The copyright of this thesis vests in the author. No quotation from it or information derived from it is to be published without full acknowledgement of the source. The thesis is to be used for private study or non-commercial research purposes only.

Published by the University of Cape Town (UCT) in terms of the non-exclusive license granted to UCT by the author.

University of Cape Town

Performance of a Penetrating Corrosion Inhibitor in Controlling Carbonation-induced Corrosion in Reinforced Concrete

Rukshani Heiyantuduwa

Thesis submitted to the Faculty of Engineering, University of Cape Town, South Africa, in partial fulfillment of the requirements for the degree of Master of Science in Engineering.

Cape Town, 2002

DIGITISED
10 JUL 2012

DECLARATION

I declare that this thesis is my own, unaided work. It is being submitted for the Degree of Masters of Science in Engineering in the University of Cape Town, Cape Town, South Africa. It has not been submitted before for any degree or examination in any other University.

Signed by candidate

(Signature of candidate)

13 day of SEPTEMBER 20 02

ABSTRACT

Reinforcement corrosion in concrete remains the most serious cause of premature deterioration of concrete structures world-wide, and many methods have been proposed to combat this problem. One method of improving the durability of concrete in aggressive environments is the use of corrosion inhibitors. In this work the effectiveness of an organic penetrating corrosion inhibitor in reducing the rate of corrosion and delaying the onset of corrosion in carbonated concrete is discussed, with reference to corrosion rates. The effectiveness of the penetrating corrosion inhibitor in reducing carbonation-induced corrosion rates was determined using a 30 MPa CEM I concrete mix. Some of the specimens were treated with the inhibitor before the carbonation process and some were treated with the inhibitor after the carbonation process. Accelerated carbonation of the samples was carried out by placing the samples in a carbonation chamber where the carbon dioxide levels and temperature were maintained at 10 % and 30 °C respectively. The carbonation depths were determined at regular intervals. Once sufficient carbonation depths had occurred the specimens were removed from the carbonation chamber and corrosion rates were monitored.

The effectiveness of the inhibitor was also determined on carbonation-induced corroding site structures. Comparisons were made between corrosion rates on treated and untreated areas to determine the effectiveness of the inhibitor.

Results of the tests conducted indicate that the penetrating corrosion inhibitor is capable of reducing corrosion rates and delaying the onset of corrosion under carbonation conditions in laboratory specimens and site structures.

ACKNOWLEDGEMENTS

My supervisors Professor Mark G. Alexander and Dr. James R. Mackechnie for their much appreciated guidance and support over the duration of this project.

The laboratory and workshop staff at the Department of Civil Engineering, University of Cape Town for their very helpful technical assistance.

Mr. Paul Adams and Mr. Rodney Van Eck from Sika South Africa for their advice and insightful comments.

Special thanks are also due to Sika South Africa for their financial support for the duration of the MSc study program.

TABLE OF CONTENTS

		Page No.
1.	**INTRODUCTION**	1
1.1	Objectives	1
1.2	Scope of work	2
1.3	Layout of thesis	2
2.	**CORROSION OF REINFORCED CONCRETE STRUCTURES**	4
2.1	Electrochemical nature of corrosion	4
2.2	Corrosion of steel in concrete	5
2.3	Serviceability of corroding concrete structures	7
2.4	Causes of corrosion	8
2.4.1	Effect of chloride ions	9
2.4.2	Effect of carbonation	11
2.4.2.1	Factors that influence rate of carbonation	13
2.4.2.2	Carbonation depth measurement	18
2.5	Problems due to the corrosion of reinforcement	19
2.6	Corrosion monitoring and testing	20
2.6.1	Half-cell potential measurements	20
2.6.2	Resistivity measurements	22
2.6.2.1	Measurement procedures	23
2.6.2.2	Interpretation of resistivity results	24
2.6.2.3	Limitations	24
2.6.3	Corrosion rate measurements	26
2.6.3.1	Galvanostatic Linear Polarisation Resistance measurements in concrete	27
2.7	Summary	28
3.	**REPAIR OF CONCRETE STRUCTURES**	30
3.1	Repair options	30
3.2	Cathodic protection	31

3.2.1 Impressed Current Systems 32
3.2.2 Sacrificial Anode System (SAS) 32

3.3 Patch repairs 33
3.3.1 Incipient Anodes 34

3.4 Coating systems, sealers and membranes 35
3.4.1 Coatings and sealers 35
3.4.2 Pore liners 36
3.4.3 Pore blockers 37

3.5 Electrochemical repair techniques 37
3.5.1 Electrochemical Chloride Extraction (ECE) 37
3.5.2 Realkalization 38

3.6 Corrosion inhibitors 39
3.6.1 Classification of corrosion inhibitors 41
3.6.1.1 Classification by action 41
3.6.1.2 Classification by chemistry and function 42

3.7 Corrosion inhibitors admixed into fresh concrete 42
3.7.1 Calcium nitrite 42
3.7.1.1 Effectiveness of calcium nitrite as an inhibitor 43
3.7.1.2 Laboratory testing and field use of calcium nitrite 43
3.7.2 Organic admixed corrosion inhibitors 44

3.8 Penetrating or migrating corrosion inhibitors for hardened concrete 45
3.8.1 Organic penetrating corrosion inhibitors 46
3.8.2 Mixed organic and inorganic penetrating corrosion inhibitors and their performance 49

3.9 Summary 51

4. EXPERIMENTAL PROCEDURES AND APPARATUS: LAB WORK 53

4.1 Concrete mixes and materials 53

4.2 Curing Regimes 55

4.3 Specimens for durability index tests 56

4.4 Blocks for monitoring corrosion 56
4.4.1 Casting programme 57

4.4.2 Application of epoxy 58
4.4.3 Application of inhibitor on test specimens 58
4.4.4 Penetration depth tests for corrosion inhibitor 59
4.4.4.1 Qualitative test 59
4.4.4.2 Quantitative test 60

4.5 Accelerated carbonation 61
4.5.1 Leec carbonation chamber 61

4.6 Measurement of cover to reinforcement 63

4.7 Exposure regimes 64

4.8 Corrosion monitoring 64
4.8.1 Copper/copper sulphate half-cell 65
4.8.1.1 Interpretation of results 65
4.8.2 Corrosion rate measurements using the Gecor 6 (Galvanostatic linear polarisation resistance meter) 67
4.8.2.1 Fundamentals of the Gecor 6 67
4.8.2.2 Use of Gecor 6 70
4.8.3 Resistivity measurements 73

4.9 Durability index tests 73
4.9.1 Oxygen permeability index test 73
4.9.2 Water sorptivity test 74

4.10 Carbonation depth tests 75
4.10.1 Sample preparation 75

4.11 Summary 76

5. 0 RESULTS OF LABORATORY STUDIES 77

5.1 Durability index tests 77

5.2 Penetration of the corrosion inhibitor 78

5.3 Accelerated carbonation of samples 79
5.3.1 Phenolphthalein test to determine depth of carbonation 79

5.4 Measurement of cover to reinforcement 81

5.5 Application of inhibitor 82

5.6 Corrosion monitoring 85

5.6.1 Corrosion rate monitoring cycles for 10 and 20 mm cover samples 85
5.6.2 Performance of the penetrating corrosion inhibitor in 10 mm cover samples 86
5.6.3 Performance of the penetrating corrosion inhibitor at 20 mm cover 92

5.7 General discussion 98

5.8 General conclusions 99

5.9 Summary 100

6. SITE WORK 101

6.1 Experimental procedure 101
6.1.1 Strength tests 103
6.1.2 Durability Index tests 103
6.1.3 Corrosion monitoring 103
6.1.4 Application of inhibitor 104

6.2 Results 104
6.2.1 Parapet walls 1, Sports Centre Building, UCT 104
6.2.1.1 Compressive strength tests 105
6.2.1.2 Durability Indexes and carbonation tests 105
6.2.1.3 Reinforcement data 106
6.2.1.4 Corrosion monitoring 107
6.2.2 Second Parapet Wall, Sports Centre Building, UCT 108
6.2.2.1 Compressive strength tests 109
6.2.2.2 Durability Indexes and carbonation depth tests 110
6.2.2.3 Reinforcement data 110
6.2.2.4 Corrosion monitoring 111
6.2.3 Concrete slabs, Civil Engineering Department, UCT 113
6.2.3.1 Compressive strength tests 114
6.2.3.2 Durability indexes and carbonation depth tests 114
6.2.3.3 Reinforcement data 115
6.2.3.4 Corrosion rate monitoring 116
6.2.4 Roof of Menzies Building, UCT 118
6.2.4.1 Compressive strength tests 120
6.2.4.2 Durability indexes and carbonation depth tests 120
6.2.4.3 Reinforcement data 120
6.2.4.4 Corrosion rate monitoring 121
6.2.4.5 Application of inhibitor 122
6.2.4.6 Depth of penetration of inhibitor 124
6.2.5 Discussion of site work results 125
6.2.6 Resultsof wetting of concrete structure (Menzies site) 127

6.3 Summary 130

7. CONCLUSIONS 132

7.1 Performance of the penetrating organic corrosion inhibitor in laboratory specimens 132
7.1.1 Discussion 133

7.2 Performance of the penetrating organic corrosion inhibitor in site structures 135
7.2.1 Discussion 136

7.3 Recommendations for further work 138

REFERENCES 139

APPENDICES 145

LIST OF TABLES

		Page No.
Table 2.1:	Types of curing regimes	14
Table 2.2:	Qualitative risk of chloride-induced corrosion	21
Table 2.3:	Relationship of corrosion rate and concrete resistivity	24
Table 2.4:	Qualitative assessment of site corrosion rates	28
Table 4.1:	Concrete mix designs (kg/m^3), 28 day strengths and measured slumps	55
Table 4.2:	Comparison of TKN and test kit results	61
Table 4.3:	Copper/copper sulphate potentials and the probability of corrosion	65
Table 4.4:	Qualitative guide for the assessment of site corrosion rates	68
Table 4.5:	Likely corrosion rate based on concrete resistivity	73
Table 4.6:	Suggested ranges for durability classification using the index values	75
Table 5.1:	Compressive strengths (MPa) obtained for different concrete grades	77
Table 5.2:	Average oxygen permeability index and water sorptivity results	77
Table 5.3:	Penetration depth of inhibitor at 28 days	78
Table 5.4:	Carbonation depths	80
Table 5.5:	Carbonation depths for 10 mm cover test specimens	81
Table 5.6:	Concrete covers (mm)	82
Table 5.7:	Qualitative test results for depth of penetration of inhibitor for samples treated with the inhibitor before the carbonation process	83
Table 5.8:	Qualitative test results for depth of penetration of inhibitor for samples treated with the inhibitor after the carbonation process	83
Table 5.9:	Measurements obtained using the Gecor and the Coulostatic method	91
Table 5.10:	Measurements obtained using the Gecor and copper/copper sulphate half-cell	91
Table 5.11:	Corrosion rate measurements obtained using the Gecor and the Coulostatic method	97
Table 5.12:	Potential measurements obtained using the Gecor and the copper/copper sulphate half-cell	98
Table 6.1:	Compressive strengths, Parapet walls 1, Sports Centre Building, UCT	105
Table 6.2:	Durability Indexes and carbonation depth results, Parapet walls 1, Sports Centre Building, UCT	106
Table 6.3:	Compressive strengths, 2nd Parapet wall, Sports Centre Building, UCT	109

Table 6.4:	Durability Indexes and carbonation depth results, 2nd parapet wall, Sports Centre Building, UCT	110
Table 6.5:	Compressive strengths, Concrete slabs, Civil Engineering Department, UCT	114
Table 6.6:	Durability and carbonation depth results, Concrete slabs, Civil Engineering Department, UCT	115
Table 6.7:	Compressive strengths, Roof of Menzies Building, UCT	120
Table 6.8:	Durability indexes and carbonation depth results, Roof of Menzies, UCT	120
Table 6.9:	Qualitative test results to determine depth of penetration of inhibitor, Roof of Menzies Building, UCT	124
Table 6.10:	Concrete conductivities and moisture contents of treated and control areas	130

LIST OF FIGURES

		Page No.
Figure 2.1:	Corrosion of steel reinforcement in concrete	6
Figure 2.2:	Three-phase corrosion damage model	7
Figure 2.3:	An example of deterioration in a bridge caused by carbonation-induced corrosion	8
Figure 2.4:	An example of deterioration in a building caused by carbonation-induced corrosion	9
Figure 2.5:	The breakdown of the passive layer and 'recycling' chlorides	11
Figure 2.6:	Schematic of the carbonation front	12
Figure 2.7:	Average depths of carbonation after 7, 28, 90 and 180 days for the types of curing shown in table 2.1	14
Figure 2.8:	Effect of relative humidity and air temperature on the depth of carbonation	16
Figure 2.9:	Effect of exposure conditions on rate of carbonation	16
Figure 2.10:	Effect of water/cement ratio on the rate of carbonation	17
Figure 2.11:	Effect of cement type on the rate of carbonation	18
Figure 2.12:	Schematic representation of the damage to the concrete cover due to rust formation	20
Figure 2.13:	Principle of Wenner probe for measuring resistivity	23
Figure 3.1:	Schematic description of cathodic protection	31
Figure 3.2:	Formation of incipient anodes after patch repair	34
Figure 3.3:	Schematic sketch of coatings and sealers	36
Figure 3.4:	Schematic sketch of pore liners	36
Figure 3.5:	Schematic sketch of pore blockers	37
Figure 3.6:	Electrochemical Chloride Extraction in concrete	38
Figure 3.7:	Schematic of progress of steel corrosion in concrete	40
Figure 3.8:	Extension of the service life of a concrete structure with corrosion inhibitor	40
Figure 3.9:	Schematic sketch of corrosion process with and without inhibitor	45
Figure 3.10:	Transport studies of penetrating organic corrosion inhibitor in concrete blocks expressed as atomic concentration ratio of nitrogen to silicon versus depth of penetration	47
Figure 3.11:	Simplified model of amino alcohol corrosion inhibitor (AACI) film forming on steel	48
Figure 3.12:	Integral corrosion current in the cracked concrete beam test	48
Figure 3.13:	Cracked concrete beam test: Corrosion currents	50
Figure 4.1:	Grading curve for fine aggregate (Klipheuwel sand)	54
Figure 4.2:	Grading curve for coarse aggregate (19 mm Greywacke stone)	54
Figure 4.3:	Schematic sketch with dimensions of concrete test blocks	57
Figure 4.4:	Wooden mould used to fabricate concrete test specimens	57
Figure 4.5:	Concrete test specimens	58
Figure 4.6:	A photograph of chromatograph paper used in a penetration test	60
Figure 4.7:	Set up of test specimens in carbonation chamber	63

Figure 4.8:	Sectional view of a copper/copper sulphate half-cell	66
Figure 4.9:	Copper/copper sulphate half-cell circuitry	67
Figure 4.10:	Confinement of current lines from central counter electrode due to the action of external counter electrode	69
Figure 4.11:	Arrangement of counter electrodes and reference electrodes (S_1 and S_2) for testing a reinforced concrete slab	69
Figure 4.12:	Scheme of sensor A	71
Figure 4.13:	Typical Gecor measurements using sensor A on test specimens	72
Figure 4.14:	Oxygen permeability cell	74
Figure 4.15:	Water sorptivity test arrangement	75
Figure 5.1:	Carbonation depths, 30 MPa concrete blocks	80
Figure 5.2:	Corrosion rate measurements for 10 mm cover test specimens	87
Figure 5.3:	Half-cell potential measurements for 10 mm cover specimens	87
Figure 5.4:	Three-point moving averages of corrosion rates for 10 mm cover samples	90
Figure 5.5:	Three-point moving average of half-cell potential data for 10 mm cover samples	90
Figure 5.6:	Relationship between resistivity of concrete and resistance	92
Figure 5.7:	Corrosion rate measurements for 20 mm cover samples	94
Figure 5.8:	Half-cell potential measurements for 20 mm cover samples	94
Figure 5.9:	Schematic relationship of fluctuation of moisture at level of the steel	95
Figure 5.10:	Three-point moving averages of corrosion rates for 20 mm cover samples	96
Figure 5.11:	Three-point moving average of half-cell potential data for 20 mm cover samples	96
Figure 6.1:	Map of the University of Cape Town showing the test sites	101
Figure 6.2:	Schematic sketch of connection to steel reinforcement	102
Figure 6.3:	Damage caused by carbonation-induced corrosion, Parapet walls 1, Sports Centre Building, UCT	105
Figure 6.4:	Reinforcement data, Parapet walls 1, Sports Centre Building, UCT	106
Figure 6.5:	Corrosion rate measurements, 1st parapet wall, Sports Centre Building, UCT	107
Figure 6.6:	Half-cell potential measurements, 1st parapet wall, Sports Centre Building, UCT	108
Figure 6.7:	Resistivity measurements, 1st parapet wall, Sports Centre Building, UCT	108
Figure 6.8:	Damage caused by carbonation induced corrosion, 2nd Parapet wall, Sports Centre Building, UCT	109
Figure 6.9:	Reinforcement data, 2nd parapet wall, Sports Centre Building, UCT	111
Figure 6.10:	Corrosion rate measurements, 2nd parapet wall, Sports Centre Building, UCT	112

Figure 6.11:	Half-cell potential measurements, 2nd parapet wall, Sports Centre Building, UCT	112
Figure 6.12:	Resistivity measurements, 2nd parapet wall, Sports Centre Building, UCT	113
Figure 6.13:	Damage caused by carbonation induced corrosion, Concrete slabs, Civil Engineering Department, UCT	114
Figure 6.14:	Reinforcement data, Concrete slabs, Civil Engineering Department, UCT	115
Figure 6.15:	Corrosion rate measurements, Concrete slabs, Civil Engineering Department, UCT	116
Figure 6.16:	Half-cell potential measurements, Concrete slabs, Civil Engineering Department, UCT	116
Figure 6.17:	Resistivity measurements, Concrete slabs, Civil Engineering Department, UCT	117
Figure 6.18:	Spalling and cracking of concrete due to carbonation-induced corrosion on parapet walls at the Menzies site.	119
Figure 6.19:	Reinforcement data, Roof of Menzies, UCT	121
Figure 6.20:	Corrosion rate measurements before and after application of inhibitor, Roof of Menzies Building, UCT	123
Figure 6.21:	Half-cell potential measurements before and after application of inhibitor, Roof of Menzies Building, UCT	123
Figure 6.22	Resistivity measurements before and after application of inhibitor, Roof of Menzies Building, UCT	124
Figure 6.23:	Dimensions of test areas and positions of cores obtained	125
Figure 6.24:	Set up of wetting system	126
Figure 6.25:	Corrosion rates for areas undergoing wetting	127
Figure 6.26:	Half-cell potentials for areas undergoing wetting	127
Figure 6.27:	Resistances for areas undergoing wetting	128
Figure 6.28:	Resistivity for areas undergoing wetting	128

1. INTRODUCTION

Reinforced concrete is a versatile, economical and successful construction material, widely used for many decades. However, sometimes it does not perform adequately as a result of poor design, poor construction, inadequate materials selection, and a more severe environment than anticipated, or a combination of these factors. [1]

The corrosion of steel in concrete has in recent decades become one of the main problems affecting the durability of reinforced concrete structures in mild as well as severe climatic conditions. Whereas in the past, much concern related directly to the performance of concrete itself e.g. resistance of concrete to sulphate attack, it seems that, at present, the most common durability problem is corrosion of steel in concrete [2].

Corrosion prevention and control must therefore be carefully considered and addressed in structural concrete. Ever since reinforcing steel has been included in the production of reinforced concrete, the potential has existed for corrosion to take place. It has been said that the corrosion of steel reinforcement is the most frequent cause of failure in reinforced concrete and is therefore of major concern [1].

The implications of damage caused by corrosion of steel in concrete structures are also large. For example, in the case of bridge decks in the USA, the yearly cost of repairs is estimated to be between $50 to $200 million [2]. Therefore the economic loss and damage due to corrosion of reinforcement makes it one of the largest problems facing infrastructure in developing and industrialised countries. However, the deterioration of reinforced concrete can be avoided by appropriate planning, design and execution. It is therefore of importance that the corrosion process is properly understood so that more durable concrete structures can be designed and better techniques be developed.

1.1 Objectives

The overall object of this work is to assess the performance of an organic corrosion inhibitor in reducing carbonation-induced corrosion, both as a preventative measure and as a repair technique. A number of tests were carried out in the laboratory and on site to determine the effectiveness of this inhibitor in these different environments.

Objectives included the following:

- To assess the performance of the inhibitor in reducing the onset of carbonation corrosion under laboratory conditions, and thereby increase the service life of a structure.
- To assess the performance of the inhibitor in reducing the rate at which carbonation corrosion takes place in already corroding structural elements under site and laboratory conditions.
- To determine the rate and depth of penetration of the corrosion inhibitor for different concrete grades.

1.2 Scope of work

Reinforcement corrosion remains the most serious cause of the premature deterioration of concrete structures world-wide and many methods have been proposed to combat this problem. One method of improving the durability of concrete in aggressive environments is the use of corrosion inhibitors. The effectiveness of a penetrating corrosion inhibitor in reducing carbonation-induced corrosion rates was evaluated using a 30 MPa CEM I concrete mix. This penetrating corrosion inhibitor could be one possible solution to the problem of reinforcement corrosion in concrete structures, and the problems occurring due to corrosion could be overcome to some extent if the inhibitor is found to be effective in stifling or slowing down the corrosion process

The effectiveness of a penetrating organic corrosion inhibitor in reducing carbonation-induced corrosion was determined by casting a number of reinforced concrete block specimens at different covers to reinforcement using a 30MPa CEM I 42.5 cement concrete mix. Six blocks were cast at a cover of 20 mm, and six blocks with 40 mm cover. Some of the specimens were treated with the inhibitor before the carbonation process and others were treated with the inhibitor after the carbonation process. Accelerated carbonation of the samples was carried out by placing the samples in a carbonation chamber where the carbon dioxide levels and temperature were maintained at 5 %, and subsequently 10 %, and 30°C respectively. The carbonation depths were determined at regular intervals. Once sufficient carbonation depths had been reached the specimens were removed from the carbonation chamber and corrosion rates were monitored.

Corrosion rates were measured using a commercial instrument, the Gecor. The Gecor uses a linear polarisation technique to determine corrosion rate values. Values of the half-cell potential and resistivity were also obtained. The data obtained are analysed and relationships established. The effectiveness of a migrating corrosion inhibitor was thereby investigated and discussed with reference to corrosion rates and carbonation depths. The depth of penetration of the inhibitor was measured by using the qualitative technique recommended by the manufacturer. Finally, recommendations are made based on the data that is presented and analysed

1.3 Layout of thesis

This work is presented in seven chapters.

- The first chapter consists of a brief introduction to the topic and objectives of this work.

- Chapters two and three comprise the literature review. The corrosion process is discussed in detail and the effects of carbonation and chloride ions on the corrosion of steel reinforcement in concrete are presented. Analysis of corrosion damage in the form of condition surveys and various available repair techniques are discussed to present the reader with an overview of the available repair methods for corrosion damaged concrete, with special attention paid to the different types of corrosion inhibitors available. Corrosion inhibitors are addressed

and the mechanisms by which they reduce the corrosion process, their different types and how they can be used in concrete repair are mentioned. Their effects on the corrosion process and how they can be used in the prevention of reinforcement corrosion and in concrete repair are also discussed. The theory behind the various electrochemical techniques used for monitoring corrosion is also introduced and discussed.

- The fourth chapter describes the experimental procedures used in this work. The method of the Galvanostatic Linear Polarisation resistance technique in the measure of corrosion rates, probability of corrosion (half-cell potentials and resistivity measurements), amount of carbonation and the depth of penetration of the corrosion inhibitor are discussed in detail. Durability Index tests are also mentioned. Basic descriptions of the test methods and important limitations in these various test methods are discussed.

- The fifth chapter presents and analyses the data obtained in the laboratory work, and discusses the effectiveness of the penetrating corrosion inhibitor with reference to corrosion rates.

- Chapter six covers the site-work. It gives a brief overview of the test procedures used. It also shows and discusses the results obtained at the various test sites monitored.

- The concluding chapter discusses the overall performance of the inhibitor and recommendations about the use of the inhibitor are made.

2. CORROSION OF REINFORCED CONCRETE STRUCTURES

The problem of corrosion is widespread in all forms of reinforced concrete structures both in South Africa and overseas. Concrete has to be reinforced with embedded steel when used to resist tensile and flexural loading, and it is the potential for corrosion of this embedded steel that is a prime issue in structural deterioration.

Electrochemical corrosion is known to pose the greatest threat to the durability of reinforced concrete structures [1]. Therefore, in order to improve the durability of these structures it is firstly essential that the corrosion process be properly understood. The sections that follow explore the basics of corrosion of steel in concrete such that durable concrete structures can be constructed and effective repair or corrosion control procedures be developed.

The purpose of this chapter is to present an overview of the corrosion process, and to introduce the two main causes of reinforcement corrosion in concrete structures, that is, chlorides and carbonation, as well as how they affect the corrosion of steel in reinforced concrete. The different methods of corrosion monitoring are also discussed.

2.1 Electrochemical nature of corrosion

Corrosion can be described as the destructive attack of a metal by an electrochemical process undergoing a number of oxidation and reduction reactions. It is a process by which a refined metal reverts back to its natural state by an oxidation reaction with the environment (e.g. oxygen and water) [1].

In the corrosion process two electrochemical reactions take place simultaneously at different sites on the steel surface. The two reactions are known as 'anodic' and 'cathodic' reactions, and the areas on the surface of the corroding metal where the reactions occur are called the anode and the cathode respectively. At the anode, metal atoms are ionised and pass into the solution around the metal as positively charged hydrated ions (anodic oxidation). Electrons are thereby left on the metal surface and therefore raise its electrical potential. The excess free electrons then flow through the metal to the cathodic region (lower potential area) of the metal where an electron acceptor such as dissolved oxygen (water and oxygen) is available to consume them to form hydroxyl ions (cathodic reduction). The flow of electrons occurs due to a potential difference that exists between the two electrodes, and as long as such a potential difference exists, electrons will flow from the anode to the cathode causing corrosion. The process continues by electro-migration of ions through the aqueous phase leading to the formation of corrosion products at the anode. If water and oxygen are not available at the cathodic sites, the corrosion process will be terminated [2].

The reactions taking place at the anode and cathode are shown below (for the purposes of the equation the metal is steel):

Anodic reaction $2Fe - 4electrons \rightarrow 2Fe^{2+}$ (2.1)

($2Fe$: metallic atoms at steel surface; $2Fe^{2+}$: ions dissolved in solution.)

Cathodic reaction $O_2 + 2H_2O + 4$ electrons $\rightarrow 4OH^-$ (2.2)

dissolved oxygen molecules. ions dissolved in solution.

2.2 Corrosion of steel in concrete

Corrosion of steel in concrete is a process similar to that described above. A characteristic feature of the corrosion of steel in concrete is the development of macro cells, that is the coexistence of passive and corroding areas on the rebar forming a galvanic element with the corroding area as the anode and the passive surface as the cathode. A corrosion current is therefore driven by a difference in potential between the anodic and cathodic areas that may exist on the same length of reinforcement. The potential difference occurs due to local differences in the environment surrounding the reinforcement or due to differences in the surface condition of the steel reinforcement [3].

Concrete is alkaline in nature, that is, it contains microscopic pores with high concentrations of soluble calcium, sodium and potassium hydroxides [1]. The alkalinity of concrete in pH terms is roughly between 12 and 13. Therefore, when steel is embedded in concrete it is in contact with highly alkaline pore solutions which form a tight and stable passivating film of ferric oxide around the steel surface protecting it against corrosion. This passive layer prevents corrosion by stopping the dissolution of Fe^{2+} ion into the surrounding pore solution, thereby preventing the flow of electrons from the anode to the cathode.

However this passivating layer is not always maintained and can be broken down by aggressive environments, which reduce the alkalinity of the concrete, or by the ingress of chloride ions. A change in pH of the environment can occur when the process of carbonation affects the concrete. The ingress of chloride ions also affects the passivity of steel, since once the chloride threshold concentration is exceeded the passive oxide layer breaks down. Once depassivation is achieved corrosion may take place. The chemical reactions are the same regardless of the depassivating medium. The steel corrodes and dissolves in the pore water and gives up electrons at the anode. The electrons created at the anode must be consumed somewhere else on the surface of the steel to preserve electrical neutrality. Therefore in the presence of water and oxygen the electrons are consumed to produce hydroxyl ions at the cathode.

The corrosion process of steel in concrete is shown schematically in figure 2.1.

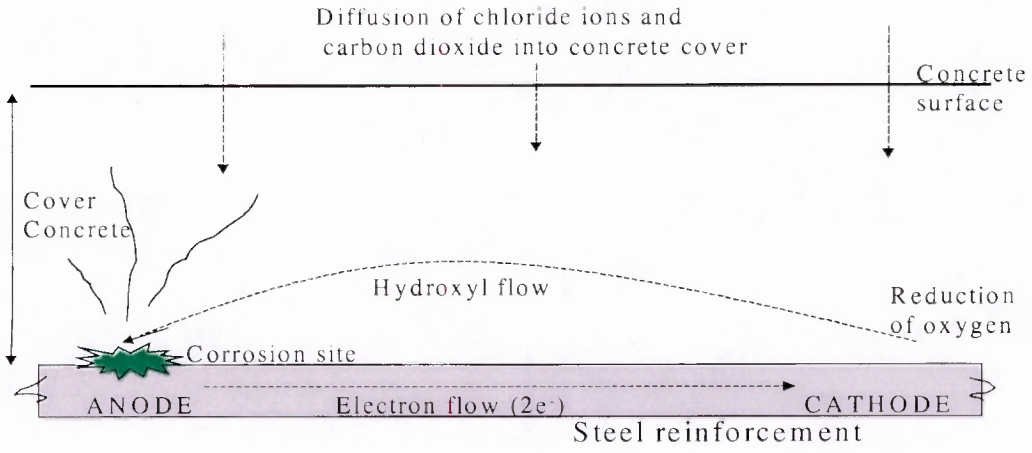

Figure 2.1: Corrosion of steel reinforcement in concrete [4]

These anodic and cathodic reactions are but the first steps in the corrosion process. If only the iron was to dissolve in the pore water without any further oxidation, cracking and spalling of the concrete would not occur. Several more stages must occur for formation of rust or expansive corrosion products, which affect the surrounding concrete. In subsequent stages ferrous hydroxide becomes ferric hydroxide and then hydrated ferric oxide or rust.

The equations are shown below [1]:

$$Fe^{2+} + 2OH^- \rightarrow \underset{\text{Ferrous hydroxide}}{Fe(OH)_2} \qquad (2.3)$$

$$4Fe(OH)_2 + O_2 + 2H_2O \rightarrow \underset{\text{Ferric hydroxide}}{4Fe(OH)_3} \qquad (2.4)$$

$$2Fe(OH)_3 \rightarrow \underset{\text{Hydrated ferric oxide (rust)}}{Fe_2O_3.H_2O} + 2H_2O \qquad (2.5)$$

The expansion associated with rust is due to the hydrated oxides, which can swell up to seven times the original steel volume [1]. This in turn causes the cracking and spalling that are observed as the usual consequence of corrosion of steel in concrete, as well as the red/brown brittle, flaky rust on the bar and the rust stains seen at cracks in the concrete [1].

2.3 Serviceability of corroding concrete structures

Serviceability is defined as the capability of a building product, component, assembly, or construction to perform the function or functions for which it is designed and constructed [5]. The loss of serviceability of corroding concrete structures can be represented by the three-phase damage model shown in figure 2.2.

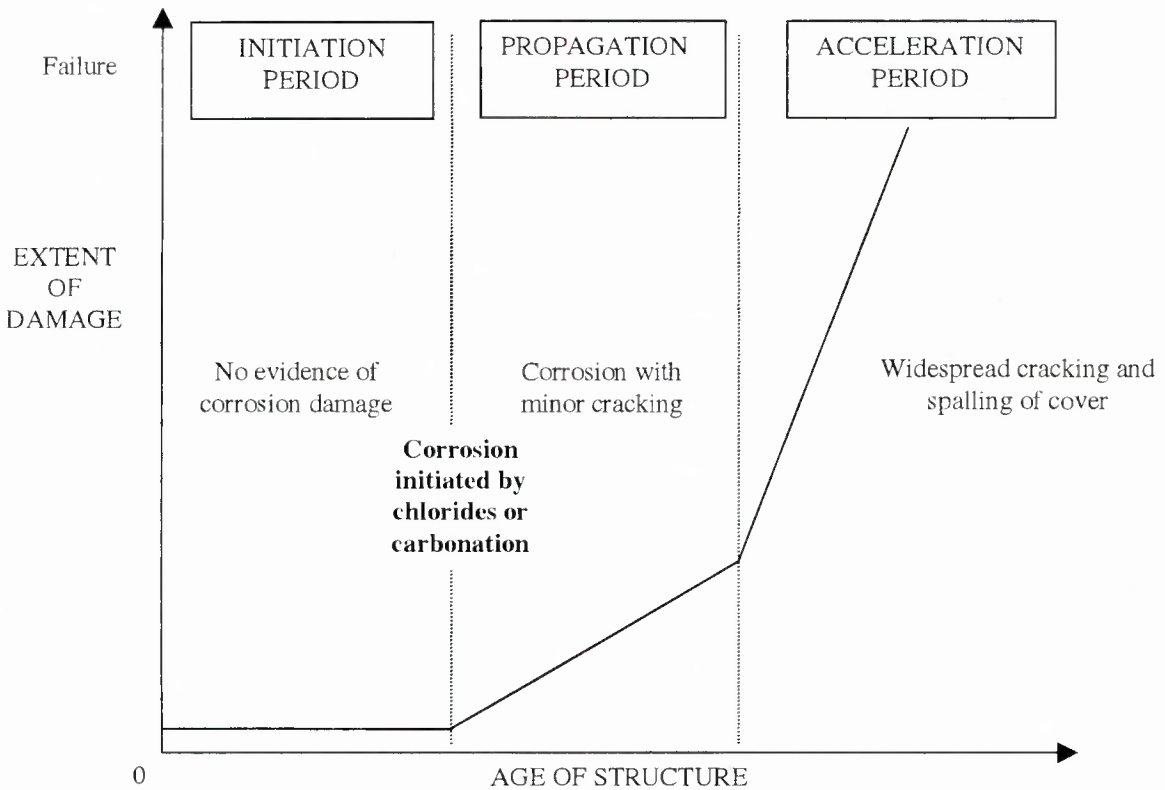

Figure 2.2: Three-phase corrosion damage model [5].

The different phases are defined as follows:

- **Initiation period** – This is the period before there is any evidence of corrosion damage, during which negligible corrosion deterioration occurs. During this period chloride ions or the carbonation front advance into the cover concrete and reach the level of the reinforcing steel.

- **Propagation period** – In this stage active corrosion begins, expansive corrosion products accumulate and cracking of the concrete cover occurs. Dominant factors affecting the rate of corrosion are the quantity of oxygen in the dissolved state, the moisture present and the electrical resistance of the concrete.

- **Acceleration period** – In this stage the rate of corrosion is accelerated due to the easy access of oxygen and water through cracks present in the cover concrete. Therefore, delamination and spalling of the cover concrete occurs.

Unfortunately once cracking and spalling of reinforced concrete structures begin there are very few cost effective measures that can be taken to restore serviceability. In repair design, non-destructive means of judging whether and how the structure is to be repaired are usually used during the initiation and propagation periods, for example by carrying out condition surveys, which will be discussed in a later section. This will enable a better specification of the performance required for the repair work.

From the perspective of use of penetrating corrosion inhibitors, their effectiveness will probably be greatest if applied during the initiation period, to prevent the onset of corrosion, or during the propagation period, to retard the rate of corrosion.

2.4 Causes of corrosion

The primary reason for reinforcement corrosion is depassivation of the steel. However, a number of causes can provide the means by which this comes about. These include porous concrete over the steel reinforcement, insufficient thickness of concrete cover to the steel reinforcement, stray electrical currents, the presence of water and oxygen, the advance of a carbonation front, and the presence of aggressive ions e.g. chlorides. There are also factors such as sulphate attack, which can affect the integrity of the concrete and thus accelerate the onset of reinforcement corrosion [6].

Figure 2.3 and 2.4 shows examples of carbonation-induced damage in concrete structures.

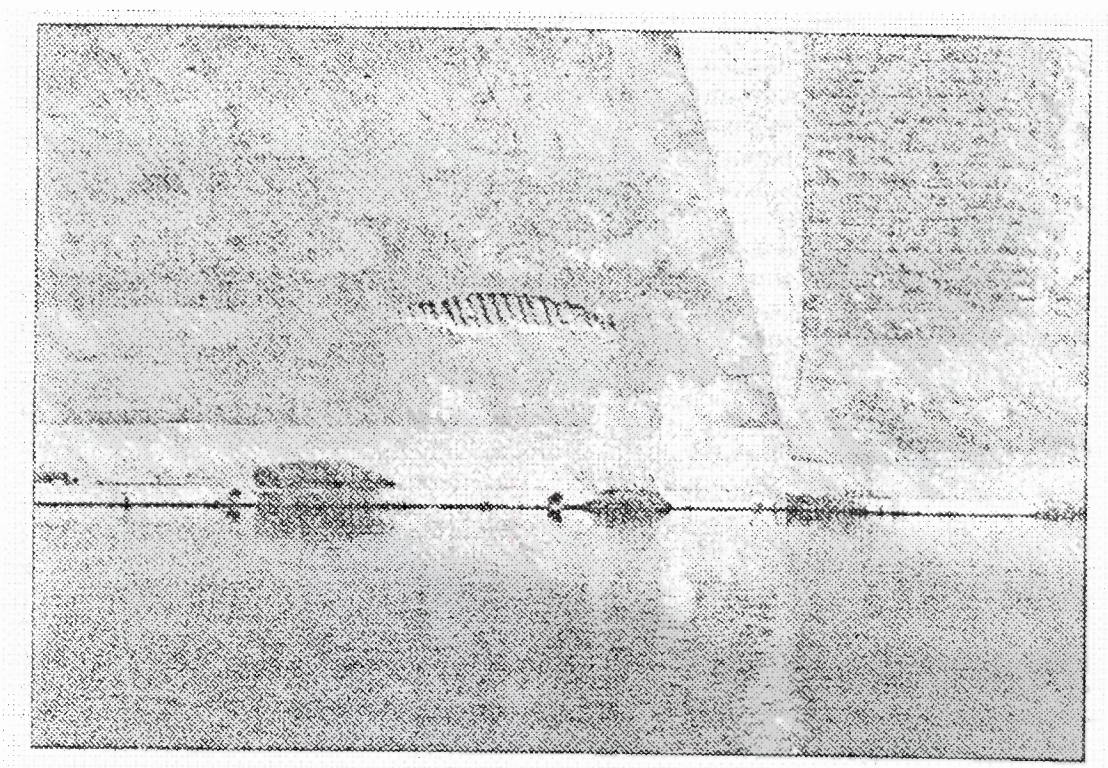

Figure 2.3: An example of deterioration in a bridge caused by carbonation-induced corrosion [7].

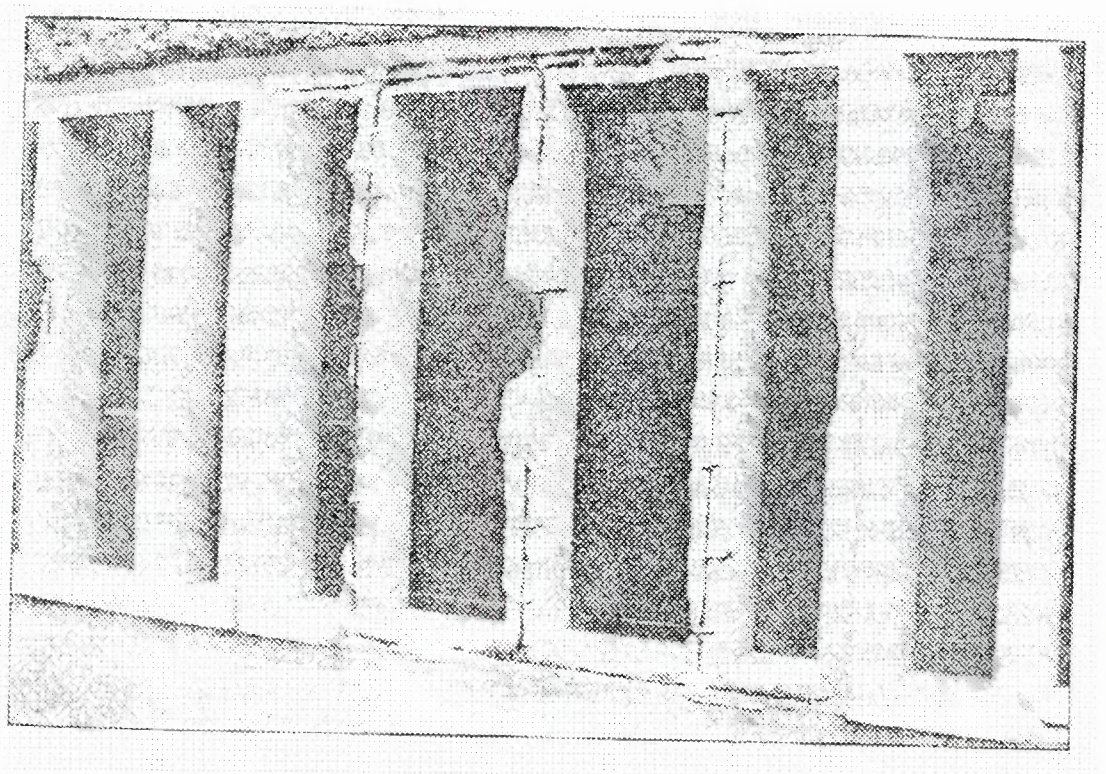

Figure 2.4: An example of deterioration in a building caused by carbonation-induced corrosion [7].

In the following sections the two main mechanisms of chloride attack and carbonation of the concrete are discussed.

2.4.1 Effect of chloride ions

The corrosion of steel in reinforced concrete due to the ingress of chlorides is a major cause for the decreased durability of structures built in marine and de-icing salt environments [8]. Chlorides are introduced into the concrete through two main processes: they can be cast into the concrete or they can diffuse through the hardened concrete from the outside.

Chlorides cast into the concrete can be due to:

- Deliberate addition of chloride set-accelerators (e.g. calcium chloride $CaCl_2$).
- Contaminated aggregates (usually sea dredged aggregates which are unwashed or inadequately washed).
- Use of seawater in the mix.

Chlorides can diffuse into the concrete as a result of:

- Sea salt spray and direct seawater wetting.
- De-icing salts.
- Chlorides in the environment.

Most chloride attack on concrete reinforcement occurs due to the diffusion of chlorides into the concrete. The passive layer around the steel is not immediately

affected when it comes into contact with chloride ions. This ferric oxide layer is able to withstand the presence of chloride ions to a certain extent. It has been suggested that there is a threshold concentration of chloride ions that must be exceeded before depassivation can take place, and that this threshold concentration is a function of the pH, or conversely the OH^- ion concentration [1]. This threshold concentration is generally given in terms of the chloride/hydroxyl ratio, which can be measured in laboratory tests [1]. When the chloride concentration exceeds 0.6 of the hydroxyl concentration, corrosion is observed [1]. This approximates typically to a concentration of 0.4% chloride by weight of cement if chlorides are cast into concrete, and 0.2% if they diffuse in [1]. This is however dependent on a number of factors e.g. cement type, chemical composition of the cement, oxygen and moisture content etc. Chlorides that enter the concrete after it has hardened e.g. de-icing salts, are more harmful than those that are present in the concrete from the start as admixtures or contamination of aggregates (assuming these cast-in chlorides do not exceed the threshold value). This is because a proportion of any chloride ions present in freshly mixed concrete will combine with tricalcium aluminate in the cement and will not be available for initiating corrosion.

The depassivation of the steel due to chloride attack occurs when the chloride ion attacks the passive layer, without there being an overall drop in pH. On reaching the iron substrate, the chloride ion acts as a catalyst for the oxidation of the iron by taking an active part in the reduction process thereby increasing the rate of breakdown of the passive layer of oxide and allowing the corrosion process to proceed.

The chloride ion combines with the iron to form the complex $FeCl_2$ and then draws this unstable ion into the solution where it reacts with the available hydroxyl ions to form $Fe(OH)_2$. This in turn releases the chloride ions back into the solution and consumes hydroxyl ions locally, as seen in the reactions below [1]:

Primary Anodic Reaction: $$Fe \rightarrow Fe^{2+} + 2e^- \quad (2.6)$$

$$Fe^{2+} + 2Cl^- \rightarrow FeCl_2 \quad (2.7)$$

Secondary Anodic Reaction: $$FeCl_2 + 2H_2O \rightarrow 2Fe(OH)_2 + 2Cl^- + 2H^+ \quad (2.8)$$

The electrons released in the oxidation reaction then flow through the steel to the cathode surface. This process would then result in a concentration of chloride ions and a reduction of the pH at the points of corrosion initiation, probably accounting for the process of pitting corrosion. The lower pH also contributes to the continual breakdown of the passive oxide film, leading to corrosion [1]. Figure 2.5 shows the chemical changes occurring at the concrete/steel interface.

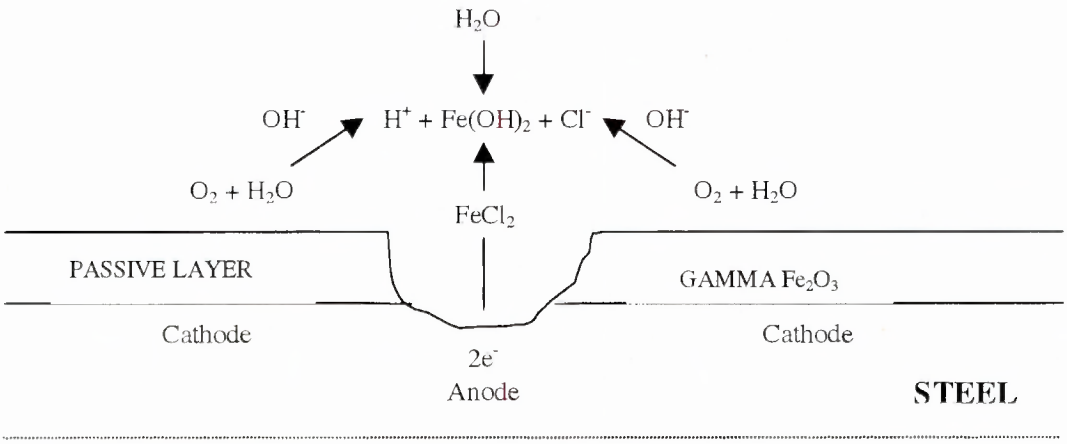

Figure 2.5: The breakdown of the passive layer and 'recycling' chlorides [1]

2.4.2 Effect of carbonation

Another major process which takes place in concrete and which may limit the service life of reinforced concrete structures is carbonation of the material. Since the focus of this thesis is to determine the effectiveness of a penetrating corrosion inhibitor on controlling carbonation-induced corrosion, the process of carbonation corrosion will be dealt with in more detail.

In this process carbon dioxide from the atmosphere diffuses into the capillary pores of the hardened cement paste and reduces the pH of the concrete. Under normal conditions the concentration of carbon dioxide in the air is approximately 0.03%. However, in industrial areas the concentration of carbon dioxide is much higher and the possibility of carbonation is increased.

Carbonation takes place as a result of the interaction of carbon dioxide with the alkali hydroxides in the concrete. The carbon dioxide gas dissolves in water to form carbonic acid, which neutralises the alkalis in the pore water, mainly forming calcium carbonate that lines the pores [1].

$$\underset{\text{Gas}}{CO_2} + \underset{\text{Water}}{H_2O} \rightarrow \underset{\text{Carbonic acid}}{H_2CO_3} \qquad (2.9)$$

$$\underset{\text{Carbonic acid}}{H_2CO_3} + \underset{\text{pore solution}}{Ca(OH)_2} \rightarrow CaCO_3 + 2H_2O \qquad (2.10)$$

There is more calcium hydroxide in the concrete pores than can be dissolved in the pore water. This helps maintain the pH at its usual level of around 12 or 13 [1]. However, as the carbonation reaction proceeds the available calcium hydroxide $Ca(OH)_2$ reacts, precipitating the calcium carbonate. If free water is present the calcium carbonate is deposited on the concrete pores at the depth at which carbonation is occurring, and as a result the pH of the pore solution is reduced from

about 12.5 in the uncarbonated region to about 8 in the region of complete carbonation. This is illustrated in figure 2.6.

When the carbonation front reaches the reinforcing steel, the low pH causes the gamma-ferric oxide layer (passivating layer) to become unstable and thus the steel is depassivated. In the presence of oxygen and moisture this leads to corrosion followed by corrosion-induced cracks parallel to reinforcement, followed by spalling which eventually leads to loss in the load bearing capacity of the structure. Cracks and spalling are induced because the corrosion product that forms can be up to seven times the volume of the steel before it is oxidised.

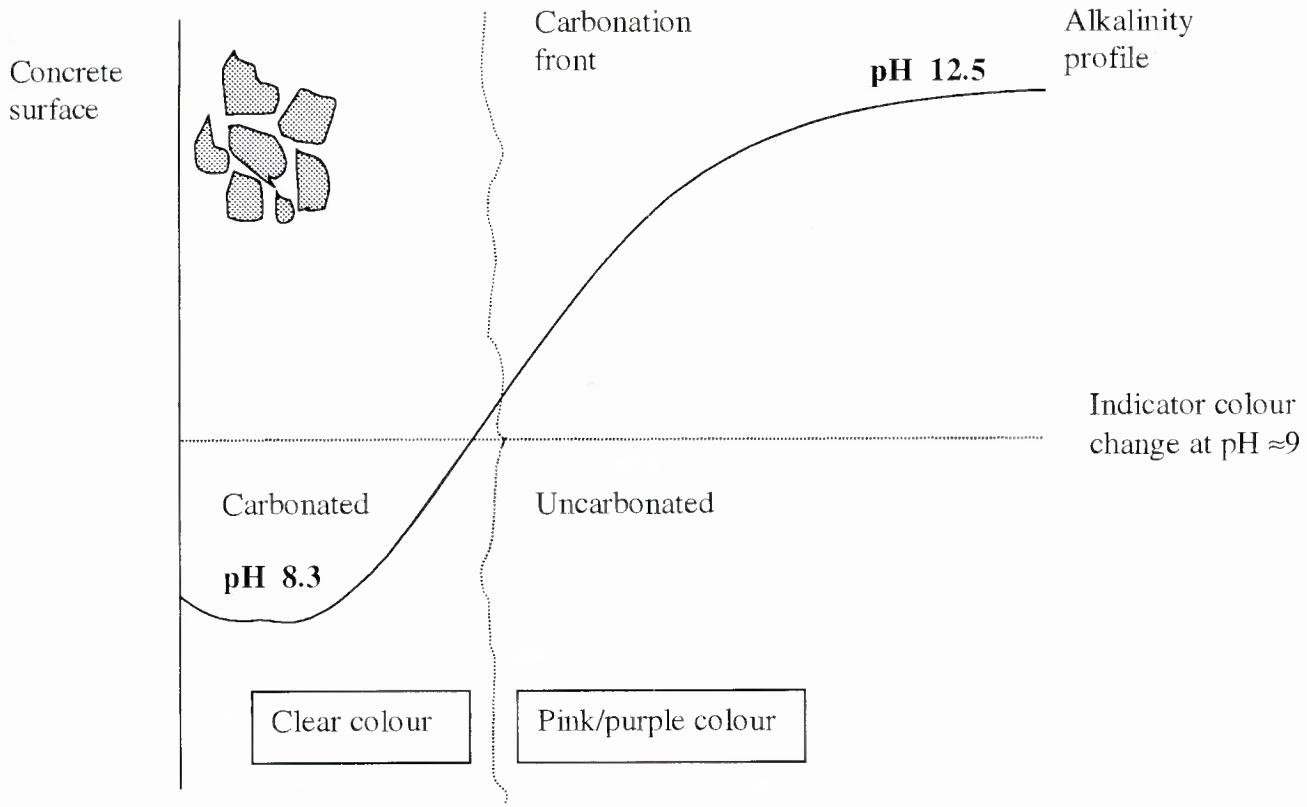

Figure 2.6: Schematic of the carbonation front [4].

Carbonation moves as a "front" into the concrete. Air is in direct contact with the external surfaces of the concrete and these surfaces will be carbonated quickly after first exposure. As air enters the capillary pores of the concrete, the carbon dioxide in the air is used up rapidly by the reaction with the hydroxides. At this stage, there is decarbonated air in the concrete, which is in intimate contact with normal air outside. In this condition there is a positive movement of carbon dioxide towards the depleted air in an attempt to restore a uniform concentration (diffusion). Since the carbon dioxide reacts rapidly with the hydroxides it cannot advance beyond a particular point until all the calcium hydroxide $Ca(OH)_2$ at that point has been converted to calcium carbonate $CaCO_3$. As the carbonation process continues the free $Ca(OH)_2$ is depleted. The C-S-H gel is however only stable in the presence of free $Ca(OH)_2$ so in the absence of free $Ca(OH)_2$ it decomposes to release calcium hydroxide leaving a

hydrated silica skeleton behind. Other hydrates in the concrete also behave similarly and therefore the carbonated layer is a framework of silica, alumina and iron oxide filled with calcium carbonate [1]. This carbonation reaction therefore also gives rise to a volume reduction, known as the "carbonation shrinkage", which is irreversible and occurs over a long period of time. In some cases it may exceed the drying shrinkage [9]. The carbonated layer is less permeable and stronger than the original concrete and therefore carbonated concrete is more resistant to the ingress of aggressive fluids. The amount of $Ca(OH)_2$ in the pore structure of the concrete also has an influence on the rate of carbonation. As the carbonated layer becomes thicker, the distance that the carbon dioxide must diffuse through to meet the hydroxide is increased.

Carbonation induced corrosion is generally a result of low covers or high permeability of the concrete.

2.4.2.1 Factors that influence rate of carbonation

A number of attempts have been made to quantify the rate of carbonation. The most commonly used relationship is that carbonation depth increases with time according to a power law. This is expressed in equation 2.11.

$$D = K\, t^{y} \qquad (2.11)$$

Where D is the carbonation depth in mm.
t is the time in years.
K is a carbonation constant for the concrete.
y is a constant that can vary from 0,3 to 0,7.

There are a number of more complicated variations of this relationship, which take into account the initial degree of alkalinity and the variable environmental conditions, which exist in the early stages of the life of concrete [10]. However, for all practical purposes this simple relationship is adequate, since in practice accurate and reliable data for these parameters are difficult to obtain.

Values for K are dependent on a number of variables such as the environment and the variables of concrete quality. The BRE report, "Carbonation Depths in Structural Quality Concrete" [10], provides details of K values for different categories of concrete under different conditions of environment.

There are a number of factors that affect the rate of carbonation. The carbonation constant K determines the rate of carbonation into a concrete surface, and is influenced by a number of factors, the most important of which are given below.

- Permeability
- Environmental conditions
- Concrete quality

Permeability

Permeability of the concrete is the most important factor affecting the rate and extent of carbonation in concrete; the higher the permeability the faster the rate of carbonation. Permeability is in turn dependent on compaction and curing.

Compaction: This is the process of expelling trapped air and proper compaction is necessary to reduce the quantity and size of the voids in the concrete and in turn reduce the permeability of the concrete.

Curing: Fresh cement paste consists of a system of solid particles uniformly dispersed throughout a water-filled space. As the cement hydrates the gel formed tends to occupy this space. With incomplete hydration the space not filled with gel becomes a capillary system which contributes to permeability. Curing tests on cement paste show that under optimum conditions the mass of curing water absorbed is roughly one quarter of the water combined with the cement at all states of hydration [11]. Therefore, it is important that sufficient curing take place for hydration to proceed under optimum conditions and in order to prevent evaporation. Active curing should begin as soon as possible. This emphasises the importance of curing for the development of strength and durability.

Research carried out on the effects of different curing periods and curing methods on carbonation rate showed that carbonation depths of specimens after ten years exposure in air with no curing were on average four to five times greater than for 90 day water cured specimens [10]. Kurtz [12] investigated the influence of extremely short-term curing on the rate of carbonation of concrete specimens, w/c = 0,45 and 0,60, subjected to different types of curing. The results of this work are shown in figure 2.7.

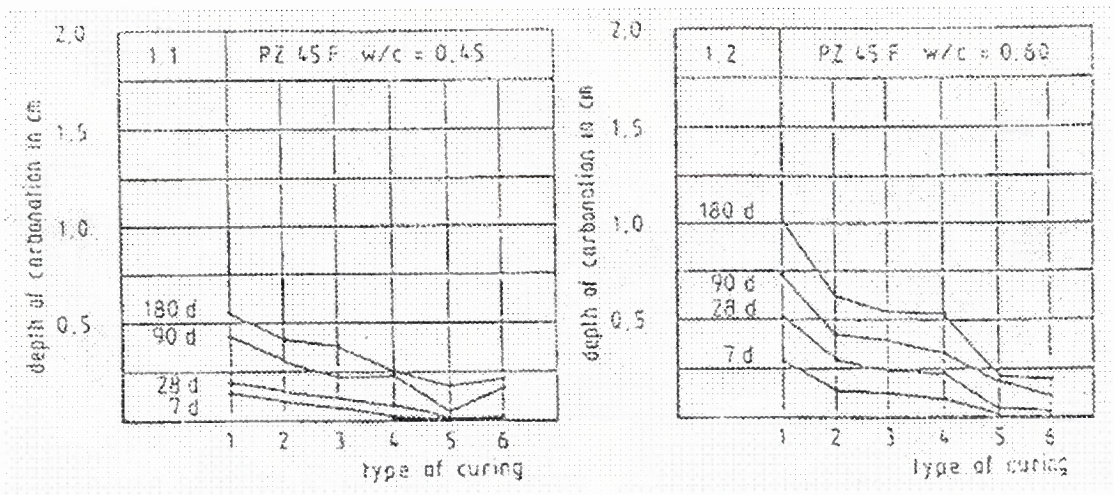

Figure 2.7: Average depths of carbonation after 7, 28, 90 and 180 days for the types of curing shown in table 2.1 [12].

Table 2.1: Types of curing regimes.

No.	Type of curing
1	6 hrs in mould, 72 hrs wind, then 20/65 climate
2	6 hrs in mould, then 20/65 climate
3	12 hrs in mould, then 20/65 climate
4	24 hrs in mould, then 20/65 climate
5	24 hrs in mould, 6 days in water, then 20/65 climate
6	6 hrs in mould, chemical curing agent, then 20/65 climate

20/65 climate – Temperature of 20 °C and a relative humidity of 65 %

It is clear that an improvement of the curing method results in a reduction in the depth of carbonation of all types of concrete, due the less permeable nature of adequately cured concrete.

Environmental conditions

The rate of carbonation is also influenced to a large extent by environmental conditions to which the concrete is subjected, particularly temperature, humidity, exposure, orientation of the structure, and carbon dioxide concentration.

Environmental conditions that are most favourable for carbonation (i.e. 50 – 65 % relative humidity) are too dry for rapid steel corrosion, which requires humidity levels above 80 % relative humidity. However, structures exposed to fluctuations in moisture conditions during the wet season are vulnerable to carbonation-induced corrosion. Wet/dry cycling on the concrete surface will accelerate carbonation by allowing carbon dioxide gas in during the dry season and then supplying water to dissolve it in the wet cycle (equation 2.8).

Temperature: influences the diffusion of carbon dioxide inside the concrete and the rate of the carbonation reaction. In both cases, a rise in ambient temperature stimulates the reactions.

Relative humidity: research done by Wierig [13] found that the rate of carbonation is strongly affected by the moisture content or relative humidity of the concrete pore solution. Little or no carbonation will take place when the pores are completely dry or when they are fully saturated. Dry calcium hydroxide reacts very slowly with carbon dioxide, and the reaction is much faster and more complete when a surface film of water, saturated with the solid, is present on the grains of the hydroxide. On the other hand if the pores of the paste are completely saturated with water the carbon dioxide gas needs to diffuse through water rather than through air, and therefore the diffusion rate is considerably slower. The rate of carbonation is a maximum when the relative humidity is at a range of about 50-65 %, as shown in figure 2.8.

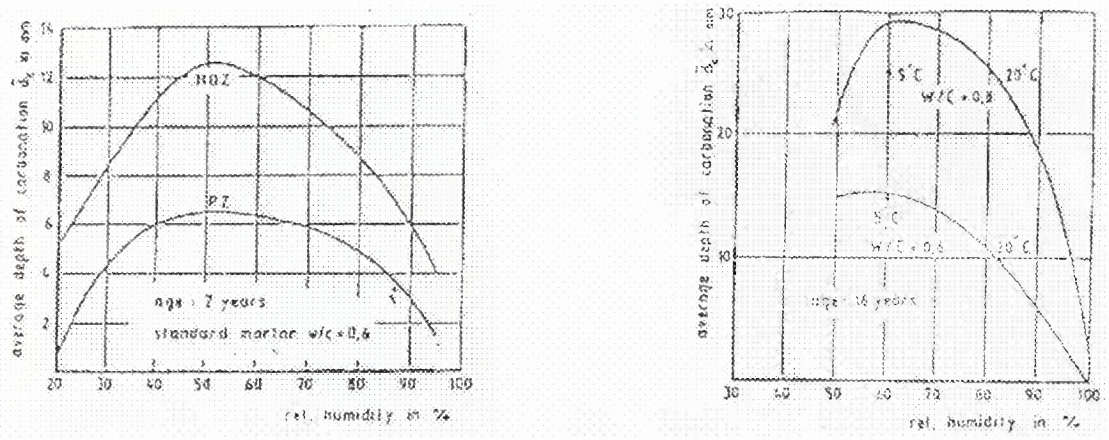

Figure 2.8: Effect of relative humidity and air temperature on the depth of carbonation [13].

Periods of relative dryness promote carbonation whereas periods of wetness promote corrosion if depassivation of the steel has already occurred. Therefore a better quality of concrete cover is necessary in climates with long dry periods and short wet periods.

Conditions of exposure: also influence the rate of carbonation. Research done by Kroone [14], Wierig [13] and Meyer [14] show that concrete subjected to cycles of wetting and drying shows a slower rate of carbonation as opposed to concrete indoors or undercover. This effect of exposure condition on carbonation is best summarised in figure 2.9.

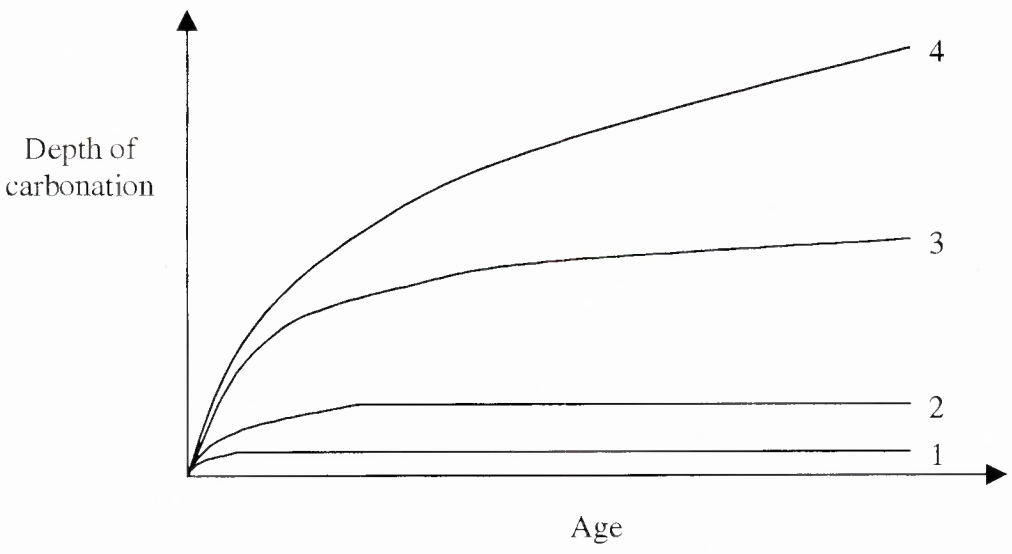

1 Constantly under water or in moist air.
2 Horizontal concrete surfaces outdoors in wet climate.
3 Outdoors in air not protected from rain and snow.
4 Constantly exposed in room air or outdoors protected from rain.

Figure 2.9: Effect of exposure conditions on rate of carbonation [14].

Orientation: of a structure influences the carbonation rates of different faces of the structure, since prevailing winds and rain direction for a particular area dictate different conditions of exposure for the different faces of the structure [14].

Carbon dioxide concentration: The rate of carbonation has been found to increase proportionally with an increase in carbon dioxide concentration [14].

Concrete quality

Water/Cement ratio: Concrete durability is influenced to a large degree by the permeability of the concrete to air and water and it is generally accepted that durability is inversely proportional to permeability. Since the rate of carbonation is dependent on the permeability of the concrete, the rate of carbonation will increase with increasing water/cement ratio. Figure 2.10 shows a typical relationship between water/cement ratio and rate of carbonation [14].

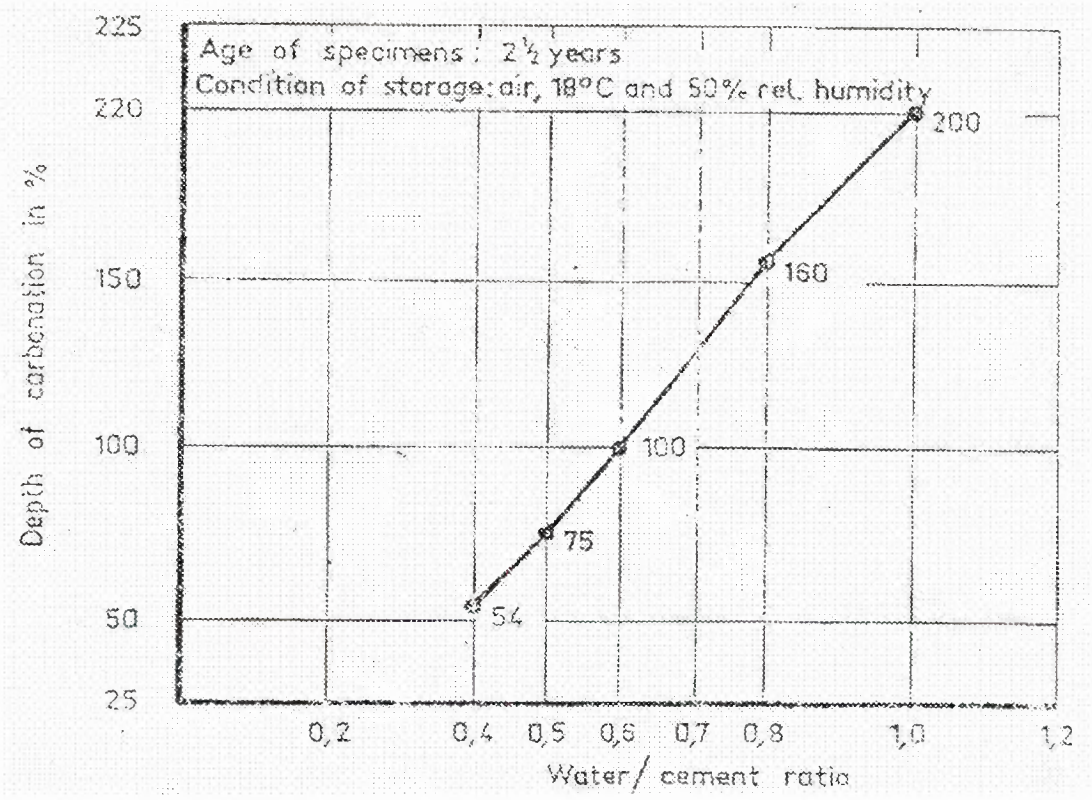

Figure 2.10: Effect of water/cement ratio on the rate of carbonation [14].

Cement content: A lower cement content results in a more porous concrete with higher permeability and therefore increased rate of carbonation. Also, the "carbonatable" content of cement is of importance, as it will affect the rate at which carbonation occurs.

Type of cement: A number of investigations have been carried out by Meyer [14] to determine the effect of different cement types on rate of carbonation. It was found that Portland cements (normal and rapid-hardening), show lower rates of carbonation

under the same conditions than concretes made from Blastfurnace cement and pozzolanic cements. The results of the tests carried out are shown in figure 2.11.

The fact that the resistance of a concrete to carbonation is a function of the type of cement used, is due to the difference in the percentage of hydration products available for carbonation, particularly free calcium hydroxide.

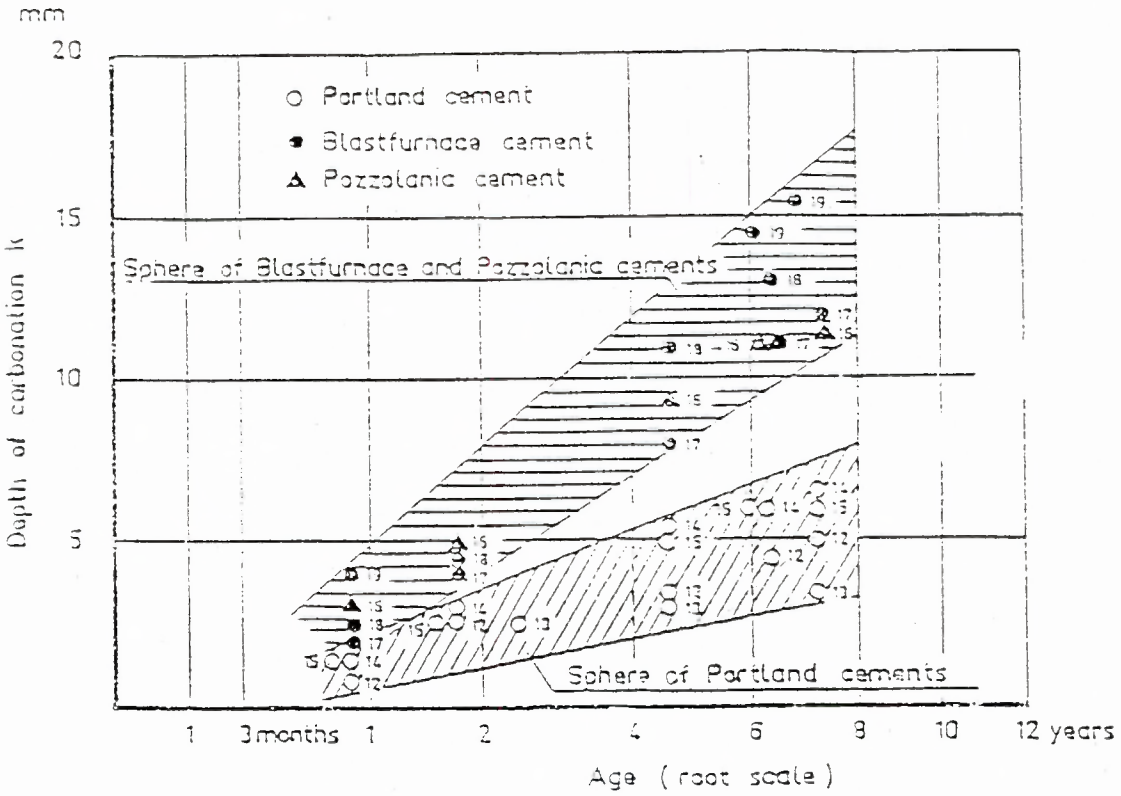

Figure 2.11: Effect of cement type on the rate of carbonation [14].

2.4.2.2 Carbonation depth measurement

Carbonation depth is measured by exposing fresh concrete, and spraying it with phenolphthalein indicator solution (1 % by mass of ethanol/water solution). The phenolphthalein solution will remain clear where the concrete is carbonated and turn pink where concrete is still alkaline (pH > 9.0). Carbonation moves through concrete as a front and reduces the alkalinity of the concrete from a pH of about 12 – 13 to about 8, with a pH level of 10.5 being sufficiently low to depassivate steel. The progress of the carbonation front was shown previously in figure 2.6.

A number of limitations however exist to carbonation testing and are as follows [1]:

- Phenolphthalein changes colour at pH 9, the passive layer of steel however breaks down at pH 10 – 11 and therefore the corrosion risk is slightly underestimated.
- Some concretes are dark in colour and detecting the colour change can be difficult.

- It is also possible for the phenolphthalein to bleach at very high pH levels e.g. after chloride removal or possibly realkalization.
- Testing should be done on freshly exposed concrete surfaces before atmospheric carbonation takes place.

2.5 Problems due to the corrosion of reinforcement

Metallic corrosion in general is a concern because of wastage of metal leading to structural damage such as collapse, perforation of containers and pipes etc. For reinforced concrete, most of the problems occurring due to the corrosion of steel are not due to the loss of the steel but due to the growth of the oxide, which leads to cracking and spalling of the concrete cover [1].

Structural collapses of reinforced concrete structures are rare, however they do occur. Two parking structures in North America are known to have collapsed due to de-icing salt-induced corrosion [1]. A post-tensioned concrete bridge collapsed in Wales due to de-icing salt attack on the strands (Woodward and Williams, 1988), and so did one in Belgium [1], and more recently the Strijdom monument collapse in Pretoria. Concrete damage would however have to be at a very advanced state before a reinforced structure is at risk.

The volume of rust which is produced during the corrosion process is up to seven times the volume of the steel that is dissolved. Since most of the rust is confined within the concrete immediately surrounding the reinforcing steel, its formation produces expansive stresses within the concrete which can lead to cracking of the cover, producing longitudinal cracks, spalling and delamination in concrete. These are schematically shown in figure 2.12.

In reinforced concrete structures, loss of the cross-sectional area of the concrete and reinforcing steel will affect load-bearing capacities of structural members. If the cross-sectional area of the concrete is decreased by spalling and delamination the load carrying capacity of the member is reduced [3]. This problem also occurs in flexural members [15]. Concrete beams are made up of concrete in compression and steel under tensile stress, and therefore when the cross sectional area of the steel is reduced by corrosion the stress in the steel is increased [15]. Eventually this may lead to structural failure.

In the case of prestressed concrete structures, reduction of cross sectional area of steel by pitting occurs due to reinforcement corrosion, eventually resulting in structural failure.

The most common problem caused by corrosion is spalling of concrete cover. A man was killed in New York City by a slab of concrete, which spalled off a bridge substructure due to de-icing salts, and a vehicle was damaged in a similar incident [1]. Spalling of concrete is therefore of concern in building safety.

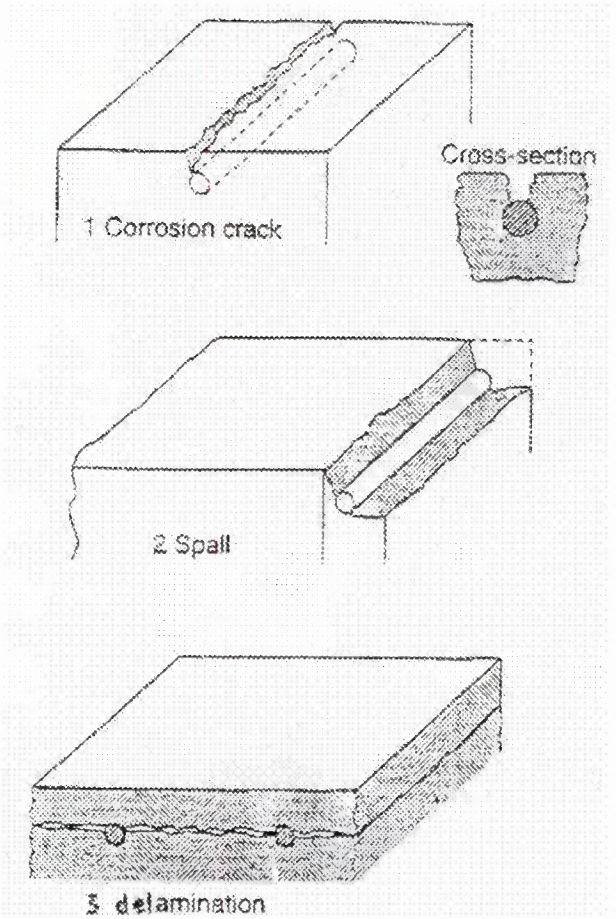

Figure 2.12: Schematic representation of the damage to the concrete cover due to rust formation [2]

2.6 Corrosion monitoring and testing

A number of different methods have been developed to determine corrosion rates and to assist in understanding the processes taking place at the steel reinforcement as a result of corrosion. However, only a few have been recommended for the measurement of corrosion in reinforced concrete structures, the most suitable being measurements using Linear Polarisation Resistance (LPR), half-cell potentials and resistivity measurements.

2.6.1 Half-cell potential measurements

In the case of chloride-induced corrosion, anodic and cathodic areas are formed along the rebar resulting in changes in electro-potential of the steel. The potentials may be measured at different points along the rebar, and data is normally recorded on a plan reflecting the survey grid in the form of a 'potential map'. The rebar potentials are determined in accordance with ASTM C876 using a copper/copper sulphate reference electrode connected to a hand held voltmeter [16]. The qualitative risk of corrosion based on a copper/copper sulphate reference electrode is shown in table 2.2 [16].

Table 2.2: Qualitative risk of chloride-induced corrosion [16]

Rebar potential (- mV $Cu/CuSO_4$)	Qualitative risk of corrosion
< 250	Low
250 - 350	Uncertain
> 350	High

The half-cell is a relatively simple device, made up of a metal in a saturated solution of its own ions (such as copper in copper sulphate, silver in silver chloride etc). In this case the metal is dissolving into the solution but simultaneously ions are precipitating out of the solution, and therefore the system remains in equilibrium. If this half-cell is connected to another metal in a solution of its own ions (e.g. iron in ferrous hydroxide, $Fe(OH)_2$) there will be a potential difference between the two 'half cells'. This situation is however not the same because corrosion in concrete is not an equilibrium process, but rather a dynamic process [2].

By using a standard half-cell that is in a constant state, and moving it along the concrete surface, the probability of corrosion in concrete can be measured. When an external half-cell is connected to the reinforcing steel in concrete the potential observed is the potential difference between the metal in its own solution and the steel in the concrete pore solution. Potentials may vary at different points on the surface of the concrete. This occurs since when steel corrodes, cathodic and anodic regions are formed along the same length of reinforcement i.e. the amount of Fe^{2+} ions varies at different points along the bar due to the presence of anodic and cathodic regions.

These half-cell potentials measure the thermodynamics of the corrosion, not the rate of corrosion. The half-cell potential is a function of the amount of iron dissolving. This is a function of the extent to which steel is depassivated i.e. the extent of carbonation or the presence of sufficient chlorides to break down the passive layer, and the presence of oxygen to sustain the passive layer. Therefore half-cell measurements should only be used to obtain an indication of the corrosion risk of the steel and should be confirmed with corrosion rate measurements. The most commonly used half-cell in corrosion measurements in concrete is the copper/copper sulphate half-cell.

This technique is however not recommended for carbonation-induced corrosion where clearly defined anodic regions are not present [4]. Since this work deals specifically with carbonation-induced corrosion, the method of determining corrosion by half-cell measurements was used only to get an indication of the risk of corrosion in a particular area, and was not used to determine the rate at which corrosion was taking place. It is also important to note that the ASTM C876 was developed for bridges (specifically decks) suffering from chloride ingress (specifically deicing salts), and the criteria in Table 2.2 have not been validated for carbonated structures.

The measurement procedure for a rebar potential survey using a half-cell is as follows [4]:

- Decide on an area of measurement, and mark up a grid pattern.
- Use a cover meter to locate the steel and determine the rebar spacing.

- Make an electrical connection to clean steel either by coring or using already exposed steel.
- Check that the steel is electrically continuous over the survey area using a multimeter.
- Wet the concrete surface that is to be tested with clean water if the concrete appears to be dry (for a reading to be made, charged ions must flow from the steel to the half cell; the concrete must therefore be damp enough for an ionic path; direct contact to the steel must not occur; the current must flow as ions, not electrons).
- Take and record the readings. For manual measurements take two immediately adjacent readings to check that they are within a few millivolts of each other.
- Check data on site to correlate with visual signs of corrosion.

However a number of limitations are associated with rebar potential measurements [4]:

- Interpretation of results must be done by a specialist.
- Rebar potentials from carbonated concrete are difficult to interpret as the reading obtained is a mixed potential of anodic and cathodic sites.
- Delaminations cause disruptions in the potential field giving false readings.
- Potentials are also influenced by environmental effects such as temperature and humidity.
- Rebar potentials cannot be directly correlated with corrosion rates.
- Stray currents may also affect measured potentials.

Corrosion rate measurements and resistivity measurements are usually required to determine whether the potential is an artefact or due to high corrosion rates [1].

2.6.2 Resistivity measurements

Resistivity is defined as the measure of the resistance to current flowing through a particular medium. Corrosion is an electrochemical phenomenon and therefore the electrical resistivity of the concrete will affect the rate at which corrosion is taking place, as an ionic current (electric current in the form of a flow of ions) must pass from the anode to the cathode for corrosion to occur. When reinforcement corrodes, electrons and hydroxyl ions are transferred between the anodic and cathodic regions giving rise to a current flow. The resistivity of concrete is affected by the amount of charged ions present in the pore solution, and therefore resistivity can be used to determine the probability of corrosion in the concrete. The higher the concrete resistivity, the lower the likely current flowing between the anodic and cathodic areas, and therefore the lower the corrosion rate. Resistivity depends on the amount of moisture in the concrete, on the permeability and interconnectivity of the pore system, and on the concentration of ionic species in the pore water [4]. Resistivity is also strongly affected by the quality of the concrete i.e. cement content, w/c ratio, curing and extenders used. Poor quality, saturated concrete has low resistivity (e.g. less than 10 kOhm.cm) and high quality, dry concrete has higher resistivities of greater than 25 kOhm.cm [1].

The carbonated layer is less permeable and stronger than the original concrete due the formation of calcium carbonate. Therefore carbonated concrete has higher resistivity, as it is more resistant to the flow of current and to the ingress of fluids.

2.6.2.1 Measurement procedures

Concrete resistivity is usually measured using the principles of the Wenner Probe. This technique was originally developed for geophysical prospecting, but has been more recently applied to concrete. The Wenner probe consists of four equally spaced probes, which make contact with the concrete surface, as shown in figure 2.13.

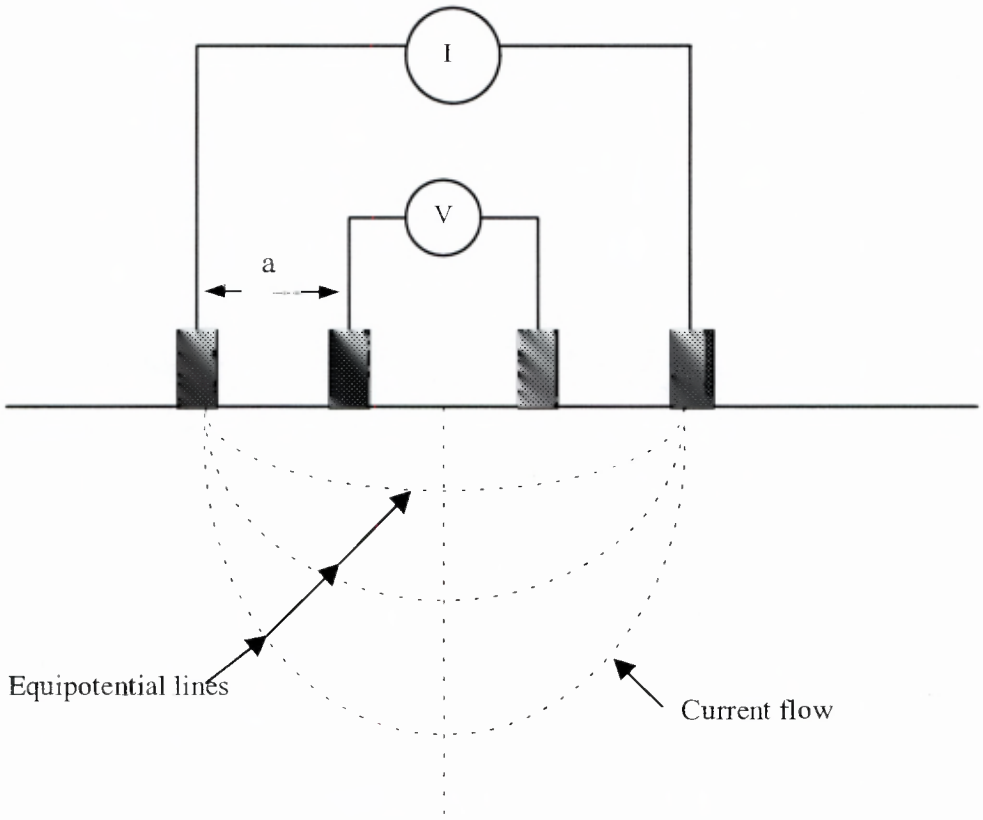

Figure 2.13: Principle of Wenner probe for measuring resistivity [17].

In this method a small alternating current (I) is passed between the two outermost contacts, and the resulting potential difference (V) between the inner two contacts is measured.

The resistivity of the concrete can then be calculated from:

$$\rho = 2\pi a(V/I) \qquad (2.12)$$

where ρ = concrete resistivity
a = the spacing between the probes
V = potential difference measured between the inner probes
I = current passed between the outer probes

It is generally agreed that the four-probe system should have a probe spacing larger than the maximum size of the aggregate used in order to avoid measuring the resistivity of the aggregate rather than that of the paste and the aggregate [17]. Also, readings should not be taken along the length of the steel since it provides a 'short circuit' path for the current during the measurement.

2.6.2.2 Interpretation of resistivity results

Resistivity measurements are useful in identifying problem areas or confirming concerns about poor quality concrete [17]. However by themselves, they are of little use as they do not give sufficient information about the state of the concrete or the extent to which corrosion has taken place. It is because of this that many researchers recommend that resistivity measurements be used alongside corrosion rate and half-cell potential measurements. Relationships between corrosion rate, resistivity and half-cell potentials have been derived and proved to be reasonably accurate in laboratory studies [1,18]. The following interpretation of resistivity measurements from the Wenner four-probe system has been cited, when referring to depassivated steel:

Table 2.3: Relationship of corrosion rate and concrete resistivity [17].

Resistivity of concrete (kΩ.cm)	Corrosion rate
< 5	Very high
5 – 10	High
10 - 20	Low to moderate
> 20	Low

2.6.2.3 Limitations

There are however a number of limitations when using the Wenner Probe technique to determine resistivity of concrete. Errors in resistivity measurements may occur due to the influences of concrete geometry, concrete nonhomogeneity, poor surface contact, surface layers of different resistivity, the presence of steel reinforcement and changes in the ambient environmental conditions [17].

Geometrical constraints

The current and potential fields produced by a Wenner resistivity instrument only give a correct measure of resistivity if they are able to exist in a semi-infinite volume of material, where the dimensions of the concrete are large in comparison to the Wenner electrode spacing (a). However, if the dimensions of the concrete element are relatively small, the current is constricted to flow into a different field pattern to that shown in figure 2.13 resulting in an over-estimation of the resistivity of the concrete. It is therefore recommended that the contact spacing should not exceed a quarter of the concrete section dimensions and the distance of the contacts from the edge of any test element should be twice the contact spacing.

In laboratory samples the relatively small dimensions of the concrete specimens may cause an over-estimation of the resistivity of the concrete. However, for on site monitoring, the dimensions of the concrete are large in comparison to the electrode

spacing of the Wenner probe and therefore accurate resistivity measurements can be obtained.

Concrete inhomogeneity

When using the Wenner resistivity technique it is assumed that the material being tested is homogeneous. However concrete contains aggregate particles with a much higher resistivity than the cement paste. If the contact spacing is small i.e. smaller than the largest aggregate size, the presence of a high-resistivity aggregate particle immediately beneath one of the surface contacts causes a random scatter in the variability of the measurement [17]. It is therefore advised to use a contact probe spacing greater than the largest aggregate size, as increasing the contact spacing causes the current field to penetrate deeper below the surface of the concrete and therefore gives a measure of a large volume of concrete, thereby making the presence of individual aggregates within the electric field less noticeable [17].

Presence of steel reinforcement

Reinforcing steel directly underneath the position of measurement will provide a 'short circuit' path to the current field and therefore give a misleading reading. This error is not however apparent when the measurement position is orthogonal to the reinforcing bar or located away from a parallel bar.

Effect of surface layer of different resistivity

A surface layer beneath the measurement contacts having a resistivity different to that of the underlying concrete has the effect of distorting the applied current field, causing errors in measurement of the resistivity of the underlying concrete [17]. The carbonation of concrete forms a relatively high-resistivity surface layer. Subsequent rainfall will produce a second low-resistivity surface layer on top of the carbonation layer. It has been found that this distortion in the current field caused due to the two surface layers will produce an artificially high resistivity measurement of the underlying concrete [19]. It is therefore recommended that resistivity measurements are not taken on recently wetted concrete surfaces especially where carbonation has taken place.

As carbonation progresses from the surface of the concrete, the products of carbonation block some of the pores in the hardened cement paste causing densification of the concrete and thus increasing the resistivity of the concrete.

Effect of ambient environmental conditions

Resistivity has been found to vary inversely with temperature, and if resistivity measurements are taken when ambient temperatures are abnormally high or low then compensation corrections must be made [17]. Also an increase in resistivity of concrete was observed with an increase in the ambient relative humidity of the air after the occurrence of rainfall indicating the double surface layer effect described earlier. It is therefore recommended that measurements be taken 24 hours after rainfall has occurred [17].

2.6.3 Corrosion rate measurements

Measurement of corrosion rate is probably the best indication of the rate of deterioration of a reinforced concrete structure. There are various techniques of measuring the rate of corrosion, including AC impedance and electrochemical noise. However, Linear Polarisation Resistance (LPR) techniques have been more widely accepted and are being used extensively in materials engineering to measure the rate at which metals corrode. This method involves the measurement of the corrosion rate (I_{CORR}), which gives a direct indication of the rate at which corrosion is taking place in a metal. Calculation of corrosion current using linear polarisation resistance depends on the assumption that the relationship between current and potential of the corroding metal is linear when the potential change is small [20].

The linear polarisation technique involves polarising of the steel with an electric current and monitoring its effect on the half-cell potential [21]. It is carried out with a sophisticated development of the half-cell incorporating an auxiliary electrode and a variable low voltage DC power supply. The half-cell potential is measured and then a small current is passed from the auxiliary electrode to the reinforcement. The polarisation resistance R_P is the change in potential measured divided by the applied current. The corrosion rate I_{CORR} is then obtained from the polarisation resistance R_P by means of the 'Stern Geary' relationship, provided the polarisation resistance R_P is measured at potentials close to the free corrosion potential E_{CORR} [22].

$$I_{CORR} = B/R_P \qquad (2.13)$$

B is a constant, which is measured from an independent experiment where the full polarisation curve needs to be determined. The value of B has been found to be dependent on the material, electrolyte, temperature, time and potential [23]. In concrete it has been determined to have a value between 26 to 52 mV depending on the passivity or active condition of the steel [1,21,23]. A value of 26 mV is used in most commercially available site based corrosion rate meters. The B value of 52 mV is generally used for actively corroding metals in seawater [23]. R_P is the polarisation resistance (in ohms), which is a ratio of the change in potential and applied current. In order for this equation to be valid and remain linear the change in potential must be kept to less than 20 mV, also the 'iR drop' must be eliminated. The 'iR drop' is the voltage that exists because a current is flowing through concrete that has an electrical resistance; this means that the current is usually switched off during the measurement process such that the potential without the iR drop is measured.

Polarisation resistance measurements can be taken in a number of ways as long as the Stern-Geary theory is applicable. LPR measurements are made according to one of two principles: either a fixed current is applied and the potential monitored, or the current caused by a change in potential is measured. By applying these two principles a number of methods can be used to measure the linear polarisation resistance. These methods include:

- **Potentiodynamic:** In this case the potential is controlled and changed such that the current can be measured. This test is started by applying a control voltage to

the working electrode (WE), such that the potential of the working electrode is displaced by 20 to 30 mV more negative than the corrosion potential. From this point onwards the potential is changed at a constant rate of 20 mV per hour until the potential of the working electrode reaches a value 20 – 30 mV more positive than the corrosion potential. The current is measured for the duration of the test [23]. This test however requires complicated electronic equipment to control the potential and the operator is required to have a thorough understanding of the procedure.

- **Galvanodynamic:** In this test the potential is measured as the current is varied at a constant rate in the area where the current-potential relationship is linear [23]. This test is however less widely used [23].

- **Potentiostatic:** In this test the potential of the working electrode is changed in steps and the current is measured when it has settled to a stable value. The polarisation resistance (R_P) is determined by using the change in potential and the measured current. The Stern-Geary equation (equation 2.13) is then used to determine the corrosion current, where the Stern-Geary constant B is taken to be 26 mV [1, 22, 24]. The corrosion rate is then given by:

  $$i_{CORR} = I_{CORR}/A \qquad (2.14)$$

  where A is the area of the working electrode in cm^2.

  For improved accuracy, a series of measurements can be taken, where in each instance the change in potential of the working electrode must be within the linear range. The corrosion rate can then be calculated from a series of points on the current versus potential curve. Each point represents a single measurement, a best-fit line can be constructed through these points, and the slope (R_P) is then determined. This method however requires sophisticated equipment to control the potential.

- **Galvanostatic:** In this test a current is applied to the system and the change in potential is monitored [23]. This test is able to measure very small corrosion rates. The current is applied in steps and the corrosion rate is determined from the potential versus current plot. This method has been found to be the most useful compared to other linear polarisation resistance techniques and will be discussed in detail in the section that follows.

2.6.3.1 Galvanostatic Linear Polarisation Resistance measurements in concrete

In situ linear polarisation resistance measurements in concrete structures are complicated as it is difficult to isolate a fixed area of steel to polarise. The large dimensions of most reinforced concrete structures complicate the uniform application of the electrical signal (polarisation) throughout the reinforcement. For this reason the values obtained are of apparent polarisation resistance R'_P rather than the actual value R_P that should be used in the Stern-Geary relationship [22]. Previous studies have shown the ability to calculate R_P from R'_P, however these calculations require the use of structures with simple geometries e.g. beams and slabs [25, 26]. Researchers have

found that the current spreads or 'fans out' across the area below the electrode where the measurement is being taken; it is therefore difficult to determine the exact polarised area [25, 26].

There are a few site-based corrosion rate measuring devices available, which use the so-called 'guard ring' approach to give more accurate results [26]. A guard ring device is used to contain the electrical signal in a restricted area of the structure for which the corrosion rate can be measured. The Gecor 6 is one such instrument, see section 4.7.2.

Table 2.4 shows the qualitative assessment of site corrosion rates using the galvanostatic linear polarisation resistance technique. The following criteria have been developed from laboratory and field investigations using the Gecor 6 instrument.

Table 2.4 : Qualitative assessment of site corrosion rates [1].

Corrosion rate ($\mu A/cm^2$)	Qualitative assessment of corrosion rate
> 10	High
1.0 - 10	Moderate
0.1 - 1.0	Low
< 0.1	Passive

The corrosion rate is measured over a known area of rebar. This means that the rebar must be located and their sizes known such that the area of the steel below the sensor is known.

There are however two main limitations to the linear polarisation technique [1]:

- They detect the instantaneous corrosion rate, which can change with temperature, relative humidity and other factors.
- They also make assumptions about the area of measurement or they define an area of measurement.

2.7 Summary

In this chapter the electrochemical nature of corrosion, its causes and mechanisms and its damaging effect on reinforced concrete structures have been discussed. It has been seen that the electro-chemical processes are the same regardless of whether the cause is carbonation or chloride attack. Particular attention was however focused on carbonation-induced corrosion, as it is the basis behind this research.

Corrosion measurement techniques were also discussed in detail. Corrosion rate measurements are the most reliable method by which the engineer can estimate the rate of corrosion in reinforced concrete structures. In this chapter the various methods of measuring corrosion rates and the probability of corrosion (half-cell potentials and resistivity measurements) were mentioned.

The use of Linear Polarisation resistance techniques in the measurement of corrosion rates was also discussed and it was concluded that the Galvanostatic method was the most appropriate method of measuring the rate of corrosion of the laboratory test specimens and on site measurement. The Gecor 6 was introduced as the most suitable Galvanostatic method for on-site determination of the polarisation resistance of reinforcement in reinforced concrete structures and for subsequent estimation of corrosion rates using the Stern-Geary equation.

3. REPAIR OF CONCRETE STRUCTURES

Steel reinforced concrete is one of the most widely used construction materials throughout the world. The alkaline environment of the concrete protects the steel from corrosion. However, when the concrete is subjected to chlorides or carbonation or both, the normally passive steel can begin to corrode [1]. In the presence of sufficient oxygen and moisture, rebar corrosion products form, which have a volume up to seven times that of the original steel causing internal stresses within the concrete. Delamination and spalling eventually occur and the integrity of the concrete structure is lost. Corrosion of the reinforcing steel is therefore a major problem, especially in the case of reinforced concrete structures with concrete cover of low quality.

The issue of concrete deterioration is significant both technically and economically. By 1987, over 20 billion US dollars were needed for repair of concrete bridges in the United States, with an estimated increase of about 500 million US dollars per year for additional necessary repair [27]. In most European countries a greater part of the infrastructure (highways, railways, housing etc) in reinforced concrete has already been constructed and has to be maintained or repaired by adequate, cost effective measures [28].

Therefore regarding the enormous cost caused by corrosion-related deterioration of the concrete infrastructure, a cost-effective means of controlling rebar corrosion and extending the service lives of reinforced concrete structures is needed [29].

Many different approaches to concrete repair and protection exist, with varying degrees of cost. These protection systems include the use of epoxy-coated reinforcement, protective coatings and membranes, cathodic protection, low water/cementious ratio concrete, silica fume concrete, desalination/realkalization, and the use of corrosion inhibitors. Within this spectrum of measures, concrete repair and protection with a corrosion inhibitor as a part of a repair/protection strategy can offer cost effective options that may prove valuable in many situations [29].

The use of inhibitors is one of many possible preventive measures that can be adopted in order to supply a supplementary protection to the concrete structure's reinforcement and therefore prolong the service life [30].

In subsequent sections the most commonly available repair techniques for both chloride and carbonation induced corrosion will be discussed, and particular attention will be paid to the use of available corrosion inhibitors, both as a repair technique and a preventive measure. The use of penetrating corrosion inhibitors in combating the problem of carbonation induced corrosion is the main focus of this research, however very little information is available on the use of these penetrating corrosion inhibitors in carbonating environments.

3.1 Repair options

A number of repair options are available. The appropriate repair and rehabilitation system must be chosen for each structure according to its type, conditions, level of

deterioration and future use. The cost effectiveness of the repairs must also be taken into consideration.
There are five commonly used approaches to repairing concrete structures damaged by reinforcement corrosion [1,4]:

- Cathodic protection
- Patch repairs
- Coating systems
- Electrochemical repair techniques
- Corrosion inhibitors

3.2 Cathodic protection

Cathodic protection (CP) has been used for a number of years and is the one method of concrete repair that is also able to stop the corrosion process completely. There are two types of cathodic protection systems that are used in concrete repair:

- Impressed Current Systems
- Sacrificial Anode Systems

In both of these systems the reinforcing steel is connected to a different metal making it an external anode and passing current from this metal to the steel such that all of the steel is made into a cathode. The reinforcement will therefore not corrode. Figure 3.1 shows a schematic diagram of an impressed current cathodic protection system.

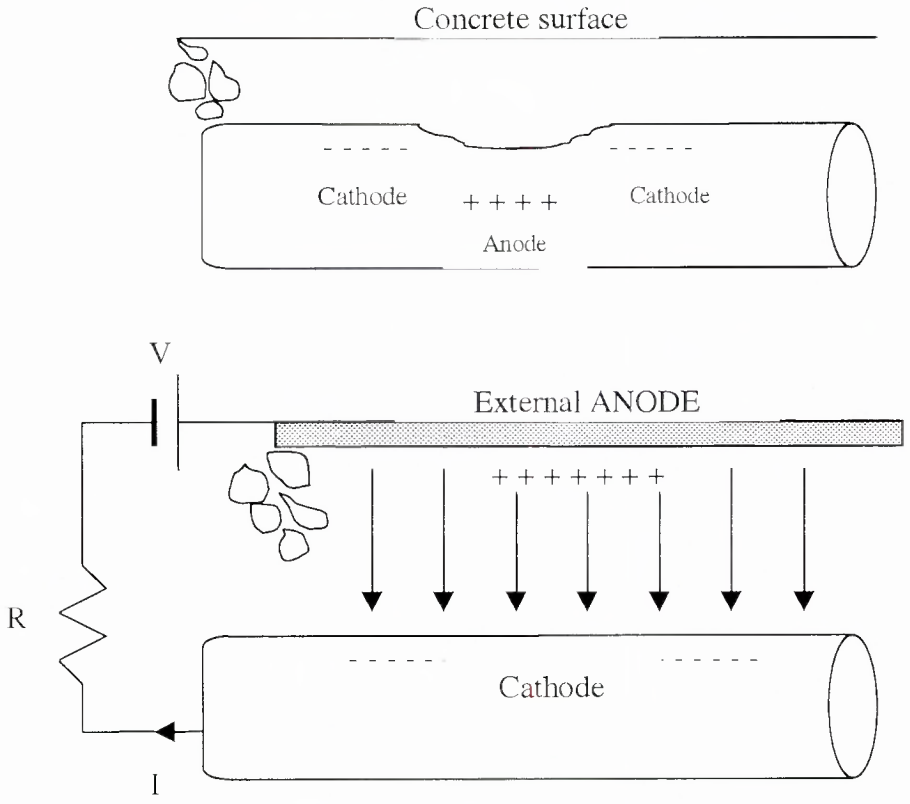

Figure 3.1: Schematic description of an impressed current cathodic protection system.

3.2.1 Impressed Current Systems

The impressed current cathodic protection system works by passing a small direct current (DC) from the external anode into the concrete to the reinforcement. The power supply passes sufficient current from the anode to the reinforcing steel to force the anode reaction to stop and make the cathodic reaction the only one to occur on the surface of the steel, and thereby effectively halts the dissolution of the iron into the pore solution. The cathodic reaction will increase the generation of hydroxyl ions and thus increase the alkalinity of the pore solution and in turn cause the re-formation of the passive ferric oxide layer.

The process of hydrogen embrittlement of steel in concrete must however be considered when using impressed current systems. Hydrogen embrittlement occurs when the potential of the reinforcement becomes too negative [31]. Monoatomic hydrogen diffuses into the steel and gets trapped at grain boundaries or other defects in the crystalline matrix of the steel, weakening it and causing failure under load. It is therefore of great importance that the current applied to the cathodic protection system is monitored and adjusted to prevent this situation.

A number of requirements have to be fulfilled before a cathodic protection system can be installed in a deteriorated concrete structure in order to ensure that the system functions properly. These include ensuring that [4]:

- Electrical continuity of the reinforcement exists in the structure.
- Repair of all delaminated, spalled, damaged and low cover areas has been completed.
- Extra reinforcement is provided where the cross-sectional area of the steel has been reduced by corrosion.
- There is sufficient current flow for the anodic reactions to stop, or severely reduce the corrosion rate.
- Potential of the steel does not exceed the hydrogen evolution potential in order to avoid hydrogen embrittlement.
- Current stays as low as possible to minimise the acidification around the anode.

3.2.2 Sacrificial Anode System (SAS)

In this system the steel is connected to a metal that normally exists at a more negative potential. When the two metals are connected the metal with the lower potential (sacrificial anode) will corrode. This anode corrodes preferentially, liberating electrons with the same effect as in the impressed current system. The most commonly used metals are magnesium, zinc and aluminium. In this system the sacrificial anode corrodes naturally when connected to the steel and therefore the steel becomes the cathode and no further corrosion takes place at the reinforcement. However, the main restriction in this system is that the zinc has only a small driving potential of ~1000 mV when coupled to steel, and for actively corroding steel the potential difference is ~600 mV. The sacrificial anode system is driven by a natural potential difference and the degree of cathodic protection therefore depends on the density of the steel in the concrete and environmental conditions. It has been found that the sacrificial anode system is not as effective in protecting the steel

reinforcement compared to an impressed current system due to the production of very little current [32, 33]. It is however becoming more accepted and is preferred for prestressed concrete as the risk for hydrogen embrittlement is minimised.

Cathodic protection design and repair of concrete structures requires an extensive corrosion survey to be done by a specialist. Once cathodic protection systems are running they are fully controlled and monitored by a series of embedded sensors [4]. This is vital since over- or under-protection of the reinforcing steel is harmful to the structure and the cathodic protection system, and therefore continuous monitoring of cathodic protection systems is usually done remotely by modem [4]. In South Africa the first major cathodic protection system was done at the Simonstown Jetty in 1996 [34]. Previous patch repairs had failed and the concrete had large amounts of chlorides making other repair techniques not cost effective. In this case an impressed cathodic protection system was used and the structure was restored to full serviceability for at least 40 to 50 years [4].

3.3 Patch repairs

In order for effective patch repair, it is important that the distinction between chloride and carbonation-induced corrosion is made. Carbonation-induced corrosion causes a more general type of corrosion with multiple pitting along the reinforcement [4]. Concrete, which has been exposed to carbonation, is usually characterised by high resistivities, which reduce macro-cell formation, therefore resulting in lower corrosion rates. Before patching is done on carbonated concrete, the cracked and spalled concrete must be removed from around the rebar to below the depth of the carbonation front. The cementitious patch material is then chosen to ensure that the steel is restored to a high pH, alkaline environment. This will therefore encourage the reformation of the passive layer to stop further corrosion.

In the case of chloride induced corrosion, pitting corrosion occurs with the formation of distinct anodic and cathodic sites. The high concentration of salts in the concrete cover indicates that macro-cell corrosion is possible with large cathodic areas driving localised intense anodes. High corrosion rates occur causing severe pitting of the reinforcement and damage to surrounding concrete [4]. If patching is required due to chloride corrosion then the usual specification is to remove concrete to about 25 mm behind the rebar ensuring that all the corroded steel is exposed and the rebar is cleaned thoroughly to remove all rust and chlorides. The cut edges and faces of the concrete must be square and clean of all dust and debris. Mechanical removal of concrete can be done using pneumatic hammers, hydro jetting or milling machines. Complete removal of chloride-contaminated concrete, where it is possible, should successfully halt corrosion by restoring passivating conditions to the steel reinforcement [4]. This form of repair is most successful when treating areas of localised low cover, before significant chloride penetration has occurred. Once chloride damage is severe it is expensive to mechanically remove chloride-contaminated concrete from depths well beyond the reinforcement [4].

Patch repairs are therefore made up of the following steps [4]:

- Removal of the delaminated and cracked concrete thereby fully exposing the corroding steel reinforcement.

- Cleaning of the corroded steel reinforcement by hydro jetting, grit blasting etc.
- Applying a protective coating on the steel surface e.g. zinc rich primer coat, anti-corrosion coating.
- Application of a repair mortar in order to replace the damaged/removed concrete.
- Application of coating or sealant to the concrete surface in order to reduce moisture contents in the concrete.

Localised patch repairs of areas that are damaged by corrosion are popular especially due to the low cost and aesthetic relief. Many patch materials are available on the market. The prebagged materials are most likely to be applied properly, especially to small repair areas, but they are more expensive than conventional cement/aggregate/water mixes [1]. Prebagged materials are generally proprietary mixes with good shrinkage compensation, minimising the risk of shrinkage cracks in and around the repair. Patch repairs are more effective in carbonation-induced corrosion than in chloride corrosion. Their limited success in chloride-induced corrosion is because the surrounding concrete is still chloride-contaminated and the reinforcement is therefore still susceptible to corrosion.

3.3.1 Incipient Anodes

Patch repairs are not usually adequate to stop further deterioration in the presence of chloride attack, as the surrounding concrete may be chloride-contaminated and therefore still susceptible to corrosion. When a structure with extensive chloride attack is patch repaired, patching the corroding areas can accelerate corrosion elsewhere, in as little as two years [1]. When the anodic reaction is stopped the generation of hydroxyl ions at the cathode is also stopped. Therefore the areas that are now protected from corrosion since they were made cathodic by the repaired anode will rise above the critical chloride/hydroxyl ratio and corrosion will once again be initiated usually around the new patch, shown in figure 3.2.

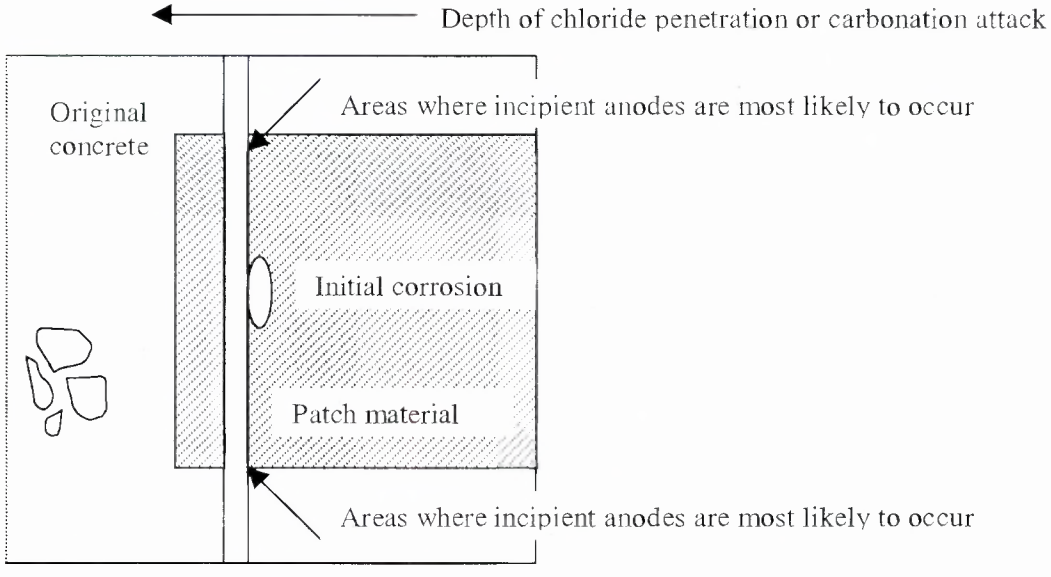

Figure 3.2: Formation of incipient anodes after patch repair [4].

'Incipient anodes' are therefore anodic areas which are formed alongside localised areas that were passivated by the patch repairs. The new corrosion sites not only affect the concrete structure but also undermine the repair leading to accelerated patch failures in as early as two years [4]. This 'incipient anode' problem can be avoided by removal of all chloride-contaminated concrete in the area around the reinforcement, thereby restoring passive conditions to the reinforcement. This problem can also be avoided by applying an electrochemical rehabilitation technique.

Patch repairs are therefore most successful when treating areas of low cover, before significant chloride penetration has occurred [4]. In many instances however patch repair is carried out once corrosion damage is severe and is thus not economically viable due to high costs induced by mechanical removal of contaminated concrete from depths well beyond the reinforcing steel.

3.4 Coating systems, sealers and membranes

Coatings are beneficial in excluding undesirable species such as chlorides and carbon dioxide, or cosmetically restoring the appearance of concrete after repair. A huge range of coatings and penetrant systems is available for concrete, with differing functions. They provide protection by eliminating or slowing down the penetration of chlorides and carbonation, or by reducing moisture movement into the concrete to keep it dry and slow the propagation of corrosion reactions. Sealers and membranes can be classified into several different types. Each type represents a family of materials with different chemical composition.

3.4.1 Coatings and sealers

These are mainly used for the purposes of waterproofing and protecting concrete from chemical attack, and consist of a continuous film applied on the concrete surface. This continuous film is made of a binder and fillers e.g. pigments, plasticizers, catalysts, fungicides etc. The performance of the film is very sensitive to the compounding of the fillers. Therefore compositions having a similar binder may be different in their performance. The coating or sealer is usually obtained in liquid form, which is either brushed or sprayed on the concrete surface to be treated. The curing by which it converts into a film, can be based on a number of mechanisms:

- Evaporation of a solvent (i.e. organic diluting liquid) or dispersant (water).
- Chemical reaction with a catalyst that is part of the formulation
- Reaction with moisture in the atmosphere or in the concrete substrate, or
- Reaction with oxygen in the atmosphere.

These materials provide a film that is stable in the alkaline environment of the concrete.

Figure 3.3 demonstrates the manner in which coatings or sealers seal the concrete surface.

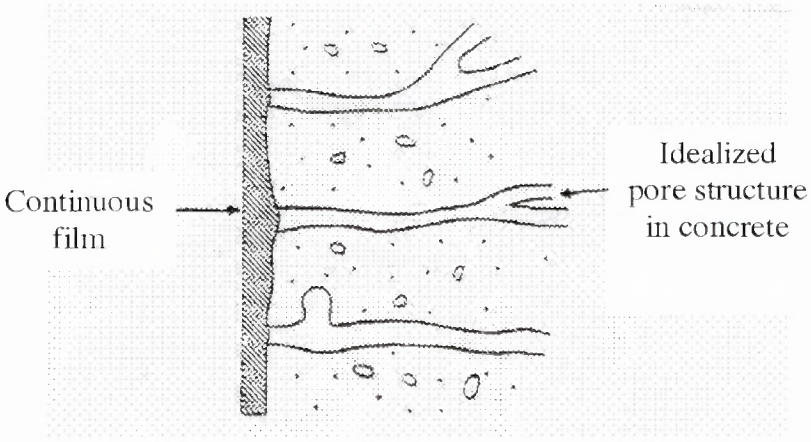

Figure 3.3: Schematic sketch of coatings and sealers [3].

3.4.2 Pore liners

Pore liners are surface treatments, which contain hydrophobic agents that line the surface of the pores in the concrete, thus reducing the surface energy, to make the concrete water repellent (i.e. non-wetting). Hydrophobic agents are mostly organic-siliceous compounds, and their hydrophobic properties are effective for at least ten years [35]. The different types of organic-siliceous compounds are:

- Siliconates
- Silicone resins
- Silanes
- Siloxanes

Silicone resin can be dissolved in an organic liquid, which after evaporation deposits a film of the resin on the pore surface. Alternatively, the resin can be formulated in such a way that it reacts with the pore water to form the water-repellent lining. Silanes also have been developed for this purpose, differing in their molecular weight. Those which polymerise in-situ to longer polymeric chains, have the advantage of being less volatile and therefore can offer longer service life. Figure 3.4 shows the general behaviour of pore liners.

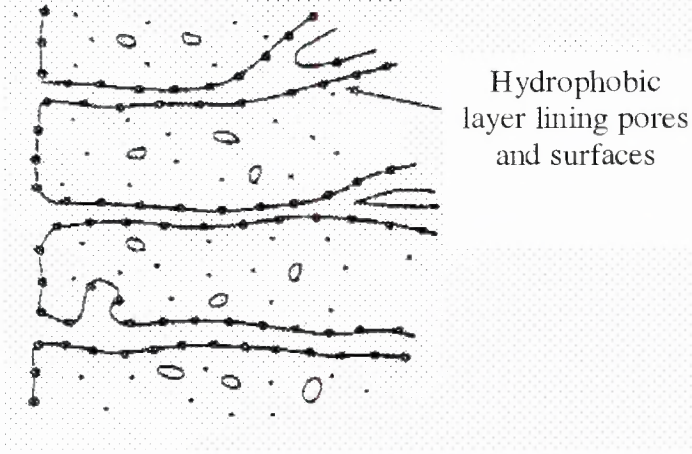

Figure 3.4: Schematic sketch of pore liners [3]

3.4.3 Pore blockers

This treatment is based on materials that penetrate into the pores and react with the concrete constituents. The resulting products are insoluble and are deposited in the pores blocking them. Figure 3.5 shows the basic principle behind pore blocking treatments.

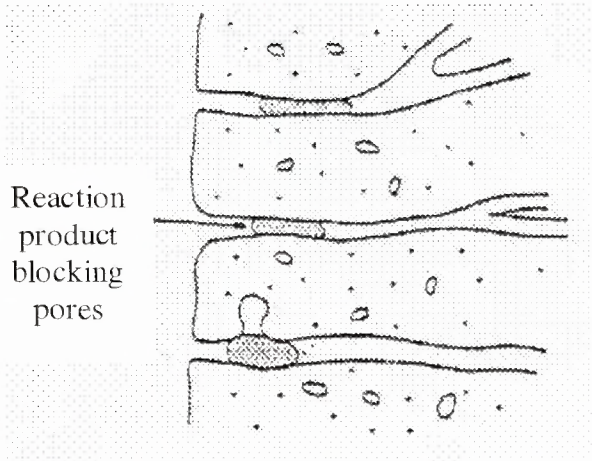

Figure 3.5: Schematic sketch of pore blockers.

The most common materials used for this purpose are liquid silicates and liquid silicofluorides. They react with $Ca(OH)_2$ to form CSH or calcium silicofluorides.

3.5 Electrochemical repair techniques

Two electrochemical repair techniques are available, electrochemical chloride extraction (ECE), and realkalization. These repair techniques restore passivating conditions by the temporary application of a strong electric field to the cover region.

3.5.1 Electrochemical Chloride Extraction (ECE)

Electrochemical Chloride Extraction (ECE) is used in marine or chloride environments. The aim of this method is the non-destructive extraction of chlorides from the concrete. A direct current is applied between the reinforcement and an external anode. The external anode mesh is placed on the surface of the concrete and is immersed in sodium or lithium-based hydroxide electrolyte. When this impressed current is passed between the anode and the reinforcement an electric field is created in the concrete, the reinforcement becomes negatively charged and therefore repels the Cl^- ions. The chloride ions are now attracted to the external anode and move towards the surface of the concrete thereby restoring passive conditions in the reinforcement. This is illustrated in figure 3.6.

Electrochemical chloride extraction takes about 4 to 12 weeks to run at current densities within the normal range of 1 to 2 A/m^2 [33]. Experimental work carried out in laboratories shows that complete extraction could take as long as eight weeks or more at current densities of 1 A/m^2 [33]. In some cases the chlorides beyond the

reinforcement are forced deeper into the concrete during the ECE process and therefore there is a risk that chlorides left in the concrete may diffuse back to the reinforcing steel leading to corrosion with time [4].

The success of this method however depends on a number of factors [4]:

- Repair of all major cracking, defects and delaminations.
- Variations in reinforcement cover cause differential chloride extraction and therefore short-circuiting.
- Susceptibility to alkali silica reaction (ASR); as negatively charged ions move towards the anode, OH^- ions are produced on the steel surface. These OH^- ions at the cathode increase the pH of the concrete pore solution. Positively charged ions, e.g. Na^+ that are present in the electrolyte, also migrate into the concrete increasing the risk of ASR. This combination of increased metal alkali content and increased concentration of OH^- ions at the surface of the steel increases the susceptibility of the concrete to alkali silica reaction.
- Hydrogen embrittlement may occur in prestressed concrete structures.
- Temporary power supplies of sufficient capacity are needed during application of ECE.

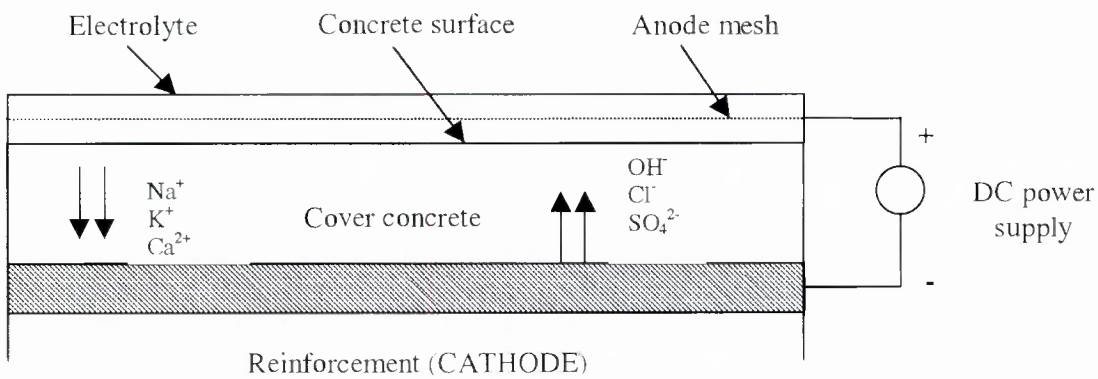

Figure 3.6: Electrochemical Chloride Extraction in concrete.

3.5.2 Realkalization

Realkalisation is used for carbonated concrete. This is the process whereby the original alkalinity of carbonated concrete is restored. This method involves placing an anode system and sodium carbonate electrolyte on the concrete surface and applying a high current density [4]. The electric field that is formed generates hydroxyl ions at the reinforcement and draws alkali metal ions into the concrete, thereby restoring alkaline conditions in the concrete [4].

3.6 Corrosion inhibitors

There are a number of definitions of a corrosion inhibitor. The definition is of great importance because many things can "inhibit" corrosion, such as coatings, cathodic protection etc. A suitable definition is provided in ISO 8044 1989: "A chemical substance that decreases the corrosion rate when present in the corrosion system at suitable concentration, without significantly changing the concentration of any other corrosion agent" [36].

The principle of most inhibitors is to develop a very thin chemical layer, usually one or two molecules thick, on the steel surface, that inhibits the corrosion attack by either forming a protective film on the substrate to be protected, or by immobilising the corrosive species and preventing them from reaching the steel. Inhibitors can prevent the cathodic reaction, the anodic reaction or both. They are consumed in the cathodic and anodic reactions, and will generally only be effective up to a given level of attack (e.g. limiting chloride content). The concern with inhibitors is that they will suppress the generalised corrosion, but if the amount available is inadequate due to low dosage or consumption, there could be localised pitting attack [37].

A corrosion inhibitor is also defined as a liquid or powder that effectively reduces the corrosion rate of steel [37]. From early usage on gas pipelines in the 1940s, specific applications for inhibitors have been developed for many industries, especially in water treatment, packaging, petroleum refining and numerous other chemical processes [37]. Inhibitors are also used in everyday items such as vehicle cooling systems and central heating systems. Their use to control the corrosion of steel reinforcement in concrete was first investigated in the late 1960s with the first commercial applications arriving a decade later [37].

In the case of steel in concrete, corrosion-inhibiting chemicals are either mixed in to the fresh concrete or travel through the hardened concrete to react on the reinforcing steel surface to slow down the rate of corrosion [1]. This difference is fundamental and will be discussed in a later section. Corrosion inhibitors can be used on buildings (frames, cladding panels, balconies, fair-faced and exposed aggregate facades), bridges, car parks, tunnels, tanks and marine structures, indeed anywhere reinforced concrete needs protection. It should however be recognised from the outset that corrosion inhibitors are not miracle cures that totally stop corrosion. They 'buy time' by increasing the time to the onset of corrosion and then by reducing the rate of eventual corrosion [37].

Figure 3.7 shows a schematic of the corrosion damage versus time relationship in concrete before application of a corrosion inhibitor.

The purpose of introducing an inhibitor into concrete is to extend the service life of a concrete structure by reducing the rate of corrosion of the steel reinforcement. This intended function of corrosion inhibitors is shown in figure 3.8.

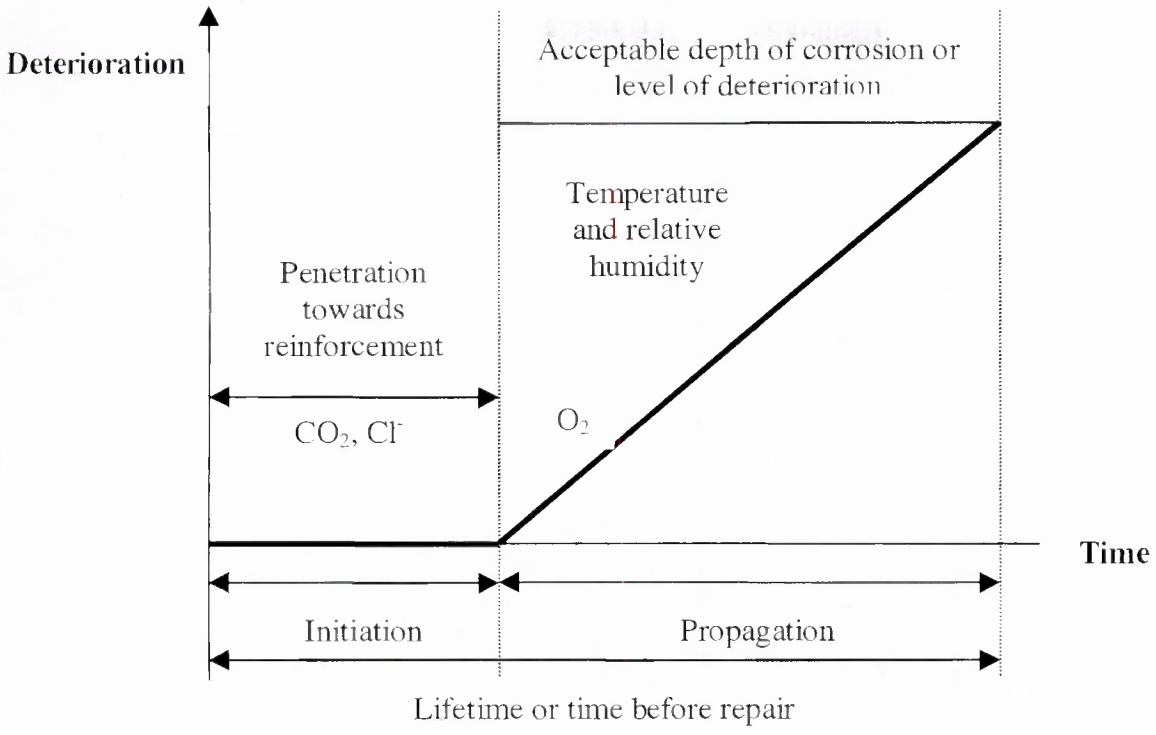

Figure 3.7: Schematic of progress of steel corrosion in concrete [38]

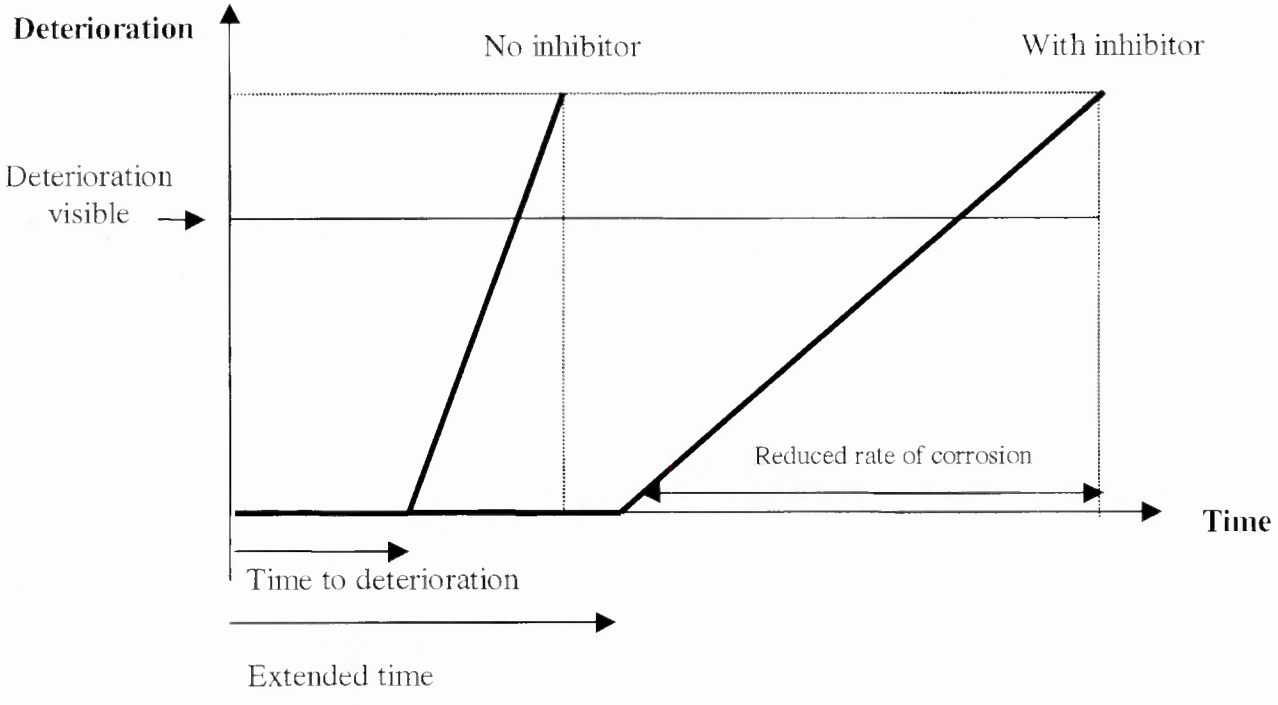

Figure 3.8: Extension of the service life of a concrete structure with corrosion inhibitor [38]

3.6.1 Classification of corrosion inhibitors

Inhibitors can be classified according to:

- Their action.
- Their chemistry and function.

3.6.1.1 Classification by action

Corrosion inhibitors are used to prevent or delay corrosion of metals exposed to aggressive environments, and can be classified according to the type of protection they impart to the reinforcement.

The three main types of inhibitors are as follows:

- Anodic inhibitors.
- Cathodic inhibitors.
- Multi-functional or mixed inhibitors.

Anodic inhibitors

Anodic inhibitors reduce the rate of reaction at the anode by accepting electrons. They usually react with the corrosion products to form a protective coating on the metal surface [1]. The most commonly used anodic corrosion inhibitor has been calcium nitrite [38]. However, sodium nitrite, sodium benzoate and sodium chromate have also been used. In the case of chloride attack, the nitrite ions in the inhibitor compete with the chloride ions for the ferrous ions at the anode, and this reaction forms a stable passive layer on the reinforcing steel, thereby reducing the rate of corrosion.

Cathodic inhibitors

Cathodic inhibitors act to prevent the reaction at the cathode. Cathodic inhibitors adsorb on the steel surface and act as a barrier to the reduction of oxygen i.e. they reduce the oxygen transport to the steel surface which is the primary cathodic reaction for steel in concrete [39]. These cathodic inhibitors increase the pH of the medium and thereby decrease the solubility of the ferrous ions. The main types of cathodic inhibitors are based on sodium hydroxide and sodium carbonate [38].

Multi-functional or mixed inhibitors

Mixed inhibitors influence both the anodic and cathodic regions. They contain molecules in which electron density distribution causes the inhibitor to be attracted to both the anode and the cathode [38]. Amino alcohol based inhibitors are typically mixed inhibitors, since they give both cathodic and anodic protection. They form an adsorptive film, which strongly adsorbs to the metal surface and interferes with the anodic and cathodic reactions in the area of adsorption. Also typical of such products is a commercial product called Ferrogard (manufactured by Sika), a multi-functional inhibitor based on an organic and inorganic, film forming, blended amino compound that allows the inhibitor to diffuse through the concrete as a vapour as well as a liquid [37].

3.6.1.2 Classification by chemistry and function

In this case, inhibitors can be described in different ways:

- Inorganic inhibitors – these usually consist of nitrites, phosphates and other inorganic chemicals; a typical example is calcium nitrite.
- Organic inhibitors - these inhibitors are a combination of amines and other organic chemicals in a water medium.
- Vapour phase or volatile inhibitors – a subgroup of the organic inhibitors (generally amino alcohols) that have a high vapour pressure.

All these inhibitors have been used widely by corrosion engineers in order to protect reinforcing steel. In some cases, their chemistry is well understood, and in other cases less so.

When used in concrete repair, inhibitors must be capable of penetrating the concrete cover to the steel reinforcement, and therefore the means of introducing them and ensuring that appropriate concentrations are maintained at the steel surface to yield the required reduction in corrosion rate is of importance. Suitable methods that have been developed will be considered in the following sections in relation to several techniques of restoration that depend on different types of corrosion inhibitor.

3.7 Corrosion inhibitors admixed into fresh concrete

There are two main types of inhibitors specifically for protecting reinforced concrete; those which are mixed into fresh concrete as an admixture; and those which are applied to the surface of the hardened concrete as a migrating or penetrating corrosion inhibitor.

The most widely applied admixed corrosion inhibitor is calcium nitrite. There are also other materials available, generally organic inhibitors with active amine and ester groups. The problem however is that many of these organic and inorganic inhibitors act as set retarders. Admixing allows a uniform distribution of the inhibitor throughout the concrete and in high performance concretes the low permeability of the cover layer helps prevent the inhibitor from being lost by evaporation [39]. However, the main problem to overcome is preventing any effects on the fresh and hardened properties of the concrete.

Sodium nitrite is identified as a good inhibitor but it results in strength loss in the concrete. Calcium nitrite also acts as a set accelerator and therefore care must be taken that "flash setting" does not occur.

3.7.1 Calcium nitrite

Calcium nitrite has been successfully employed in the USA since 1978 as a corrosion-inhibiting admixture in a number of parking, marine and highway structures.

Calcium nitrite is an anodic inhibitor. The mechanism by which it inhibits the corrosion process is by preventing the continuation of the corrosion reaction by reacting with the ferrous ions, Fe^{2+}, in regions where the passive oxide layer has been disrupted by the presence of chloride ions or carbonation. The nitrites that are present react with the ferrous ions and hydroxyl ions to form the more stable ferric oxide layer.

$$2Fe^{2+} + 2OH^- + 2NO_2^- \rightarrow 2NO + Fe_2O_3 + H_2O \quad (3.1)$$

In the case of corrosion due to chloride attack the chloride and nitrite ions compete at flaws in the passivation film for the same ferrous ion and therefore the concentrations of the chloride and nitrite ions will determine the type of reaction that will take place. When insufficient nitrite is present, and the chloride concentration is larger than a threshold value, corrosion will take place. Thus nitrite is an anodic inhibitor, and it acts to raise the threshold level in the case of chloride-induced corrosion, or to increase time to the onset of carbonation-induced corrosion.

3.7.1.1 Effectiveness of calcium nitrite as an inhibitor

Calcium nitrite is one of the most commonly used inhibitors. It has been stated that calcium nitrite reduces corrosion without affecting the properties of concrete. However, researchers have found that calcium nitrite decreases the compressive strength of concrete, causes other effects such as efflorescence, and increases its susceptibility to alkali-aggregate reaction [40]. Damage to concrete induced by calcium nitrite has also been reported by Hope et al. [41]. This observation was based on experiments carried out on concrete cylinders, each with a centrally placed length of reinforcement, containing admixed chloride, which were soaked in a saturated calcium nitrite solution. Severe deterioration occurred in the case where the specimens were soaked after two weeks of curing, and no deterioration was detected when the specimen was cured for two months prior to soaking.

Calcium nitrite also behaves as a set accelerator and therefore care must be taken that "flash setting" does not take place. Adequate air entrainment is recommended for concrete mixes which include calcium nitrite, as there is some concern about freeze thaw resistance.

3.7.1.2 Laboratory testing and field use of calcium nitrite

The South Dakota Department of Transportation carried out an extensive study on the effectiveness of calcium nitrite as a corrosion inhibitor, in which reinforcing bars were embedded in concrete cylinders with and without admixed chlorides [42]. The cylinders containing the admixed chlorides underwent corrosion almost immediately (1 day) whereas the samples containing calcium nitrite remained passive for 700 days. Calcium nitrite was also found to improve the corrosion resistance of samples without the admixed chlorides. Chloride analyses at the reinforcing bar showed that calcium nitrite prevented corrosion at chloride-to-nitrite ratios of 1.6 to 2.2 at chloride levels in excess of 5.3% (by weight of cement) [43].

Though most work with calcium nitrite has considered the protection against chloride ions, work done by Andrade et al [44,45,46] shows that it also protects steel in carbonated concrete.

The commercial use of calcium nitrite as a corrosion inhibitor started as early as 1978 with applications on bridge decks in the United States. These older bridge decks in Illinois, New Hampshire, and Maine contain calcium nitrite. Several were recently cored and the results show that the nitrite is still present in original quantities and corrosion measurements indicate complete passivity [42].

In a series of investigations carried out as part of the Strategic Highway Research Programme (SHRP) in the USA, calcium nitrite was found to be more effective than several other proposed corrosion inhibitors, as a treatment for small reinforced concrete specimens, which had been precorroded in a saline environment. This was supposed to simulate the effects of de-icing salt applied to a bridge deck [48]. Recent work at Aston University found that, when calcium nitrite was used on moderately precorroded reinforced concrete specimens by means of repeated ponding with an aqueous solution of a specified strength, followed by application of an overlay containing a recommended dosage of the inhibitor, there were significant reductions in the overall corrosion rates of bars embedded at depths of 12 mm. However, provided that the initial chloride content was relatively low, for non-carbonated concrete or very low for carbonated concrete [48, 49].

Many other concrete structures have also used calcium nitrite where steel corrosion is a threat and all signs point to confidence in calcium nitrite's performance.

A commercially available concrete repair system of this sort based on calcium nitrite has been introduced in the USA [50, 51]. In Japan, systems based on lithium nitrite have also been used, which are claimed to reduce both reinforcing-steel corrosion and ASR [52].

3.7.2 Organic admixed corrosion inhibitors

A number of proprietary organic inhibitors for use in fresh concrete have been introduced, including various amines, alkanolamines, their salts with organic and inorganic acids and emulsified esters, alcohols and amines [1]. Tests conducted to determine the inhibition mechanism of amines and amino alcohol based inhibitors found a surface layer made up of amino alcohols and associated radicals on the surface of the steel reinforcement. Also, these inhibitors were able to displace chloride ions from the steel surface and form an inhibitive film around the reinforcement thus protecting it from corrosion [53]. There is rather limited information in the literature about the detailed compositions of these products and it is therefore difficult to evaluate claims and counterclaims regarding their supposed mechanism of action and effectiveness in different applications. Also these newer inhibitors have yet to establish a record of long-term performance comparable with that of calcium nitrite [1].

A test programme into the effects of amino alcohol based admixed inhibitors on the properties of fresh and hardened concrete was conducted by Mott MacDonald, Special

Services Division, and the results showed that at recommended levels of addition the inhibitor does not significantly affect the following factors [53]:

Fresh concrete:
- Water content (slight plasticising effect)
- Air entrainment
- Setting time (slight retarding effect)

Hardened concrete:
- Compressive strength
- Pull-out strength
- Porosity
- Permeability
- Freeze/thaw resistance
- Shrinkage (up to 28 days)

Researchers have also shown that the inhibitive film formed around the steel cannot be easily removed by rinsing the steel with water, thus indicating that the dilution of the inhibitor is unlikely [3].

3.8 Penetrating or migrating corrosion inhibitors for hardened concrete

Vapour phase inhibitors or penetrating corrosion inhibitors have been used to impregnate packaging, greases and waxes for many years to protect steel machinery and components [1]. In the 1980s it was realised that they might be effective in penetrating through concrete pores and protecting the reinforcing steel. Several companies now offer proprietary formulations, which are again amine- and ester-based, with amino alcohols as the main volatile component [1].

Tests carried out on the ability of these surface applied amine and alkanolamine-based inhibitors to control the rate of corrosion of steel in concrete or mortar which has been subjected to prior contamination with chloride salts or carbonation have been reported in the USA and Europe [47]. The American research supported by the SHRP [54] initiative showed positive results when the inhibitor was applied, by a) ponding to small-scale laboratory specimens and b) by alternate spraying and drying to large-scale sections of a bridge deck.

Figure 3.9 shows the corrosion process with and without the inhibitor.

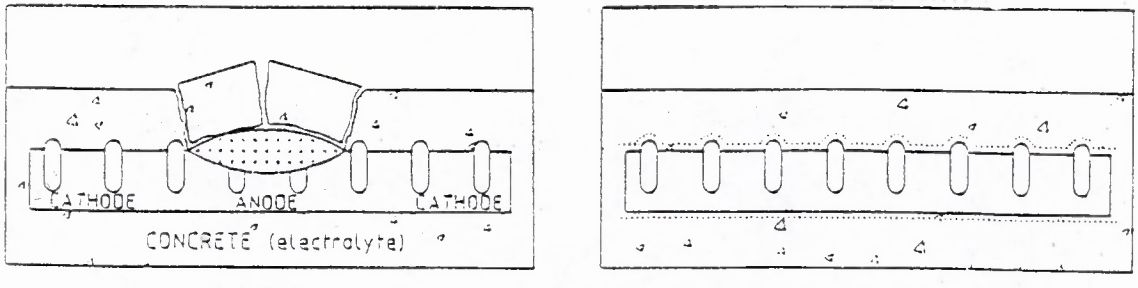

Unprotected reinforcing steel

Reinforcing steel protected by corrosion Inhibitor

Figure 3.9: Schematic sketch of corrosion process with and without inhibitor

3.8.1 Organic penetrating corrosion inhibitors

These new corrosion inhibitors are considered to be a class of inhibitor that contain organic amines, amino-alcohols, fatty acids or a combination of these [55]. These corrosion inhibitors are available in the market as surface applied penetrating corrosion inhibitors. Due to the relatively new nature of these corrosion inhibitors their long-term performance is not well documented.

These inhibitors are able to diffuse considerable distances through concrete both in the pore solution phase and, because of their relatively high vapour pressures, through the gaseous phase of the material when exposed to unsaturated environments [56,57]. They penetrate to the steel surface developing a multi-molecular layer on the steel. In principle their ability to diffuse as a vapour gives them an advantage over liquid inhibitors. However they can also diffuse out of the concrete unless trapped in place [58]. Penetrating corrosion inhibitors diffuse poorly through saturated concrete but once the inhibitor has formed the multi-molecular layer on the steel surface, it is very durable and lasting [58]. However, it is acknowledged that these inhibitors will not work under all corrosion conditions and an upper limit with respect to the chloride content of the concrete is often specified [58].

The effectiveness of this class of compound has been shown by means of various experiments and in large-scale tests using a mixed inhibitor based on amino-alcohol with anodic and cathodic effects on steel [59]. These tests reported that this type of corrosion inhibitor has no negative effects on the setting time of the cement and on the fresh and hardened concrete properties [60].

Site surveys and experimental test results have also shown that the inhibitor can penetrate through concrete at a rate of between 2.5 to 20 mm per day and to a depth of at least 80 mm in 28 days, depending on the quality of concrete [60]. Tests carried out as part of the SHRP reported that penetrating corrosion inhibitors penetrated from the repair material through to the subsequent layer of steel reinforcement [54].

Laboratory testing done to determine the concentration of the inhibitor at different depths of the concrete are shown in figure 3.10 [53], in terms of the atomic concentration ratio of nitrogen to silicon versus depth of penetration. Since no other nitrogen component is present, the ratio was used to express the amount of amino alcohol in the samples. Calibration results were used to correct the intensity ratios into absolute mass concentrations. The nitrogen to silicon ratio was also used as an additional indicator for the presence of an organic additive.

Depth profiles presented in figure 3.10 show that a concentrated band of the inhibitor passes through the cover concrete over a period of days, allowing the penetration of the inhibitor to embedded steel surfaces irrespective of the orientation of the application [53]. It was also found that the inhibitor reached a transport rate of 7 mm/day, averaging around 2.5 mm/day with the rate of transportation declining as the depth of penetration increased [53]. The rate of penetration is however dependent on the grade and hence the porosity and permeability of the concrete.

Brundle and Grunze [60] carried out laboratory tests using X-Ray Photon Spectrometry (XPS) and Secondary Ion Mass Spectrometry (SIMS) surface analysing techniques. After establishing the accuracy and usefulness of using XPS and SIMS to detect the presence of amino-alcohols, these two techniques were used to provide semi-quantitative information on the coverage and thickness of amino-alcohol corrosion inhibitors on steel samples exposed to solutions of high pH and varying concentrations of saline solution. This was used to show the effectiveness of the inhibitors in forming continuous protective films in contaminated environments [59].

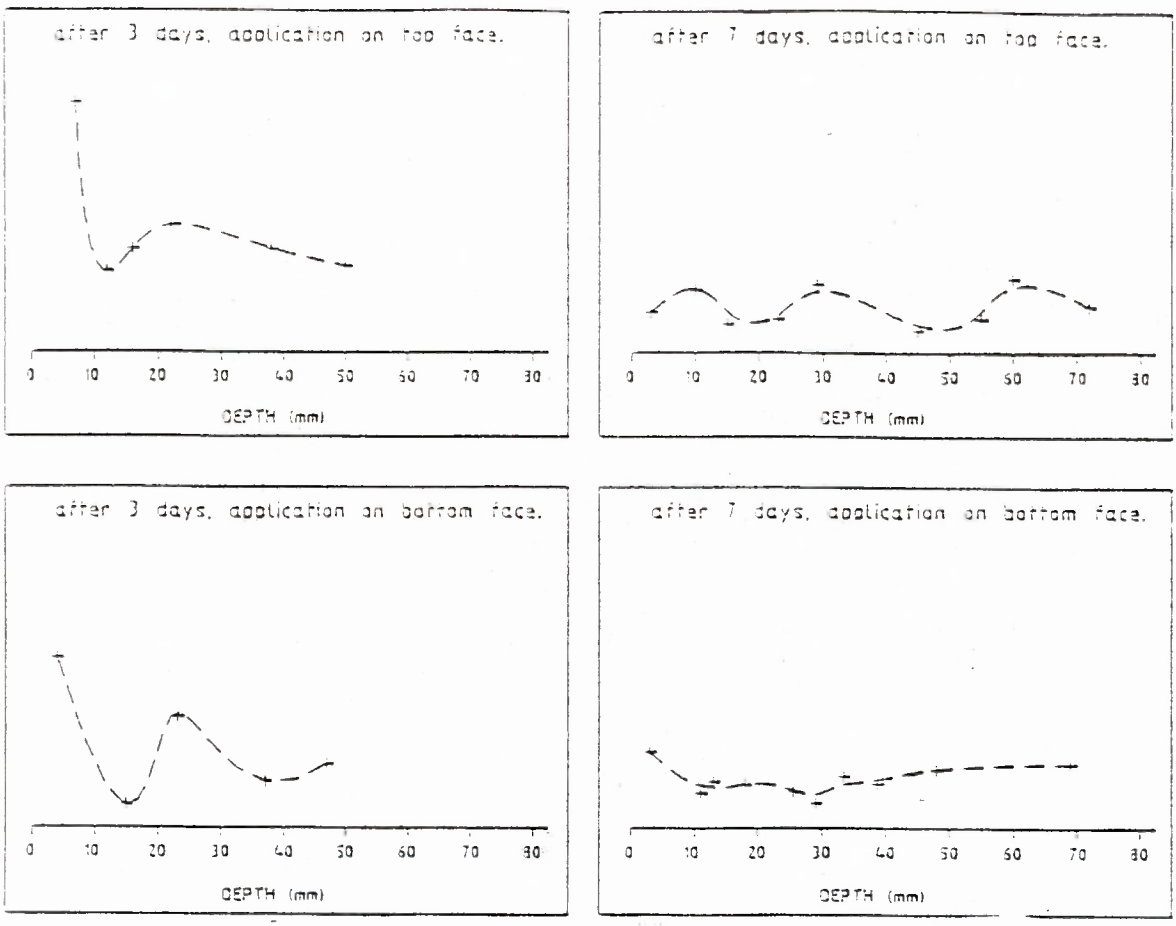

Figure 3.10: Transport studies of penetrating organic corrosion inhibitor in concrete blocks expressed as atomic concentration ratio of nitrogen to silicon versus depth of penetration [53].

Figure 3.11 gives a schematic of such a protective film around a reinforcing bar. This amino alcohol blended protective film is very similar to a passive layer around the steel, which retards the start of corrosion and reduces the corrosion rate. It provides both anodic and cathodic corrosion protection. The protective inhibitor film both inhibits ferrous decomposition (anodic reaction), and restricts oxygen access to the steel surface (cathodic reaction).

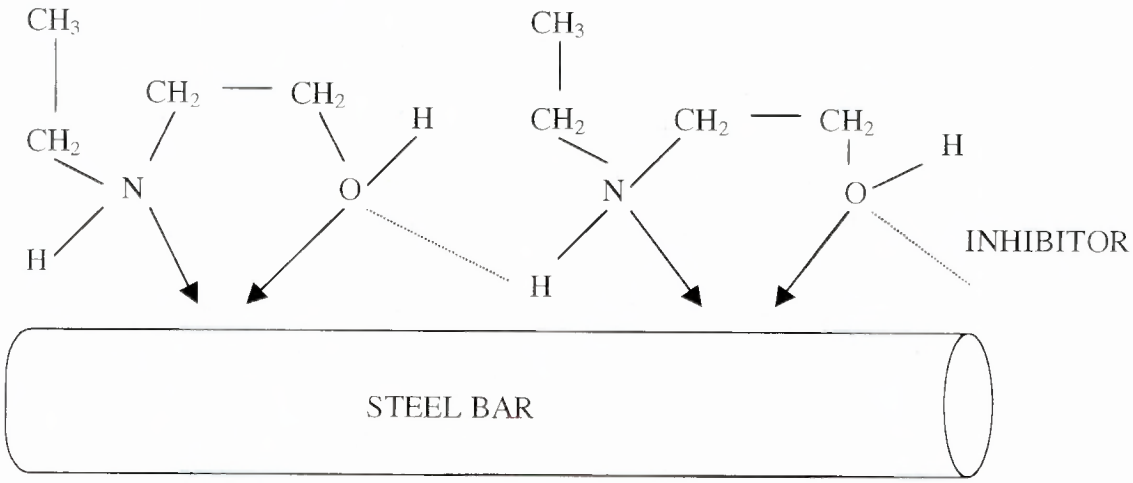

Figure 3.11: Simplified model of amino alcohol corrosion inhibitor (AACI) film forming on steel [40].

The cracked concrete beam corrosion test according to ASTM G 109-92 [61] was also carried out by Brundle to evaluate the ability of an amino-alcohol corrosion inhibitor to protect reinforcing steel embedded in cracked concrete by extending the time to corrosion [59]. This test evaluates the ability of these inhibitors to protect reinforcing steel embedded in cracked concrete subject to cyclic wetting with salt solution and drying [40]. As a result it was reported that time to corrosion was extended when the concrete contains an organic corrosion inhibitor, see figure 3.12 [40].

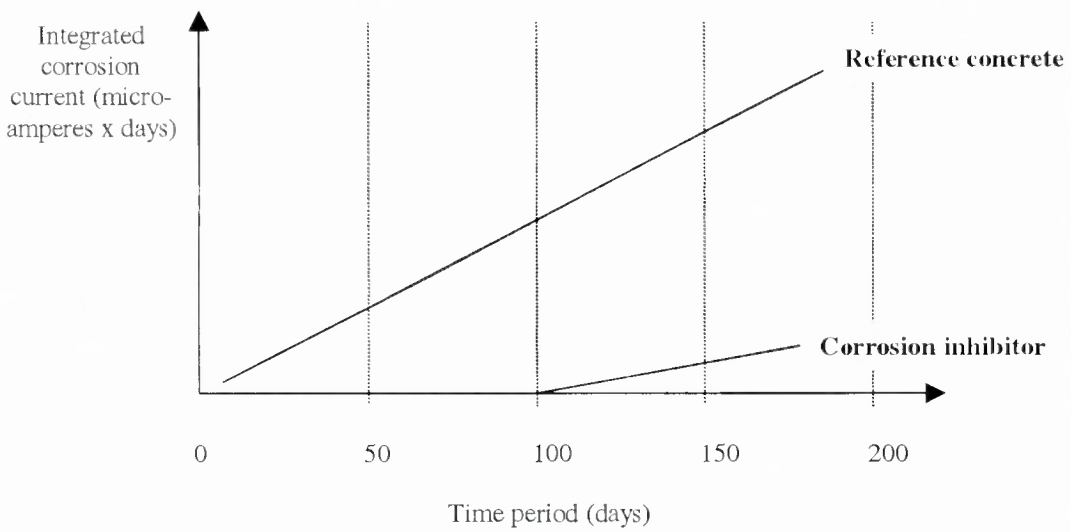

Figure 3.12: Integral corrosion current in the cracked concrete beam test [40].

It has also been reported that corrosion inhibitors of this type adsorb on the surface of the reinforcing steel in a layer of 20-100 Å, and displace chloride ions from the steel surface. They can also convert the hydroxides (rust) into passivating oxides. These inhibitors also appear to be active in alkaline and neutral (carbonated) environments making it suitable for chloride contaminated areas and carbonated areas. The time to corrosion is therefore extended and the rate of corrosion slowed down [40].

3.8.2 Mixed organic and inorganic penetrating corrosion inhibitors and their performance

A mixed organic and inorganic inhibitor is a multi-functional inhibitor or mixed corrosion inhibitor based on an organic (amino-alcohol) and inorganic, film forming, blended amino compound. This material allows the inhibitor to diffuse through the concrete as a vapour as well as a liquid [37]. This product, like all other inhibitors, forms a protective film on the steel surface, which retards the onset of corrosion and reduces the rate of corrosion. The protective film inhibits both the ferrous decomposition (anodic reaction) and restricts oxygen access to the steel surface (cathodic reaction).

The advantage of these more recent products compared to the first generation basic amino-alcohol inhibitors is that they display improved penetration rates and depths and a greater affinity for the steel, therefore producing a thicker protective layer which also forms faster than previously [37].

The diffusion of inhibitors through concrete has been verified by laboratory testing and monitoring of actual repairs undertaken in the USA as part of the Strategic Highways Research Program (SHRP) [54]. This amino-alcohol based inhibitor was reported to penetrate to the layer of steel reinforcement beneath the repaired area. These test results proved the suitability of this inhibitor for use in concrete repairs.

Analysis using Secondary Ion Mass Spectrometry and X-Ray Photon Spectrometry carried out by Brundle and Grunze identified the surface layer to be made of the parent amino alcohol and the associated radicals, which covers the anodic and cathodic sites with a continuous film [60]. The layer appeared to be typically 10^{-8} m thick and masked any trace of iron on the spectrograph, which is indicative of a high integrity film providing a barrier layer to any aggressive ions [30, 53]. Experimental test results (aqueous phase) reported that this amino alcohol corrosion inhibitor, when applied in simulated concrete pore water solutions containing chloride ions, also forms an inhibitive film ($\approx 10^{-8}$ m), and displaces the chloride ions from the steel surface [61].

Tests on cracked concrete beams subject to cyclic wetting with salt solution and drying, using an adapted ASTM Standard Test method for evaluation of inhibitors, reported that this type of inhibitor can retard the onset of corrosion and reduce the magnitude of corrosion [53]. The free corrosion potential and corrosion current were measured and the time to the onset of corrosion recorded [53]. Results obtained are shown in figure 3.13.

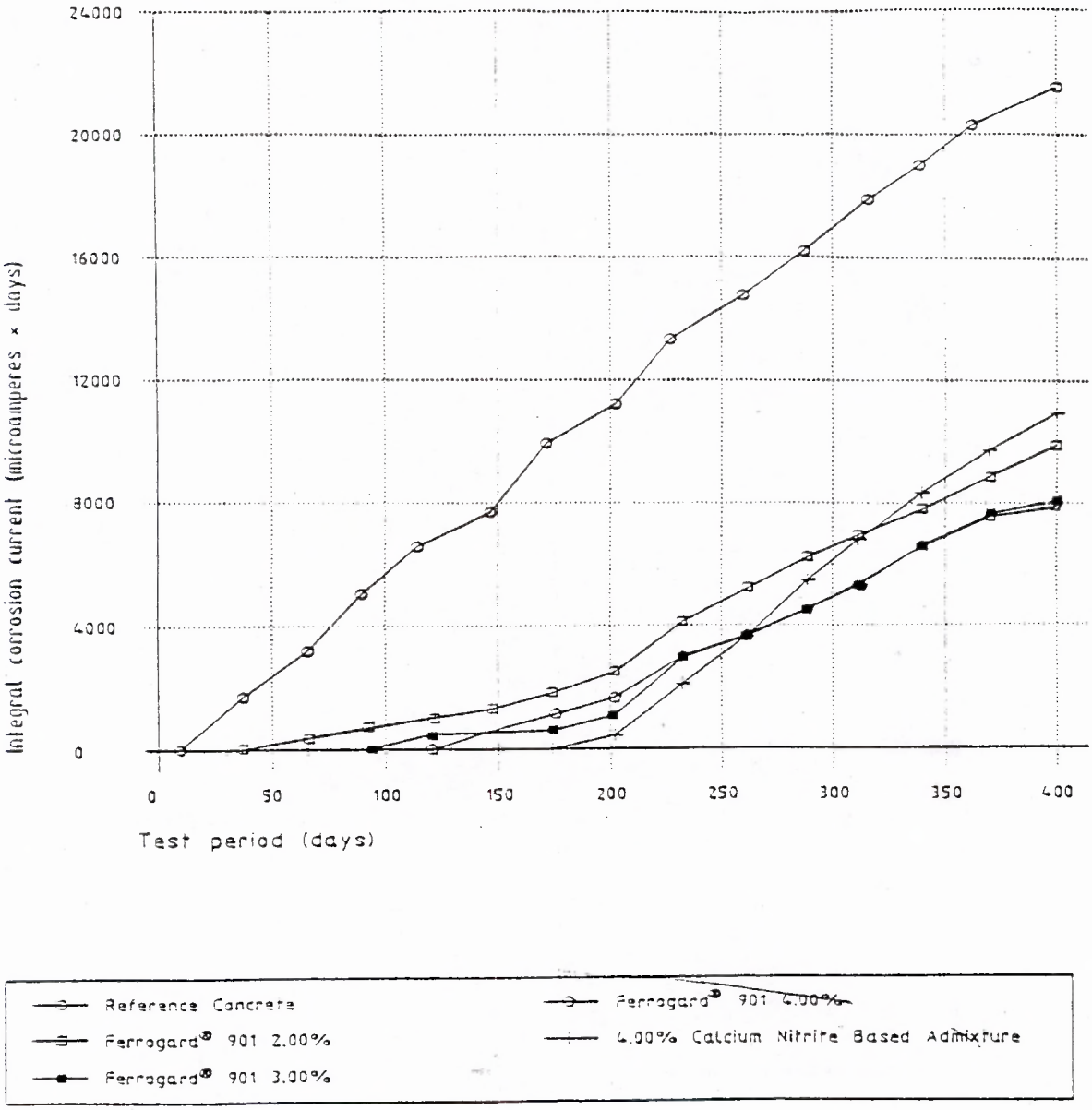

Figure 3.13: Cracked concrete beam test: Corrosion currents [53].

Figure 3.13 shows the effectiveness of the inhibitor in delaying the onset of corrosion and subsequently reducing the overall magnitude. These results confirmed other work previously carried out by Wiss, Janney, Elstner Associates Inc., and SHRP [54].

Site surveys from SHRP [54] also reported that the inhibitor was successful in inhibiting the corrosion of steel reinforcement in concrete bridge decks. Further testing on the overlay and repair areas showed that this amino alcohol inhibitor had penetrated to the subsequent layer of reinforcement below the repaired area.

Ongoing tests carried out at the Swedish Cement and Concrete Research Institute, on mortar and concrete samples exposed to marine environments, salt spray and artificial

sea water, have shown that the inhibitor is successful in retarding the onset of corrosion, most notably for the concrete samples [53, 58].

A trial test was carried out using an inhibitor of this type on a multi-storey car park in St. Austell, Cornwall, U.K. [62]. A study of the structure showed significant levels of chlorides at the depth of reinforcement, and cracking and spalling of the concrete. Half-cell potentials and corrosion rate measurements using the Gecor 6 instrument showed that corrosion was taking place. Initial testing and surface penetration was started on the 24 September with application of the inhibitor through a period of four days. Follow-up corrosion rate measurements were then determined about six weeks after application. In the treated areas the reduction in corrosion rates was found to be between 60 % and 91 % where the corrosion rate changed from 0.122 $\mu A.cm^2$ to 0.048 $\mu A.cm^2$, and from 0.125 $\mu A.cm^2$ to 0.012 $\mu A.cm^2$ respectively. This trial study was therefore able to verify that the application of this inhibitor can lead to enhanced durability and extended service life of reinforced concrete structures [62].

Based on evaluation of results obtained from various test programmes, this inhibitor appeared to [53]:

- Improve resistance to the initiation of pitting corrosion in chloride contaminated concrete and reduce the risk of general corrosion in carbonated concrete.
- Retard the onset of corrosion in new structures, and reduce the risk of incipient anode corrosion taking place in areas adjacent to repairs,
- Achieve a rate and penetration depth of up to 20 mm per day and 80 mm in 28 days respectively [53].
- Adsorb on the surface of the reinforcing steel in a layer of 20-100 Å and displace chloride ions from the steel surface.
- Be active in alkaline and neutral (carbonated concrete) environments.

3.9 Summary

In this chapter the most commonly used methods of concrete repair have been discussed. The methods discussed were: cathodic protection, patch repairs, coating systems, electrochemical repair techniques and corrosion inhibitors. Patch repairs are the most commonly used method of repair and the least expensive in the short term. Cathodic protection is usually found to be the most effective but unfortunately the most expensive method of repair. Coating systems can slow down the rate of corrosion but should only be applied to structures that are not severely damaged. Electrochemical repair techniques were also found to be very effective, however they are expensive. Since the use of corrosion inhibitors is the focus of this work, they were discussed in detail.

A corrosion inhibitor for steel reinforcement in concrete was defined as a chemical substance that reduces the corrosion of a metal without reducing the concentration of the corrosive agents. Corrosion inhibitors were found to either influence the cathodic or anodic reactions or both (i.e. they reduce either iron dissolution at the anode and oxygen access at the cathode or both). The net result is that the current density reduces, increasing the time to the onset of corrosion and reducing the rate of corrosion. This chapter introduced the various types of corrosion inhibitors available

and the mechanisms by which they are able to effectively inhibit the corrosion of reinforced concrete.

When correctly used, it appears that corrosion inhibitors can make a valuable contribution to a long-term concrete repair and maintenance strategy.

These various repair methods have been discussed, giving an indication of the available methods of repair, in order to be able to compare the methods with the penetrating corrosion inhibitor method investigated in this work.

4. EXPERIMENTAL PROCEDURES AND APPARATUS : LAB WORK

The performance of an amino alcohol-based penetrating corrosion inhibitor was investigated using various experimental techniques. The penetrating corrosion inhibitor used was a water-based impregnation for steel reinforced concrete, which penetrates to the surface of the steel reinforcement [63]. This inhibitor is adsorbed onto the surface of the reinforcing steel, and forms a protective film on the substrate to be protected, with the object of delaying the start of corrosion and reducing the rate of corrosion.

A number of laboratory tests were conducted under controlled conditions to determine the effectiveness of the penetrating inhibitor. Concrete specimens were cast in the laboratory and exposed to an accelerated carbonating environment, which promoted the rapid ingress of carbon dioxide into the concrete specimens. The inhibitor was applied on some samples before the carbonation process (BC) and on some samples after the carbonation process (AC), and the corrosion rates of the samples were monitored. The rate of carbonation of the concrete specimens in the carbonation chamber was also monitored at regular intervals, to determine if sufficient carbonation depths were being reached. The depth of penetration of the inhibitor was monitored using a qualitative test technique.

Site tests were also performed on four different sites on the campus of the University of Cape Town. These sites were initially chosen for detailed monitoring of repairs using the penetrating corrosion inhibitor. The structures were selected due to visual evidence of reinforcement corrosion and their relatively easy accessibility. It was expected that the visually severe conditions existing in these structures might represent the upper limit of possible successful performance of the penetrating corrosion inhibitor.

Using these results the performance of the inhibitor in delaying or reducing carbonation-induced corrosion was assessed.

4.1 Concrete mixes and materials

The concretes used in this investigation comprised CEM I 42.5 N mixes of grades 20, 30, 40 and 50 MPa. The aggregates used were:

- Fine aggregate: "Klipheuwel" sand with a fineness modulus of 2,50.
- Coarse aggregate: 19 mm crushed Greywacke

The grading curves for the two aggregates are shown in figures 4.1 and 4.2 respectively.

Klipheuwel sand is a siliceous pit sand having a very good particle shape and a continuous grading. The concrete water requirement is low, making it a good sand for concrete. The grading analysis was performed according to SABS 829:1994 [64]. It was found that the material grading fell within the limits recommended by SABS 1083:1994 [65], with a fineness modulus of 2,50. A single batch of sand was used throughout this research project.

Greywacke, more commonly known in the Western Cape as Malmesbury Shale, is a greywacke that was developed by thermal metamorphism of argillaceous rocks of the Malmesbury Group. A typical grading curve for 19-mm greywacke stone is given in Figure 4.2.

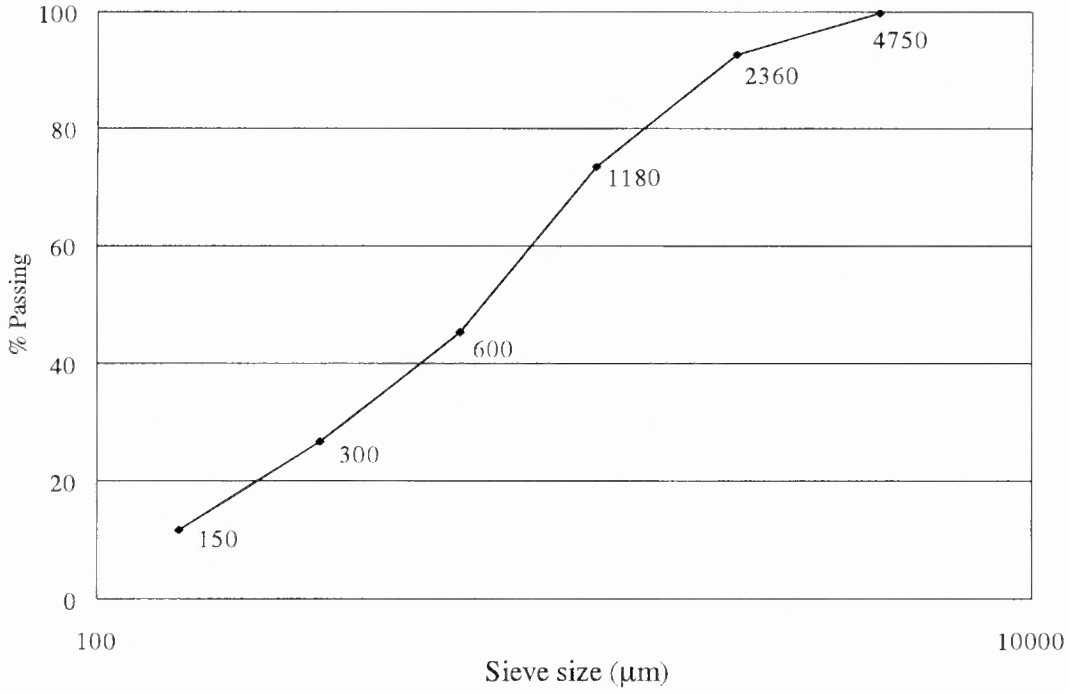

Figure 4.1: Grading curve for fine aggregate (Klipheuwel sand)

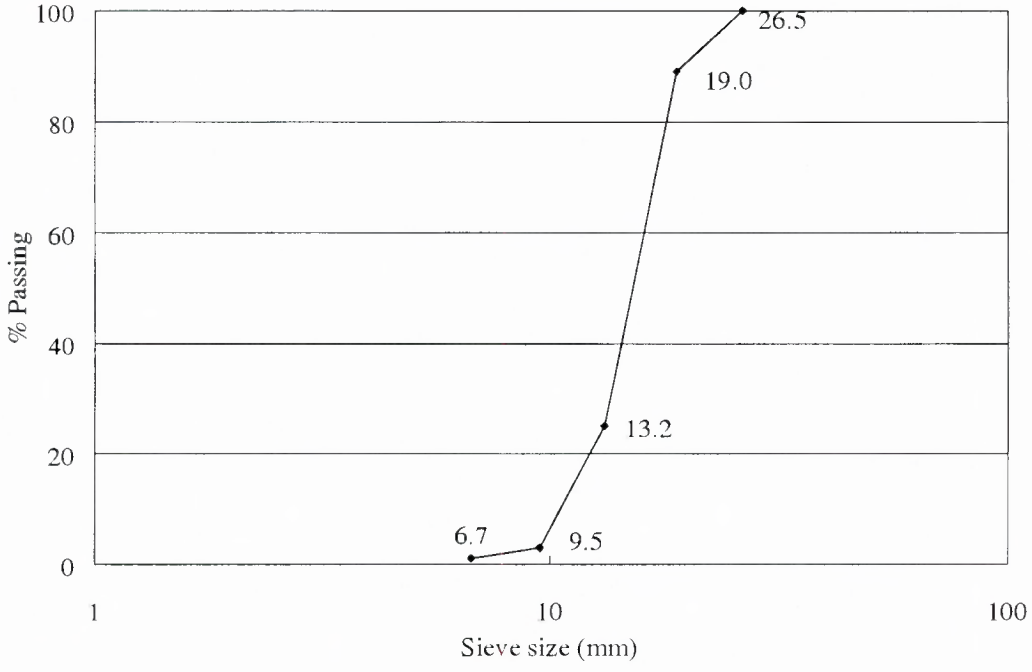

Figure 4.2: Grading curve for coarse aggregate (19 mm Greywacke stone)

The cement used for this investigation was CEM I 42.5 N, which is an ordinary Portland cement. Portland cement consists of a mixture of calcium silicates, calcium aluminates and other compounds, which have hydraulic properties. The proportions of the different compounds present in the cement vary from one factory to another and also within each specific factory the cement may vary from one batch to another. The cement used in this work was obtained from one batch. A typical oxide composition and fineness analysis of the cement is shown in Appendix A.

Twenty-four 100 mm cubes were cast for compressive strength tests for each of the different concrete grades. The cube samples were wet-cured in the water bath for 27 days after stripping samples at one day. The temperature in the water bath was maintained at a temperature of 25±2 °C **(Wet cured)**. Compressive strengths were obtained at 7, 14, and 28 days.

Details of the concrete mix proportions are shown in Table 4.1, as well as the average 28 day compressive strength and the measured slump of the concrete.

Table 4.1: Concrete mix designs (kg/m^3), 28 day strengths and measured slumps.

Grade	**20 MPa**	**30 MPa**	**40 MPa**	**50 MPa**
w/c ratio	0.83	0.73	0.60	0.52
Water content	180	180	180	180
CEM I 42.5N	217	247	300	346
Stone	1100	1100	1100	1100
Sand	897	871	826	787
28 day* strength (MPa)	22.0	30.1	39.8	50.1
Measured slump (mm)	80	80	80	75

* Average strength obtained by crushing three 100 mm cubes per concrete grade.

The water contents of all the mixes were kept constant and a slump of 75 mm was used as the reference value.

4.2 Curing Regimes

Three different curing regimes were used:

- In the first regime the samples were wet cured in the water bath for 6 days at a temperature of 25±2 °C after stripping from the mould at one day, and then dry cured in the laboratory for 21 days at a temperature of 25±5 °C and a relative humidity of 68±5 %. This regime was used for durability index samples and the corrosion monitoring specimens. **(Dry 1)**
- In the second regime the samples were dry cured in the laboratory at a temperature and relative humidity of 25±5 °C and 68±5 % respectively for 27 days after stripping from the mould at one day. This regime was used for durability index samples. **(Dry 2)**

- In the third regime the samples were wet cured in the water bath for 27 days after stripping from the mould at one day. The temperature in the water bath was maintained at a temperature of 25±2 °C. This regime was used for compressive strength tests. **(Wet cured)**

4.3 Specimens for durability index tests

A further twenty-four 100 mm cubes were cast for durability index testing (oxygen permeability index and water sorptivity) for each of the concrete grades shown in table 4.1.

Durability Index tests were carried out to characterise the concrete according to transport mechanisms; oxygen permeability for permeation and water sorptivity for absorption.

For the durability index tests some samples were cured using the **Dry 1** regime and others using the **Dry 2** curing regime.

In order to determine the depth of penetration of the penetrating corrosion inhibitor, 100 mm cubes were cast for each of the strength grades shown in table 2.1. The **Dry 1** curing regime was used.

4.4 Blocks for monitoring corrosion

The 30 MPa concrete mix was used to cast the corrosion test specimens. The permeability and sorptivity values of the grade 30 concrete in particular indicated a concrete in which the penetrating corrosion inhibitor was likely to be absorbed relatively easily, and was also likely to be retained (results discussed in Chapter Five).

The curing regime involved wet curing the specimens in the water bath for six days after stripping at one day and then dry curing in the laboratory at a temperature of 25±5 °C and relative humidity of 68±5% (**Dry 2** curing regime). The concrete specimens were 120x120x380 mm in dimension, and each specimen contained a Y16 steel reinforcement bar longitudinally through its centre. The bars embedded in the concrete were thoroughly cleaned with a wire brush and degreased with acetone before casting. Each bar had an electrical connection emerging from the concrete. The electrical connection was made from a copper wire, attached to one end of the bar by drilling a 2 mm diameter hole into the side of the bar, and passing the wire into the hole before tightly connecting them using pliers. The reinforcement bar at both ends was wrapped with insulation tape and covered with plastic heat-shrinkable tubing to prevent accidental contamination from the sides.

The wooden moulds used to cast the concrete test specimens were such that the reinforcing bars were originally embedded in the concrete at either 20 mm or 40 mm cover from the top surface of the specimen. Figure 4.4 shows the arrangement of the components in the concrete mould. A schematic sketch showing the dimensions of the concrete test blocks is illustrated in Figure 4.3.

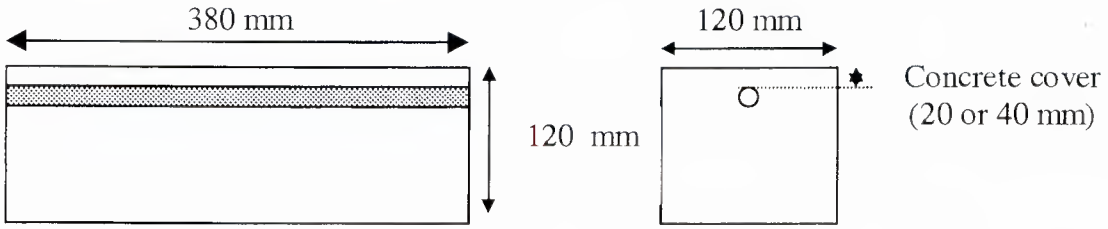

Figure 4.3: Schematic sketch with dimensions of concrete test blocks

The concrete was cast in three layers and compacted carefully using a vibrating table, to ensure proper compaction and to prevent the reinforcement being displaced. This was however not completely achieved as some of the reinforcement was displaced during compaction.

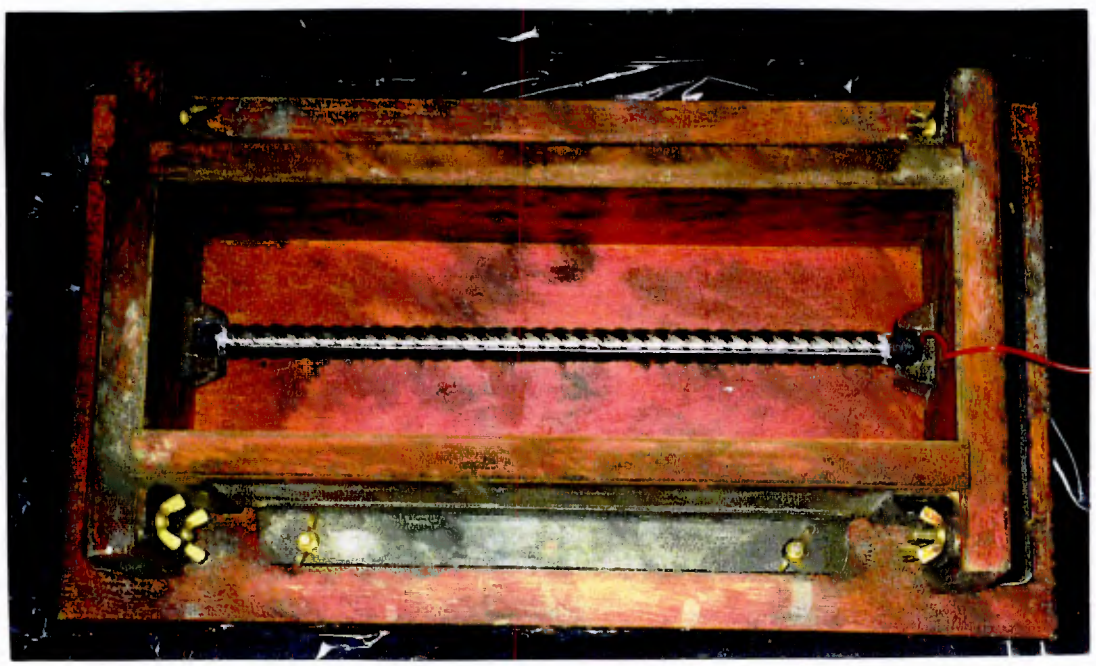

Figure 4.4: Wooden mould used to fabricate concrete test specimens.

4.4.1 Casting programme

Twelve concrete blocks were cast using the Grade 30 CEM I concrete mix, six blocks for each cover to reinforcement. Each group of six had two control specimens, two specimens that were treated with the inhibitor before the carbonation process (BC), and two specimens that were treated with the inhibitor after the carbonation process (AC). After casting, the concrete specimens were cured under PVC plastic at normal room temperature for 24 hours, at the end of which they were removed from their moulds and wet cured in the curing tanks for six days. The temperature of the curing baths was maintained at 25±2 °C. They were then dry cured in the laboratory for two and a half months. The environment was maintained at a relative humidity of 68±5 % and a temperature of 25±5 °C. Figure 4.5 gives details of the different specimens.

The casting and configuration of the block specimens resulted in the following variables being defined:

- Two cover depths to reinforcement (10 mm and 20 mm).
- Three concrete systems (controls, concrete treated with the inhibitor before the carbonation process, and concrete treated with the inhibitor after the carbonation process).

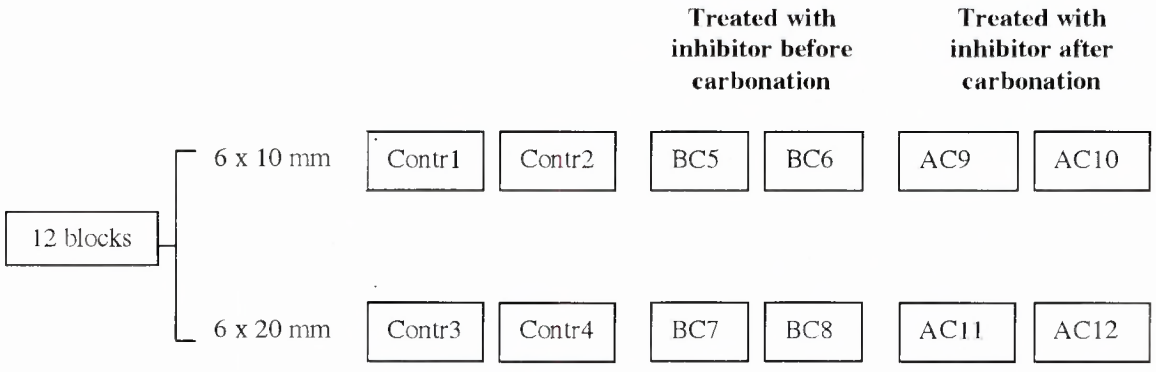

Figure 4.5: Concrete test specimens

4.4.2 Application of epoxy

After 21 days of the dry curing period a coat of epoxy (Sikadur 32 Epoxy Resin Bonding Agent) was applied on all four vertical faces (sides) of the concrete test specimens and the corresponding 100 mm concrete cube samples. This was done to ensure that during the carbonation process there would be only one controlled front of carbonation instead of carbonation occurring from all sides.

The cube samples were not exposed to accelerated carbonation; they were simply used to determine the depth of penetration of the inhibitor for different concrete grades. The epoxy was applied on these cube samples such that uniformity was maintained between the cubes and test specimens.

4.4.3 Application of inhibitor on test specimens

The penetrating corrosion inhibitor was applied on two each of the 10 mm cover and 20 mm cover test specimens before the carbonation process, and likewise on two each of the 10 mm cover and 20 mm cover specimens after the carbonation process. The inhibitor was applied at a rate of 0,1 litres per square meter on each of the test specimens over three consecutive days, so as to conform with material application specifications by the manufacturers (i.e. 0,3 to 0,5 litres per square meter). The corresponding cube specimens were treated with the inhibitor in the same fashion. On the fourth day the concrete surfaces that were treated with the inhibitor were wetted using a sponge. The following day the samples were exposed to the wetting and drying cycles mentioned later (in section 4.7).

Twenty-eight days after the application of the inhibitor the depth of penetration of the inhibitor was determined on each of the treated block samples and cubes by taking two 20 mm diameter cores and slicing them at 15 mm increments, before pulverising the slices. Using a qualitative method for analysing the penetration of the inhibitor (as specified by the manufacturers) the concentration of the inhibitor at the various depths was obtained.

In order to determine the depth of penetration of the penetrating corrosion inhibitor for the different concrete grades, 100 mm cubes were cast for each of the strength grades shown in table 4.1. The **Dry 2** curing regime was used. These cubes were coated with the inhibitor in the same way as the block samples and left for 28 days before qualitative testing.

It was found that the inhibitor had penetrated to a depth of between 45 mm and 60 mm in the block samples and similarly on the cube samples.

For the concrete test specimens the 30 MPa CEM I mix was used as it proved to be the most effective with penetration of the inhibitor. This is discussed in a later section (section 5.2).

4.4.4 Penetration depth tests for corrosion inhibitor

The depth of penetration of the penetrating corrosion inhibitor can be evaluated using two different tests. The first test is a test specified by the Manufacturer for quick and easy detection of the inhibitor in the concrete specimen. This is a qualitative test, which shows the presence of the inhibitor by a noticeable colour change on a specially prepared chromatograph paper.

The second test is a quantitative test (the TKN test), which is typically used in wastewater treatment laboratories. Both of these tests determine the presence of nitrogen in the concrete. Therefore powdered samples should not be obtained by drilling of the concrete since the heat generated by the drilling process causes decomposition of the nitrogen-containing molecules, thereby causing less of the inhibitor to be detected. Instead core samples should be obtained from the concrete specimens and these used to obtain powdered samples of the concrete in order for effective determination of the depth of penetration of the inhibitor.

4.4.4.1 Qualitative test

A 20 mm diameter concrete core of length about 70 to 80 mm was taken from the concrete specimens. The core sample was then sliced at 15 mm increments into disc samples. Each of these discs was then crushed into a fine powder using a mortar and pestle and stored separately in carefully labelled airtight plastic bags.

A small powdered sample of one gram was then weighed using a balance, and saturated with approximately one millilitre of distilled water in a small glass container. The glass container with the solution of powdered concrete and distilled water was mixed together and allowed to settle until a clear supernatant was visible in

the container. The supernatant was extracted using a one-millilitre syringe with a micro-filter attached to its front. The solution in the syringe was dispensed through the micro-filter into a second clean container. A micropipette was placed in the second container with the filtrate and was used to draw small amounts of the filtrate. This liquid was drawn onto a strip of chromatograph paper to form a mark of approximately 5 mm in diameter. The chromatograph paper was then dried using a portable hair dryer until the wet mark disappeared. This process was repeated five times and each time the liquid was drawn onto the same position on the chromatograph paper such that the supernatant ionic contents were effectively concentrated at that particular point. This entire process was carried out at each of the 15 mm increments such that the samples of a single core were placed on the same strip of chromatograph paper. At this point the sample preparation was complete.

In the next stage of the test the strip of chromatograph paper was sprayed with two indicator solutions, supplied by the manufacturers. The first indicator solution was sprayed on and dried, after which the second indicator solution was sprayed on and dried using the portable hair dryer at a higher speed.

A noticeable colour change was observed at each of the positions where the solution was placed for each of the 15 mm increments indicating that the inhibitor was present, see figure 4.6. The colours that indicate the presence of the inhibitor range from brick red where the concentration is high to a very pale pink where the concentration of the inhibitor is low.

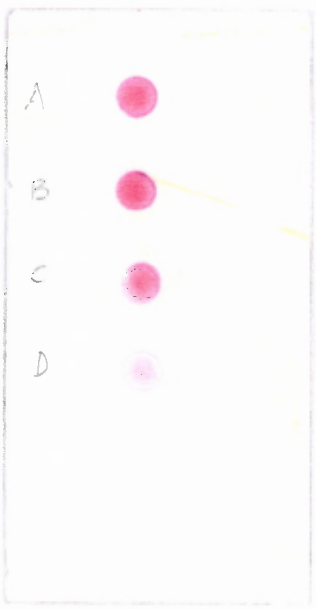

Figure 4.6: A photograph of chromatograph paper used in a penetration test

4.4.4.2 Quantitative test

This test is called the Total Kjeldahl Nitrogen (TKN) test and is used to assess the penetration of the inhibitor into the concrete based on traces of nitrogen from the amino-alcohol material. The TKN test involves many different processes such as acid

digestion, titration and distillation [66]. The values from the TKN test are expressed as organic nitrogen in milligrams per gram of concrete.

For the purposes of this study the qualitative assessment of the penetration of the inhibitor into the concrete developed by the manufacturers was decided to be sufficient, due to its simplicity.

In previous research done by Rylands [3], the results of numerous TKN and qualitative tests were compared and a general relationship was established for an easy comparison of the colours obtained in the qualitative test and values obtained in the TKN test [3]. This relationship is shown in table 4.2 [3].

Table 4.2: Comparison of TKN and test kit results [3].

Test kit colour	Qualitative rating	Organic nitrogen (mg/g of concrete)
Brick red	Excellent	0.55 - 2.20
Pink	Good	0.17 - 0.55
Pale pink	Adequate	0.06 - 0.28
Trace	Inadequate	< 0.06

4.5 Accelerated carbonation

The carbon dioxide content in the atmosphere is roughly 0.03 %, thus the carbonation process in concrete will take a number of years. For the purposes of this research it was therefore necessary to accelerate the carbonation process. This was done by introducing a more concentrated carbonating environment, where a higher carbon dioxide level was maintained, using a Leec carbonation chamber. The chamber was maintained at a carbon dioxide level and temperature of 10 % and 30 °C respectively to ensure accelerated carbonation of the samples. Regular monitoring of the carbon dioxide content, temperature and relative humidity of the chamber was also carried out to ensure that the required carbon dioxide and temperature levels were maintained.

4.5.1 Leec carbonation chamber

The carbon dioxide concentration is controlled to a pre-set level with an accuracy of better than 0.2% carbon dioxide in air. The carbon dioxide/air mixture is continuously monitored and a digital meter on the control panel shows the percentage of carbon dioxide. A built-in thermal conductivity detector cell is used to measure the carbon dioxide level. If the carbon dioxide concentration falls below the pre-set level the control system causes a solenoid valve to automatically inject additional carbon dioxide to bring the chamber's atmosphere back to the desired level. When the door is opened, two-stage rapid recovery of the carbon dioxide level is automatically achieved by the sensing system. This is achieved by proportioning both 'coarse' and 'fine' flow carbon dioxide to the incubator until a pre-set fraction of the set carbon dioxide level has been reached. The 'fine' flow then overrides the system and brings the carbon dioxide level slowly to the percentage carbon dioxide operating level.

When the doors are open the circulating fan and carbon dioxide solenoid supply valves shut off.

The carbon dioxide concentration can be altered by adjusting the digital carbon dioxide operating level. The carbon dioxide gas enters the chamber through a gas inlet nozzle, and ordinary commercial carbon dioxide gas is used at between 0,25-0,5 bar pressure to feed the system.

The temperature in the chamber is controlled by an advanced microprocessor, which has been programmed to give optimum control. Sensors placed throughout the chamber and on the door, allow quick recovery and stable control. The temperature can also be adjusted to a required value and maintained at this temperature.

The circulating fan located at the top of the chamber circulates the carbon dioxide/air mixture around the chamber, thereby ensuring that the mixture of gas and concentration of carbon dioxide in the chamber is uniform throughout.

The humidity in the chamber can be increased to as high as 99% relative humidity by filling the reservoir in the base of the chamber. There are also a number of safety alarms fitted in the chamber, which maintains the carbon dioxide gas levels and temperatures at the set values.

For the purposes of this research the chamber was maintained at a carbon dioxide level of 10% and a temperature of about 30°C to ensure accelerated carbonation of the samples. A concentration of 10 % carbon dioxide was chosen rather than a higher concentration, as greater carbon dioxide concentrations would generate an artificially dense carbonation layer. Regular monitoring of the carbon dioxide content, temperature and relative humidity of the chamber was also carried out to ensure that the carbon dioxide and temperature levels were maintained at 10% and 30°C respectively. The values of the relative humidity were determined to be about 85%±5%.

Roughly 28 days after application of the penetrating corrosion inhibitor on the six specimens treated with the inhibitor before the carbonation process, these specimens were placed in the carbonation chamber for accelerated carbonation. At the same time, the six 'after carbonation' specimens were placed in the carbonation chamber.

The set up in the carbonation chamber is shown in figure 4.7.

Figure 4.7: Set up of test specimens in carbonation chamber

4.6 Measurement of cover to reinforcement

Initially it was decided to use concrete covers of 20 mm and 40 mm, however during the carbonation rate monitoring period (discussed in a later section) it was seen that in order to achieve carbonation depths of about 40 mm a further seven or eight months was necessary. It was therefore decided to reduce the cover of the 40 mm sample to 10 mm by slicing 30 mm off the 40 mm cover blocks leaving a cover of about 10 mm. This was done about four months after commencing carbonation.

During the dry curing period, cover measurements were carried out on the concrete test specimens at three different positions along the reinforcement bar to determine the cover to reinforcement. The instrument used was an electronic micro-cover meter (Koelectric Limited). An alternating magnetic field is used to detect the presence of magnetic materials such as steel rebars. There are however a number of limitations to consider when using cover meters. The congestion of rebars and deep covers gives inaccurate results. Also, iron-bearing aggregates in the concrete tested can lead to misleading readings, as they will influence the magnetic field.

However for the purposes of determining covers of laboratory block samples, the cover meter used was sufficient and accurate measurements were obtained. The cover results obtained for each of the test specimens are included in sections to follow.

4.7 Exposure regimes

Three different regimes of wet and dry cycles were used in order to optimise the rate at which corrosion would take place. These regimes were used on a 'trial and error' basis in order to find the optimum regime. The regimes used were as follows:

- **First regime (7 days wet and 7 hours dry):** Samples were placed in the water bath at 22±2°C, and three hours prior to corrosion rate testing the samples were removed and allowed to surface dry. About 4 hours after corrosion monitoring the samples were replaced in the water bath. The test specimens were therefore in the water bath except for seven hours during corrosion rate testing when the samples were exposed to laboratory conditions. The wetting regime was such that the test specimens were semi-immersed (about 20 mm deep) in the water bath, with the inhibitor treated surface exposed to the moisture. This cycle was initially followed on the basis that too little moisture will electrolytically stifle the corrosion rate whilst saturated conditions will limit the availability of oxygen to the cathode. It was however found that the high level of saturation attained with short drying periods was limiting the availability of oxygen to the cathode, thereby stifling the corrosion process. This first regime continued for a period of three months and one and a half months for the 10 mm and 20 mm cover samples respectively.

- **Second regime (3 days wet and 4 days dry):** The samples were now allowed to surface dry for four days before they were replaced in the water bath for the next three days. This regime was introduced as it was thought that excessive saturation might be limiting the availability of oxygen to the cathode. The drying period was thus extended in this cycle. This new wetting and drying regime however resulted in very erratic results with large differences between the corrosion rates at the end of the wet and dry cycles. Therefore a third wetting and drying regime was introduced. The second regime lasted for a period of two months.

- **Third regime (5 days wet and 2 days dry):** This third regime had a longer wetting period and a shorter drying period than regime 2. The samples were dried for 2 days and then they were replaced in the water bath for the remaining five days. This regime was found to be the most effective and was adopted for the remainder of the testing period. This regime allowed the concrete to dry out sufficiently to allow the availability of oxygen to the cathode and also sufficient moisture was present for corrosion to take place. This regime continued for the remainder of the testing period (approximately six months).

During the drying period in the above regimes the specimens were exposed to relatively stable laboratory conditions. The temperature in the laboratory was found to vary with seasonal changes. In the winter the temperature varied from about 15 to 17°C and in the summer period it ranged from 20 to 30 °C. The relative humidity was also measured and it was found to be 65±5 %.

4.8 Corrosion monitoring

A number of different methods have been developed to determine corrosion rates and to assist in understanding the processes taking place at the steel reinforcement as a result of corrosion.

For the purposes of this research, the following methods were used for corrosion monitoring:

- Copper/copper sulphate half-cell to measure half-cell potentials.
- Gecor 6, a commercial instrument, which uses a linear polarisation resistance technique to measure the rate at which corrosion is taking place.
- Wenner probe to determine resistivity of the concrete.

4.8.1 Copper/copper sulphate half-cell

The apparatus required for a standard copper sulphate half-cell is described in ASTM C 876-91 [16]. It is made of a rigid tube of a dielectric, non reactive material, a porous wooden or plastic plug that remains wet by capillary action, and a copper rod that is immersed within the tube in a saturated solution of copper sulphate [16]. The saturated copper sulphate is prepared by dissolving reagent grade copper sulphate crystals in distilled water; the solution is considered to be saturated when an excess of crystals lie at the bottom of the solution. It is also specified in ASTM C 876-91 [16] that the rigid tube should have an inside diameter of not less than 25 mm; the diameter of the porous plug should not be less than 13 mm; the diameter of the immersed copper rod should not be less than 6 mm and length should not be less than 50 mm [16]. A sponge was attached to the front of the cell to provide a low electrical resistance liquid bridge between the half-cell and the concrete surface. Before potential measurements were taken the sponge was pre-wetted with a low electrical resistance contact solution, in this case normal tap water. The potential was then measured by connecting a high impedance voltmeter between the half-cell and the reinforcing steel.

4.8.1.1 Interpretation of results

Half-cell potentials do not indicate the rate at which corrosion is taking place, but rather give an indication of the corrosion risk of the steel [2]. Table 4.3 shows copper/copper sulphate half-cell potentials and the probability of corrosion [16].

Table 4.3: Copper/copper sulphate potentials and the probability of corrosion [16]

Potential (mV)	% Probability
> - 250	90 % probability that no reinforcing steel corrosion is occurring in that area at time of measurement.
- 250 to - 350	Corrosion activity of the reinforcing steel is uncertain.
< - 350	90 % probability that reinforcing steel corrosion is occurring in that area at time of measurement.

However, in some circumstances the potentials obtained are not representative of the corrosion condition of the concrete. Very negative potentials can be found in saturated conditions where the cathodic reaction is stifled due to the lack of oxygen to form a passive layer. In such cases the half-cell potentials are more negative than – 500 mV even though corrosion is not taking place. Other problems also arise in the presence of carbonation. In this case the anodes and cathodes are formed close to each other, and therefore the potential measured is usually an average of the potentials at the anode and the cathode. In carbonated concrete the pores are partly blocked by the calcium carbonate deposits, and this increases the resistivity of the concrete (i.e. reduced conductivity of the concrete), which in turn reduces the potential measurements. Also, potentials can be positive in some areas and slightly negative in adjacent areas, and it is therefore important to consider the change in potential over a certain area instead of a potential value at a single point. Potential mapping is therefore advisable, so that a 'contour map' of potentials can be drawn up indicating clearly areas where large shifts in potentials occur, as these are the areas where corrosion is likely.

The above shows the limitations of potential measurements in carbonated concrete. They measure the thermodynamics of the corrosion, not the rate of corrosion. Due to this problem, potentials measured are only used as an indication of the corrosion risk of the steel.

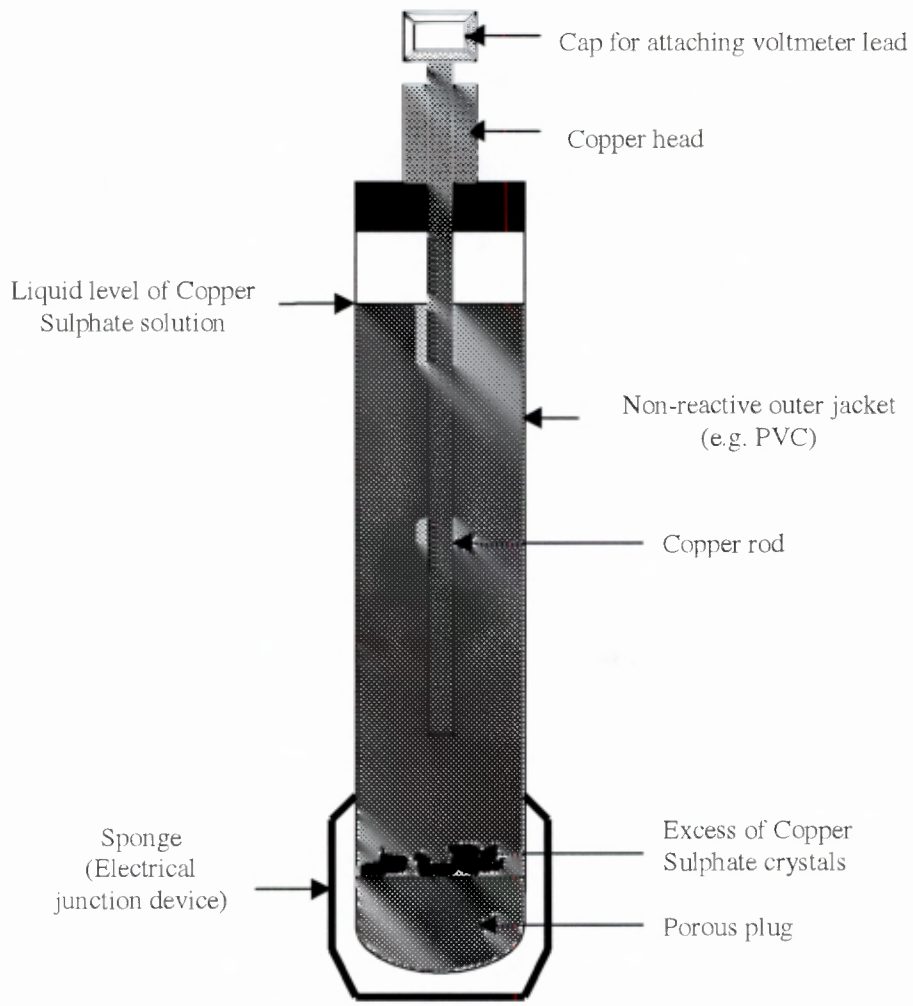

Figure 4.8: Sectional view of a copper/copper sulphate half-cell [16].

Figure 4.8 shows a cross section through a copper/copper sulphate half-cell and figure 4.9 shows the set up for measuring half-cell potentials using the copper/copper sulphate half-cell.

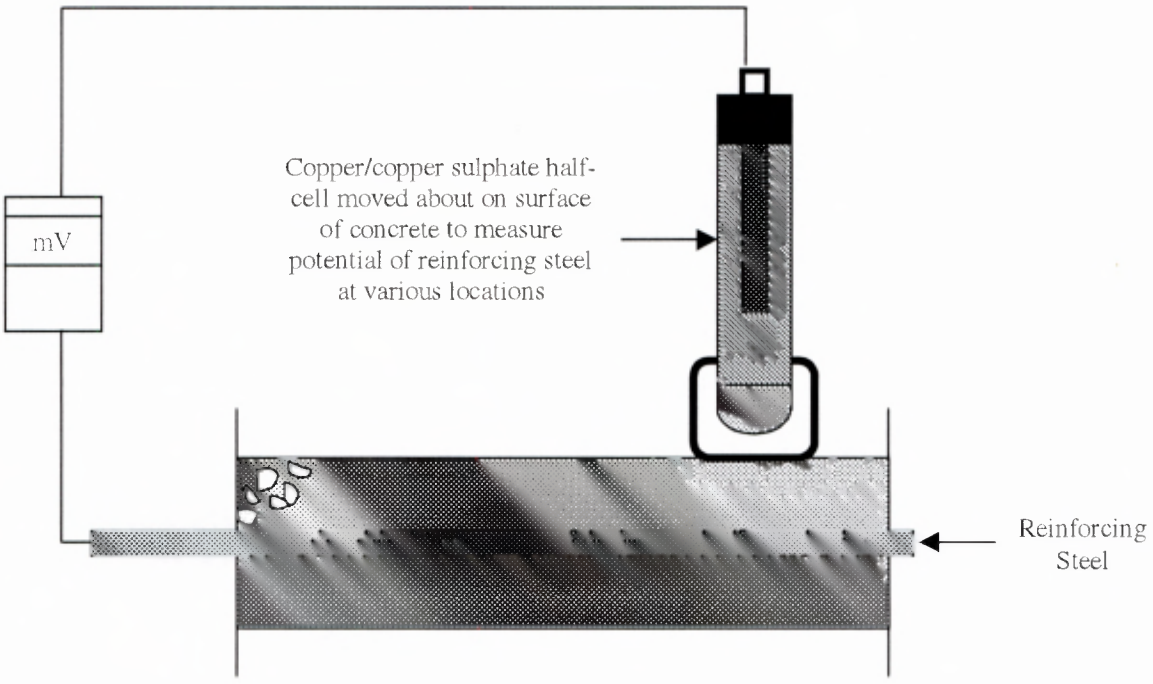

Figure 4.9: Copper/copper sulphate half-cell circuitry.

4.8.2 Corrosion rate measurements using the Gecor 6 (Galvanostatic linear polarisation resistance meter)

The Gecor 6 was developed to measure the corrosion rate of steel in concrete by using the galvanostatic linear polarisation resistance technique. This is a non-destructive technique that works by applying a small current to the reinforcing bar and measuring the change in the half-cell potential. The polarisation resistance R_P is the change in potential, measured by the Gecor 6, divided by the applied current. The Gecor 6 obtains the corrosion rate I_{CORR} from the polarisation resistance R_P by means of the Stern-Geary relationship, where the constant B is assigned the value 26 mV in the Gecor 6 [18]. The Gecor 6 is able to accurately confine the area of measurement by the use of a sensor controlled guard ring [18]. This means that corrosion rate measurements are not carried out over an undefined area, but show the 'true' corrosion rate at the place of measurement.

4.8.2.1 Fundamentals of the Gecor 6

The main difference of the Gecor 6 to other already existing galvanostatic linear polarisation resistance measurement devices is the use of a pair of extra reference electrodes (sensors) for a more precise bounding of the action of the electrical signal [18]. This galvanostatic device is specially adapted to be used along with a guard ring device. The guard ring device is made up of two concentric counter electrodes (CE) to

which different currents can be applied simultaneously (figure 4.10). The current applied from an external counter electrode (CE) tends to repel the lines of current of the electrical signal applied from an internal (central) counter electrode, restricting them to an area located close to this central counter electrode. A pair of electrodes (S_1 and S_2) is located between the two counter electrodes and spaced a fixed distance apart (figure 4.11). These are two small reference electrodes. A voltmeter is connected between these two electrodes (S_1 and S_2). A reference electrode (RE) is placed in an orifice in the centre of the inner counter electrode i.e. the electrodes (S_1 and S_2) are orientated radially with respect to the circular counter electrode (see figure 4.11). The electrodes S_1 and S_2, are positioned in such a way between the counter electrode that the current confinement can be measured.

Before any electrical signal is applied the voltmeter will always indicate a certain potential difference. This potential difference between the two sensors is taken as a reference value before the current is applied [18]. When a set current is applied to the reinforcement through the central counter electrode, the voltmeter reading between the sensors is modified due to the change in the electric field. An additional current higher than that applied to the internal counter electrode is applied to the external counter electrode such that the potential difference between the sensors returns to the reference value. When this condition occurs then a uniform current has been confined to a fixed area of steel, the current lines therefore covering a circular area with a radius equal to the distance between the centre of the central counter electrode and the central point between the sensors (figure 4.11) [18].

From this the polarisation value is read, and this value, along with the surface area of the steel affected by the current applied from the counter electrode, and the intensity of this current are used to obtain the value of the polarisation resistance R_P. The corrosion rate I_{CORR} is then obtained from the polarisation resistance R_P by means of the Stern-Geary relationship, see equation 2.13.

Experience however indicates that corrosion rates fluctuate significantly in response to environmental and material influences and single readings in time are generally unreliable as indication of the overall corrosion rate [4]. Table 4.4 shows a qualitative guide for the assessment of corrosion rates of site structures [4,26].

Table 4.4: Qualitative guide for the assessment of site corrosion rates

Corrosion rate ($\mu A/cm^2$)	Qualitative assessment of corrosion rate
> 10	High
1.0 - 10	Moderate
0.1 – 1.0	Low
< 0.1	Passive

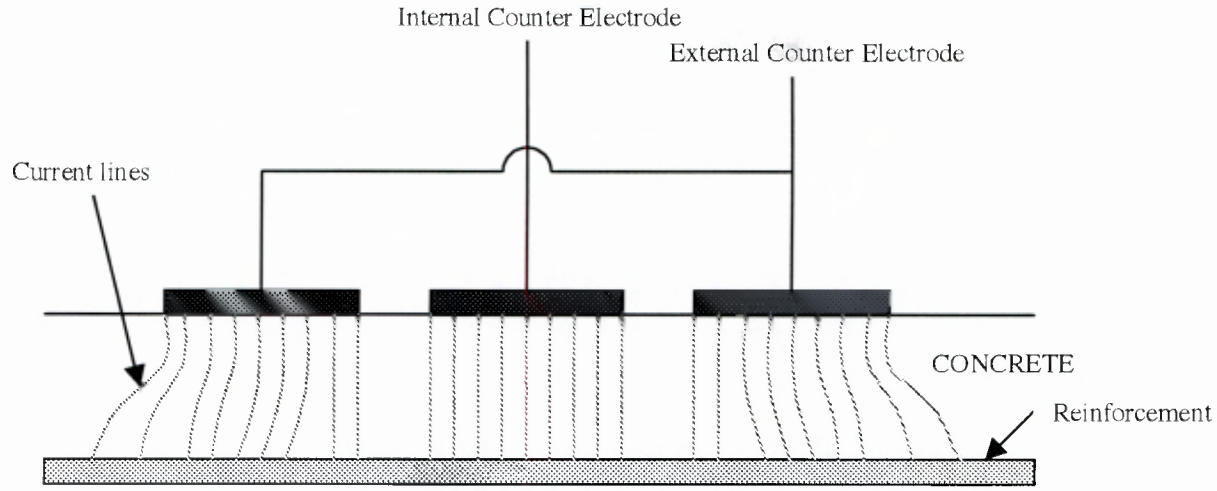

Figure 4.10 Confinement of current lines from central counter electrode due to the action of external counter electrode [18]

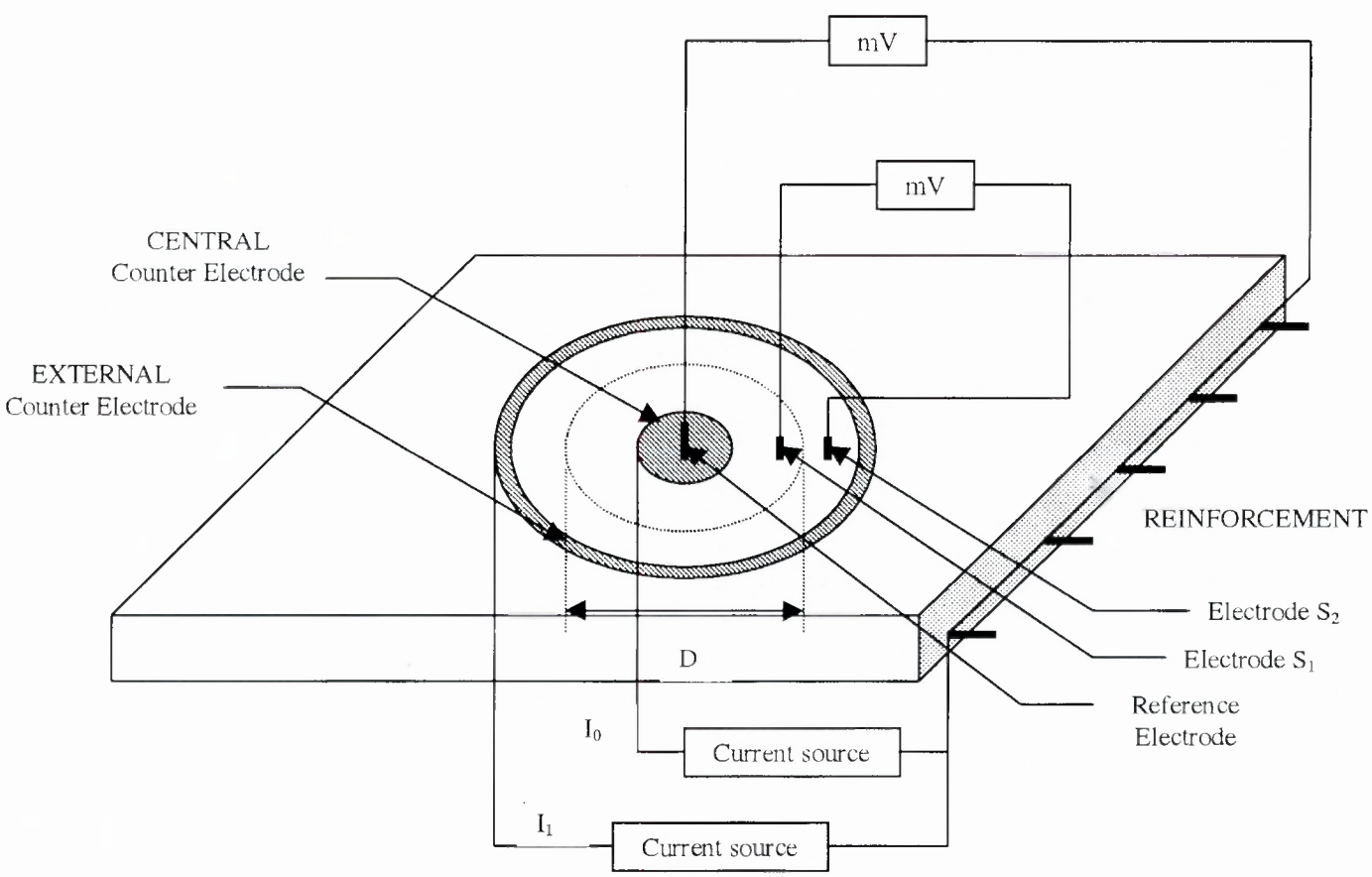

Figure 4.11: Arrangement of counter electrodes and reference electrodes (S_1 and S_2) for testing a reinforced concrete slab [18]

4.8.2.2 Use of Gecor 6

The Gecor 6 has three major components: the rate meter, and two separate sensors. The LG-ECM-06 meter controls the system, collects the measurements and processes the data. The meter and the sensor A measure the corrosion rate in $\mu A/cm^2$ over a defined area of rebar, the corrosion potential E_{CORR} measured relative to a copper/copper sulphate half-cell, and the electrical resistance of the concrete as required for the calculation of the I_{CORR}. The meter and the sensor B measure the concrete resistivity, the ambient relative humidity and temperature. For the purposes of this research, only the meter and sensor A were used. Figure 4.12 shows the scheme of sensor A.

The complete system is portable and easy to use. A measurement will take between 2 to 5 minutes. The microprocessor control system selects the correct parameters and carries out the measurement.

Measurements were taken by placing the sensor on the surface and making an electrical connection to the reinforcing steel. The sensor includes a sponge pad, which is wetted to ensure good electrical connection to the surface. Figure 4.13 shows the set up of a typical measurement to determine corrosion rates in test specimens.

If Gecor 6 measurements are taken on site, it is recommended that readings are taken over a grid in which the grid size is dependent on the rebar spacing. A 0.5 m grid spacing would be the closest spacing, except on small structures or units with severe changes in condition.

For this work, the sensor A was placed directly over a rebar of known diameter, either a single bar or at a cross over in order to get best results. There must not be a metallic (electronic) short circuit from the bar to the surface caused by a tie wire, nail etc as this will distort the reading. There must also be complete electrical contact between the half-cells in the sensor and the concrete surface. Any local deformations or insulating layers such as coatings, debris, deposits or contaminants must be removed or avoided by grinding or choosing another location. Small deformations in the surface can be 'ironed out' by using additional sponge pads. Minor voids, delaminations or cracks within the concrete must also be avoided, as these will cause the signal to deviate from the required path therefore giving misleading readings.

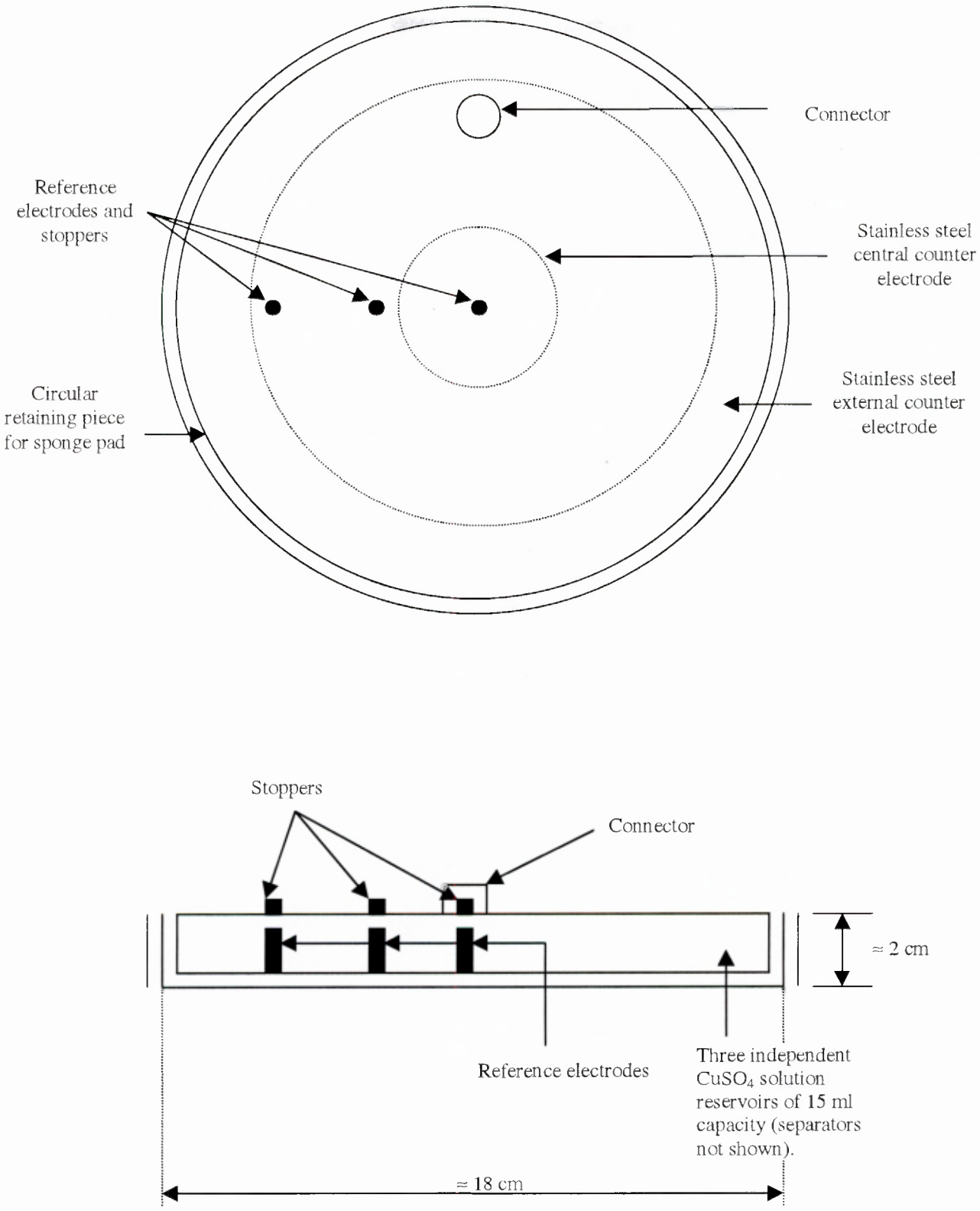

Figure 4.12: Scheme of sensor A

Figure 4.13 Typical Gecor measurements using sensor A on test specimens

The concrete surface was also wetted with normal tap water before a reading was taken to enhance the measurement obtained. Also prior to taking readings on site, a connection was made to the reinforcement. A piece of rebar is usually exposed, by coring, excavation or connection to exposed steel, which is bonded to the reinforcement, and a cable attached. The steel must be cleaned to ensure a good electrical contact. It is essential that there is good electrical continuity between the rebar connection and the steel rebar being measured by the Gecor sensor. Reasons for discontinuity include construction joints with separate rebar cages, excessive corrosion and light reinforcement content. If discontinuities are found it is necessary to make regular rebar connections rather than just one or two. The sensor must be maintained flat against the surface of the concrete throughout the measurement.

The flow of external or stray currents into and out of the reinforcing network can change the polarisation of the steel giving unsteady half-cell readings. This usually occurs near DC power lines or rails, cathodic protection systems and other DC power sources. Therefore for accurate corrosion rate measurements stray currents must be isolated from the measurement location. This was however not a concern in this work.

Environmental conditions also have an effect on the corrosion rate measurements taken using the Gecor 6. The corrosion rate meter does not function in extreme conditions of temperature or humidity. The device should therefore not be operated at temperatures below 0 °C or above 50 °C and the environmental relative humidity should not exceed 80 %.

4.8.3 Resistivity measurements

Resistivity was measured using a Wenner Probe connected to a portable resistivity meter. The Wenner probe is made up of four electrodes. An alternating current is applied through the concrete between the two outer electrodes and the potential difference is measured across the two inner elecrodes. The concrete resistivity is then determined and the assessment of likely corrosion rates can be made.

Once the concrete resistivity is known a rough assessment of likely corrosion rate can be made as shown in table 4.5. This assessment assumes conditions are favourable for corrosion. A resistivity measurement in itself provides little information about the extent of reinforcement corrosion. Also, carbonated concrete has been found to have very high resistivities due to the formation of calcium carbonate, which reduces the permeability of the concrete. This reduction in permeability results in reduced moisture levels within the concrete. In addition, oxides formed around the steel cause a dense skin reducing the ingress of moisture to the surface of the steel, and thus reducing the conductivity of current in the steel. It is for these reasons that it is recommended that resistivity measurements be used in conjunction with corrosion rate and half-cell potential data.

Table 4.5: Likely corrosion rate based on concrete resistivity [4]

Resistivity (k.ohm.cm)	Likely corrosion rate given corrosive conditions
< 12	High
12 - 20	Moderate
> 20	Low

4.9 Durability index tests

Twenty-eight days after casting, the cubes were removed from the respective curing regimes and were cored with a diamond tipped core barrel. Concrete core samples of 68 mm diameter were obtained. Site cores were also obtained. The cores were then sliced into 25 mm thick disks using a water-cooled moveable bed diamond saw. Site cores were also prepared in the same manner.

4.9.1 Oxygen permeability index test

This test was done to obtain the gas permeation properties of the concrete. Permeation describes the process of movement of fluids through the pore structure under an externally applied pressure whilst the pores are saturated with the particular fluid. Permeation is therefore a measure of the capacity for concrete to transfer fluids. It is dependent on the concrete microstructure, the moisture condition of the material and the characteristics of the permeating fluid [67]. This test therefore assesses the overall microstructure of the outer surface of cast concrete, and is very sensitive to micro-voids and cracks which act as 'short circuits' for the permeating gas [68]. This test can therefore be used to assess the state of compaction, presence of bleed voids and channels and the degree of the interconnectedness of the pore structure [68].

Four samples were tested and the average obtained for one result. The disc samples were preconditioned in the oven at 50 °C and at a relative humidity of less than 20 % for seven days. After this seven-day period the testing was carried out as specified in Alexander et al [68]. Figure 4.14 shows the basic set up of the oxygen permeability cell.

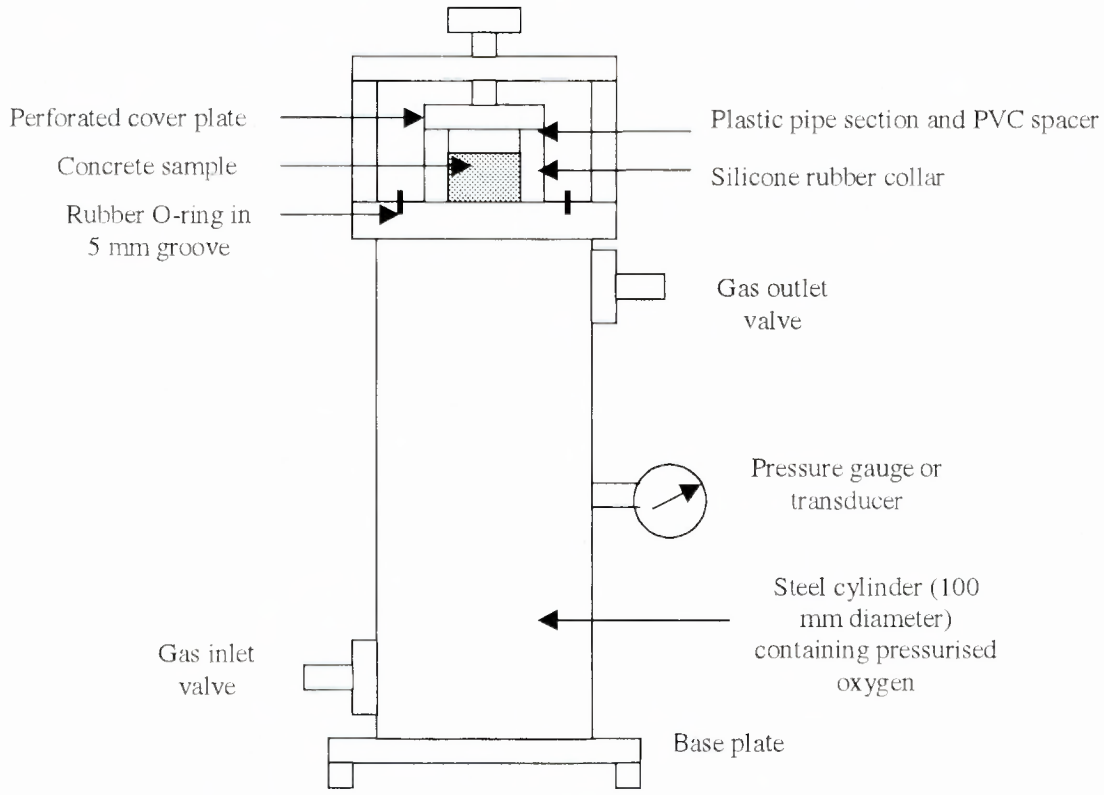

Figure 4.14: Oxygen permeability cell [68]

4.9.2 Water sorptivity test

This test uses the mass of water absorbed from the bottom face (usually the near-surface face) of a concrete sample as a measure of the sorptivity of the concrete sample. Absorption is the process whereby fluid is drawn into a porous, unsaturated material under the action of capillary forces. The capillary suction is dependent on the pore geometry and the saturation level of the concrete. Water absorption caused by wetting and drying at the concrete surface is an important transport mechanism near the surface but becomes less significant with depth. The rate of movement of a wetting front through a porous material under the action of capillary forces is defined as sorptivity. This test therefore measures the physical properties of the surface layer (5 –15 mm) of the test concrete, by means of the mechanism of capillary suction [68]. This test has also been found to be sensitive to the nature and duration of early curing of the concrete cover and can therefore be used on site to assess construction quality [68].

In this case the same samples used in the oxygen permeability index test were also used for measuring sorptivity. The disc samples were once again pre-conditioned in the oven at 50 °C to ensure uniformly low moisture contents at the start of the test.

The circular edges of the discs were sealed with epoxy to ensure uni-directional absorption. The water sorptivity test was then carried out on the samples as specified [68]. Four samples were used, and the average obtained for one result.

The arrangement for the water sorptivity test is shown in figure 4.16

Suggested ranges for durability classification of concrete for water sorptivity and oxygen permeability, based on site and on laboratory data are shown in table 4.6.

Table 4.6: Suggested ranges for durability classification using the index values [67]

Durability class	Oxygen Permeability Index (log scale)	Water sorptivity (mm/√h)
Excellent	> 10	< 6
Good	9.5 - 10	6 – 12
Poor	9.0 - 9.5	12 - 15
Very poor	< 9.0	> 15

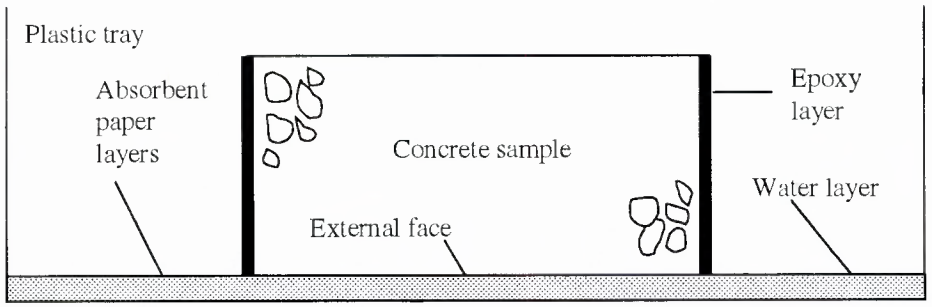

Figure 4.16: Water sorptivity test arrangement [68]

4.10 Carbonation depth tests

The depth of carbonation in a concrete structure can be established by chemical methods. It is measured by exposing fresh concrete and spraying on phenolphthalein indicator solution. This can be done either by breaking away a fresh surface, or by coring and splitting, or by cutting the core in the laboratory. The phenolphthalein indicator solution will remain clear where concrete is carbonated and turn purple/pink where concrete is still alkaline i.e. no carbonation.

4.10.1 Sample preparation

The concrete test specimens were removed from the carbonation chamber at regular intervals and 20 mm diameter cores were cut out of the specimens using the coring machine in the laboratory. Two cores were taken at each interval; these cores were then cleaned, washed and allowed to surface dry. Carbonation depth was then measured by spraying the fresh concrete cores with phenolphthalein indicator solution

(1 % by mass in ethanol/water solution), and the carbonation depth measured at six points along the outer surface of the core using a vernier calliper. The carbonation depths obtained for each core were then recorded and an average value obtained.

The concrete test specimens remained in the carbonation chamber until sufficient carbonation depths were reached. The object of this method of exposure was to allow the carbon dioxide to penetrate the concrete as rapidly as possible.

4.11 Summary

In this chapter the concrete mixes and materials used were introduced, and the various methods of measuring corrosion rates, probability of corrosion (half-cell potentials and resistivity measurements), amount of carbonation and the depth of penetration of the penetrating inhibitor were discussed in detail.

The Gecor 6 was introduced as the most suitable galvanostatic method for on-site determination of the polarisation resistance of reinforcement in reinforced concrete structures and for subsequent estimation of corrosion rates using the Stern-Geary equation. A basic description of the test set up was also described.

Durability index tests used to determine the fluid transport parameters of the concrete were also covered. . Basic descriptions of the test methods and important limitations in these various test methods were also described.

The results of all these test methods will be discussed with reference to corrosion rates in the chapter that follows.

5. RESULTS OF LABORATORY STUDIES

The concrete grade used to produce the corrosion block specimens was determined by casting twenty-four 100 mm cubes for durability index testing (i.e. oxygen permeability and water sorptivity), compressive strength tests and inhibitor penetration at each of the different strength grades shown in table 5.1. For the compressive strength tests the 100 mm cubes were cured using the wet curing regime mentioned in section 4.2. The compressive strengths were determined at 7, 14 and 28 days, in accordance with SABS Method 863:1994 [69]. The average cube compressive strengths are shown in table 5.1.

Table 5.1: Compressive strengths (MPa) obtained for different concrete grades.

Age (days)	Mean Compressive Strength (MPa)			
	Concrete grade			
	20 MPa	30 MPa	40 MPa	50 MPa
7	15.8	22.1	27.3	38.0
14	17.0	24.9	32.2	43.0
28	22.0	30.1	39.8	50.1

The 28-day strengths of the concrete shown in table 5.1 indicate that the required compressive strengths were obtained.

5.1 Durability index tests

Oxygen permeability index and water sorptivity tests were carried out as described in section 4.9. For each test result, four samples were tested. The average results obtained are given in table 5.2.

Table 5.2: Average oxygen permeability index and water sorptivity results.

Concrete grade (MPa)	Average oxygen permeability index (**Dry 1** cured)	Average oxygen permeability index (**Dry 2** cured)	Average Sorptivity (**Dry 1** cured) (mm/√h)	Average Sorptivity (**Dry 2** cured) (mm/√h)
20	8.91	10.01	12.7	6.60
30	9.33	10.14	14.2	6.30
40	9.65	10.23	9.80	5.20
50	9.91	10.44	6.20	4.80

Dry 1-Samples dry cured in the laboratory at temperature and relative humidity of 25±5°C and 68±5 % respectively for 27 days after stripping at one day.
Dry 2- Samples stripped at one day, then wet cured in the water bath for 6 days at temperature of 25±2°C, and then dry cured in the laboratory for 21 days at a temperature and relative humidity of 25±5°C and 68±5 % respectively.

Values of oxygen permeability and water sorptivity were within expected ranges. The grade 30 concrete mix was chosen to cast the corrosion test specimens as the relatively high oxygen permeability index (i.e. relatively low permeability) indicated a concrete with a good overall microstructure and macrostructure of the outer surface of

the concrete, provided adequate curing is carried out. It also indicated a concrete with good compaction and the absence of bleed voids and channels. Also, the water sorptivity of the grade 30 mix indicated a concrete that would permit the relative ease of movement of a wetting front under the action of capillary forces. The denser microstructure of the grade 30 concrete as compared to the grade 20 concrete indicated a concrete in which the penetrating corrosion inhibitor would more likely be retained.

5.2 Penetration of the corrosion inhibitor

The penetration depth of the corrosion inhibitor was determined 28 days after its application by taking cores from the 100 mm cubes of different strengths, one face of which had been coated with the penetrating corrosion inhibitor. Two cores were removed from each of the coated cube specimens and were tested using the qualitative test kit. The depth of penetration was determined using the qualitative method described in section 4.4.4.1. The results obtained are shown in table 5.3.

Table 5.3: Penetration depth of inhibitor at 28 days

Concrete grade (MPa)	Depth (mm)	Indicator colour	Qualitative rating	Organic nitrogen (estimated) (mg/g of concrete)
20	0-15	Red	Excellent	0.55 – 2.20
	15-30	Pink	Good	0.17 – 0.55
	30-45	Trace	Inadequate	0.06 – 0.28
	45-60	-	-	-
30	0-15	Red	Excellent	0.55 – 2.20
	15-30	Pink	Good	0.17 – 0.55
	30-45	Pink	Good	0.17 – 0.55
	45-60	Pink	Good	0.17 – 0.55
40	0-15	Red	Excellent	0.55 – 2.20
	15-30	Pink	Good	0.17 – 0.55
	30-45	Pale pink	Adequate	0.06 – 0.28
	45-60	Pale pink	Adequate	0.06 – 0.28
50	0-15	Red	Excellent	0.55 – 2.20
	15-30	Pink	Good	0.17 – 0.55
	30-45	Pale pink	Adequate	0.06 – 0.28
	45-60	Pale pink	Adequate	0.06 – 0.28

In the 20 MPa concrete the degree of penetration was poorer than that of the other concrete grades. This was attributed to the volatile nature of the inhibitor, and the relatively high permeability of the concrete. The inhibitor moves through the concrete as a front. The results indicate lower concentrations of the inhibitor deeper into the concrete, attributed to the loss of the inhibitor at the surface of the concrete due to the volatile nature of the inhibitor molecules and the higher porosity of the 20 MPa concrete. This implies that the low grade 20 MPa concrete loses much of the inhibitor from the surface before the inhibitor can penetrate deeper into the concrete. In the case of the 40 and 50 MPa concretes the penetration of the inhibitor was lower than that of the 30 MPa concrete, due to the lower permeability and denser nature of these

concretes. The grade 30 concrete in particular indicates a concrete in which the penetrating corrosion inhibitor is likely to penetrate effectively and be retained, and was therefore used to cast the corrosion test specimens.

The results also show that the inhibitor generally had penetrated the concrete to a depth of between 45 and 60 mm, well beyond the reinforcement (10 mm and 20 mm). It is suggested that a concentration of more than 0.06 mg of organic nitrogen per gram of concrete is sufficient to inhibit corrosion. The indicator colours shown in table 5.3 show that more than sufficient amounts of the inhibitor were present at all depths. It was therefore expected that some degree of inhibition would occur.

Grade 30 concrete was therefore chosen for a number of reasons:

- Typical structural grade.
- "Penetrable" by inhibitor and wetting fronts.
- Retains inhibitor well.
- Higher grade concretes are inherently more durable, and therefore the inhibitor is less likely to be used in these cases.

5.3 Accelerated carbonation of samples

The test blocks were kept in the carbonation chamber until sufficient carbonation depths had been reached. This chamber was initially maintained at a carbon dioxide level of 5±1 %, and at a temperature of 30±1 °C to ensure accelerated carbonation of the samples. Regular monitoring of the carbon dioxide content, temperature and relative humidity of the chamber was also carried out to ensure that the required levels were maintained.

5.3.1 Phenolphthalein test to determine depth of carbonation

Cores of 20 mm diameter were taken from seven (see table 5.4) of the corrosion test specimens at regular intervals during accelerated carbonation and were sprayed with phenolphthalein indicator to test for the depth of carbonation. This procedure was carried out to determine if the required carbonation depths were reached. After the first two coring procedures were carried out at ages of 21 and 56 days, it was apparent that sufficient carbonation depths had not been reached. The carbon dioxide content in the chamber was therefore increased to 10 %, and was maintained at this level to accelerate the rate of carbonation even further. The temperature was unchanged and remained at 30 °C. The results of the phenolphthalein tests to determine the depth of carbonation are shown in table 5.4.

Table 5.4: Carbonation depths

Sample number	Date	Number of days	Carbonation depth (mm)	CO_2 concentration (%)
Control 1	9/10/00	21	10.0	5
Control 3	9/10/00	21	10.7	
BC 5	13/11/00	56	17.0	5
Control 4	4/12/00	77	20.0	5
BC 8	4/12/00	77	19.5	
AC 11	4/12/00	77	20.0	
Control 1	4/01/00	107	22.0	5

In order to determine the additional number of days that would be required to carbonate the 40 mm cover blocks that were in the carbonation chamber a graph was plotted. The graph shows the number of days versus carbonation depth and is illustrated in figure 5.1. A power curve was also fitted to the results in order to permit extrapolation. The power curve has the relationship:

$$\text{Carbonation depth (mm)} = 2.3807\ t^{0.4848} \qquad (5.1)$$

where t is the time in days.

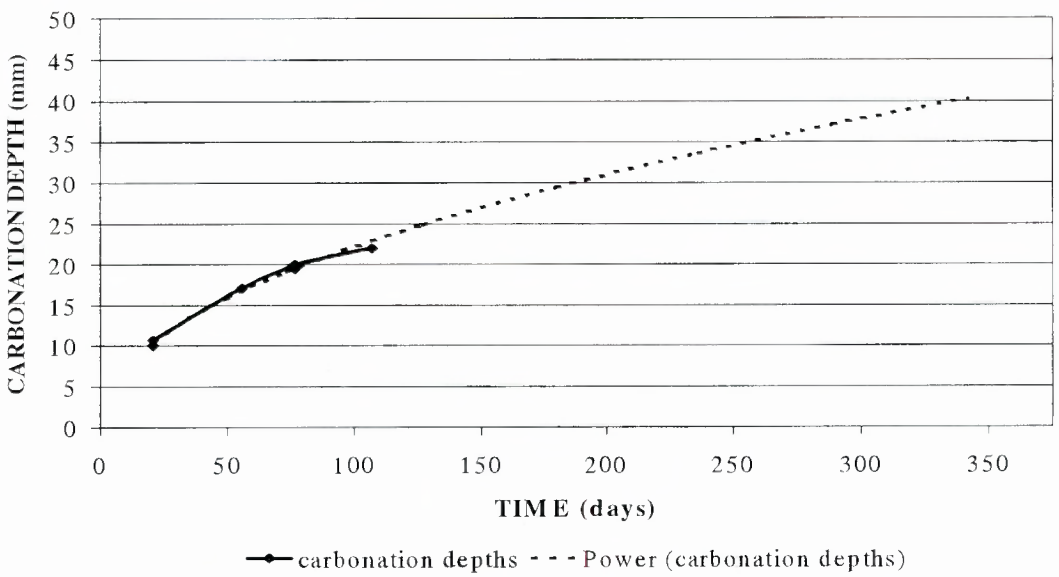

Figure 5.1: Carbonation depths, 30 MPa concrete blocks.

From figure 5.1 it was apparent that in order to achieve a carbonation depth of 40 mm a further seven or eight months would be required. It was therefore decided to reduce the cover of the 40 mm blocks to about 10 mm. This was done since only about two months would then be required to obtain the new desired carbonation depth of 10 mm;

also a cover of 10 mm, while not occurring very often, was not entirely unrealistic based on cover surveys carried out by other investigations. Therefore, 30 mm was sliced off the 40 mm cover test specimens using the diamond saw in the laboratory, leaving a cover of about 10 mm.

Carbonation depths were thereafter monitored on the 'new' 10 mm cover test specimens at regular intervals. Carbonation depths obtained are shown in table 5.5.

Table 5. 5: Carbonation depths for 10 mm cover test specimens

Sample	Number of days	Carbonation depth (mm)	CO_2 concentration (%)
Control 1	28	6	10
Control 2	28	7	
BC 5	50	11	10
BC 6	50	9	
AC 10	50	10	
BC 5	62	13	10
Control 1	62	11	
AC 9	62	15	

In the 20 mm cover test specimens the carbonation depth achieved at 28 days was generally greater (10 mm) than in the case of the 10 mm cover specimens (6 mm). This can be attributed to the fact that since the cover was reduced from 40 to 10 mm by slicing off the surface 30 mm of the concrete, the carbonation face now has different micro-structural properties. This new face would be less permeable compared with the initial 10 mm layer of surface concrete, thereby affecting the rate at which carbonation is taking place.

Once sufficient carbonation depths were obtained the test block samples were removed from the carbonation chamber and were placed in the laboratory environment. The relative humidity was measured regularly and was found to vary between 60 and 65 %. The temperature in the laboratory at the time was 25±5 °C. The 'AC' test specimens were left in the laboratory environment to dry for two weeks prior to application of the inhibitor in order for the concrete to stabilise and dry sufficiently for quick penetration of the corrosion inhibitor.

5.4 Measurement of cover to reinforcement

Measurements were carried out on the concrete test specimens at a number of positions to determine the cover to reinforcement, using an electronic micro-cover meter (Koelectric Limited). The results obtained on each of the concrete specimens are shown in table 5.6.

Table 5.6: Concrete covers (mm)

Sample	Concrete cover at three different points (mm)	Average concrete cover (mm)
Cont 1	6, 7, 9	7.3
Cont 2	7, 9, 8	8.0
Cont 3	27, 27, 26	26.7
Cont 4	25, 25, 26	25.3
BC 5	8, 9, 9	8.7
BC 6	9, 10, 11	10.0
BC 7	25, 27, 26	26.0
BC 8	23, 24, 26	24.3
AC 9	5, 6, 6	5.7
AC 10	8, 8, 8	8.0
AC 11	27, 27, 26	26.7
AC 12	29, 29, 28	28.7

The variations in the cover to reinforcement were due to the shifting of the reinforcing bars during the casting of the concrete. A variation in cover was also observed in the 10 mm cover samples due to the slicing off 30 mm of the original 40 mm cover concrete samples (discussed in later section).

5.5 Application of inhibitor

During the drying period the surfaces of the samples that were to be treated with the penetrating inhibitor after carbonation were cleaned thoroughly using a wire brush. The surface was cleaned further by blowing off the loose material and dust particles. The corrosion inhibitor was then applied on the concrete specimens at a rate of 0.1 litres per square meter for each of the three applications as specified by the manufacturer. The three coats were applied using a normal paintbrush. Each coat of the penetrating inhibitor was allowed to dry for twenty-four hours before application of the next coat. Twenty-four hours after the application of the final coat, the concrete was wetted with normal tap water, and this procedure was repeated for two consecutive days. The application of water saturates the surface layer of the concrete to a certain extent thereby preventing the evaporation or escape of the inhibitor from the concrete and thus aiding its penetration.

28 days after the application of the inhibitor the qualitative test for determining the depth of penetration of the inhibitor was performed by taking 20 mm diameter cores from the appropriate test specimens. The concentration of the penetrating corrosion inhibitor was also measured 5 and 10 months after application.

The results obtained are shown in tables 5.7 and 5.8 for specimens treated with the inhibitor before and after the carbonation process respectively.

Table 5.7: Qualitative test results for depth of penetration of inhibitor for samples treated with the inhibitor before the carbonation process.

	Depth (mm)	BC 5 Cover = 8.7 mm		BC 6 Cover = 10.0 mm		BC 7 Cover = 26.0 mm		BC 8 Cover = 24.3 mm	
		Indicator colour	Qualitative rating	Indicator colour	Qualitative rating	Indicator colour	Qualitative rating	Indicator colour	Qualitative rating
28 days	0 - 15	Red	Excellent	Pink	Good	Pink	Good	Red	Excellent
	15 - 30	Pink	Good	Pink	Good	Pink	Good	Pink	Good
	30 - 45	Pink	Good	Pink	Good	Pink	Good	Pink	Good
	45 - 60	Pink	Good	Pink	Good	Pink	Good	Pink	Good
5 months	0 - 15	Pink	Good	Pink	Good	Pink	Good	Pink	Good
	15 - 30	Pink	Good	Pink	Good	Pink	Good	Pink	Good
	30 - 45	Pink	Good	Pink	Good	Pink	Good	Pink	Good
	45 - 60	Pink	Good	Pink	Good	Pink	Good	Pink	Good
10 months	0 - 15	Pale pink	Adequate	Pale pink	Adequate	Pale pink	Adequate	Pale pink	Adequate
	15 - 30	Pale pink	Adequate	Pink	Good	Pale pink	Adequate	Pink	Good
	30 - 45	Pink	Good	Pink	Good	Pink	Good	Pink	Good
	45 - 60	Pink	Good	Pink	Good	Pink	Good	Pink	Good

Table 5.8: Qualitative test results for depth of penetration of inhibitor for samples treated with the inhibitor after the carbonation process.

	Depth (mm)	AC 9 Cover = 5.7 mm		AC 10 Cover = 8.0 mm		AC 11 Cover = 26.7 mm		AC 12 Cover = 28.7 mm	
		Indicator colour	Qualitative rating	Indicator colour	Qualitative rating	Indicator colour	Qualitative rating	Indicator colour	Qualitative rating
28 days	0 - 15	Red	Excellent	Red	Excellent	Red	Excellent	Red	Excellent
	15 - 30	Pink	Good	Red	Excellent	Red	Excellent	Pink	Good
	30 - 45	Pink	Good	Pink	Good	Pink	Good	Pink	Good
	45 - 60	Pink	Good	Pink	Good	Pink	Good	Pink	Good
5 months	0 - 15	Pink	Good	Pink	Good	Pink	Good	Pink	Good
	15 - 30	Pink	Good	Pink	Good	Pink	Good	Pink	Good
	30 - 45	Pink	Good	Pink	Good	Pink	Good	Pink	Good
	45 - 60	Pink	Good	Pink	Good	Pink	Good	Pink	Good
10 months	0 - 15	Pale pink	Adequate	Pale pink	Adequate	Pink	Good	Pale pink	Adequate
	15 - 30	Pale pink	Adequate	Pink	Good	Pink	Good	Pale pink	Adequate
	30 - 45	Pink	Good	Pink	Good	Pink	Good	Pink	Good
	45 - 60	Pink	Good	Pink	Good	Pink	Good	Pink	Good

The rapid penetration of the penetrating corrosion inhibitor into the Grade 30 concrete was due to the volatile nature of the material that encourages quick vapour phase transmission. Also the permeability and dryness of the concrete played a significant role in causing a swift ingress and high concentration of the inhibitor.

Vapour diffusion is an important mechanism especially in unsaturated concrete. However, in the presence of moisture where most of the pore structure may be

saturated this is significantly reduced. It is therefore of importance that samples are air dried prior to application of the inhibitor for optimum penetration of the penetrating corrosion inhibitor.

The performance of the penetrating corrosion inhibitor was also dependent on its ability to penetrate the concrete and reach the steel reinforcement that was undergoing corrosion. Penetration results given previously for different concrete grades generally showed excellent penetration. However, the results indicated that the penetration is dependent on the grade and hence the porosity and permeability of the concrete.

The penetration data from the 30 MPa corrosion test specimens where the inhibitor was applied before accelerated carbonation indicates that the inhibitor had penetrated the concrete to a depth of between 45 and 60 mm, well beyond the reinforcement depth of 10 and 20 mm, 28 days after application. The degree of penetration can be attributed to the nature of the inhibitor and the permeability of the grade 30 concrete. The relatively dry nature of the concrete after it was allowed to surface dry for a few weeks prior to application of the inhibitor also allowed for the rapid absorption of the penetrating inhibitor. The concentrations of the inhibitor shown in table 5.8 were considered sufficient for corrosion inhibition to occur.

The penetration of the inhibitor was also tested 5 and 10 months after application. The five month penetration results for the samples treated with the inhibitor before the carbonation process showed that more than adequate amounts of the inhibitor were still present at all depths. After ten months the inhibitor was still present at all depths, however the concentration of the inhibitor was higher at deeper levels (30 – 45 mm and 45 – 60 mm) compared to shallower levels (0 – 15 mm and 15 – 30 mm). This result suggested that the inhibitor was moving through the concrete as a front; it also indicated that some of the inhibitor was lost at the surface of the concrete. This was attributed to the volatile nature of the inhibitor molecules. The concentration of the inhibitor at the surface was different at 1 month, 5 months and 10 months. The concentrations determined at 10 months after application of the penetrating corrosion inhibitor were lower than the concentrations determined at one and five months. This difference in concentration of the inhibitor observed at the same depth in concrete at 1, 5 and 10 months could be attributed to local differences in the surface condition of the concrete. Most importantly however the results showed that at cover levels of 10 and 20 mm adequate amounts of the corrosion inhibitor were present in all cases at 1, 5 and 10 months, and therefore inhibition of corrosion activity should be observed through a reduction in corrosion rates measured if the inhibitor is effective.

The penetration data obtained by taking cores from samples treated with the inhibitor after the carbonation process were very similar to the results obtained from the samples treated with the inhibitor before the carbonation process. At 28 days the inhibitor had penetrated the concrete to a depth of between 45 to 60 mm, with more than adequate concentrations of the penetrating corrosion inhibitor at all depths in the samples tested. This indicated that sufficient amounts of the inhibitor had reached the reinforcement and that a decrease in corrosion activity in the specimens treated could be expected after the application. The degree of penetration at an early age was once again attributed to the permeability of the grade 30 concrete and also the dry nature of the concrete after it was allowed to surface dry for a few weeks prior to the application of the inhibitor.

The penetration of the inhibitor into the samples treated with the inhibitor after the carbonation process was also tested 5 and 10 months after application. The five-month penetration results indicated that more than adequate amounts of the inhibitor were present at all depths in all the test specimens. After ten months the inhibitor was still present at all depths but at higher concentrations at deeper levels than at the surface. This indicated that the corrosion inhibitor was lost at the surface of the concrete, as had occurred in the specimens treated with the inhibitor before the carbonation process. Also, as in the case of the samples treated with the inhibitor before the carbonation process, the concentration of the inhibitor at the surface was different at 1, 5 and 10 months. This was once again attributed to the local differences in the surface condition of the concrete, the volatile nature of the inhibitor molecules, and the permeability of the 30 MPa concrete. These results once again showed that adequate amounts of the penetrating corrosion inhibitor were present at the level of the reinforcement (10 and 20 mm) in all cases, and therefore a decrease in corrosion activity should be observed after the application of the inhibitor if the inhibitor is effective.

5.6 Corrosion monitoring

5.6.1 Corrosion rate monitoring cycles for 10 and 20 mm cover samples

Corrosion rate measurements were taken using the galvanostatic linear polarisation resistance technique (Gecor 6) mentioned previously in section 4.8.2.2. The first wetting and drying cycle described in section 4.7 was initially used. The samples were placed in a water bath and three hours prior to corrosion rate monitoring being done, the samples were removed and allowed to surface dry in the laboratory environment which maintained a temperature and relative humidity of 25±5 °C and 65±5 % respectively. About four hours after corrosion monitoring the samples were replaced in the water bath. The samples were therefore continuously left in the water bath except for seven hours during Gecor testing when the samples were removed from the water bath and placed in laboratory conditions. This procedure was carried out on a fortnightly basis and corrosion rates were monitored. This initial wetting and drying cycle was followed until cycle number 28 (i.e. 14 weeks in total) and cycle number 13 (i.e. 7 weeks in total) for the 10 and 20 mm cover test specimens respectively.

However, due to an increase in values of measured resistivity of the concrete samples using the Wenner probe, it was decided to introduce a different wetting and drying cycle with a longer drying period. This increase in resistivity of the concrete was thought to be due to the effect of a different resistivity at the surface layer of the concrete tested. A surface layer beneath the measurement contacts having a resistivity different to that of the underlying concrete has the effect of distorting the applied current field, causing errors in measurement of the resistivity of the underlying concrete [17]. The carbonation of concrete forms a relatively high-resistivity surface layer. The wetting of the concrete produces a second low-resistivity surface layer on top of the carbonation layer. It has been found that this distortion in the current field caused due to the two surface layers will produce an artificially high resistivity measurement of the underlying concrete [17].

The second regime was introduced at cycle number 28 and cycle number 13 in the 10 and 20 mm cover test specimens respectively. The samples were allowed to surface dry for four days before they were replaced in the water bath for the next three days. This cycle was introduced as it was thought that excessive saturation might be limiting the availability of oxygen to the cathode, thereby stifling the corrosion process. This new wetting and drying cycle however resulted in very erratic results with large differences between the corrosion rates at the end of the wet and dry cycles.

Therefore a third wetting and drying cycle was introduced at cycle number 38 and cycle number 23 (i.e. seven weeks later) in the 10 mm and 20 mm cover samples respectively. This new cycle had a longer wetting period and a shorter drying period. The samples were allowed to surface dry for two days after a Gecor measurement was taken on a Monday and then they were replaced in the water bath for the remaining five days. Prior to a Gecor measurement the test specimens were allowed to surface dry for about two hours.

5.6.2 Performance of the penetrating corrosion inhibitor in 10 mm cover samples

Initial corrosion rate measurements on the 10 mm cover specimens were started on the 17 April 2001, and were taken on a daily basis for a period of five days. During this period very unstable and low corrosion rate values ranging from 0.001 to about 0.09 $\mu A/cm^2$ were obtained. This was ascribed to the dry nature of the concrete, since too little moisture will electrolytically stifle the corrosion rate. At this stage no wetting regimes were used. The specimens were stored in a special room where the temperature and relative humidity were maintained at 25±2 °C and 68±5 % respectively. Due to the erratic nature of the results obtained the samples were placed in a water bath for two consecutive days before corrosion monitoring was carried out on the 24 April 2001. The corrosion rate measurements and the half-cell potential measurements obtained using the Gecor are shown in figures 5.2 and 5.3, where the corrosion rates and half-cell potentials are expressed as averages of the two samples in each case.

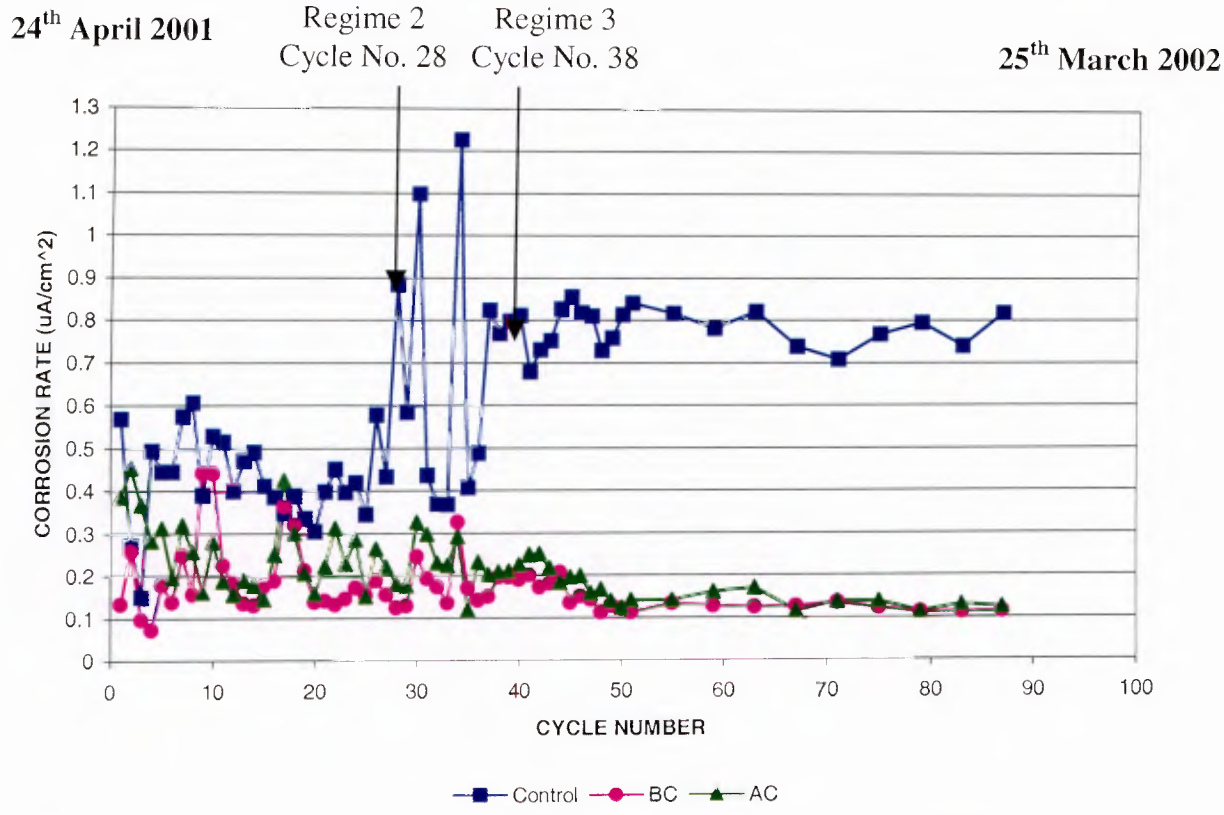

Figure 5.2: Corrosion rate measurements for 10 mm cover test specimens.

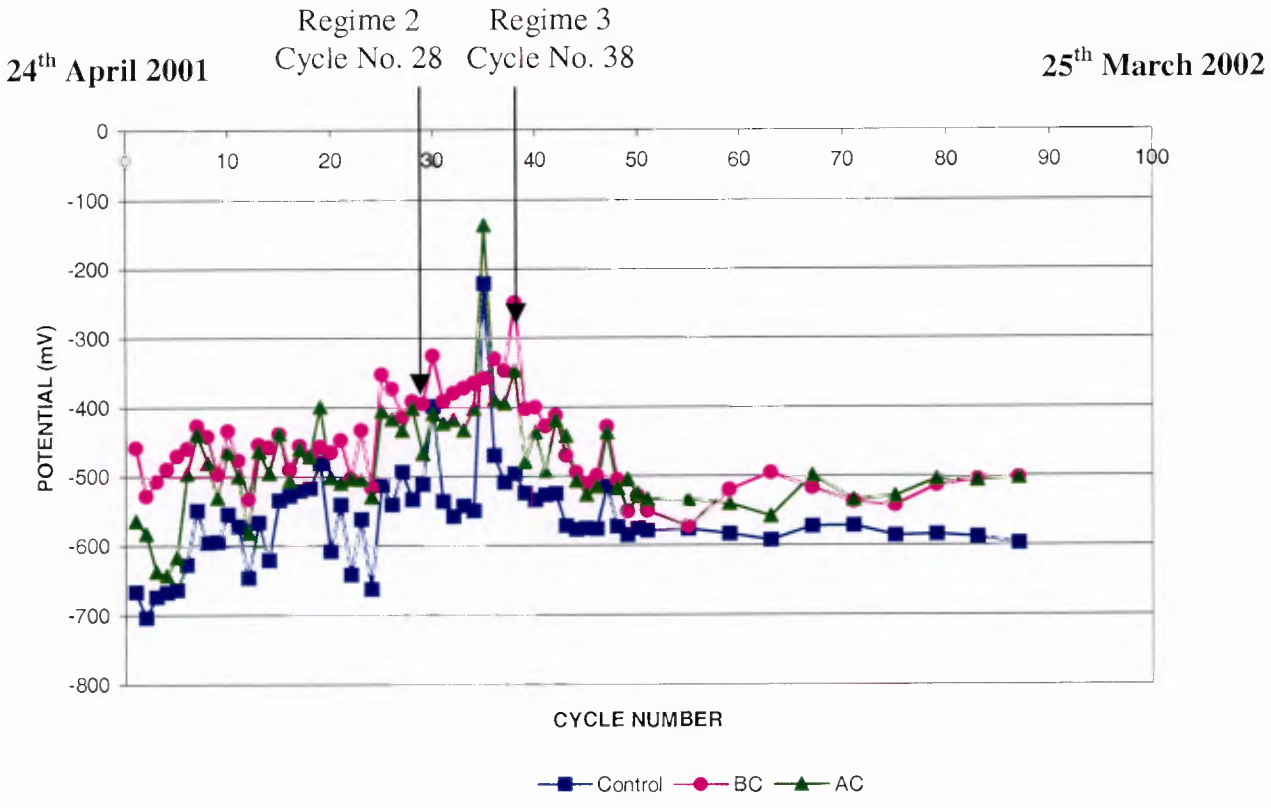

Figure 5.3: Half-cell potential measurements for 10 mm cover specimens.

From the corrosion rate data of the six test specimens shown in figure 5.2 it can be seen that the corrosion rates measured in the first regime were variable. On introduction of the second wetting and drying regime at cycle number 28 (6 August 2001), a significant change in the pattern of the corrosion rate measurements was observed in the control samples where no inhibitor was applied. Corrosion rate measurements were taken at the end of the wetting and again at the end of the drying period. At the end of the wetting cycle a large increase in corrosion rates measured was observed and at the end of the drying period the corrosion rates measured were comparatively low. This indicated that sufficient conditions were obtained at the end of the wet cycle to induce high corrosion rates, which reduced at the end of the drying cycle (i.e. moisture and oxygen were optimised at the steel in terms of corrosion at the end of the wet cycle, and at the end of the drying cycle too little moisture was available stifling the corrosion process). It also implies that measured corrosion rates are highly sensitive to the 'micro-environment' at the level of the steel. A wetter concrete gives higher corrosion rates, as opposed to a somewhat drier concrete, which gives lower corrosion rates. Also, this phenomenon is far more marked in low cover samples than in samples with higher cover, as observed in the 20 mm cover specimens, due to quicker wetting and drying.

This large difference between the corrosion rates at the end of the wet and dry cycles was however only observed in the control specimens where no inhibitor was applied. In samples treated with the penetrating inhibitor before and after the carbonation process, there were no large fluctuations in the corrosion rates observed. It was therefore deduced that the penetrating inhibitor was able to control corrosion rates even when the wetting and drying cycles were varied in an attempt to obtain very high corrosion rates, a further indication of its effectiveness. On introduction of the third wetting and drying regime at cycle number 38 much more stable corrosion rates were observed.

Regime 3 was found to be the most effective regime, yielding the most stable corrosion rates. It is therefore observed that a move from 3-day wet (regime 2) to 5 day wetting regime (regime 3) stabilised corrosion rates. Sufficient moisture and oxygen are now present for corrosion to occur. Sufficient moisture is obviously present, since even 3 day wetting (regime 2) was sufficient to provide adequate corrosion rates. Four day drying (regime 2) had the effect of starving the system of moisture (drying out too much), while 2 day drying (regime 3) did not. Therefore, the effectiveness of these cycles will also depend on the nature of the concrete (i.e. permeability, porosity etc.).

The results obtained therefore show the effectiveness of the inhibitor in the 10 mm cover specimens. The control specimens with no inhibitor applied maintained the highest corrosion rates and the most negative potentials. The corrosion rates in this case ranged from about 0.1 to 1.2 $\mu A/cm^2$ corresponding to very active corrosion. The potentials in the control samples ranged from about -220 to -700 mV also indicative of active corrosion.

The corrosion rates of the blocks where the penetrating corrosion inhibitor was applied before the carbonation process (BC) showed much lower values of corrosion rates and half-cell potentials in comparison to the control specimens. The ranges in this case were between 0.05 and 0.5 $\mu A/cm^2$, and –240 and –570 mV respectively. In

the samples treated with the penetrating inhibitor after the initiation of carbonation the corrosion rates and half-cell potentials were also much lower in comparison to the control samples, maintaining values of between 0.07 and 0.5 $\mu A/cm^2$, and –135 and –640 mV respectively. Further, the specimens treated with the inhibitor before and after the carbonation process showed a steady decrease in corrosion rate, gradually reaching the 0.1 $\mu A/cm^2$ line.

Three Point moving Average

From the three-point moving average data shown in figures 5.4 and 5.5 it is easier to observe the trends. A steady increase in the corrosion rates of the control samples was observed as opposed to a steady decrease in corrosion rates in the samples that were treated with the inhibitor before and after the carbonation process.

The trends observed for the half-cell potentials however were not as conclusive as the corrosion current densities observed. This implies that the different regimes were having their effects primarily through their effects on moisture content at the steel in the cover region, since if oxygen was really 'starved' at the cathode, very negative potentials would have been observed.

Readings were relatively stable and did not exhibit large fluctuations. Negative potentials greater than –250mV were observed during the testing period. There was little discernable difference between the various systems being tested. However, a slight positive shift in potential in specimens treated with the penetrating inhibitor as compared to the control samples was observed. This difference in potential was considered to be due to the action of the penetrating corrosion inhibitor. The inhibitor is adsorbed onto the steel surface. The adsorbed organic layer inhibits corrosion by interfering with anodic dissolution of iron while simultaneously disrupting the reduction of oxygen at the cathode thereby reducing corrosion rates and half- cell potentials.

These results therefore clearly indicate:

a) That the penetrating corrosion inhibitor is capable of delaying the onset of corrosion, as shown in the blocks that were treated with the inhibitor before the carbonation process, and
b) The effectiveness of the penetrating inhibitor in its ability to reduce the corrosion rate, as seen in the specimens that were treated with the inhibitor after the initiation of corrosion due to carbonation.

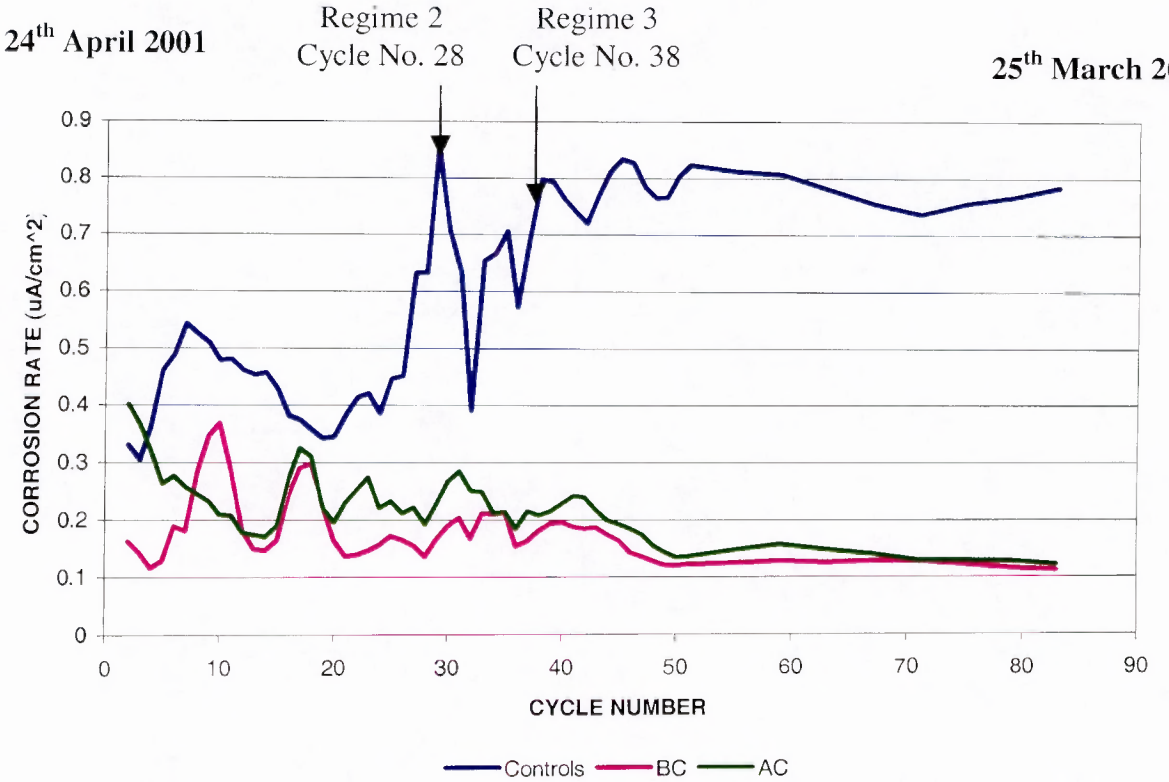

Figure 5.4: Three-point moving averages of corrosion rates for 10 mm cover samples

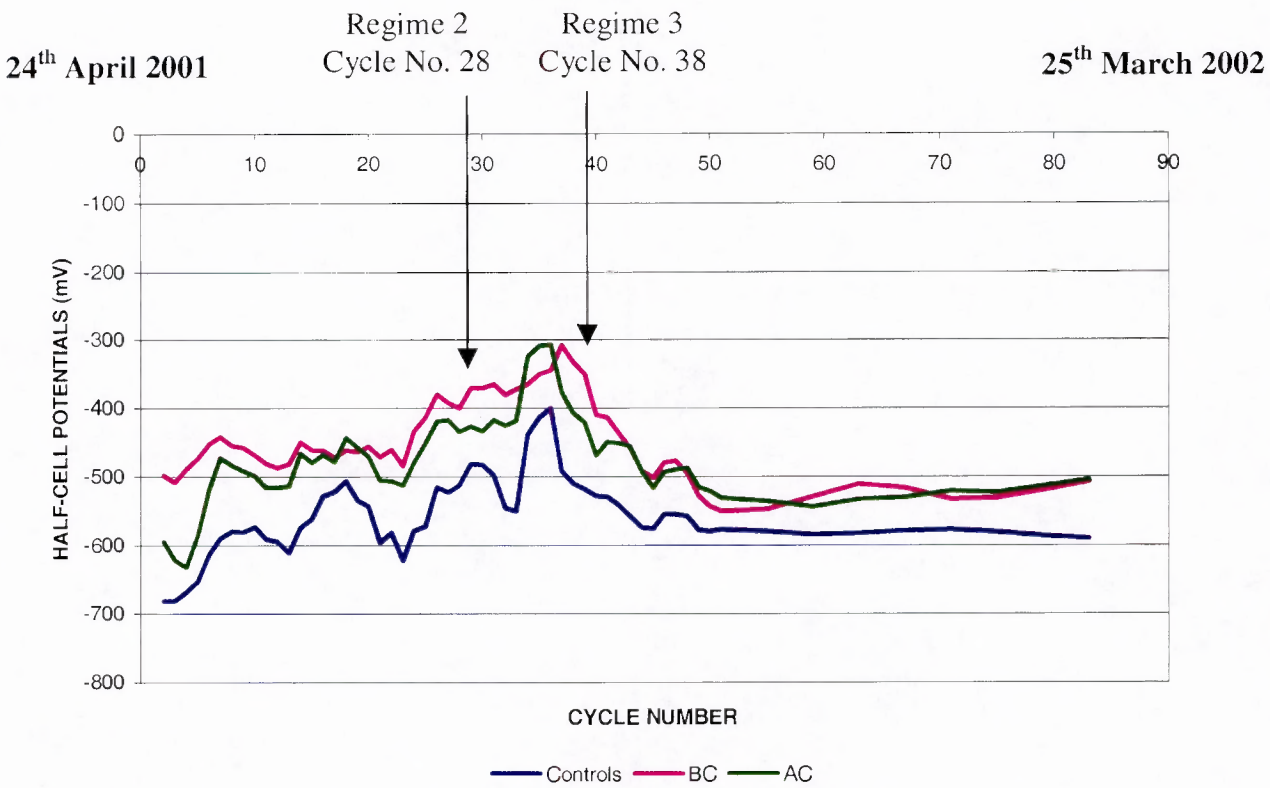

Figure 5.5: Three-point moving average of half-cell potential data for 10 mm cover samples.

In order to validate the corrosion rate measurements obtained using the Gecor, corrosion rate measurements were also taken using the Coulostatic method (Galvanostatic pulse method) between cycles 1 and 5. Detailed results obtained for corrosion rates and half-cell potentials using the Coulostatic method are shown in the Appendix D. Table 5.9 shows the comparative results obtained using the Gecor 6 and the Coulostatic method.

Table 5.9: Measurements obtained using the Gecor and the Coulostatic method.

Cycle No.	1		2		3		4		5	
Sample	Gecor	Coulostatic	Gecor	Coulostatic	Gecor	Coulostatic	Gecor	Coulostatic	Gecor	Coulostatic
	($\mu A/cm^2$)		($\mu A/cm^2$)		($\mu A/cm^2$)		($\mu A/cm^2$)		($\mu A/cm^2$)	
Cont 1	0.797	0.555	0.150	0.110	0.107	0.009	0.579	0.623	0.542	0.522
Cont 2	0.341	0.412	0.390	0.412	0.193	0.115	0.408	0.410	0.345	0.406
BC 5	0.213	0.210	0.192	0.222	0.032	0.100	0.017	0.100	0.184	0.222
BC 6	0.053	0.009	0.320	0.345	0.161	0.179	0.127	0.133	0.174	0.170
AC 9	0.351	0.321	0.556	0.500	0.440	0.509	0.422	0.419	0.322	0.345
AC 10	0.418	0.388	0.351	0.320	0.291	0.311	0.140	0.150	0.301	0.288

These results confirm the accuracy of the corrosion rates taken using the Gecor 6 as values obtained fall within the same ranges.

The half-cell potential measurements taken using the Gecor 6 were also validated using measurements taken using a copper/ copper sulphate half-cell, see table 5.10. Results obtained once again confirmed the reliability of potential measurements obtained using the Gecor 6 as very similar results were obtained. The half-cell potentials were also measured between cycles 1 and 5 and are shown in Appendix D.

Table 5.10: Measurements obtained using the Gecor and copper/copper sulphate half-cell

Cycle No.	1		2		3		4		5	
Sample	Gecor	Half-cell	Gecor	Half-cell	Gecor	Half-cell	Gecor	Half-cell	Gecor	Half-cell
	(mV)		(mV)		(mV)		(mV)		(mV)	
Cont 1	-715.4	-758.9	-727.6	-633.5	-756.2	-688.7	-740	-699.8	-735	-705.5
Cont 2	-617.5	-600	-679.7	-600.5	-592	-569.7	-594.2	-555.8	-592.1	-610.2
BC 5	-497.3	-466.5	-509.4	-501.2	-525.2	-511.2	-490.6	-512	-451.6	-455
BC 6	-419.4	-456.2	-547.6	-577.3	-596.8	-540.6	-488.3	-500.3	-489.2	-399.2
AC 9	-597.6	-625.4	-620.8	-645.3	-698.3	-503.8	-699.5	-645.9	-688.4	-611.2
AC 10	-531.9	-500	-545.9	-550.8	-576.9	-498.5	-586.2	-500	-545.3	-500.2

However, it appears that the Gecor 6 is always slightly higher for half-cell potential values obtained. Resistance measurement data is shown in Appendix D.

Relationship between resistivity (k.ohm.cm) measured using the Wenner probe and resistance (k.ohm) measured using the Gecor

Resistivity measurements were taken using the Wenner probe and resistance was also measured using the Gecor 6 at each cycle. When the relationship between resistivity and resistance for each specimen was compared, a definite pattern was observed. This relationship was analysed using all the data recorded for the entire test period. The linear relationship established between these two data sets is shown in figure 5.6. The correlation coefficient (R) was found to be 0.906. The relationship between resistivity of the concrete and the resistance measured using the Gecor 6 was used to determine resistivity of the concrete when only the Gecor was used to measure resistances.

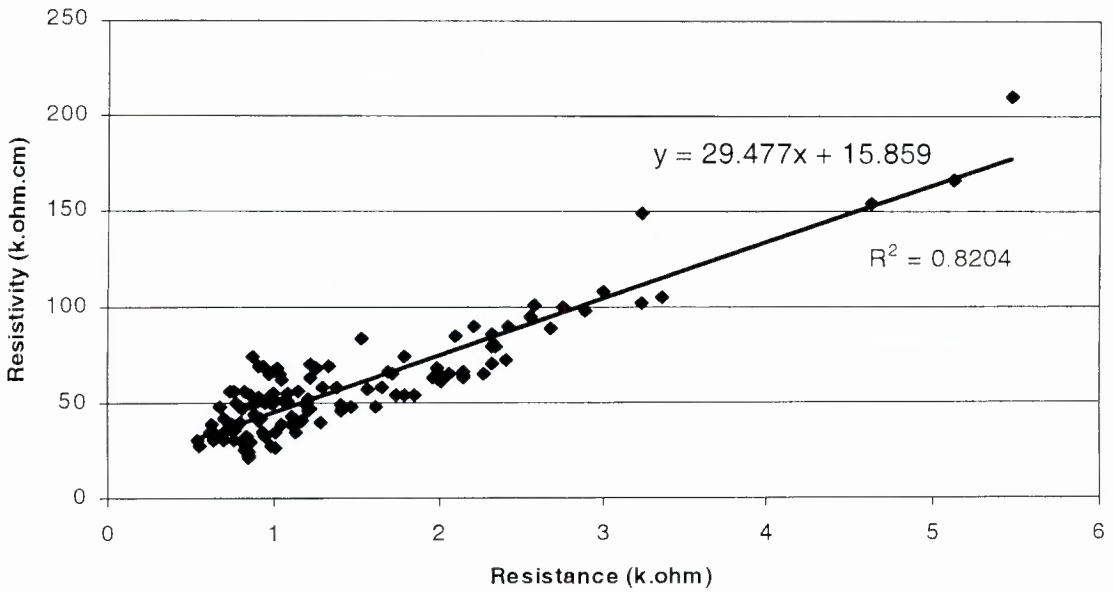

Figure 5.6: Relationship between resistivity of concrete and resistance

It is important to note that this relationship was only used as a guide to determine the resistivity of the concrete using the Gecor. This investigation was also carried out on site investigations (results also included in figure 5.6). It is therefore assumed that this relationship holds true for the site concrete.

5.6.3 Performance of the penetrating corrosion inhibitor at 20 mm cover

Corrosion rate measurements were first carried out on the 18 June 2001, seven days after removal from the carbonation chamber. The same wetting and drying cycles were used as for the 10 mm cover samples. The samples were placed in a water bath for seven days prior to initial Gecor measurement to ensure that sufficient moisture was present for corrosion to be initiated. The samples were placed in the water bath, and three hours before Gecor testing was done, the samples were removed and allowed to surface dry. Four hours after corrosion monitoring the samples were replaced in the water bath. The samples were therefore continuously left in the water bath except for the seven hours during which the samples were placed under

laboratory conditions. Corrosion rate measurements and half-cell potential measurements obtained using the Gecor for the 20 mm cover specimens are shown in figures 5.7 and 5.8 where the corrosion rates and the half-cell potentials are expressed as averages of the two samples in each case.

From the corrosion rate data shown in figure 5.7 it was seen that initially low corrosion rates were observed in the specimens treated with the inhibitor as well as in the control samples with no inhibitor. This was attributed to the unstable nature of the concrete in the initial stages, after removal from the extreme exposure conditions in the carbonation chamber. The results show that similar trends to the 10 mm cover test specimens were also maintained in the 20 mm cover specimens, i.e. the penetrating corrosion inhibitor was capable of delaying the onset of corrosion, as shown in the blocks that were treated with the inhibitor before the carbonation process; and the effectiveness of the penetrating inhibitor in its ability to reduce the corrosion rate, as seen in the specimens that were treated with the inhibitor after the initiation of corrosion due to carbonation.

However, lower corrosion rates and less negative half-cell potentials were observed compared with the 10 mm cover samples. This was attributed to the higher cover to reinforcement, thereby resulting in a lower rate at which corrosion is taking place. The control samples with no inhibitor applied once again maintained the highest corrosion rates and the most negative potentials. The corrosion rates and half-cell potentials in this case ranged from about 0.1 to 0.5 $\mu A/cm^2$, and -210 to -615 mV respectively. The corrosion rate values of the 20 mm cover specimens that were treated with the inhibitor before the carbonation process and after the carbonation process showed much lower corrosion rates of between 0.09 and 0.23 $\mu A/cm^2$, and 0.1 and 0.24 $\mu A/cm^2$ respectively. The half-cell potentials maintained in the specimens treated with the penetrating inhibitor before and after the carbonation process were also very similar to half-cell potentials in specimens with no inhibitor, maintaining potentials of between –315 and -600 mV, and –315 and –565 mV respectively.

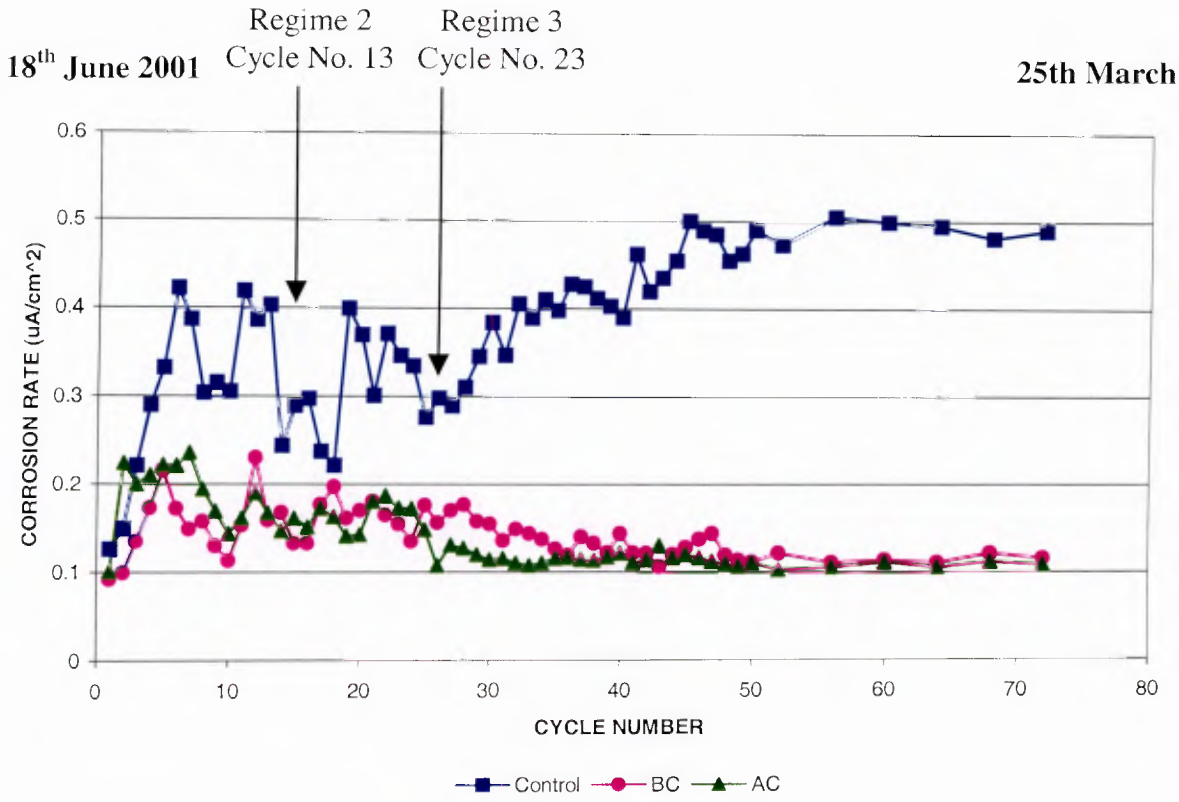

Figure 5.7: Corrosion rate measurements for 20 mm cover samples

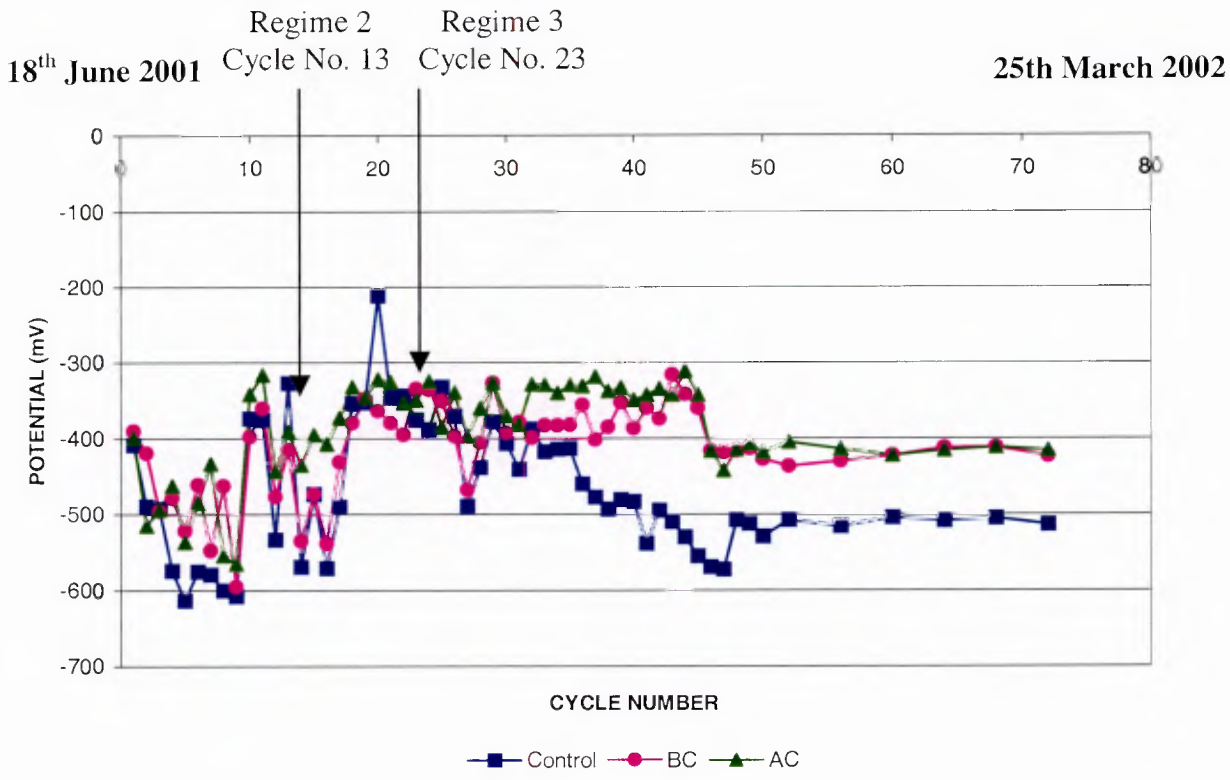

Figure 5.8: Half-cell potential measurements for 20 mm cover samples.

As observed previously in the 10 mm cover specimens, the samples treated with the inhibitor before and after accelerated carbonation also showed a steady decrease in the corrosion rate observed towards the 0.1 $\mu A/cm^2$ level. The drastic fluctuations observed due to the introduction of the second wetting and drying regime in the 10 mm cover samples, were, however, not observed in the 20 mm control samples This was attributed to the higher cover to reinforcement in this case. It was previously mentioned that the corrosion rates measured are highly sensitive to the 'micro-environment' at the level of the steel. In the 20 mm cover sample, the fluctuation in moisture at the level of the steel is much reduced due to the higher cover, implying that moisture conditions at the steel are far more stable; this is illustrated schematically in figure 5.9.

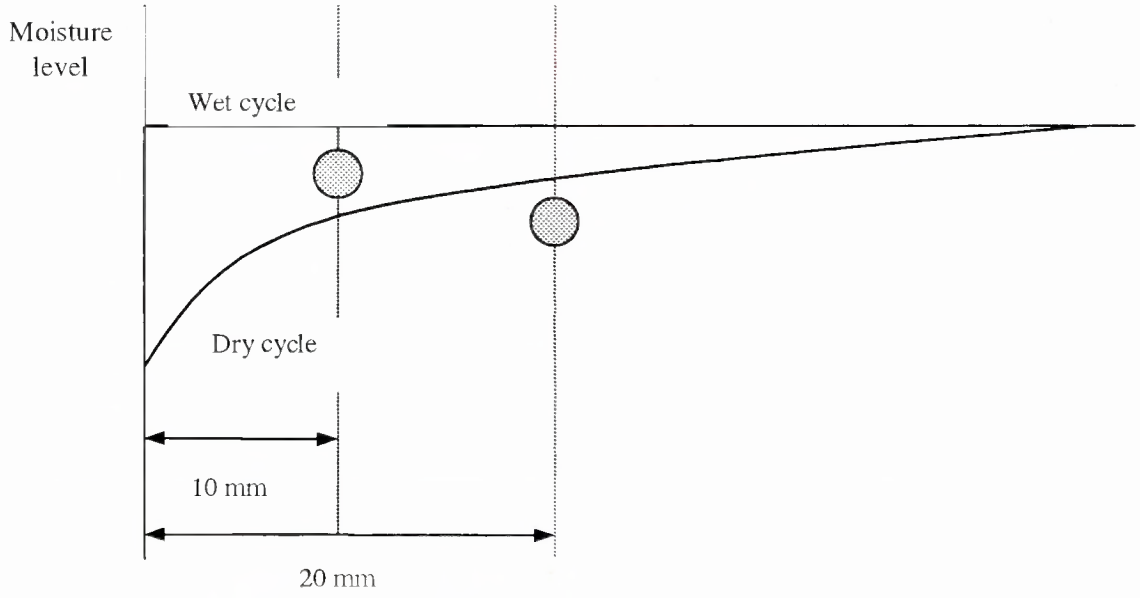

Figure 5.9: Schematic relationship of fluctuation of moisture level in cover region due to wetting and drying cycles

Also, corrosion rates and half-cell potentials were less affected by the introduction of the second regime, as the 3 day wet cycle is not sufficient to allow adequate moisture to reach the level of the steel, and thus affect corrosion measurements.

The introduction of the third wetting and drying regime (5 days wet and 2 days dry) stabilised the results to a certain extent. This was observed to be the optimal regime, appearing to provide sufficient moisture not to electrolytically stifle the corrosion rate, whilst avoiding saturated conditions limiting the availability of oxygen to the cathode. Thus, these conditions appeared to permit a fairly stable rate at which corrosion was taking place. The advantage of this limited wetting and drying regime was that it promoted uniform conditions in which to determine corrosion trends effectively.

Three Point moving Average

Three-point moving averages of the data are shown in figures 5.10 and 5.11. Once again clear trends were observed from the three-point moving average data.

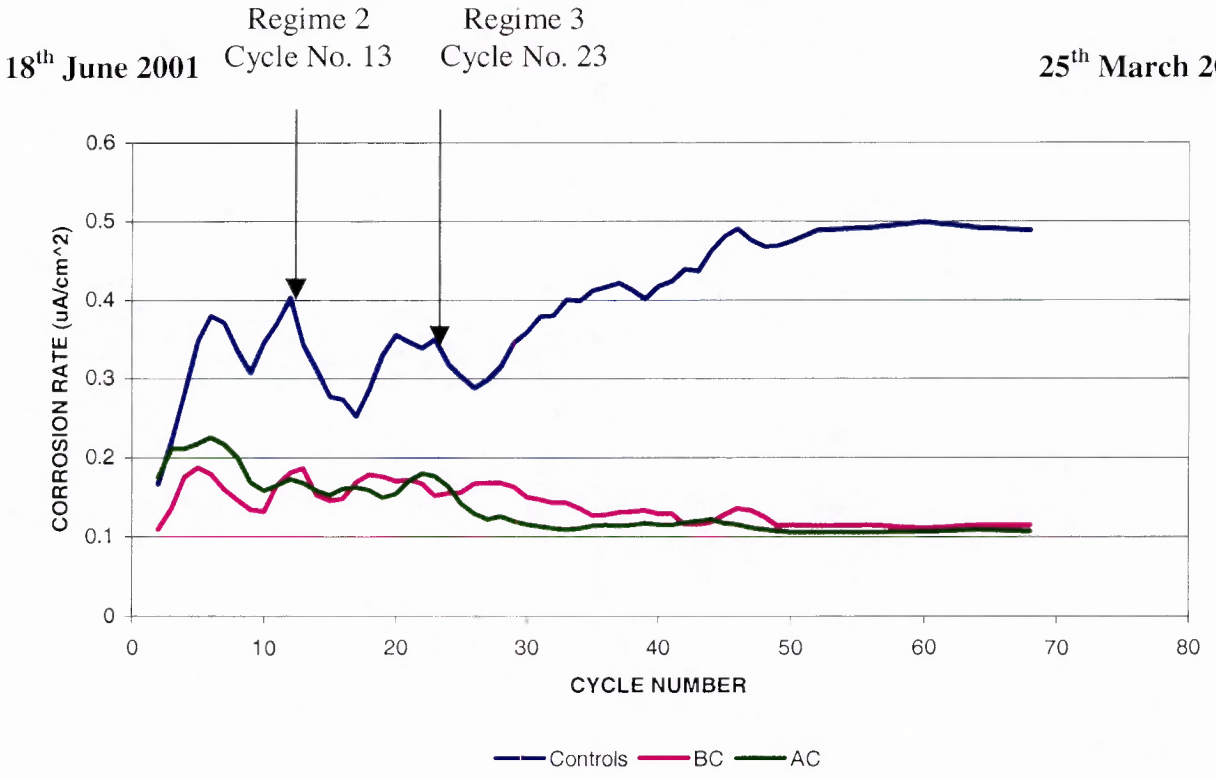

Figure 5.10: Three-point moving averages of corrosion rates for 20 mm cover samples.

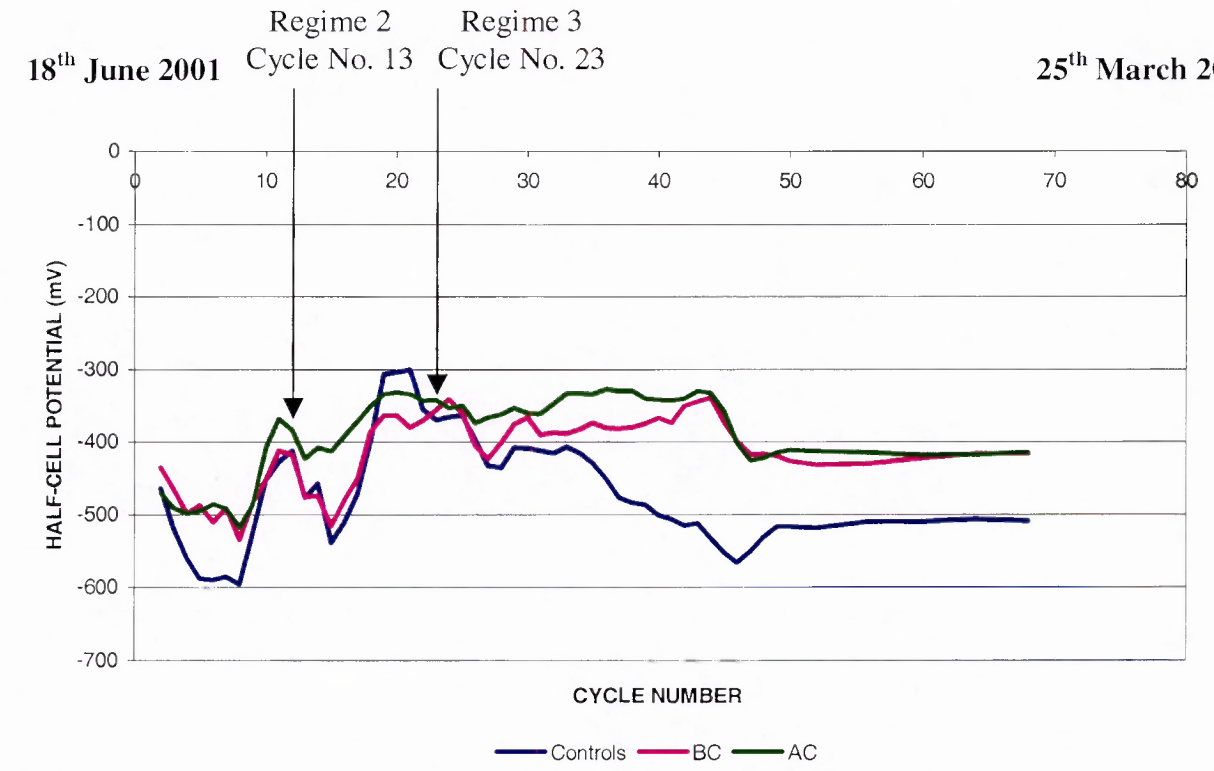

Figure 5.11: Three-point moving average of half-cell potential data for 20 mm cover samples.

A steady increase and a steady decrease in corrosion rates were observed for control specimens and specimens treated with the inhibitor before and after carbonation respectively. The half-cell potential data in this case showed slight differences between the various systems being tested. However, on introduction of the third wetting and drying cycle a positive shift in the samples treated with the penetrating inhibitor was observed as opposed to the control samples.

These results once again indicate:

a) That the penetrating corrosion inhibitor is capable of delaying the onset of corrosion.
b) The effectiveness of the penetrating inhibitor in its ability to reduce the corrosion rate.

In order to validate corrosion rate and half-cell potential measurements taken using the Gecor, corrosion rate measurements were also taken using the Coulostatic method and half-cell potential measurements were taken using a copper/copper sulphate half-cell between cycles 1 and 5. The corrosion rates and half-cell potentials obtained were found to be consistent with the Gecor 6 measurements. Corrosion monitoring was therefore continued using only the Gecor 6. Table 5.11 and 5.12 shows the results obtained.

Table 5.11: Corrosion rate measurements obtained using the Gecor and the Coulostatic method.

Cycle No.	1		2		3		4		5	
Sample	Gecor	Coulostatic	Gecor	Coulostatic	Gecor	Coulostatic	Gecor	Coulostatic	Gecor	Coulostatic
	($\mu A/cm^2$)		($\mu A/cm^2$)		($\mu A/cm^2$)		($\mu A/cm^2$)		($\mu A/cm^2$)	
Cont 3	0.140	0.155	0.155	0.135	0.244	0.250	0.325	0.302	0.405	0.400
Cont 4	0.112	0.149	0.145	0.144	0.198	0.205	0.255	0.288	0.259	0.240
BC 7	0.095	0.109	0.100	0.108	0.119	0.132	0.140	0.145	0.122	0.111
BC 8	0.088	0.110	0.098	0.112	0.150	0.141	0.205	0.200	0.309	0.268
AC 11	0.099	0.122	0.294	0.285	0.145	0.158	0.122	0.142	0.255	0.213
AC 12	0.102	0.115	0.154	0.150	0.255	0.210	0.298	0.250	0.188	0.195

Table 5.12: Potential measurements obtained using the Gecor and the copper/copper sulphate half-cell

Cycle No.	1		2		3		4		5	
Sample	Gecor	Half-cell	Gecor	Half-cell	Gecor	Half-cell	Gecor	Half-cell	Gecor	Half-cell
	(mV)		(mV)		(mV)		(mV)		(mV)	
Cont 3	-402.3	-398.0	-501.2	-489.6	-545.2	-540.1	-592.6	-567.3	-645.0	-600.8
Cont 4	-415.5	-399.8	-477.3	-466.5	-440.3	-438.5	-555.4	-550.2	-581.5	-558.2
BC 7	-398.2	-375.0	-450.2	-450.8	-468.5	-460.2	-455.2	-444.9	-543.6	-540.2
BC 8	-382.5	-365.2	-388.4	-355.4	-523.2	-511.3	-502.5	-500.0	-499.3	-487.5
AC 11	-399.1	-395.1	-520.4	-512.0	-422.2	-410.0	-405.3	-400.9	-539.0	-526.3
AC 12	-400.5	-399.0	-510.3	-500.3	-566.7	-555.2	-520.3	-518.5	-535.2	-531.0

Once again half-cell potentials measured using the Gecor 6 were slightly more negative.

5.7 General discussion

The performance of the penetrating corrosion inhibitor is largely dependent on its ability to penetrate the concrete and reach the corroding steel reinforcement. The effectiveness of the penetrating corrosion inhibitor was evaluated in 30 MPa concrete. The action of the inhibitor was evaluated at 10 and 20 mm covers to reinforcement. Penetration results obtained with different concrete grades (20, 30, 40 and 50) generally showed excellent penetration. However, results indicated that the penetration is dependent on the grade and hence porosity of the concrete. The penetration data obtained from corrosion test specimens treated with the inhibitor before and after accelerated carbonation also indicated rapid penetration of the inhibitor to depths of up to 60 mm, well beyond the 10 and 20 mm cover of the reinforcing steel. Ten months after application of the inhibitor sufficient concentrations were found to be present at all depths. However, higher concentrations were measured at deeper levels (30-45 mm and 45-60 mm) compared to shallower levels (0-15 mm and 15-30 mm), indicating the loss of inhibitor at the surface of the concrete. Most importantly however, the results showed that adequate concentrations of the inhibitor was present at 1, 5 and 10 months for inhibition of corrosion activity.

Three different wetting regimes were used during corrosion monitoring of which the third regime (5 days wet and 2 days dry) was found to be the most effective, yielding the most stable corrosion rates as sufficient moisture and oxygen were present for corrosion to take place.

Corrosion results obtained for the 10 mm cover test specimens show the effectiveness of the inhibitor. The control specimens maintain the highest corrosion rates and the most negative half-cell potentials corresponding to very active corrosion. Test specimens treated with inhibitor before and after accelerated carbonation showed much lower values of corrosion rates and half-cell potentials. Also, a steady decrease

in corrosion rate gradually reaching the 0.1 $\mu A/cm^2$ line was observed in the treated specimens, as opposed to a steady increase in corrosion rates of the control samples.

Similar trends to the 10 mm cover test specimens were observed in the 20 mm cover specimens. However, lower corrosion rates and less negative half-cell potentials were observed. This was attributed to the higher cover to reinforcement resulting in a lower rate of corrosion. Fluctuations in corrosion rates on introduction of the various wetting regimes were less drastic in the 20 mm cover test specimens as compared to the 10 mm cover test specimens, implying more stable moisture conditions at the level of the steel (20 mm).

The half-cell potential results indicate that:

- A positive shift in half-cell potential was observed in specimens treated with the corrosion inhibitor before and after the carbonation process.
- A steady positive shift in half-cell potentials continued after cycles number 50 and 45 in the 10 and 20 mm cover specimens treated with the inhibitor respectively
- The observed trend in half-cell potentials of specimens treated with the inhibitor indicates that the inhibitor had an effect on the corrosion process.

The corrosion rate results indicate that:

- A steady increase in corrosion rates of the control samples was observed as opposed to a steady decrease in corrosion rates in the specimens that were treated with the inhibitor before and after the carbonation process.
- Corrosion rates remain active immediately following treatment with the inhibitor.
- However, corrosion rates approached passive levels of 0.1 $\mu A/cm^2$ with time in concrete specimens treated with the penetrating corrosion inhibitor.

These results indicate that the penetrating corrosion inhibitor had a positive effect on the corrosion rate of the reinforcement and is therefore capable of corrosion inhibition in carbonation induced corrosion environments, provided sufficient concentrations of the inhibitor is present at the level of the reinforcement.

5.8 General conclusions

- Penetration of the inhibitor was found to be rapid through the concrete tested. The penetration results observed at the various concrete grades (20, 30, 40 and 50) however, indicate that the penetration is dependent on the grade and hence the porosity of the concrete. Grade 30 concrete used for the corrosion test specimens indicates excellent penetration, where sufficient concentrations of the inhibitor were present up to depths of 60 mm, well beyond the reinforcement depths of 10 and 20 mm ten months after application.

- The penetrating corrosion inhibitor was capable of delaying the onset of corrosion. This is observed as a decrease in corrosion rates and half-cell potentials in specimens that were treated with the inhibitor before the carbonation process in both 10 and 20 mm cover samples. Corrosion rates were found to decrease steadily, gradually reaching 0.1 $\mu A/cm^2$; also a slight positive shift in half-cell potentials in treated specimens was observed.

6. SITE WORK

Four different sites on the campus of the University of Cape Town were initially chosen for detailed monitoring of repairs using the penetrating corrosion inhibitor: a set of parapet walls of the walkways at the Sports Centre Building; concrete slabs at the back of the Civil Engineering Building; and a parapet wall on the roof of the Menzies Building. These structures were selected due to visual evidence of reinforcement corrosion and their relatively easy accessibility. It was expected that the visually severe conditions existing in these structures might represent the upper limit of possible successful performance of the penetrating corrosion inhibitor. Figure 6.1 shows a site map with the positions of the individual test sites.

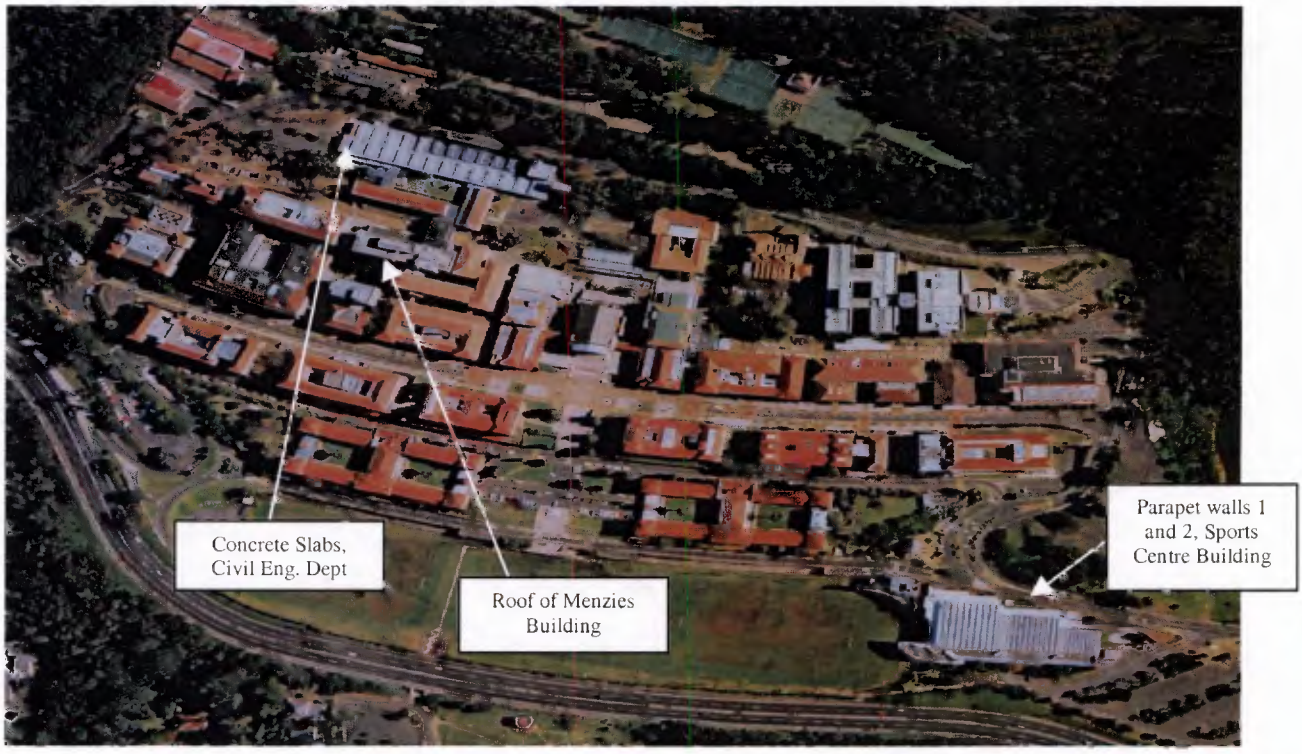

Figure 6.1: Map of the University of Cape Town showing the test sites.

6.1 Experimental procedure

At each of the sites the same experimental procedure was carried out. Initially a condition survey was performed in order to determine the cause and extent of deterioration. Two similar areas were located for corrosion monitoring in the same general vicinity.

Firstly, each of the sites was visually inspected. Telltale signs of corrosion e.g. rust stains, cracking, spalling and delaminations were observed, indicating that corrosion was taking place, and that there was a need for an effective repair technique. A cover survey was then carried out at each of the sites using the micro-cover meter and suitable areas with relatively low covers were located on the different sites. Covers to reinforcement that were considered as ideal for investigation were between 10 mm

and 20 mm to ensure that there was a good chance of corrosion. However, such low covers were difficult to locate in most cases.

Once two suitable areas were located on each site based on the above information, the rebar configuration was marked on the concrete surface and was used as a guide when cores were taken and connections made. Cores were taken using a hand held coring machine.

One core from each of the two areas was drilled to intersect the rebar by a few millimetres in order to make a good connection for coupling with the Gecor instrument to take corrosion rate measurements. A brass screw connected to a copper wire was securely knocked into the indent made on the steel rebar to connect to the external cable of the Gecor. The steel was cleaned to ensure good electrical contact. The set up is illustrated in figure 6.2.

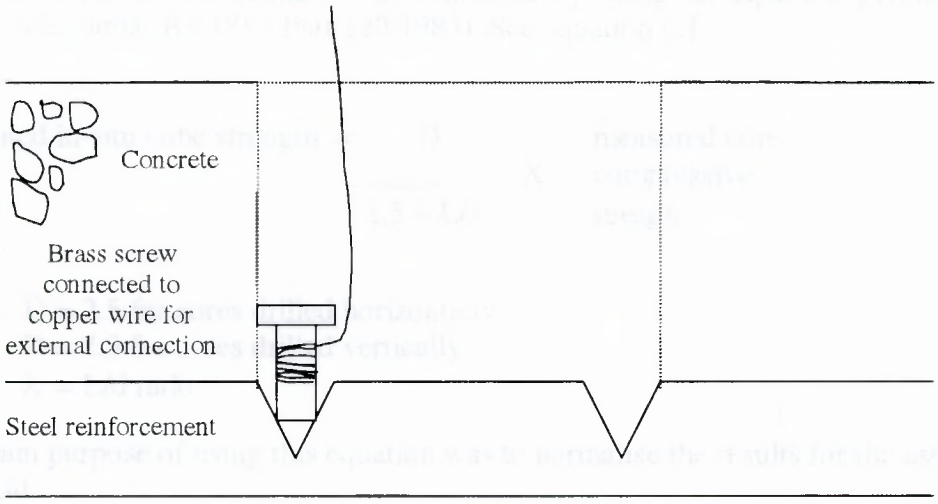

Figure 6.2: Schematic sketch of connection to steel reinforcement.

The Gecor and copper/copper sulphate half-cell electrode were used to measure the rebar potentials in a grid, and the area of greatest corrosion activity (most negative potential) was determined. For the case of carbonation-induced corrosion this usually coincided with the area of lowest cover to reinforcement. Knowing the alignment and diameter of the reinforcement bars, Gecor measurements were then carried out according to the same procedure as the laboratory.

Cores were also taken to determine concrete characteristics. Three cores of 45 mm diameter were taken at each of the two areas on each site. A core length of about 90 mm was taken. On return to the laboratory, the cores were thoroughly cleaned and tested for carbonation in the usual way by spraying on 1% phenolphthalein indicator solution. The core was then tested for strength and durability indexes. A 25 mm length sample was cut off using a continuous blade for the durability index testing; the remaining piece of the core sample was used to determine the compressive strength of the concrete, by trimming and grinding the core ends before testing.

Figure 6.3: Damage caused by carbonation-induced corrosion, Parapet walls 1, Sports Centre Building, UCT

6.2.1.1 Compressive strength tests

The compressive strength results are shown in table 6.1. The actual compressive strength was calculated by using equation 6.1.

For areas A and B, the range of compressive strengths obtained was quite large. This may partly have been due to the fact that the size of the cores was relatively small, affecting the accuracy. The concrete strength for the areas was estimated to be in the range of 25 to 35 MPa.

Table 6.1: Compressive strengths, Parapet walls 1, Sports Centre Building, UCT

Area	Sample	Diameter (mm)	Height (mm)	Load (kN)	Compressive Strength (MPa)	L/d	Estimated in-situ cube strength (MPa)
A	A1	45.3	44.0	61.0	37.8	0.971	37.5
	A2	45.3	40.9	37.0	22.9	0.903	22.0
	A3	45.4	31.8	58.0	35.8	0.700	30.5
B	B1	45.3	43.9	42.0	26.0	0.969	25.5
	B2	45.5	20.8	68.0	41.8	0.457	28.5
	B3	45.5	42.7	59.0	36.3	0.938	35.5

6.2.1.2 Durability Indexes and carbonation tests

The results for the durability indexes and carbonation depth are shown in table 6.2.

Table 6.2: Durability Indexes and carbonation depth results, Parapet walls 1, Sports Centre Building, UCT

Area	Sample	Oxygen Permeability Index	Average Oxygen Permeability Index	Water Sorptivity ($mm/h^{1/2}$)	Average Water Sorptivity ($mm/h^{1/2}$)	Carbonation Depth (mm)
C	C1	9.98		5.54		15.6
	C2	9.57	9.79	6.35	6.24	14.8
	C3	9.82		6.84		13.1
D	D1	9.60		5.86		13.4
	D2	9.64	9.58	3.87	4.90	18.7
	D3	9.50		4.98		17.3

The values obtained corresponded to relatively good quality concrete (refer to table 4.6). An average carbonation depth of 16 mm was measured indicating that the carbonation front has extended to the embedded steel, and therefore localised corrosion should be expected.

6.2.1.3 Reinforcement data

The upper rebar layer in this case had a rebar diameter of 12 mm and an average concrete cover of about 20 mm (range: 15 to 30 mm).
The lower rebar layer has a rebar diameter of 12 mm and an average concrete cover of about 50 mm (range: 31 to 64 mm). Figure 6.4 shows detailed cover data.

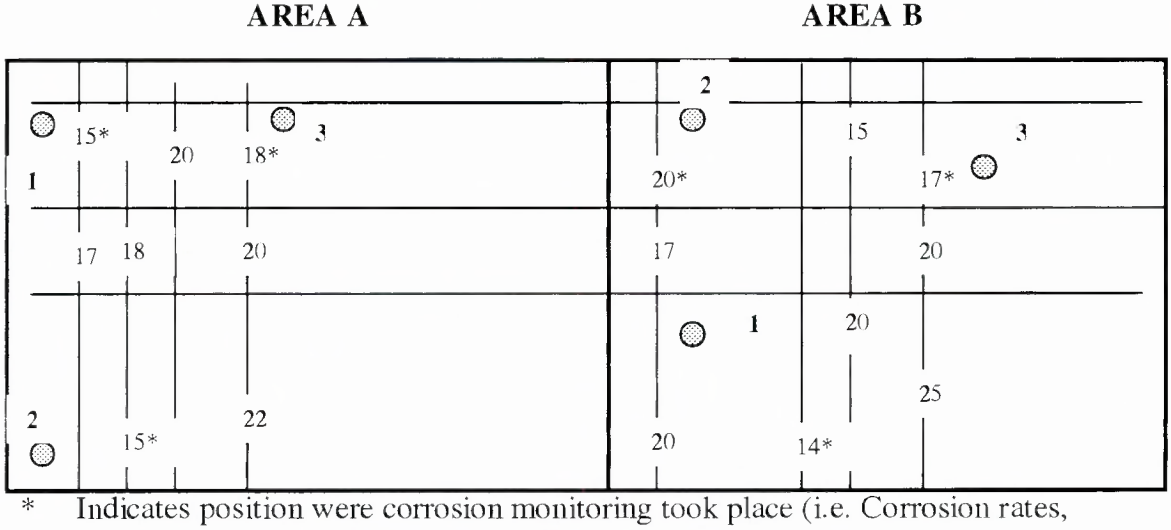

* Indicates position were corrosion monitoring took place (i.e. Corrosion rates, half-cell potentials and resistivity measurements).

⊙ Indicates position where cores were taken for durability index tests and carbonation depths.

13 Indicates cover to reinforcement in mm at marked position

Figure 6.4: Reinforcement data, Parapet walls 1, Sports Centre Building, UCT Each area is 1200 mm wide and 1000 mm high.

6.2.1.4 Corrosion monitoring

Corrosion measurements were taken using the Gecor 6 at three different points on each of the two areas. At these points maximum negative potentials were occurring indicating that carbonation corrosion was highest at these points. Readings were taken twice a week, on consecutive days in order to obtain consistency in results. The corrosion rate, half-cell potential and resistivity results obtained are shown in figures 6.5, 6.6 and 6.7 respectively. They are represented as averages of three measurements across each test area.

The Appendix shows the detailed results. As observed from figures 6.5, 6.6 and 6.7, very low corrosion rates were observed at this site which were consistent with the low negative potentials observed with the copper/copper sulphate half-cell measurements and the high resistivity measurements. Corrosion rates measured were in the range of between 0.01 and 0.07 $\mu A/cm^2$ (actual values) indicating passive conditions although visible signs of corrosion were apparent on the site. Cracks were visible along the reinforcement and rust stains and delaminations were also present. Spalling of the concrete at certain patches on the test area was also observed. However, since the corrosion rate measurements together with the half-cell potential data and resistivity data indicate that corrosion is not taking place it is thought correct to assume that corrosion was not actively taking place during this monitoring period due to the relatively dry nature of the concrete. Corrosion monitoring of this site was therefore discontinued as it was decided that the application of the inhibitor was of no advantage.

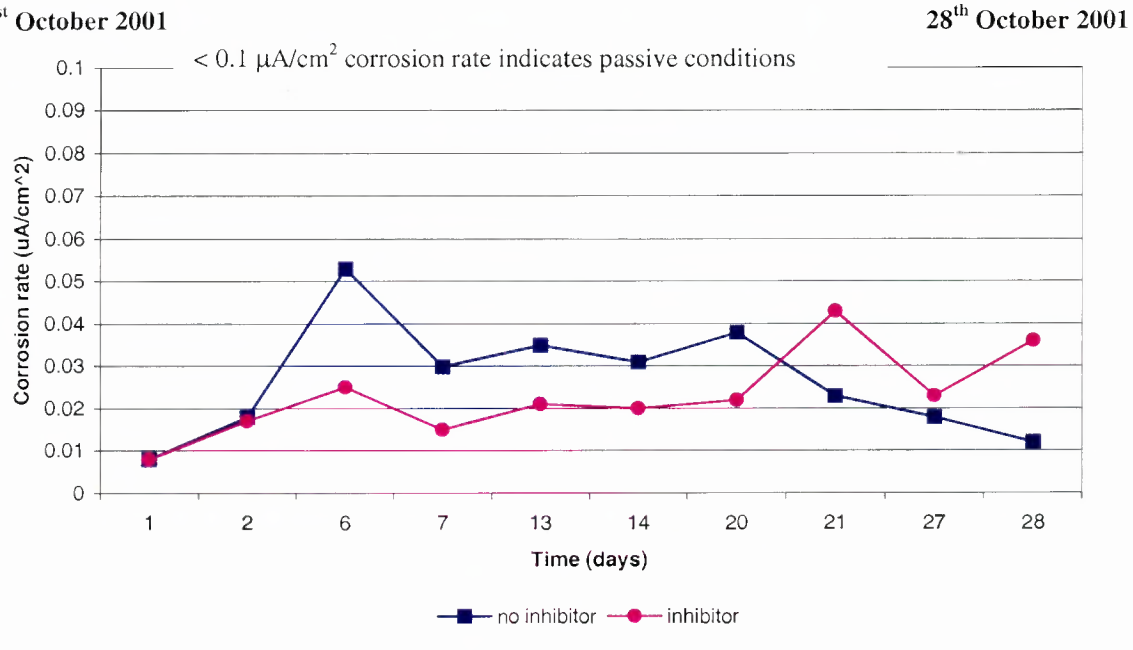

Figure 6.5: Corrosion rate measurements, 1st parapet wall, Sports Centre Building, UCT

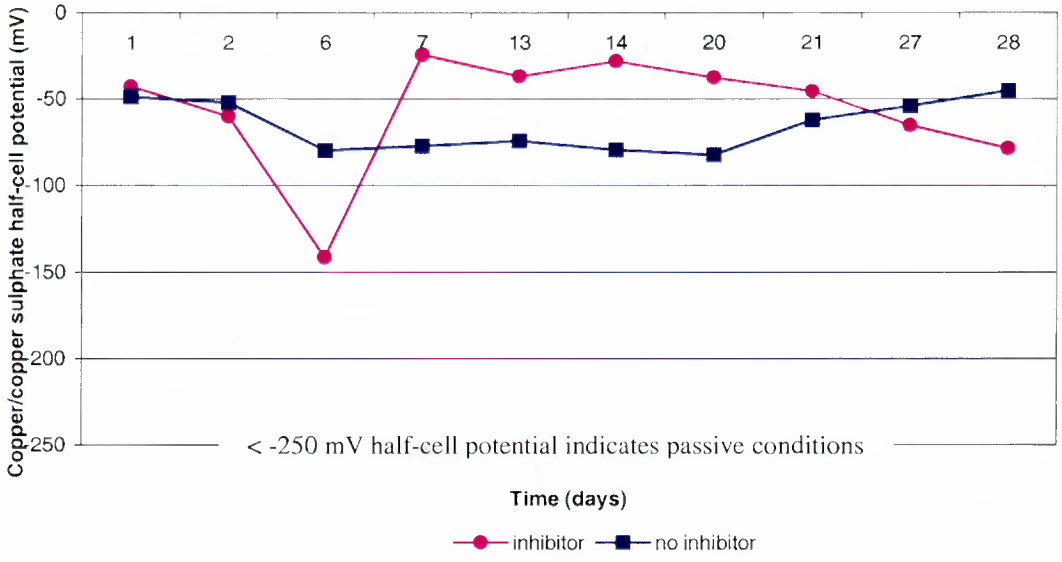

Figure 6.6: Half-cell potential measurements, 1st parapet wall, Sports Centre Building, UCT

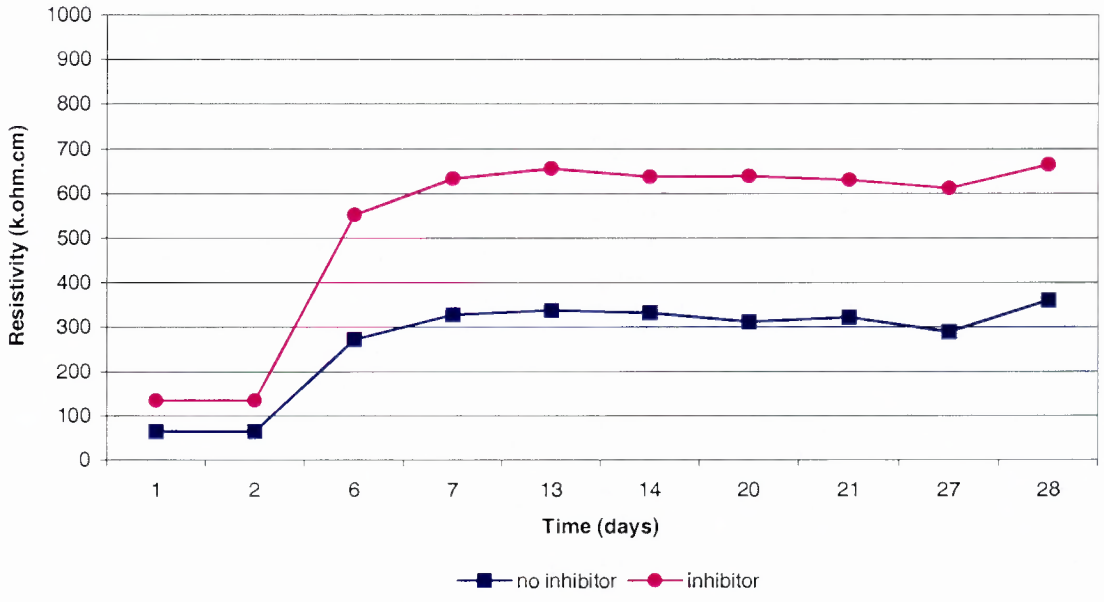

Figure 6.7: Resistivity measurements, 1st parapet wall, Sports Centre Building, UCT

6.2.2 Second Parapet Wall, Sports Centre Building, UCT

The test areas were labelled:

AREA C : Area not to be treated with inhibitor
Samples C1, C2 and C3 were cored samples from area C.

AREA **D** : Area to be treated with inhibitor.
Samples D1, D2 and D3 were cored samples from area D.

Each area was 1200 by 1000 mm in size. This structure is believed to be about 25 years old. Figure 6.8 shows damage observed due to carbonation corrosion at this site.

Figure 6.8: Damage caused by carbonation-induced corrosion, 2nd Parapet wall, Sports Centre Building, UCT

6.2.2.1 Compressive strength tests

The results obtained for compressive strengths are shown in table 6.3. The actual compressive strength was calculated by using equation 6.1.

Table 6.3: Compressive strengths, 2nd Parapet wall, Sports Centre Building, UCT

Area	Sample	Diameter (mm)	Height (mm)	Strength (kN)	Compressive Strength (MPa)	L/d	Estimated in-situ cube strength (MPa)
C	C1	45.5	44.2	70.0	43.1	0.971	42.5
	C2	45.3	32.1	72.0	44.7	0.709	38.5
	C3	45.3	30.5	74.0	45.9	0.673	38.5
D	D1	45.3	50.3	49.0	30.4	1.110	31.5
	D2	45.5	45.2	73.5	45.2	0.993	45.0
	D3	45.4	44.4	69.0	42.4	0.977	42.0

Once again, the range of compressive strengths obtained was quite large. This may partly have been due to the relatively small size of the core samples, affecting the

Figure 6.13: Damage caused by carbonation induced corrosion, Concrete slabs, Civil Engineering Department, UCT

6.2.3.1 Compressive strength tests

The compressive strength test results are shown in table 6.5.

Table 6.5: Compressive strengths, Concrete slabs, Civil Engineering Department, UCT

Area	Sample	Diameter (mm)	Height (mm)	Strength (kN)	Compressive Strength (MPa)	L/d	Estimated in-situ cube strength (MPa)
E	E1	45.5	73.2	37.0	22.8	1.609	24.5
	E2	45.5	72.0	38.0	23.3	1.582	25.0
F	F1	45.5	50.2	31.4	19.3	1.103	18.5
	F2	45.4	49.3	30.2	18.6	1.086	17.5
	F3	45.4	47.6	31.0	19.2	1.048	18.0

The range of compressive strengths obtained were quite large due to the relatively small size of the cores used affected accuracy. Concrete strength for the area was estimated to be in the range of 20 to 25 MPa.

6.2.3.2 Durability indexes and carbonation depth tests

The results obtained for durability indexes and carbonation depths are shown in table 6.6.

Table 6.6: Durability and carbonation depth results, Concrete slabs, Civil Engineering Department, UCT

Area	Sample	Oxygen Permeability Index	Average Oxygen Permeability Index	Water Sorptivity ($mm/h^{1/2}$)	Average Water Sorptivity ($mm/h^{1/2}$)	Carbonation Depth (mm)
E	E1	9.37		12.28	8.75	17.3
	E2	9.56	9.46	5.21		20.0
F	F1	9.62		6.53		15.6
	F2	9.63	9.40	7.98	8.21	22.0
	F3	8.94		10.11		21.4

The values obtained corresponded to relatively good quality concrete (refer to table 4.6). An average carbonation depth of 19 mm was measured indicating that the carbonation front has extended to the embedded steel at particular areas, and therefore localised corrosion should be expected.

6.2.3.3 Reinforcement data

The upper rebar layer in this case had a rebar diameter of 12 mm and an average concrete cover of about 15 mm (range: 13 to 25 mm). Figure 6.14 shows a schematic sketch of the positions of lowest cover and maximum carbonation
The lower rebar layer had a rebar diameter of 12 mm and an average concrete cover of about 40 mm (range: 30 to 55 mm).

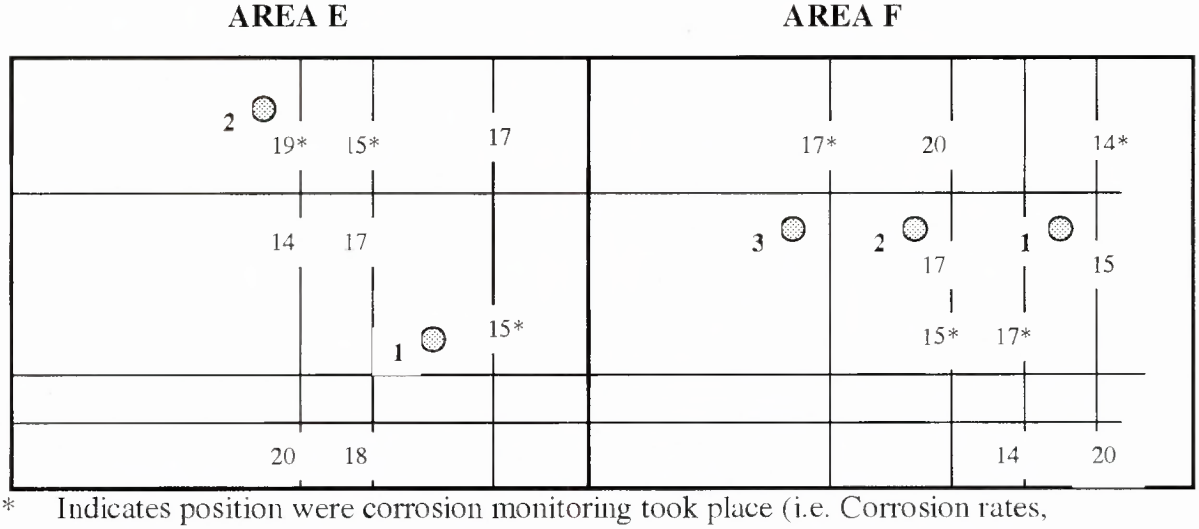

* Indicates position were corrosion monitoring took place (i.e. Corrosion rates, half-cell potentials and resistivity measurements).

○ Indicates position where cores were taken for durability index tests and carbonation depths.

13 Indicates cover to reinforcement in mm at marked position

Figure 6.14: Reinforcement data, Concrete slabs, Civil Engineering Dept, UCT Each area is 1200 mm wide and 1000 mm high.

6.2.3.4 Corrosion rate monitoring

The corrosion rate, half-cell potential and resistivity results obtained are shown in figures 6.15, 6.16 and 6.17 respectively. They are represented as averages of three measurements across each test area. Detailed results are presented in the Appendix.

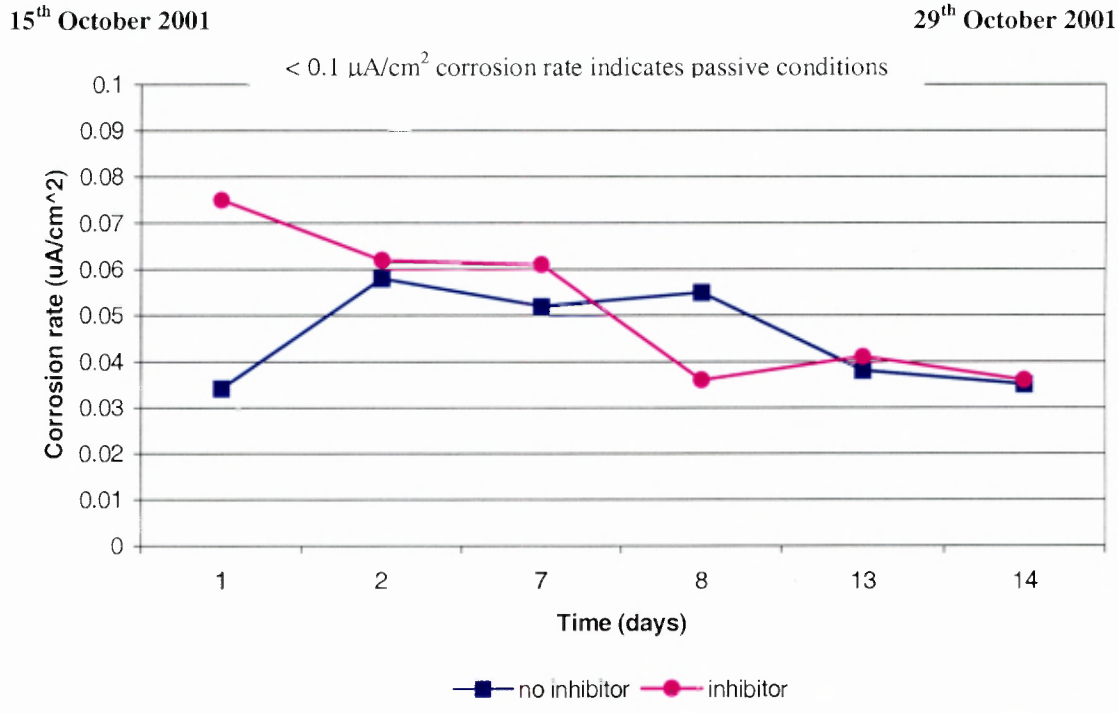

Figure 6.15: Corrosion rate measurements, Concrete slabs, Civil Engineering Department, UCT

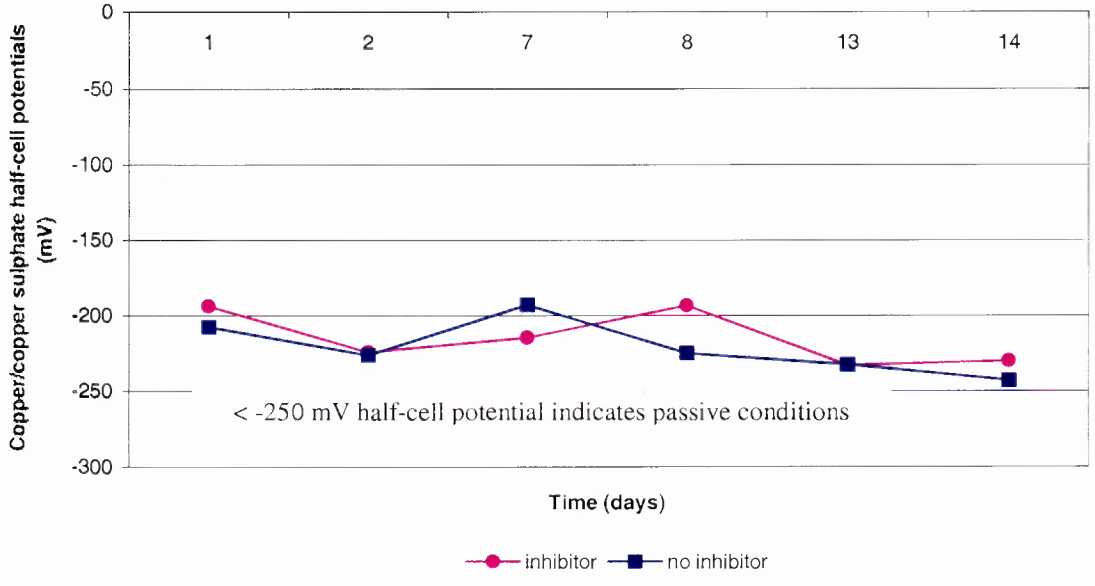

Figure 6.16: Half-cell potential measurements, Concrete slabs, Civil Engineering Department, UCT

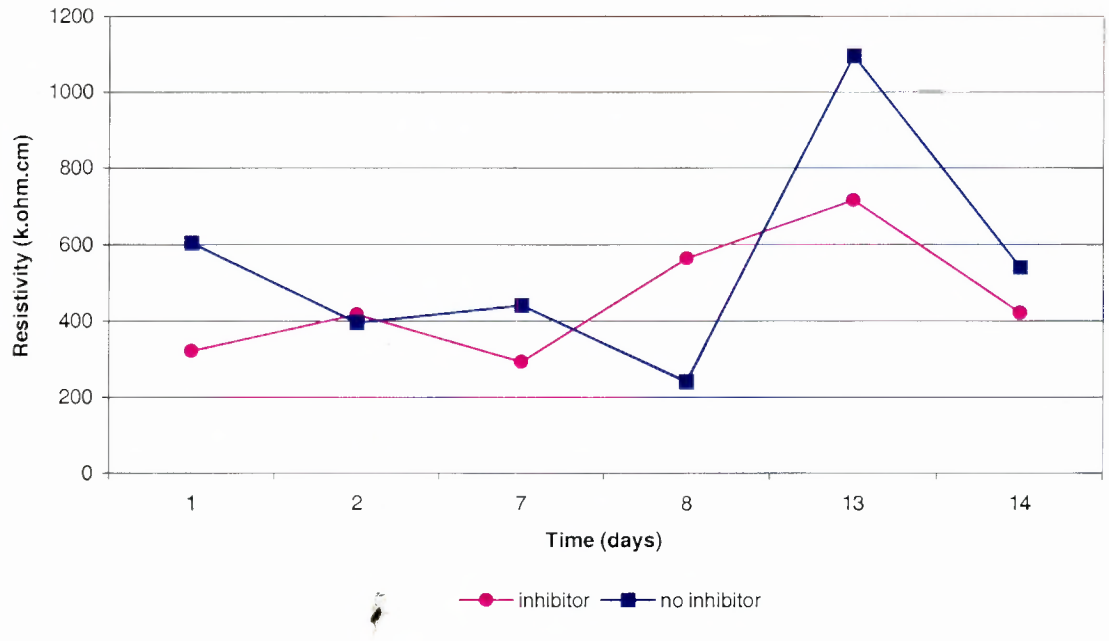

Figure 6.17: Resistivity measurements, Concrete slabs, Civil Engineering Department, UCT

Once again corrosion rates observed were low but higher than those observed on the two previous sites. The corrosion rates measured were in the range of between 0.01 and 0.099 $\mu A/cm^2$, once again indicating passive corrosion conditions. The copper/copper sulphate potentials were also more negative, however still less than negative 250 mV confirming the passive state of the reinforcement. Resistivities measured were very high. Although all corrosion measurements indicate the passive state of the reinforcement, cracking and spalling of the concrete, rust stains and exposed rebar was visible at this test site. It is therefore once again assumed that corrosion is not actively taking place. Corrosion monitoring of this site was therefore also discontinued, as the application of the penetrating corrosion inhibitor would be of no advantage.

Discussion of results

In all the sites discussed in the above sections evidence of corrosion and corrosion damage were observed, however no reasonable corrosion rates were measured. All corrosion measurements obtained (corrosion rates, half-cell potentials and resistivities) indicate the passive state of the reinforcement.

The corrosion process is determined by factors such as:

- The conductivity of the cover concrete zone
- The availability of oxygen and water in the surrounding environment
- The penetrability of oxygen and water to the level of the reinforcing steel

Carbonation corrosion is known not to occur when the pores in the concrete are either completely dry or completely saturated. Various sources differ slightly as to the

optimum relative humidity (RH) range for maximum carbonation corrosion. It is suggested in Fulton (1986) that corrosion requires humidity levels above 80 %. The corrosion rate measurements taken on these sites were during the Cape Town summer period (December, January, February and March), where ambient RH ranges between 40 and 55 %. The Cape Town climate is therefore less favourable for steel corrosion during the summer period. This is therefore consistent with the very high values of resistivity of the concrete measured at all sites indicating very low conductivity of the cover concrete due to its dry nature.

The values of water sorptivity and oxygen permeability were consistent with good quality concrete (see table 4.6). Oxygen permeability indexes ranged from 9.5 to 11.0 indicating concrete of low permeability and good microstructure. Water sorptivity ranged from about 4.0 to 8.0, which is characteristic of well cured concrete. The average carbonation depths measured at the test sites were in the range of 15 to 20 mm, and at all the corrosion measurement positions the carbonation depths had reached the steel reinforcement. The process of carbonation would act to close the pore structure of the concrete, resulting in reduced fluid transport properties of the surface cover zone. The penetrability and availability of oxygen and water to the level of the reinforcing steel is questionable.

Therefore the lack of 'reasonable' corrosion measurements obtained although evidence of corrosion and corrosion damage is present can be accounted to be due to one or a combination of the following factors:

- The generally dry environment of the environment, limiting the availability of water at the level of the reinforcing steel.
- The reduced fluid penetrability of the cover concrete zone, limiting the availability of water and oxygen at the level of the reinforcing steel.

A broader investigation was therefore required in order to validate these findings and to assess the potential rate of corrosion in areas where the steel was found to have been depassivated.

6.2.4 Roof of Menzies Building, UCT

The test areas were labelled as shown below:

AREA **G** : Area that is not to be treated with the inhibitor
Samples G1 and G2 are cored samples from area G.

AREA **H** : Area that is to be treated with the inhibitor.
Samples H1, H2 and H3 are cored samples from area H.

Figure 6.18 shows some of the damage that was observed due to carbonation corrosion at the Menzies site.

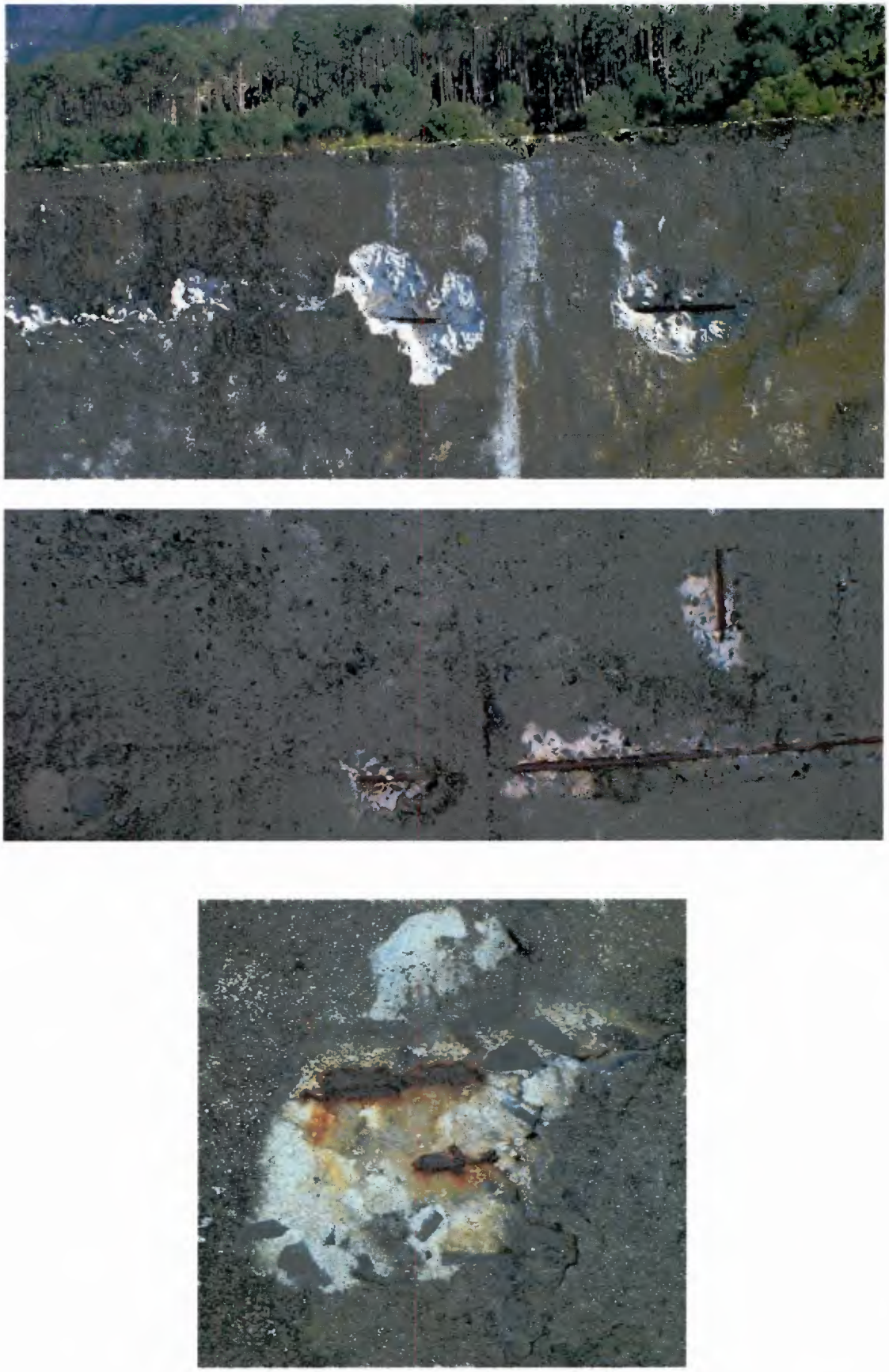

Figure 6.18: Spalling and cracking of concrete due to carbonation-induced corrosion on parapet walls at the Menzies site.

6.2.4.1 Compressive strength tests

The compressive strength results are shown in table 6.7.

Table 6.7: Compressive strengths, Roof of Menzies Building, UCT.

Area	Sample	Diameter (mm)	Height (mm)	Strength (kN)	Compressive Strength (MPa)	l/d	Estimated in-situ cube strength (MPa)
G	I1	45.5	52.1	35.0	21.5	1.145	22.5
	I2	45.4	48.3	33.4	20.6	1.064	21.0
H	J1	45.5	72.4	35.5	21.8	1.591	25.6
	J2	45.4	71.0	37.1	22.7	1.557	26.5

The concrete strength for the areas was estimated to be in the range of 20 and 25 MPa.

6.2.4.2 Durability indexes and carbonation depth tests

Durability indexes and carbonation depth results are shown in table 6.8.

The values obtained corresponded to relatively good quality concrete (refer to table 4.6). An average carbonation depth of 32 mm was measured indicating that the carbonation front has extended well beyond the embedded steel in all areas, and therefore corrosion should be expected.

Table 6.8: Durability indexes and carbonation depth results, Roof of Menzies, UCT

Area	Sample	Oxygen Permeability Index	Average Oxygen Permeability Index	Water Sorptivity ($mm/h^{1/2}$)	Average Water Sorptivity ($mm/h^{1/2}$)	Carbonation Depth (mm)
G	G1	9.97		6.20		35.0
	G2	9.54	9.76	5.54	5.87	32.0
	G3					30.0
H	H1	9.66		5.20		28.0
	H2	9.57	9.62	6.15	5.68	33.0
	H3					35.0

6.2.4.3 Reinforcement data

The upper rebar layer in this case had a rebar diameter of 12 mm and an average concrete cover of about 12 mm (range: 8 to 20 mm). Figure 6.19 shows a schematic sketch of the positions of lowest cover and maximum carbonation
The lower rebar layer had a diameter of 12 mm and an average concrete cover of about 35 mm (range: 30 to 40 mm).

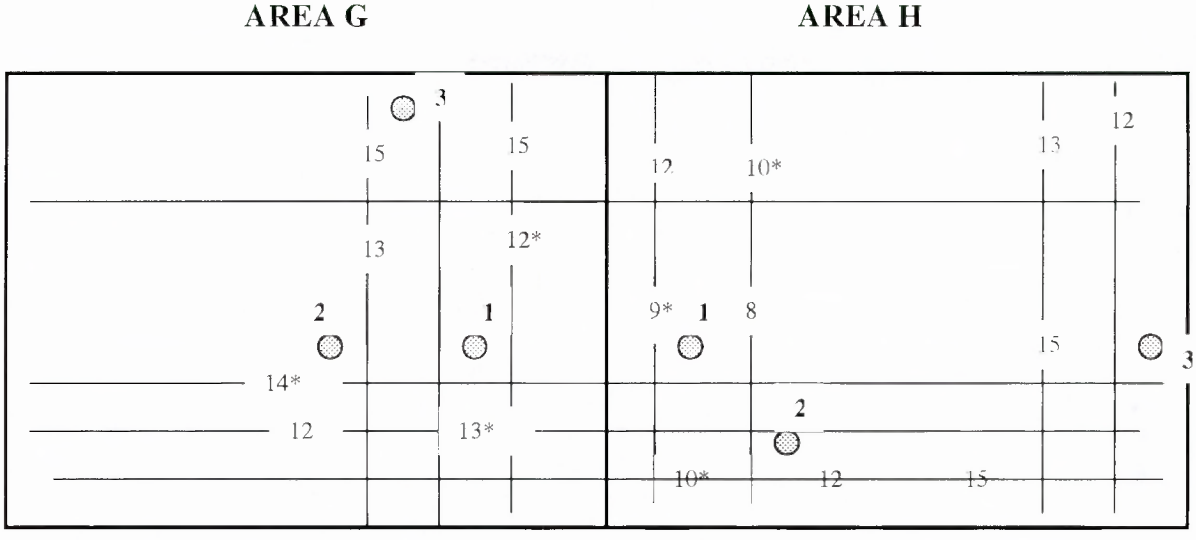

* Indicates position were corrosion monitoring took place (i.e. Corrosion rates, half-cell potentials and resistivity measurements).

◎ Indicates position where cores were taken for durability index tests and carbonation depths.

13 Indicates cover to reinforcement in mm at marked position

Figure 6.19: Reinforcement data, Roof of Menzies, UCT
Each area is 1200 mm wide and 1000 mm high.

6.2.4.4 Corrosion rate monitoring

The corrosion rate, half-cell potential and resistivity results obtained are shown in figures 6.20, 6.21 and 6.22 respectively. They are represented as averages of three measurements across each test area. Detailed results are presented in the Appendix I.

On this site much higher corrosion rates were measured, with values higher than 0.1 $\mu A/cm^2$ in most instances indicating active corrosion in the area. The corrosion rates measured were in the range of between 0.012 to 0.39 $\mu A/cm^2$ (actual values). The half-cell potentials measured also showed negative values of more than 250 mV indicating the probability of active corrosion. The resistances measured were however high. Corrosion rates were monitored for a period of about a month until stable corrosion rate measurements were maintained. Due to the active nature of the corrosion rate results obtained the inhibitor was applied on this site in order to determine its effectiveness in reducing the rate at which corrosion is taking place.

As compared to the previously discussed sites, the Menzies site showed much higher corrosion rates and half-cell potentials, this can be accounted to a number of factors:

- Low covers-cover to reinforcement on this site ranged from about 8 to 20 mm and an average cover of 12 mm was found as opposed to the previous sites where average covers ranged between 15 and 20 mm.

- Higher carbonation depths- an average carbonation depth of 32 mm was measured as compared to the previous sites whose carbonation depths ranged form 15 to 20 mm. This meant that the carbonation front had moved well beyond the steel reinforcement at all positions.
- More exposure-the Menzies site is fully exposed to the varying weather conditions as opposed to the other sites, which are sheltered to a certain extent.
- Poorer concrete- the Menzies site concrete had a lower concrete grade as compared to the other sites, and therefore more permeable and susceptible to carbon dioxide ingress. Also more severe corrosion damage was observed at this particular site.
- The possibility of chloride contamination in the concrete was considered to be minimal due to the distance away from aggressive chloride environments.

The high resistivites measured can be accounted for by the generally dry environment of the concrete, limiting the availability of water at the level of the reinforcing steel. Also the carbonation of the cover concrete may have reduced fluid penetrability of the cover concrete zone, limiting the availability of water at the level of the reinforcing steel, thereby reducing the conductivity of the cover concrete zone

6.2.4.5 Application of inhibitor

The inhibitor was applied on the area that was to be treated with the penetrating corrosion inhibitor, as specified by the manufacturers. Since application was on site, the maximum application of 0.5 litres per square meter was used. Before application of the inhibitor the area to be treated was cleaned with a wire brush to remove all loose materials, which may affect the absorption of the inhibitor. The inhibitor was applied in five coats by painting on the product using a normal paintbrush at roughly 10 hour intervals. On completion of application of the inhibitor the concrete surface treated was wetted twice by spraying on clean water, roughly at twenty-four hour intervals.

Twenty-eight days after the application of the inhibitor corrosion rate measurements were started using the Gecor 6 in order to determine the effectiveness of this penetrating corrosion inhibitor. Corrosion rate measurements were continued until sufficient data was obtained. The results obtained are shown in figure 6.5. Penetration depth of the inhibitor was also measured.

The results presented in figure 6.20 showed that corrosion rates were reduced after the introduction of the penetrating corrosion inhibitor in Area G. The corrosion rates observed in the treated area G were less than those previously measured. They were also less than the corrosion rates observed in the control area H where no inhibitor was applied. These trends therefore indicate the effectiveness of the penetrating corrosion inhibitor in its ability to slow down the rate at which corrosion is taking place.

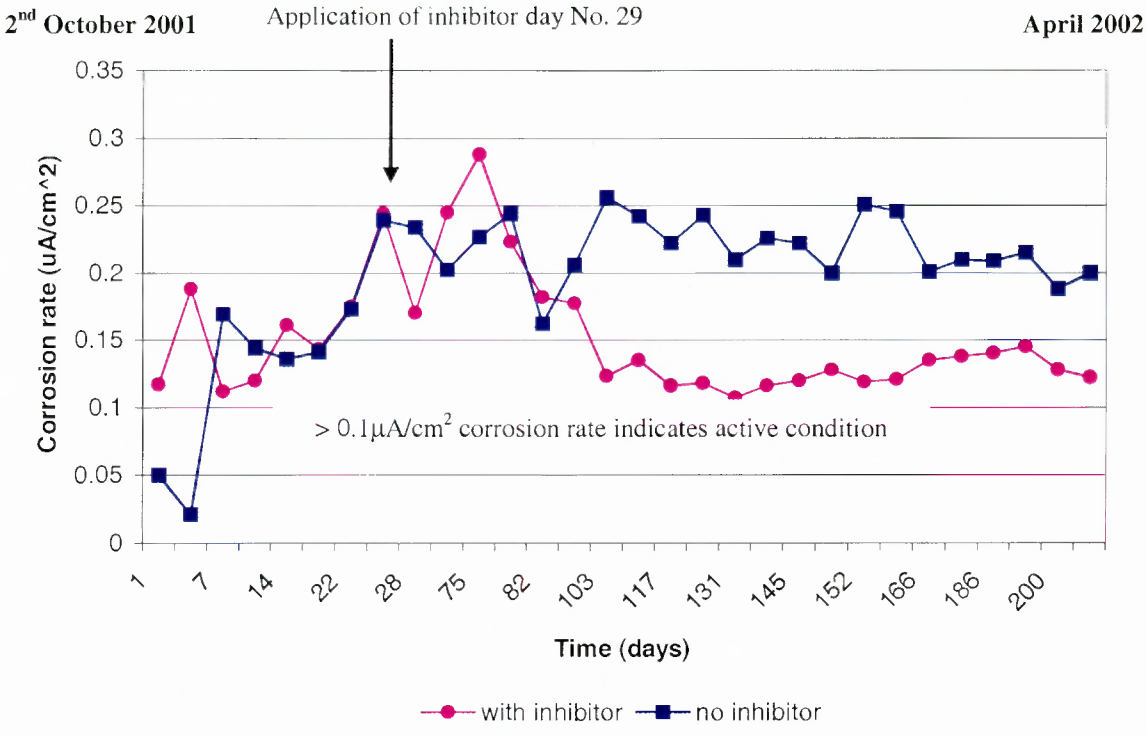

Figure 6.20: Corrosion rate measurements before and after application of inhibitor, Roof of Menzies Building, UCT.

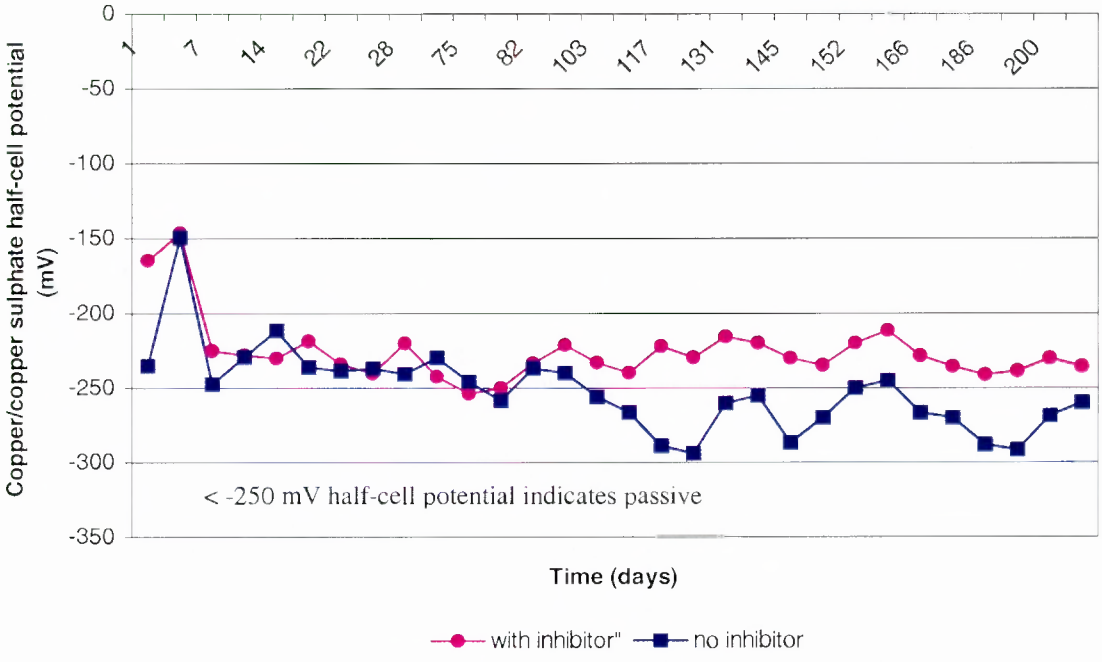

Figure 6.21: Half-cell potential measurements before and after application of inhibitor, Roof of Menzies Building, UCT.

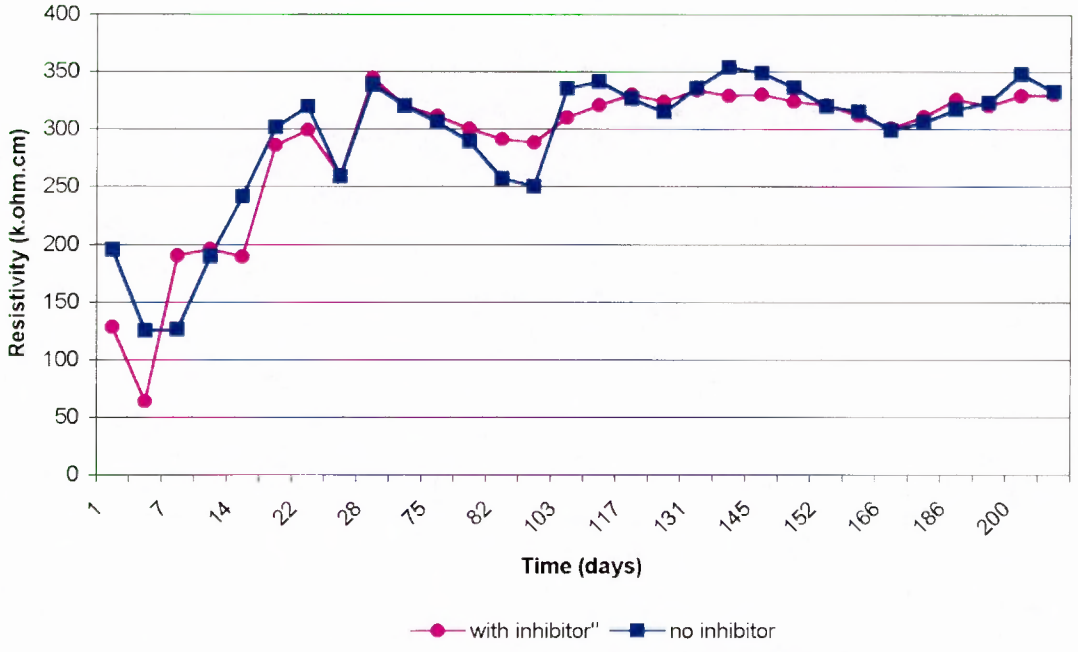

Figure 6.22: Resistivity measurements before and after application of inhibitor, Roof of Menzies Building, UCT.

6.2.1.1 Depth of penetration of inhibitor

28 days after the application of the inhibitor on Area G, two cores were taken at different points within the area G. These cores were then qualitatively analysed to determine the depth of penetration of the inhibitor. The results obtained are shown in table 6.9.

Table 6.9: Qualitative test results to determine depth of penetration of inhibitor, Roof of Menzies Building, UCT.

Date	Area	Core number	Depth (mm)	Indicator colour	Qualitative rating
10/12/01	G	1	0 - 15 15 - 30 30 - 45 45 - 60	Red Pink Pink Pale pink	Excellent Good Good Adequate
10/12/01	H	2	0 - 15 15 - 30 30 - 45 45 - 60	Pink Pink Pink Pale pink	Good Good Good Adequate

Figure 6.23 shows the test areas and the positions at which the two cores were obtained.

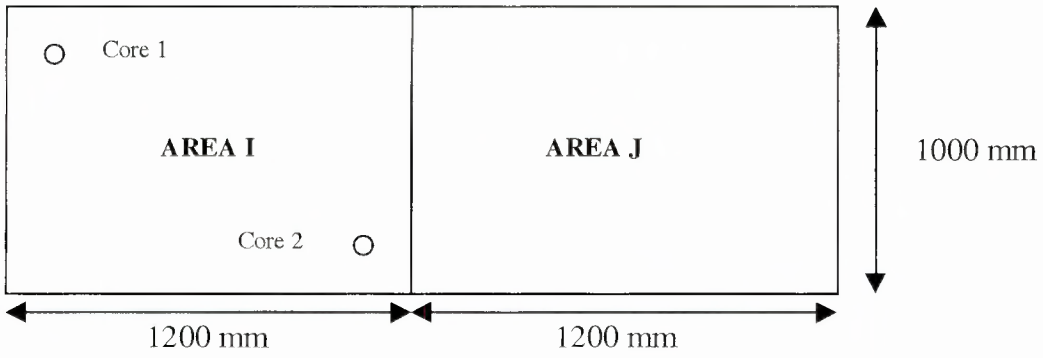

Figure 6.23: Dimensions of test areas and positions of cores obtained.

The results of the qualitative test showed that the inhibitor had penetrated to a depth of between 45 and 60 mm. Thus the inhibitor had penetrated the concrete beyond the steel reinforcement, which was found to be at a cover of between 10 and 20 mm. The degree of penetration can be attributed to the nature of the inhibitor, the permeability of the concrete and the sorptivity of the concrete. The results shown in table 6.9 suggest that more than adequate concentration of the inhibitor is present for sufficient corrosion inhibition to occur.

6.2.5 Discussion of site work results

From site work carried out on the initial three sites around UCT, very low corrosion rates were observed at three of these sites which were consistent with the low negative potentials observed with the copper/copper sulphate half-cell measurements and the high resistivity measurements. Corrosion rates measured were in the range of between 0.001 and 0.01 $\mu A/cm^2$ indicating passive conditions although visible signs of corrosion were apparent on the site. Cracks were visible along the lines of reinforcement and rust stains and delaminations were also present. Spalling of the concrete at certain localised points on the test area was also observed. However, since the corrosion rate measurements together with the half-cell potential data and resistivity data indicate that corrosion is not taking place it is thought correct to assume that corrosion is not actively taking place.

Therefore the lack of 'reasonable' corrosion measurements (very low values of corrosion current densities and high resistivity values using the Gecor and Wenner probe) obtained although evidence of corrosion and corrosion damage is visible can be accounted for by one or a combination of the following factors:

- The generally dryness of the environment, limiting the availability of water at the level of the reinforcing steel, thereby reducing the conductivity of the cover concrete zone.
- Oxides formed around the steel causing a dense skin reducing the ingress of moisture to the surface of the steel, and also reducing the conductivity of the steel/concrete interface.
- The reduced fluid penetrability of the cover concrete zone due to carbonation, limiting the availability of water at the level of the reinforcing steel.

A broader investigation was therefore required in order to validate these findings and to assess the potential rate of corrosion in areas where the steel was found to have depassivated.

It was therefore proposed that a wetting system, which allows saturation of the corrosion monitoring area, be erected at the Menzies site. This system consisted of PVC piping running along the top of the parapet wall with 0.5 mm diameter holes drilled at 100 mm intervals for regular wetting of the walls. Wetting of the test area where no inhibitor had been applied was initiated. This was a continuous application lasting for a period of about four weeks during which regular corrosion rate, half-cell potential and resistivity monitoring occurred. This was done in order to determine if the presence of moisture would increase the rate of corrosion and stabilise the somewhat erratic nature of the measurements. This wetting procedure was repeated on the area treated with the penetrating corrosion inhibitor, starting later. Figure 6.24 shows the set up of the wetting system.

Figure 6.24: Set up of wetting system

On completion of this wetting period, cores, 100 mm deep and 68 mm diameter, were taken and sliced at 25 mm increments with minimal water usage during the coring and slicing process. These disc samples were used to determine the moisture content and conductivity of the concrete at the different depths (0-25 mm, 25-50 mm, 50-75 mm).

At the end of this exercise it was intended that some closure be obtained with regard to the erratic and inconsistent nature of the corrosion rate, half-cell potential and resistivity measurements obtained at the various sites monitored previously at the University of Cape Town.

6.2.6 Results of wetting of concrete structure (Menzies site)

Corrosion monitoring was continued at two-day intervals initially and then at weekly intervals in order to obtain relevant trends. The corrosion rate, half-cell potential and resistivity results obtained are shown in figures 6.25 to 6.28 for the control area and the area treated with the corrosion inhibitor.

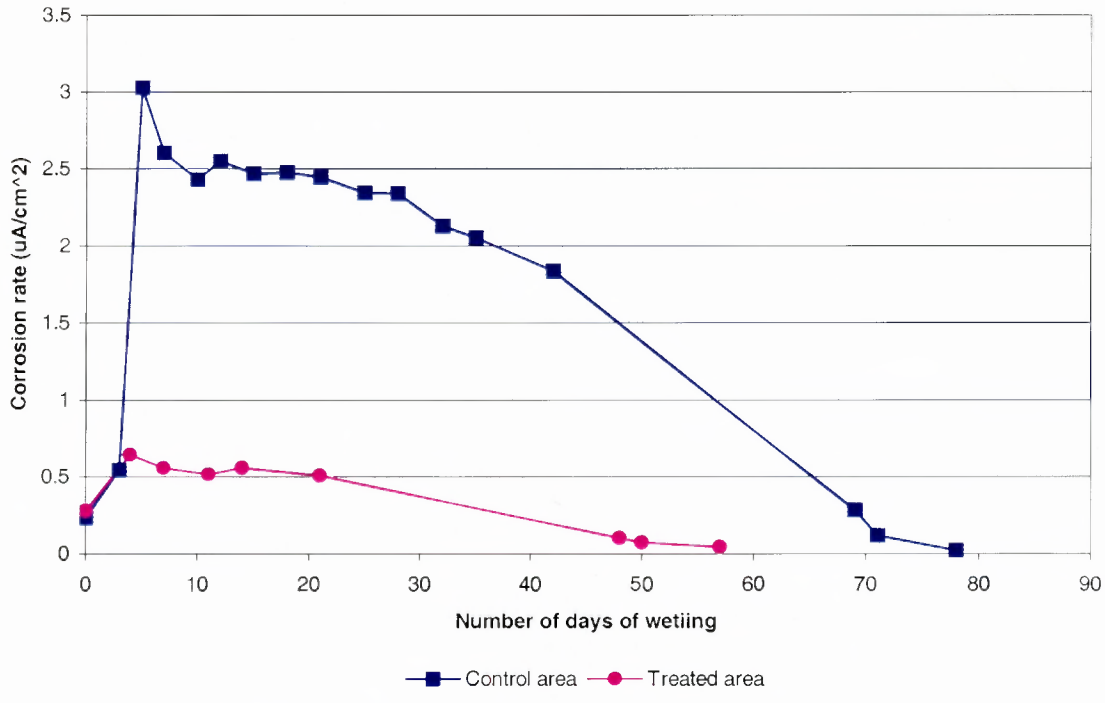

Figure 6.25: Corrosion rates for areas undergoing wetting

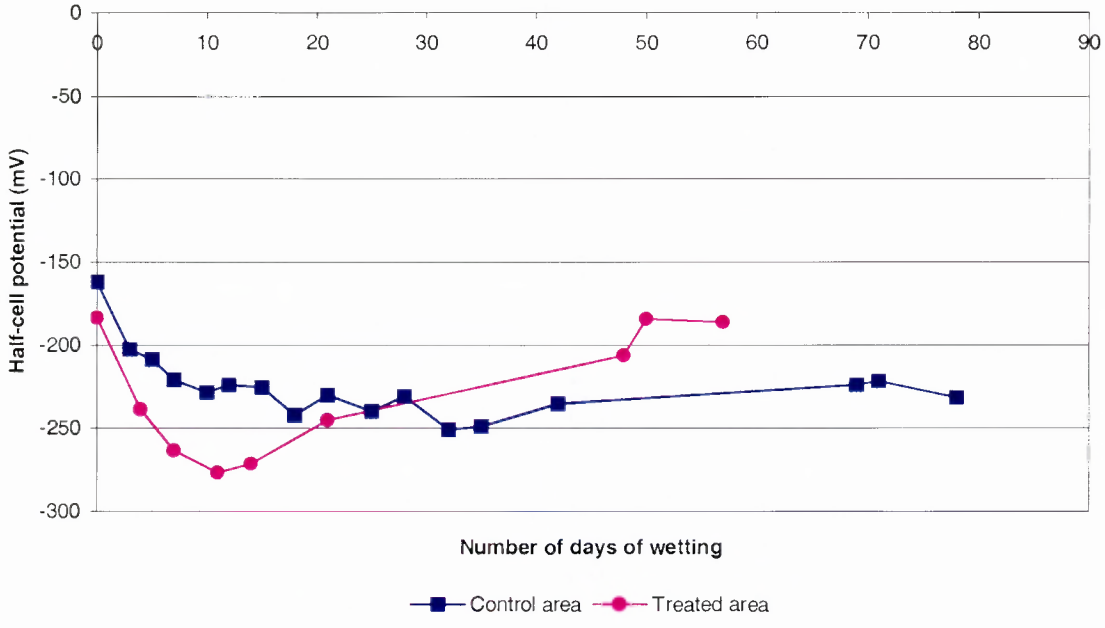

Figure 6.26: Half-cell potentials for areas undergoing wetting

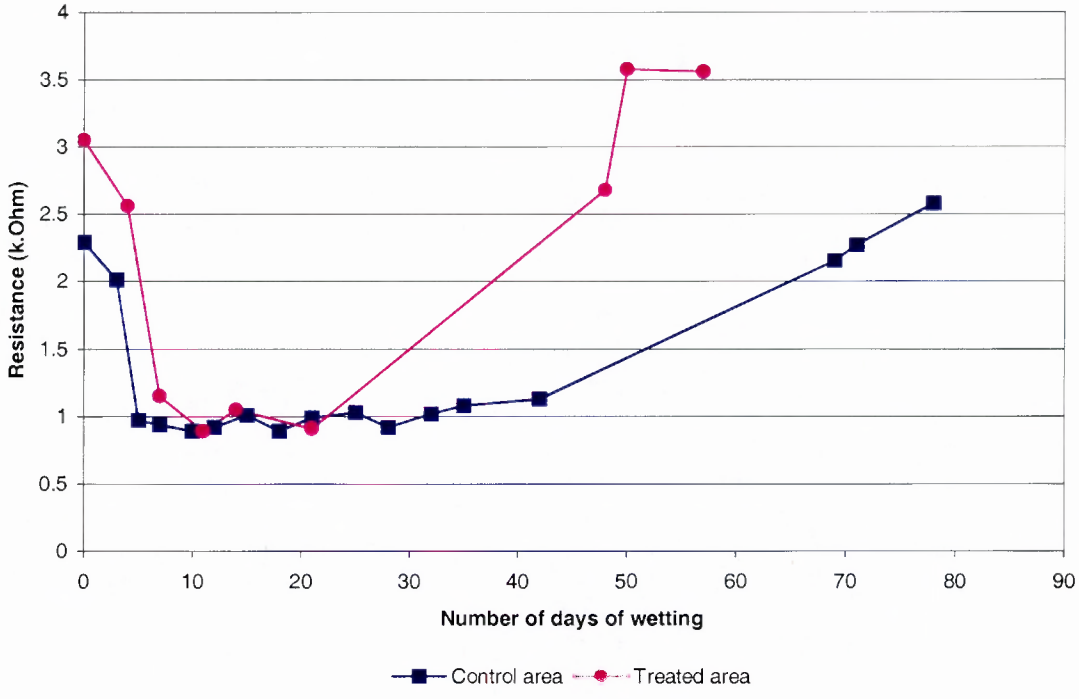

Figure 6.27: Resistances for areas undergoing wetting

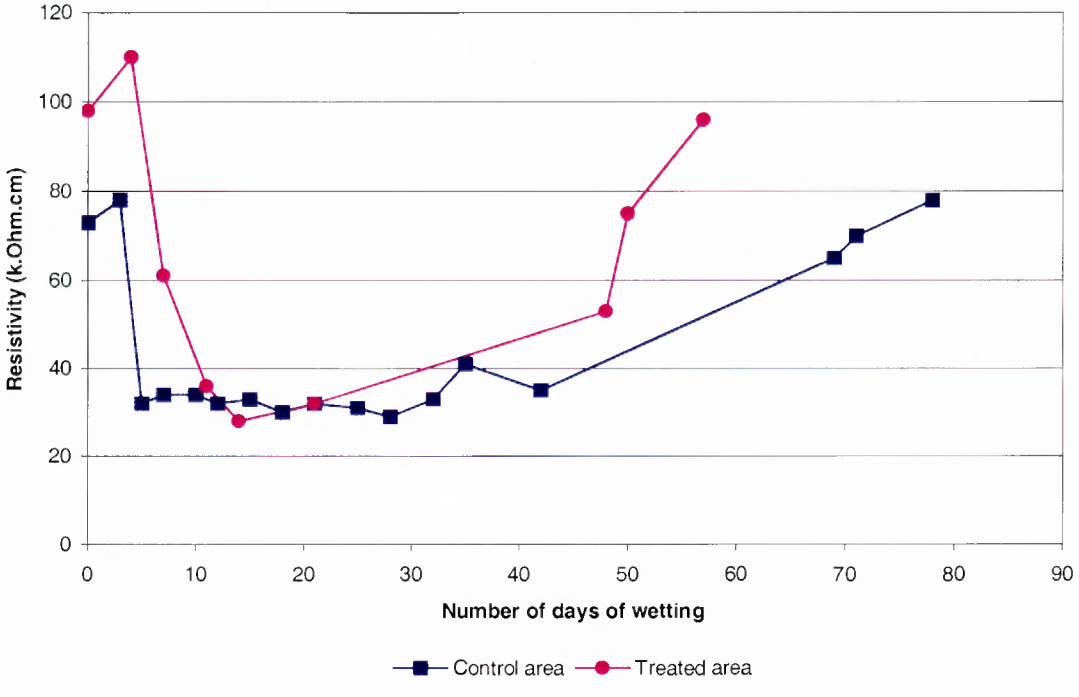

Figure 6.28: Resistivity for areas undergoing wetting

Discussion of results from wetting experiment

It was mentioned in previous sections that the corrosion process is determined by factors such as the conductivity of the cover concrete zone, the availability of oxygen and water in the surrounding environment and the penetrability of oxygen and water to the level of the reinforcing steel. Corrosion measurements obtained from the wetting of the concrete confirmed the importance of the above-mentioned points.

Prior to the start of the wetting system the corrosion rates for the control and treated areas were 0.237 and 0.282 $\mu A/cm^2$ respectively. The wetting system was applied continuously for a period of about three months. As moisture levels in the concrete got progressively higher an increase in corrosion rates and negative half-cell potentials and a decrease in concrete resistivity was observed. An increase in moisture content of the cover concrete increases the conductivity of the concrete thereby increasing corrosion rates and negative half-cell potentials. Also, an increase in conductivity (i.e. decrease in resistivity) indicates a freer movement of ions between the cathodic and anodic regions, thereby aiding the corrosion process. The corrosion rates and half-cell potentials in both cases (control and treated areas) increased gradually until a plateau value was obtained. These values were relatively stable for a small period of time after which a gradual reduction in corrosion rates and half-cell potential was observed. This general trend was observed in both the control and treated areas. However, a much lower plateau corrosion rate and half-cell potential was observed on the treated area, indicating the effectiveness of the penetrating corrosion inhibitor in reducing the rate at which corrosion is taking place.

The reduction of corrosion rates and half-cell potentials after a period of about 30 days is as a result of one or more of the following:

- The saturated nature of the concrete after repeated wetting was limiting availability of oxygen to the cathode, thereby stifling the corrosion process and hence reducing corrosion rates and negative half-cell potentials.
- An increase in resistivity was observed with the corresponding decrease in corrosion rate and half-cell potential. This increased resistance to ionic flow in the concrete is also a possible reason for the reduction in corrosion rates and half-cell potentials.

The 25 mm thick disc samples obtained from three cores taken at each of the two areas (treated and control area) were used to determine moisture contents and natural conductivities of the concrete to confirm the nature of the reduction in corrosion rates and half-cell potentials. Concrete conductivities were obtained using the chloride conductivity test developed by Streicher at the University of Cape Town where the ionic flux occurs by conduction due to a 10 V potential difference [68]. The apparatus consists of a two cell conduction rig in which the concrete core samples are exposed on either face to 5 M NaCl solution. The movement of chlorides is accelerated by applying a 10 V potential difference, and the conductivity determined by measuring the current flowing through the concrete specimen. The conductivity of concrete may be defined as follows [68]:

$$\sigma = it/VA \qquad (6.2)$$

where σ - concrete conductivity (mS/cm)
i - current (mA)
V - voltage (V)
t - specimen thickness (cm)
A - cross sectional area (cm^2)

The conductivity measurements were used to confirm the resisitivity of the saturated concrete in comparison to resistivity results measured on site using the Wenner probe. Resistivity is the inverse of conductivity. The results obtained are shown in table 6.10.

6.10: Concrete conductivities and moisture contents of treated and control areas.

Sample	Thickness (mm)	Current (mA)	Voltage (V)	Conductivity (mS/cm x 10^{-3})	Resistivity (k.Ohm.cm)	Degree of Saturation# (%)
Treated-1-A	25.4	2.2	10.08	15.3	65.3	86.5
Treated-1-B	25.4	2.5	10.03	17.4	57.5	88.0
Treated-1-C	26.2	2.0	10.01	14.4	69.4	86.9
Treated-2-A	26.1	1.9	10.00	13.7	73.0	81.2
Treated-2-B	26.2	2.4	10.00	17.3	57.8	83.3
Treated-2-C	26.1	2.1	10.07	15.0	66.7	90.6
Treated-3-A	26.0	1.8	10.02	12.9	77.5	77.1
Treated-3-B	25.5	1.8	10.07	12.6	79.4	84.5
Treated-3-C	25.5	1.4	10.03	9.81	102.0	44.4
Control-1-A	26.0	2.1	9.98	15.1	66.2	83.2
Control-1-B	23.7	2.4	10.00	15.7	63.7	86.2
Control-1-C	27.9	1.9	9.98	14.6	68.5	73.2
Control-2-A	26.3	2.1	9.98	15.2	65.8	84.6
Control-2-B	26.9	1.9	10.07	14.0	71.4	89.3
Control-2-C	25.8	1.6	10.07	11.3	88.5	86.3
Control-3-A	25.7	1.7	10.13	11.9	84.0	86.0
Control-3-B	25.3	2.0	10.00	13.9	72.0	90.9
Control-3-C	25.1	1.8	10.03	12.4	80.6	85.5

***A= depth of 0-25 mm B= depth of 25-50 mm C= depth of 50-75 mm**

 # Degree of saturation = (wet mass – dry mass)/(saturated mass – dry mass)

The values of conductivity obtained indicate concrete of relatively low resistivity of between 57 and 105 k.ohm.cm in the lab samples. These results were consistent with those obtained on site using the Wenner probe indicating it true nature. On saturation of the concrete structure a reduction in resistivity of the concrete was initially observed due to an increase in conductivity of the concrete. However, as saturation progressed resistivities increased with corresponding decreases in corrosion rates and half-cell potentials. It is therefore correct to assume that the reduction of corrosion rates and half-cell potentials observed were due to this increased resistance to the flow of current in the concrete. Conductivities were also observed to be higher at depths of between 0 and 50 mm.

6.3 Summary

Findings from site monitoring of structures treated with the organic corrosion inhibitor may be summarised as follows:

- Penetration of corrosion inhibitor was found to be rapid through concrete. The penetration results however indicate that the penetration is dependent on the grade and hence the porosity of the concrete.

- Rebar potentials shifted slightly positive after treatment with the inhibitor. Further monitoring is likely to indicate further positive shifts as evidenced in lab work.

- Corrosion rates remained active immediately following treatment with the inhibitor.

- However, corrosion rates approached passive levels with time in concrete treated with the inhibitor.

- The lack of 'reasonable' corrosion measurements (very low values of corrosion current densities and high resistivity values using the Gecor and Wenner probe) obtained was accounted for by the generally dryness of the environment, limiting the availability of water at the level of the reinforcing steel, thereby reducing the conductivity of the cover concrete zone.

7. CONCLUSIONS

The first chapters of this work involved a brief introduction to the corrosion of steel in reinforced concrete structures. Different methods of repairing and rehabilitating deteriorating concrete as well as corrosion prevention methods were discussed. Particular attention was paid to the problem of carbonation-induced corrosion in reinforced concrete and the use of penetrating corrosion inhibitors as a repair technique. Corrosion prevention and rehabilitation methods were discussed in order to place in context the effectiveness of the penetrating organic corrosion inhibitor tested in this work. Various corrosion measurement techniques (corrosion rate measurements, half-cell potentials and resistivities) were also discussed, and their limitations and interpretations stated.

Findings from this work have been valuable in that a better understanding of the penetrating surface-applied corrosion inhibitor was gained with respect to carbonation-induced corrosion, both in light of laboratory and site observations. The penetrating corrosion inhibitor was found to have a beneficial effect on protecting reinforcement in concrete. Penetrating corrosion inhibitors are unique in the sense that they can be applied to the surface of existing reinforced concrete structures as well as new structures to extend the useful life of the structure. The performance of the penetrating corrosion inhibitor in 30 MPa concrete specimens at 10 and 20 mm cover, and on site structures is summarised below. All the test specimens and areas used to assess the action of the inhibitor were treated with the amount recommended by the manufacturers.

7.1 Performance of the penetrating organic corrosion inhibitor in laboratory specimens

The performance of this penetrating corrosion inhibitor is largely dependent on its ability to penetrate the concrete and reach the corroding steel reinforcement. The performance of the inhibitor in 30 MPa concrete specimens at 10 and 20 mm covers is summarised below. Two specimens were treated with the inhibitor before the carbonation process, and two specimens were treated with the inhibitor after the carbonation process. Two control specimens were also cast to compare with treated specimens. The concentration of the inhibitor was determined at 1, 5 and 10 months. Corrosion rate measurements, half-cell potentials and resistivity measurements were taken. From the results obtained the following conclusions were made:

- The penetrating corrosion inhibitor showed excellent penetration in the 30 MPa concrete. At 28 days after treatment the inhibitor was found to have penetrated between 45 mm and 60 mm into the samples.

- The rate of penetration is dependent on the grade and hence the porosity of the concrete.

- 10 months after application of the inhibitor sufficient concentrations of the inhibitor were present at 60 mm depths. However, lower concentrations were detected at shallow levels compared to deeper levels. Sufficient inhibitor was still present at the 10 mm and 20 mm cover depths.

- A positive shift in half-cell potential was observed in specimens treated with the corrosion inhibitor before and after the carbonation process. On average, this shift amounted to + 100 mV.

- The observed trend in half-cell potentials of specimens treated with the inhibitor indicates that the inhibitor had an effect on the corrosion process.

- A steady increase in corrosion rates of the control samples was observed as opposed to a steady decrease in corrosion rates in the specimens that were treated with the inhibitor before and after the carbonation process.

- Corrosion rates approached passive levels of 0.1 $\mu A/cm^2$ with time, in concrete specimens treated with the penetrating corrosion inhibitor. In contrast, corrosion rates approached 0.8 and 0.5 $\mu A/cm^2$ in the 10 and 20 mm cover control samples respectively.

- The penetrating corrosion inhibitor is capable of delaying the onset of corrosion, as shown in the blocks that were treated with the inhibitor before the carbonation process, provided sufficient concentrations of the inhibitor are present at the level of the steel reinforcement.

- The ability of the penetrating inhibitor to reduce the rate at which corrosion takes place was also demonstrated, as seen in the specimens that were treated with the inhibitor after the initiation of corrosion due to carbonation, provided sufficient concentrations of the inhibitor are present at the level of the steel reinforcement.

7.1.1 Discussion

Grade 30 concrete was found to have relatively low permeability (high oxygen permeability index) indicating a concrete with a good overall microstructure and macrostructure of the outer surface of the concrete, provided adequate curing is carried out. The denser microstructure of the grade 30 concrete as compared to the grade 20 concrete indicated concrete in which the penetrating corrosion inhibitor was more likely to be retained. The water sorptivity of the grade 30 mix indicated a concrete that would permit the relative ease of movement of a wetting front under the action of capillary forces.

The penetration results observed at the various concrete grades (20, 30, 40 and 50 MPa) indicated that penetration is dependent on the grade and hence the porosity and permeability of the concrete. Penetration of the inhibitor may therefore be even slower in

higher grades of concrete and concrete containing cement extenders like FA and GGBS. Also the penetration of the inhibitor would be slower through carbonated concrete due to its denser microstructure. It is essential that sufficient concentrations of the corrosion inhibitor are available at the steel surface to ensure satisfactory conditions for corrosion inhibition. In some severe cases where structures are exposed directly to regular wetting, satisfactory penetration of corrosion inhibitors may not be possible beyond the near surface region. This is because of high internal moisture levels that would discourage capillary action and absorption and only allow extremely slow diffusion.

The grade 30 concrete in particular indicates a concrete in which the penetrating corrosion inhibitor is likely to penetrate effectively and be retained, and was therefore used to cast the corrosion test specimens.

The results also show that the inhibitor generally had penetrated the concrete to a depth of between 45 and 60 mm, well beyond the reinforcement (10 mm and 20 mm). The manufacturers of the inhibitor suggest that a concentration of more than 0.06 mg of organic nitrogen per gram of concrete is sufficient to inhibit corrosion. The results obtained show that more than sufficient amounts of the inhibitor were present at all depths. At 28 days a concentration of between 0.17 and 0.55 mg of organic nitrogen per gram of concrete was measured at the level of the steel reinforcement (10 mm and 20 mm). It was therefore expected that some degree of inhibition would occur.

After ten months the inhibitor was still present at all depths but at higher concentrations at deeper levels than at the surface. This indicated loss of the corrosion inhibitor at the surface of the concrete. However, adequate amounts of the penetrating corrosion inhibitor were present at the level of the reinforcement (10 and 20 mm) in all cases, and therefore a decrease in corrosion activity should be observed after the application of the inhibitor.

The performance of the penetrating corrosion inhibitor in treated specimens clearly indicates its ability to inhibit corrosion in carbonation-contaminated environments, provided sufficient concentrations are present at the level of the reinforcement. A steady increase in the corrosion rates of the control samples was observed, as opposed to a steady decrease in corrosion rates in the samples that were treated with the inhibitor before and after the carbonation process.

Potentials more negative than –250mV were observed during the testing period. A slight positive shift in potential in specimens treated with the penetrating inhibitor as compared to the control samples was observed. This difference in potential was considered to be due to the action of the penetrating corrosion inhibitor. The inhibitor is adsorbed onto the steel surface. The adsorbed organic layer inhibits corrosion by interfering with anodic dissolution of iron while simultaneously disrupting the reduction of oxygen at the cathode thereby reducing corrosion rates and half- cell potentials.

Resistivity measurements were taken using the Wenner probe and resistance was also measured using the Gecor 6 at each cycle. A linear relationship between resistivity and resistance for each specimen was observed. This relationship was analysed using all the

data recorded for the entire test period. The relationship between resistivity of the concrete and the resistance measured using the Gecor 6 was used to determine resistivity of the concrete when only the Gecor was used to measure resistances. It is important to note that this relationship was only used as a guide to determine the resistivity of the concrete using the Gecor.

7.2 Performance of the penetrating organic corrosion inhibitor in site structures

Initially the performance of the inhibitor was to be tested on four different sites situated at the University of Cape Town. However, at three of the sites, very low corrosion rates, low half-cell potentials and high resistivity measurements were observed. Corrosion rates measured were indicative of passive conditions although visible signs of corrosion were apparent on the sites. Cracks were visible along the lines of reinforcement and rust stains and delaminations were also present. Spalling of the concrete at certain localised points on the test area was also observed. However, the corrosion rate measurements together with the half-cell potential data and resistivity data indicated that corrosion was not taking place at that time. Probable reasons could be ascribed to one or a combination of the following factors:

- The generally dry environment, limiting the availability of water at the level of the reinforcing steel, thereby reducing the conductivity of the cover concrete zone.
- Oxides formed around the steel causing a dense skin on the surface of the steel, thus reducing the conductivity of the steel/concrete interface.
- The reduced fluid penetrability of the cover concrete zone due to carbonation, limiting the availability of water at the level of the reinforcing steel.

However, one of the UCT sites (the Menzies site) showed much higher corrosion rates and half-cell potentials; nevertheless, high resistivites of the order of 350 k.ohm.cm were still obtained. Due to the higher corrosion rate results obtained at the Menzies site corrosion monitoring was continued and the penetrating corrosion inhibitor was applied. Corrosion measurements were initiated a month prior to application of the inhibitor and continued for three months after its application. From the results of the test, the following conclusions were made:

- Penetration of corrosion inhibitor was found to be rapid through the site concrete (approximately Grade 20).

- Rebar potentials shifted slightly positive after treatment with the penetrating inhibitor. Further monitoring is likely to indicate further positive shifts as evidenced in lab work.

- Corrosion rates remained active immediately following treatment with the inhibitor.

- However, corrosion rates approached passive levels (0.1 $\mu A/cm^2$) with time in concrete treated with the inhibitor.

7.2.1 Discussion

The penetration of the inhibitor is dependent on the porosity and moisture condition of the concrete. The present concrete grade of the Menzies structure was found to be between 20 and 25 MPa, hence the rapid penetration. Twenty-eight days after application of the inhibitor sufficient concentrations were found at depths of between 45 and 60 mm, which are well beyond the level of steel reinforcement (≈ 20 - 30 mm). In some severe cases where structures are exposed directly to regular wetting, satisfactory penetration of corrosion inhibitors is not possible beyond the near surface region. This is because of high internal moisture levels that discourage capillary action absorption and only allow extremely slow diffusion.

The corrosion rates observed in the treated area (between 0.1 and 0.145 $\mu A/cm^2$) were lower than those previously measured on the same area prior to treatment with the inhibitor. They were also lower than the corrosion rates observed in the control area (between 0.169 and 0.256 $\mu A/cm^2$) where no inhibitor was applied. Results obtained showed that corrosion rates were gradually approaching passive levels in the area treated with the inhibitor. A positive shift in half-cell potentials was also observed. These trends therefore indicate the effectiveness of the penetrating corrosion inhibitor in its ability to slow down the rate at which corrosion is taking place.

The high resistivity measured can be accounted for by the generally dry environment of the concrete during the summer months, limiting the availability of water at the level of the reinforcing steel. Also the carbonation of the cover concrete may have reduced fluid penetrability of the cover concrete zone, limiting the availability of water, thereby reducing the conductivity i.e. increasing the resistivity of the cover concrete zone

The relatively low corrosion measurements obtained were ascribed to one or a combination of the following factors:

- The dryness of the environment, limiting the availability of water at the level of the reinforcing steel, thereby reducing the conductivity of the cover concrete zone.

- Oxides formed around the steel causing a dense skin reducing the ingress of moisture to the surface of the steel, and thus reducing the conductivity of the steel/concrete interface.

- The reduced fluid penetrability of the cover concrete zone due to carbonation, limiting the availability of water at the level of the reinforcing steel.

A broader investigation was therefore implemented to validate these assumptions and to assess the potential rate of corrosion in areas where the steel was found to have depassivated. To do this the concrete at the Menzies site was wetted continuously for a period of three months during which regular corrosion rate, half-cell potential and resistivity measurements were obtained. This wetting procedure was repeated on the area treated with the penetrating corrosion inhibitor.

The corrosion rates and half-cell potentials in both cases (control and treated areas) increased rapidly until a plateau value was obtained (2.5 $\mu A/cm^2$ in the control area and 0.5 $\mu A/cm^2$ in the treated area). These values were relatively stable for a period of time ($\approx$ 1 month) after which a gradual reduction in corrosion rates and half-cell potential, and a increase in concrete resistivity, was observed. This general trend was observed in both the control and treated areas. Plateau corrosion rates and half-cell potentials observed on the treated area were lower than those observed in the control area, indicating the effectiveness of the penetrating corrosion inhibitor in reducing the rate at which corrosion was taking place.

From the results obtained the following conclusions were made:

- The relatively low corrosion rates measured were accounted for by the general dryness of the environment, limiting the availability of water at the level of the reinforcing steel, thereby reducing the conductivity of the cover concrete zone.

- The penetrating corrosion inhibitor was effective in reducing the rate at which corrosion was taking place as was observed on the area treated with the inhibitor.

- Since the half-cell potentials at the end of the wetting experiment were not highly negative, the low corrosion rates obtained must be ascribed to the increased resistivity, and not oxygen starvation at the cathode.

From the laboratory and site work the following general conclusions can therefore be made:

- The penetrating corrosion inhibitor showed excellent penetration into concrete. The penetration results however indicate that the penetration is dependent on the grade and hence the porosity of the concrete. Penetration of the inhibitor may therefore be slow in higher grades of concrete and concrete with refined pore structures. Also the penetration of the inhibitor would be slower through carbonated concrete due to its denser microstructure. It is essential that sufficient concentrations of the corrosion inhibitor are available at the steel surface to ensure satisfactory conditions for corrosion inhibition.

- The penetrating corrosion inhibitor was effective in delaying the onset of corrosion as seen in the concrete samples treated with the penetrating inhibitor before the carbonation process. Laboratory findings suggest that the application of the penetrating corrosion inhibitor prior to carbonation is significantly able to increase the service life of reinforced concrete structure by delaying the onset of corrosion.

- The penetrating corrosion inhibitor was also able to slow the corrosion rate as seen in the blocks that were treated with the inhibitor after the initiation of corrosion by carbonation and also on site structures. Laboratory and site findings show that the

presence of sufficient concentrations of the penetrating corrosion inhibitor at the reinforcement will reduce the overall corrosion rate considerably.

From the results obtained in this study it was found that a penetrating corrosion inhibitor in laboratory specimens was effective in delaying the onset of corrosion and in reducing the rate at which corrosion takes place. It is therefore expected that such an inhibitor should be effective when applied to the surface of an existing structure or new structures to extend the useful life of the reinforced concrete. However, the cost needs to be carefully considered before repairs are initiated to provide the most appropriate repair solution from a technical and economic perspective.

7.3 Recommendations for further work

Some key issues that were found during this research that require further investigation are listed below:

- More detailed investigation into the effect of porosity and permeability on the rate of penetration of penetrating corrosion inhibitors.

- Comparison between the effectiveness of penetrating organic corrosion inhibitors and inorganic corrosion inhibitors (calcium nitrite) in controlling carbonation-induced corrosion.

- Investigation into the effectiveness of using penetrating corrosion inhibitors in conjunction with silane treatments to reduce carbonation-induced corrosion.

- Long-term corrosion monitoring of structures exposed to carbonation-induced corrosion in order to get a better understanding of corrosion measurements obtained i.e. low corrosion rates and negative half-cell potentials and high resistivities.

- Detailed cost analysis of the various corrosion prevention techniques.

REFERENCES

1. Broomfield, J. P., Corrosion of Steel in Concrete, Understanding, Investigation and Repair, Chapman and Hall London, 1996.

2. Bentur, A., Diamond, S. and Berke, N. S., Steel Corrosion in Concrete, Chapman and Hall London, 1997.

3. Rylands, T., Corrosion of Reinforcement in Concrete: The effectiveness of Organic Corrosion Inhibitors, MSc Thesis, University of Cape Town, 1999

4. Alexander, M. G. and Mackechnie, J. R., Repair principles for corrosion-damaged Reinforced Concrete Structures, Research Monogram No. 5, Department of Civil Engineering, University of Cape Town, March 2001.

5. Tuutti, K., Corrosion of Steel in Concrete, (1982) Swedish foundation for concrete research.

6. Fraczek, J., A Review of Electrochemical principles as applied to corrosion of Steel in Concrete or Grout environment, Corrosion, Concrete and Chlorides: Steel Corrosion in concrete causes and restraints, Gibson, F. W. (Ed), Michigan: American Concrete Institute, 1987, pp 13-22.

7. Hobbs, D. W., Marsh, B. K., Matthews, J. D. and Petit, S., Minimum requirements Concrete to resist carbonation-induced corrosion of reinforcement, Minimum requirements for durable concrete, Hobbs, D. W. (Ed)., British Cement Association, 1998, pp 11-42.

8. Berke, N. S., Hicks, M. C., Hoopes, R. J. and Tourney, P. J., Use of Laboratory Techniques to evaluate long-term durability of steel reinforced concrete exposed to chloride ingress, Durability of concrete in Malhotra, V. M. (Ed). Michigan: American Concrete Institute,1994, pp 229-331.

9 Parrott, L. J., A Review of carbonation in reinforced concrete, Cement and Concrete Association and Building Research Establishment Report, 1986.

10. Currie, R. J., Carbonation depths in structural-quality concrete, Building Research Establishment Report, 1986.

11. Mathews, J. D., Carbonation of ten-year-old concretes with and without added pulverised-fuel ash, Proceedings of 2nd International Conference on Ash Technology and Marketing, Barbican Centre, London, September, 1984.

12. Kurz, M., The influence of extremely short-term curing on the rate of carbonation in concrete, Proceedings of the RILEM Seminar, Hannover, 1984.

13. Wierig, H. J., Longtime studies on the carbonation of concrete under normal outdoor exposure, Proceedings of the RILEM Seminar, Hannover, 1984.

14. Meyer, A., Investigation on the carbonation of concrete, Proceedings of the 5th International Symposium on the Chemistry of Cement, Toyoko, 1969.

15. Fadayomi, J., Corrosion inhibitors, Concrete, Vol. September, 1997, pp 21-23.

16. American Society for Testing Materials, Standard Test Method for half-cell Potential measurements of reinforced concrete, ASTM C876, Philadelphia, 1991.

17. Gowers, K. R. and Millard, S. G., Measurement of Concrete Resistivity for Assessment of Corrosion Severity of Steel using Wenner Technique, ACI Materials Journal, September-October 1999, pp. 536-541.

18. Feliu, S., Gonzalez, J. A., Andrade, C. and Feliu, S. Jnr., Confinement of the Electrical Signal for In-situ Measurements of Polarisation Resistance in Reinforced Concrete, ACI Materials Journal, September- October 1990, pp. 457-460.

19. Millard, S. G. and Gowers, K. R., Structures and Building, British Institute of Civil Engineering, V.94, 1992, pp. 389.

20. Kinney, K. D. and Munteanu, V. F., The Electrochemical Evaluation of a Complex Corrosion Inhibitor, Proceedings of the International Conference on Corrosion and Rehabilitation of Reinforced Concrete Structures. US DoT, FHWA, Washington, 1999, Published as a CD Rom, Pub. No. FWH-SA-99014.

21. Gonzales, Felui, Andrade and Rodriguez, On site detection of corrosion in reinforced concrete structures, Materials and Structures, Vol. 24, 1991, pp. 346-350.

22. Stern, M. and Geary, A. L., Electrochemical Polarisation: Theoretical Analysis of the shape of Polarisation Curves, Journal of the Electrochemical Society, Vol. 104 No. 1, January 1957, pp. 56-63.

23. Page, C. L., Lambert, P. and Vassie, P. R. W., Investigation of Reinforcement Corrosion, Part II, Electochemical Monitoring of Steel in Chloride Contaminated Concrete, Materials and Structures, Vol. 24, 1991, pp.351- 358.

24. Millard, S. G., Corrosion Rate Measurement of In-situ Reinforced Concrete Structures, Proceedings of the Institution of Civil Engineers, Structures and Buildings, Vol. 99, February 1993, pp. 84-88.

25. Feliu, S., Gonzalez, J. A., Andrade, C. and Feliu, V., On Site determination of the Polarisation Resistance in a Reinforced Concrete Beam, Corrosion, Vol. 44, No.10, October 1988, pp. 761-765.

26. Feliu, S., Gonzalez, J. A., Andrade, C. and Feliu, V., On Site determination of the Polarisation Resistance in Reinforced Concrete Slabs, Corrosion Science (Oxford), Vol. 29, No. 1, January 1989, pp. 105-113.

27.Gianetti, F., Corrosion Inhibitor (Part 1), Concrete Engineering International, Volume March, 1998, pp 31-36.

28.Elsener, B., Buchler, M. and Bohni, H., Corrosion Inhibitors for Steel in Concrete, Proc. Eurocorr'97, Trondheim, 1997, pp 469-474.

29.Marazzani, B., Testing of the corrosion-inhibiting impregnation Sika Ferrogard 903 on carbonated slabs containing slightly to moderately corroded rebars, Report Sika, Madrid, February 1999.

30.Cigna, R., Mocalli, A., Peroni, E., Erisoni, L. and Maeder, U., Influence of Corrosion Inhibitors containing Aminoalcohols on the Prolongation of the Service Life of Reinforced Concrete Structures, Proc. Int. Conf. – Corrosion and Rehabilitation of Reinforced Concrete Structures, Orlando, 1998.

31.Emmons, P. H., Concrete Repair and Maintenance Illustrated, R. S. Means Company Inc., Construction Publisher and Consultants, Kingston, MA.

32.Bijen, J. M., Maintainance and Repair of Concrete Structures, Heron, Volume 34, 1989, No 2.

33.Manning, D. G., Cathodic Protection of Concrete Highways Bridges, Corrosion Of Reinforcement in Concrete, Page, C. L., Treadaway, K. W. J. and Bamforth, P. B. (Editors)., Published for the Royal Society of Chemical Industry by Elsevier Applied Science, London, 1990.

34.Stevenson, C. E., Unpublished MSc Thesis in progress, University of Cape Town, 2001.

35.Schutt, W. R., Cathodic Protection for Reinforced Concrete Structures, The USA Experience, Corrosion of Reinforcement in Concrete, Treadaway, K. W. J. and Bamforth, P. B. (Editors)., Published for the Royal Society of Chemical Industry by Elsevier Applied Science, London, 1990.

36.International Standards Organisation, Corrosion of metals and alloys, Basic terms and definitions, ISO 8044, 1989.

37.Fadayomi, J., Corrosion inhibitors, Concrete, Vol. September, 1997, pp 21-23.

38.Laamenen, P. H. and Byfors, K., Corrosion Inhibitors in Concrete – AMA (alkanolamines) – Based Inhibitors – State of the art Report, Nordic Concrete Research, No. 19, 1996, pp 29-40.

39.Mulheron, M. and Nwaubani, S. O., Corrosion Inhibitors for High performance Reinforced Concrete Structures, Proc. Int. Symposium – The Role of Admixtures In High Performance Concrete, Mexico, 1999.

40.Burge, T. A., The role of corrosion inhibitors in high performance concrete, SIKA AG, CH-8048, Zurich, Switzerland.

41. Hope, B. B. and Thompson, S. V., Damage to Concrete Induced by Calcium Nitrite, ACI Materials Journal, Sep-Oct 1995, Vol. 92 No. 5, pp. 529-531.

42. South Dakota Dept of Transportation Report (Use of Calcium Nitrite)

43. Berke, N. S., Corrosion inhibitors in Concrete, Concrete International, pp. 24, July 1991.

44. Andrade, C., Alonso, C. and Gonzalez, J. A., Some laboratory experiments on the inhibitor effect of sodium nitrite on reinforcement corrosion, Cement, Concrete and Aggregates, 1986, 8, No. 2, pp. 110-116.

45. Alonso, C., Acha, M. and Andrade, C., Inhibiting effect of nitrites on the corrosion of rebars embedded in carbonated concrete, Proceedings of RILEM International Symposium on Admixtures for Concrete-Improvement of Properties (ed. E. Vasquez), Chapman and Hall, London, 1990, pp. 219-228.

46. Alonso, C. and Andrade, C., Effect of nitrite as a corrosion inhibitor in contaminated and chloride-free carbonated mortars, ACI Materials Journal, 1990, 87, No. 2, pp. 130-137.

47. Page, C. L., Ngala, V. T. and Page, M. M., Corrosion Inhibitors in Concrete Repair Systems, Magazine of Concrete Research, Vol. 52, No. 1, February 2000, pp 25-37.

48. Gonzalez, J. A., Ramirez, E., Bautista, A. and Feliu, S., The behaviour of pre-rusted steel in concrete, Cement and Concrete Research, 1996, Vol. 26, pp 501-511.

49. Grace Construction Products, Application Guide : Postrite, W.R.Grace and Co., Cambridge, MA, 1994.

50. Cogliano, J. and Rosenberg, A., Treating concrete structures to inhibit corrosion by heating the structure, cooking same under controlled temperature gradient, and applying an inhibiting agent to an internal portion of the structure, United States Patent 5039556, August 1991.

51. Berke, N. S., Dallaire, M. P., Weyers, R. E., Henry, M. B., Peterson, J. E. and Prowell, B. D., Impregnation of concrete with corrosion inhibitors, In Corrosion Forms and Control for Infrastructure (ed. V. Chaker), American Society for Testing and Materials, Philadelphia, 1992, STP-1137, pp. 300-327.

52. Takukura, M., Hori, T., Sakaguchi, Y. and Nakamura, Y., Method for Preventing Hardened Cementitious Material from Deteriorating, European Patent Application EP 0 312 387 A1, 1988.

53. MacDonald, M., Sika Ferrogard 901 and 903 Corrosion Inhibitors: Evaluation of Test Programme, Sika Report, 1996.

54. Al-Qadi, I. L., Prowell, B. D., Weyers, R. E., Dutta, T. and Gouru, H., SHRP-S-666, Concrete Bridge Protection and Rehabilitation: Chemical and Physical Techniques, Corrosion Inhibitors and Polymers, Strategic Highway Research Programme, National Research Council, Virginia Polytechnic Institute and State University.

55. Vennesland, O., Humstad, E. P., Gautefall, O. and Nustad, G., Electrochemical Removal of Concrete effect on Bond Strength and Removal Efficiency, Corrosion of Reinforcement in concrete Construction, pp. 448, Edited by C. L Page, P. B Bramforth and J. W Figg, Published by the Royal Socoety of Chemistry, 1996.

56. Bjegovic, D., Sipos, L., Ukrainczyk, V. and Miksic, B., Diffusion of the MCI 2020 and 2000 corrosion inhibitors into concrete, Proc. of Corrosion and corrosion Protection of Steel in Concrete, (ed. R. N. Swamy), Sheffield Academic Press, 1994, pp 865-877.

57. Miksic, B., Gelner, L., Bjegivic, D. and Sipos, L., Migrating Corrosion Inhibitors for reinforced Concrete, Proc. of the 8th European Symposium on Corrosion Inhibitors, Ferrara, 1995, Sez. V, Suppl. 10, pp 569-588.

58. Broomfield, J. P., The pros and cons of Corrosion Inhibitors, Construction Repair, Vol. 11, No. 4, 1997, pp 16-17.

59. Broomfield, J. P. Corrosion inhibitors for steel in concrete, Concrete Journal, June 1999, pp. 44-47.

60. Report on X-ray Photon Spectrometry (XPS) and Secondary Ion Mass Spectrometry (SIMS) studies of Amino alcohol exposed to gold and steel surfaces; CR Brundle Associates, San Jose, CA; M. Grunze, Angewandte Physikalische Chemie, Universitat Heidelberg.

61. ASTM G 109-92, Standard Test Method for Determining the Effects of Chemical Admixtures on the Corrosion of embedded Steel Reinforcement in Concrete exposed to Chloride Environments.

62. Broomfield, J. P., St. Austell Car Park Sika Ferrogard 903 Corrosion Inhibitor Trial, Unpublished report, Sika, 1996.

63. Sika Information Manual, Product Summary, Sika, 1999

64. South African Bureau of Standards. "Sieve analysis, fines content and dust content of aggregates." SABS, Pretoria. SABS Method 829, 1994.

65. South African Bureau of Standards. "Specification for aggregates from natural sources." SABS, Pretoria. SABS Method 1083, 1994.

66. Standard Methods (1985), Standard methods for the examination of water and wastewater (16th edition), APHA, AWWA, WEF, Alexandria, VA, USA.

67. Alexander, M. G., Mackechnie, J. R. and Ballim, Y., Guide to the use of durability indexes for achieving durability in concrete structures, Research Monogram No. 2, Department of Civil Engineering, University of Cape Town, March 1999.

68. Alexander, M. G., Ballim, Y., and Mackechnie, J. R. Concrete durability index testing manual, Research Monogram No.1, Department of Civil Engineering, University of Cape Town, March 1999

69. South African Bureau of Standards. "Compressive strength of concrete (including making and curing of the test cubes)." SABS, Pretoria. SABS Method 863, 1994

APPENDICES

APPENDIX A

Materials and mixes

Grading analysis of fine aggregate (Klipheuwel sand).

Sieve size (μm)	Mass retained (g)	Cumulative % retained	% of material passed
4750	1.20	0.20	100
2360	35.1	7.30	93
1180	96.0	26.6	73
600	139.7	54.7	45
300	92.6	73.3	27
150	75.2	88.4	12

Grading analysis of coarse aggregate (Greywacke stone).

Sieve size (mm)	Cumulative % retained	% of material passed
26.5	0	100
19	10.92	89.08
13.2	74.92	25.08
9.5	97.03	2.97
6.7	98.92	1.08
0.075	99.75	0.25

Oxide analysis of cement (CEM I 42.5N).

Oxides	Proportion of sample (%)
CaO	67.16
SiO_2	22.25
Al_2O_3	4.42
Fe_2O_3	3.42
Mn_2O_3	0.08
TiO_2	0.22
MgO	1.01
P_2O_5	0.09
SO_3	0.58
K_2O	0.56
Na_2O	0.21
Na_2O_{eq}	0.58

APPENDIX B

Compressive strengths

Compressive strengths (MPa) obtained for different concrete grades.

Concrete grade (MPa)	Age (days)	Compressive strength (MPa)	Mean compressive strength (MPa)
20	7	16.0	15.8
		14.7	
		16.7	
	14	17.6	17.0
		15.2	
		18.3	
	28	27.2	22.0
		26.4	
		26.2	
30	7	22.2	22.1
		22.0	
		22.1	
	14	25.8	24.9
		23.4	
		25.5	
	28	30.1	30.1
		30.3	
		29.8	
40	7	27.2	27.3
		27.5	
		27.2	
	14	30.9	32.2
		33.4	
		32.6	
	28	38.5	39.8
		37.4	
		43.5	
50	7	38.4	38.0
		37.9	
		37.7	
	14	45.2	43.0
		42.1	
		41.7	
	28	49.6	50.1
		51.0	
		49.7	

APPENDIX C

Durability Index test results

Oxygen Permeability Index test results

Concrete grade (MPa)	Dry 1 cured		Dry 2 Cured	
	Oxygen Permeability Index	Average Oxygen Permeability Index	Oxygen Permeability Index	Average Oxygen Permeability Index
20	9.02	8.91	10.12	10.01
	8.79		10.1	
	8.93		9.82	
30	9.50	9.33	10.28	10.14
	9.15		10.13	
	9.33		10.0	
40	9.79	9.65	8.88	10.23
	9.53		10.4	
	9.64		10.06	
50	9.99	9.91	10.52	10.44
	9.61		10.57	
	10.13		10.22	

Water Sorptivity test results

Concrete grade (MPa)	Dry 1 cured		Dry 2 Cured	
	Water Sorptivity Index (mm/√h)	Average Water Sorptivity (mm/√h)	Water Sorptivity Index (mm/√h)	Average Water Sorptivity (mm/√h)
20	10.6	12.7	6.3	6.6
	13.4		6.3	
	14.2		7.1	
30	13.8	14.2	5.5	6.3
	15.0		6.7	
	13.9		6.8	
40	7.9	9.8	5.0	5.2
	10.9		5.4	
	10.5		5.1	
50	6.6	6.2	4.9	4.8
	5.2		4.1	
	6.7		5.4	

APPENDIX D

Corrosion measurements for 10 mm cover test specimens

Corrosion rates of 10 mm cover test specimens (Gecor 6 measurements)

Cycle number	Date	Corrosion rate (uA/cm^2)					
		Control 1	Control 2	BC 5	BC 6	AC 9	AC 10
1	24-Apr-01	0.797	0.341	0.213	0.053	0.351	0.418
2	27-Apr-01	0.150	0.390	0.192	0.320	0.556	0.351
3	30-Apr-01	0.107	0.193	0.032	0.161	0.440	0.291
4	04-May-01	0.579	0.408	0.017	0.127	0.422	0.410
5	07-May-01	0.542	0.345	0.184	0.174	0.322	0.301
6	14-May-01	0.633	0.256	0.168	0.106	0.127	0.265
7	18-May-01	0.828	0.322	0.231	0.263	0.197	0.441
8	21-May-01	0.788	0.425	0.140	0.172	0.162	0.350
9	25-May-01	0.555	0.224	0.444	0.440	0.707	0.214
10	29-May-01	0.519	0.539	0.611	0.271	0.179	0.380
11	01-Jun-01	0.542	0.488	0.242	0.208	0.152	0.220
12	04-Jun-01	0.646	0.149	0.212	0.152	0.071	0.237
13	08-Jun-01	0.686	0.254	0.150	0.118	0.112	0.267
14	11-Jun-01	0.690	0.292	0.160	0.100	0.132	0.222
15	15-Jun-01	0.555	0.266	0.159	0.192	0.112	0.174
16	18-Jun-01	0.482	0.288	0.180	0.195	0.244	0.254
17	22-Jun-01	0.520	0.176	0.523	0.200	0.562	0.288
18	25-Jun-01	0.588	0.188	0.388	0.250	0.344	0.255
19	29-Jun-01	0.480	0.190	0.240	0.185	0.200	0.210
20	02-Jul-01	0.415	0.192	0.150	0.124	0.168	0.145
21	06-Jul-01	0.544	0.250	0.144	0.135	0.288	0.155
22	09-Jul-01	0.574	0.325	0.132	0.130	0.385	0.236
23	13-Jul-01	0.490	0.300	0.140	0.150	0.255	0.198
24	16-Jul-01	0.550	0.288	0.150	0.192	0.277	0.291
25	23-Jul-01	0.485	0.203	0.164	0.142	0.122	0.178
26	26-Jul-01	0.710	0.445	0.104	0.236	0.240	0.283
27	30-Jul-01	0.544	0.320	0.120	0.188	0.190	0.250
28	06-Aug-01	1.216	0.554	0.146	0.102	0.117	0.245
29	13-Aug-01	0.500	0.666	0.118	0.137	0.156	0.194
30	17-Aug-01	1.413	0.785	0.268	0.219	0.288	0.364
31	20-Aug-01	0.205	0.666	0.248	0.135	0.255	0.339
32	27-Aug-01	0.177	0.558	0.188	0.158	0.196	0.261
33	03-Sep-01	0.441	0.290	0.125	0.145	0.288	0.158
34	10-Sep-01	1.621	0.830	0.398	0.254	0.347	0.234
35	14-Sep-01	0.544	0.268	0.187	0.151	0.119	0.116
36	17-Sep-01	0.663	0.311	0.155	0.126	0.242	0.220
37	24-Sep-01	0.828	0.820	0.188	0.109	0.182	0.222
38	01-Oct-01	0.750	0.788	0.201	0.188	0.212	0.203
39	08-Oct-01	0.800	0.795	0.215	0.174	0.205	0.215
40	12-Oct-01	0.798	0.824	0.189	0.188	0.245	0.202

41	15-Oct-01	0.754	0.601	0.210	0.190	0.266	0.232
42	19-Oct-01	0.710	0.750	0.156	0.185	0.200	0.300
43	22-Oct-01	0.812	0.690	0.144	0.215	0.178	0.255
44	26-Oct-01	0.850	0.802	0.188	0.223	0.164	0.200
45	29-Oct-01	0.888	0.822	0.138	0.132	0.205	0.184
46	02-Nov-01	0.750	0.886	0.144	0.156	0.187	0.210
47	05-Nov-01	0.900	0.718	0.158	0.125	0.128	0.185
48	09-Nov-01	0.666	0.789	0.110	0.114	0.135	0.198
49	12-Nov-01	0.745	0.770	0.125	0.132	0.109	0.168
50	16-Nov-01	0.800	0.823	0.120	0.122	0.115	0.130
51	19-Nov-01	0.788	0.891	0.112	0.110	0.156	0.125
55	03-Dec-01	0.890	0.741	0.109	0.156	0.112	0.169
59	17-Dec-01	0.650	0.910	0.123	0.130	0.110	0.210
63	31-Dec-01	0.756	0.885	0.100	0.146	0.154	0.185
67	14-Jan-02	0.821	0.655	0.133	0.119	0.115	0.113
71	28-Jan-02	0.690	0.723	0.122	0.145	0.123	0.151
75	11-Feb-02	0.745	0.789	0.119	0.125	0.152	0.122
79	25-Feb-02	0.789	0.800	0.108	0.113	0.111	0.115
83	11-Mar-02	0.755	0.724	0.112	0.112	0.140	0.120
87	25-Mar-02	0.821	0.814	0.105	0.120	0.112	0.134

Half-cell potential of 10 mm cover test specimens (Gecor 6 measurements)

Cycle number	Date	Potentials (mV)					
		Control 1	Control 2	BC 5	BC 6	AC 9	AC 10
1	24-Apr-01	-715.4	-617.5	-497.3	-419.4	-597.6	-531.9
2	27-Apr-01	-727.6	-679.7	-509.4	-547.6	-620.8	-545.9
3	30-Apr-01	-756.2	-592.0	-525.2	-596.8	-698.3	-576.9
4	04-May-01	-740.0	-594.2	-490.6	-488.3	-699.5	-586.2
5	07-May-01	-735.0	-592.1	-451.6	-489.2	-688.4	-545.3
6	14-May-01	-671.9	-583.5	-460.7	-458.6	-529.8	-464.3
7	18-May-01	-617.2	-480.8	-461.8	-391.0	-476.2	-402.2
8	21-May-01	-650.8	-540.2	-460.2	-423.4	-506.4	-454.2
9	25-May-01	-677.2	-512.6	-464.3	-528.7	-570.4	-492.5
10	29-May-01	-700.3	-408.0	-462.5	-405.7	-492.2	-436.9
11	01-Jun-01	-693.4	-450.2	-462.2	-490.5	-560.2	-440.8
12	04-Jun-01	-717.3	-576.1	-467.3	-597.4	655.1	-508.7
13	08-Jun-01	-653.6	-480.1	-453.8	-454.3	-492.4	-435.5
14	11-Jun-01	-692.4	-550.4	-422.3	-492.6	-501.3	-490.2
15	15-Jun-01	-627.7	-442.3	-438.0	-439.4	-450.2	-426.9
16	18-Jun-01	-545.3	-512.1	-489.2	-490.5	-503.2	-510.4
17	22-Jun-01	-548.2	-494.1	-460.7	-451.4	-500.2	-420.2
18	25-Jun-01	-580.4	-455.2	-497.5	-444.3	-485.5	-456.8
19	29-Jun-01	-540.2	-420.1	-488.5	-425.3	-398.5	-400.5
20	02-Jul-01	-687.6	-529.0	-449.7	-479.6	-548.4	-455.8
21	06-Jul-01	-594.3	-488.2	-450.1	-444.5	-520.3	-500.3
22	09-Jul-01	-668.8	-614.9	-461.3	-544.3	-569.3	-439.1
23	13-Jul-01	-623.5	-500.3	-420.1	-445.2	-512.2	-498.3
24	16-Jul-01	-694.4	-632.2	-469.1	-564.8	-602.4	-457.5
25	23-Jul-01	-576.0	-449.8	-406.3	-298.0	-436.8	-374.9
26	26-Jul-01	-587.0	-496.2	-411.3	-335.4	-453.6	-381.3
27	30-Jul-01	-571.6	-416.8	-405.4	-420.3	-412.2	-455.6
28	06-Aug-01	-580.9	-487.1	-406.1	-375.9	-434	-370.3
29	13-Aug-01	-544.4	-480.2	-417.3	-372.4	-546.9	-388.2
30	17-Aug-01	-402.9	-395.1	-370.8	-278.9	-450.8	-368.5
31	20-Aug-01	-571.3	-502.4	-443.1	-340.3	-445.7	-401.7
32	27-Aug-01	-595.1	-522.3	-415.7	-343.6	-441.7	-401.7
33	03-Sep-01	-578.6	-507.9	-445.8	-298.0	-485.5	-382.7
34	10-Sep-01	-589.4	-511.5	-433.1	-296.9	-428.5	-376.1
35	14-Sep-01	-300.4	-140.9	-188.9	-526.0	-144.5	-128.4
36	17-Sep-01	-537.8	-402.2	-400.3	-258.9	-409.2	-369.1
37	24-Sep-01	-548.3	-470.0	-411.9	-281.4	-417.1	-373.2
38	01-Oct-01	-524.7	-468.4	-304.8	-192.4	-390.7	-303.5
39	08-Oct-01	-550.2	-499.3	-400.6	-405.5	-458.3	-500.2
40	12-Oct-01	-580.8	-488.3	-401.8	-398.2	-483.2	-390.0
41	15-Oct-01	-562.1	-492.4	-403.8	-452.6	-487.1	-498.3
42	19-Oct-01	-555.8	-495.3	-425.1	-400.2	-426.1	-412.0
43	22-Oct-01	-589.2	-555.2	-488.2	-452.0	-460.1	-423.5

45	29-Oct-01	-584.3	-566.3	-512.1	-510.0	-532.1	-522.2
46	02-Nov-01	-566.5	-587.4	-500.3	-498.2	-511.3	-520.5
47	05-Nov-01	-558.1	-471.1	-400.4	-456.2	-484.9	-390.2
48	09-Nov-01	-566.3	-580.3	-500.3	-510.8	-523.0	-512.3
49	12-Nov-01	-582.1	-589.9	-560.2	-542.1	-498.2	-512.3
50	16-Nov-01	-584.2	-567.3	-523.0	-536.2	-520.1	-530.6
51	19-Nov-01	-569.4	-589.7	-587.5	-512.3	-546.3	-522.3
55	03-Dec-01	-590.2	-562.1	-591.0	-555.2	-502.3	-566.1
59	17-Dec-01	-556.3	-612.3	-513.2	-526.5	-500.1	-580.5
63	31-Dec-01	-587.5	-598.6	-456.2	-536.1	-562.4	-555.3
67	14-Jan-02	-600.3	-545.2	-510.0	-525.0	-499.6	-499.6
71	28-Jan-02	-578.2	-566.3	-506.2	-569.3	-523.5	-546.1
75	11-Feb-02	-586.4	-586.0	-511.1	-575.4	-545.4	-513.6
79	25-Feb-02	-599.6	-569.3	-500.3	-526.9	-500.3	-509.5
83	11-Mar-02	-580.2	-596.1	-501.4	-510.1	-502.0	-510.5
87	25-Mar-02	-594.4	-600.5	-506.0	-500.2	-500.4	-505.3

Resistance of 10 mm cover test specimens (Gecor 6 measurements).

Cycle number	Date	Resistance (k. ohms)					
		Control 1	Control 2	BC 5	BC 6	AC 9	AC 10
1	24-Apr-01	0.64	0.74	0.53	0.58	0.72	0.64
2	27-Apr-01	0.50	0.62	0.80	0.67	0.67	0.60
3	30-Apr-01	0.62	0.68	0.92	0.67	0.65	0.82
4	04-May-01	0.50	0.62	0.57	0.62	0.59	0.72
5	07-May-01	0.55	0.64	0.57	0.62	0.56	0.70
6	14-May-01	0.56	0.70	0.91	0.85	0.77	0.71
7	18-May-01	0.64	0.77	1.09	0.85	0.97	0.95
8	21-May-01	0.54	0.66	0.88	0.85	0.78	0.68
9	25-May-01	0.77	0.74	0.99	0.83	0.83	0.82
10	29-May-01	0.63	0.91	1.06	0.77	0.88	0.92
11	01-Jun-01	0.60	0.82	0.98	0.80	0.85	0.90
12	04-Jun-01	0.62	0.79	1.05	0.83	0.87	0.99
13	08-Jun-01	0.70	0.94	1.26	1.02	0.93	1.21
14	11-Jun-01	0.68	0.84	0.98	0.83	0.76	0.98
15	15-Jun-01	0.80	0.80	0.94	0.83	0.92	0.93
16	18-Jun-01	0.75	0.62	0.50	0.90	0.88	0.64
17	22-Jun-01	0.84	0.70	0.99	0.77	0.84	0.95
18	25-Jun-01	0.95	0.88	0.70	0.85	0.99	0.95
19	29-Jun-01	0.98	0.77	0.80	0.65	0.90	0.87
20	02-Jul-01	0.64	0.84	1.12	0.87	0.95	0.99
21	06-Jul-01	0.66	0.85	0.99	1.02	0.70	0.85
22	09-Jul-01	0.70	0.89	1.14	1.08	0.86	1.17
23	13-Jul-01	0.70	0.88	1.09	1.00	0.99	0.80
24	16-Jul-01	0.78	0.96	1.18	1.17	1.30	1.18
25	23-Jul-01	0.69	0.93	1.18	1.11	1.15	1.29
26	26-Jul-01	0.51	0.64	0.84	0.76	0.78	0.92
27	30-Jul-01	0.52	0.78	0.97	0.85	0.70	0.66
28	06-Aug-01	0.75	1.30	1.77	1.82	1.99	2.26
29	13-Aug-01	1.52	1.25	1.77	1.76	1.04	1.78
30	17-Aug-01	0.68	0.85	1.11	1.00	0.78	1.13
31	20-Aug-01	1.75	1.41	2.15	1.86	2.22	2.02
32	27-Aug-01	1.47	1.17	1.62	1.41	1.57	1.66
33	03-Sep-01	0.41	0.52	1.02	0.90	0.75	1.09
34	10-Sep-01	0.61	0.76	1.06	1.09	1.18	1.30
35	14-Sep-01	1.58	2.40	2.79	3.33	3.59	3.23
36	17-Sep-01	1.35	1.25	1.34	1.57	1.52	1.69
37	24-Sep-01	0.79	1.09	1.85	1.49	1.07	1.58
38	01-Oct-01	1.44	1.64	2.30	2.48	1.60	2.51
39	08-Oct-01	1.50	1.22	1.10	1.45	1.78	2.00
40	12-Oct-01	1.09	1.41	1.79	1.69	1.29	1.80
41	15-Oct-01	0.99	1.08	1.88	1.30	1.54	1.62
42	19-Oct-01	0.98	0.88	1.05	1.10	1.33	1.25
43	22-Oct-01	0.87	0.90	1.50	1.02	1.12	1.10

44	26-Oct-01	0.99	1.03	1.46	1.22	1.11	1.06
45	29-Oct-01	0.88	0.85	0.95	0.63	0.99	0.68
46	02-Nov-01	0.60	0.58	0.88	0.75	0.98	0.68
47	05-Nov-01	0.52	0.51	0.7	0.60	0.53	0.80
48	09-Nov-01	0.60	0.56	0.87	0.66	0.89	0.75
49	12-Nov-01	0.58	0.62	0.70	0.98	0.68	0.77
50	16-Nov-01	0.60	0.69	0.85	0.45	0.62	0.78
51	19-Nov-01	0.55	0.63	0.65	0.56	0.75	0.90
55	03-Dec-01	0.69	0.58	0.78	0.50	0.45	0.65
59	17-Dec-01	0.88	0.78	0.98	0.69	0.50	0.78
63	31-Dec-01	0.75	0.75	0.88	0.99	0.66	0.50
67	14-Jan-02	0.70	0.69	0.96	0.87	0.96	0.98
71	28-Jan-02	0.90	0.88	0.56	0.82	0.85	0.88
75	11-Feb-02	0.50	0.99	0.66	0.60	0.70	0.65
79	25-Feb-02	0.89	0.84	0.68	0.70	0.90	0.60
83	11-Mar-02	0.99	1.02	0.85	0.70	0.88	0.80
87	25-Mar-02	0.90	0.88	1.12	0.99	0.90	0.68

Corrosion rates of 10 mm cover test specimens (Coulostaic method measurements).

Cycle number	Date	Corrosion rate (uA/cm^2)					
		Control 1	Control 2	BC 5	BC 6	AC 9	AC 10
1	24-Apr-01	0.555	0.412	0.210	0.009	0.321	0.388
2	27-Apr-01	0.110	0.412	0.222	0.345	0.500	0.320
3	30-Apr-01	0.009	0.115	0.100	0.179	0.509	0.311
4	04-May-01	0.623	0.410	0.100	0.133	0.419	0.150
5	07-May-01	0.522	0.406	0.222	0.170	0.345	0.288

$Cu/CuSO_4$ Half-cell potential of 10 mm cover test specimens.

Cycle number	Date	Potentials (mV)					
		Control 1	Control 2	BC 5	BC 6	AC 9	AC 10
1	24-Apr-01	-758.9	-600.0	-466.5	-456.2	-625.4	-500.0
2	27-Apr-01	-633.5	-600.5	-501.2	-577.3	-645.3	-550.8
3	30-Apr-01	-688.7	-569.7	-511.2	-540.6	-503.8	-498.5
4	04-May-01	-699.8	-555.8	-512.0	-500.3	-645.9	-500.0
5	07-May-01	-705.5	-610.2	-455.0	-399.2	-611.2	-500.2

Resistivity measurements for 10 mm cover test specimens (using the Wenner probe)

Cycle number	Date	Resistivity (k. ohms.cm)					
		Control 1	Control 2	BC 5	BC 6	AC 9	AC 10
1	24-Apr-01	31	37	25	30	23	20
2	27-Apr-01	20	35	40	26	22	25
3	30-Apr-01	25	48	54	25	20	26
4	04-May-01	20	28	30	23	24	31
5	07-May-01	18	25	23	20	28	31
6	14-May-01	25	31	51	25	57	42
7	18-May-01	32	37	51	22	53	51
8	21-May-01	31	34	49	22	51	50
9	25-May-01	31	37	53	26	56	47
10	29-May-01	39	41	32	36	75	55
11	01-Jun-01	23	28	30	26	28	31
12	04-Jun-01	20	26	32	29	55	50
13	08-Jun-01	35	35	69	27	31	38
14	11-Jun-01	25	30	29	25	26	34
15	15-Jun-01	27	25	32	29	30	28
16	18-Jun-01	25	22	20	32	27	24
17	22-Jun-01	29	27	32	25	30	28
18	25-Jun-01	30	28	22	27	33	30
19	29-Jun-01	31	27	25	23	27	27
20	02-Jul-01	35	33	38	30	33	28
21	06-Jul-01	25	27	35	30	27	26
22	09-Jul-01	23	28	35	29	30	33
23	13-Jul-01	25	27	29	26	32	29
24	16-Jul-01	27	30	36	32	38	41
25	23-Jul-01	32	38	49	45	37	35
26	26-Jul-01	28	32	26	25	28	32
27	30-Jul-01	21	26	32	22	26	28
28	06-Aug-01	25	45	53	59	63	75
29	13-Aug-01	72	52	57	61	58	55
30	17-Aug-01	26	28	36	25	29	35
31	20-Aug-01	55	46	66	55	90	65
32	27-Aug-01	48	40	48	49	57	58
33	03-Sep-01	25	22	36	27	28	35
34	10-Sep-01	26	24	36	28	32	40
35	14-Sep-01	55	76	85	97	115	101
36	17-Sep-01	42	38	48	55	43	52
37	24-Sep-01	25	38	50	42	38	51
38	01-Oct-01	46	50	74	79	52	78
39	08-Oct-01	48	37.5	35	48	51	65
40	12-Oct-01	35	38.5	55	52	40	61
41	15-Oct-01	25	28	56	44	49	50
42	19-Oct-01	32	30	35	33	46	40
43	22-Oct-01	26	30	39	35	30	31

44	26-Oct-01	24	28	44	32	34	35
45	29-Oct-01	27	26	30	22	31	32
46	02-Nov-01	22	20	30	23	31	22
47	05-Nov-01	16	21	26	22	29	25
48	09-Nov-01	28	20	32	21	27	24
49	12-Nov-01	25	28	24	32	23	25
50	16-Nov-01	22	31	26	25	28	31
51	19-Nov-01	20	21	20	18	24	30
55	03-Dec-01	18	16	20	20	16	21
59	17-Dec-01	27	30	35	25	18	24
63	31-Dec-01	26	28	33	31	20	16
67	14-Jan-02	25	23	29	35	32	29
71	28-Jan-02	30	28	20	25	30	32
75	11-Feb-02	20	25	35	28	30	20
79	25-Feb-02	26	25	20	25	28	18
83	11-Mar-02	32	35	27	25	30	27
87	25-Mar-02	30	28	37	35	32	25

APPENDIX E

Corrosion measurements for 20 mm cover test specimens

Corrosion rates of 20 mm cover test specimens (Gecor 6 measurements)

Cycle number	Date	Corrosion rate (uA/cm^2)					
		Control 3	Control 4	BC 7	BC 8	AC 11	AC 12
1	18-Jun-01	0.140	0.112	0.095	0.088	0.099	0.102
2	22-Jun-01	0.155	0.145	0.100	0.098	0.294	0.154
3	25-Jun-01	0.244	0.198	0.119	0.150	0.145	0.255
4	29-Jun-01	0.325	0.255	0.140	0.205	0.122	0.298
5	02-Jul-01	0.405	0.259	0.122	0.309	0.255	0.188
6	06-Jul-01	0.455	0.388	0.121	0.222	0.282	0.160
7	09-Jul-01	0.364	0.410	0.154	0.144	0.222	0.250
8	13-Jul-01	0.305	0.302	0.162	0.153	0.188	0.200
9	16-Jul-01	0.288	0.342	0.120	0.140	0.150	0.188
10	23-Jul-01	0.290	0.320	0.114	0.112	0.122	0.165
11	26-Jul-01	0.488	0.350	0.200	0.105	0.140	0.182
12	30-Jul-01	0.450	0.322	0.271	0.188	0.135	0.244
13	06-Aug-01	0.408	0.398	0.166	0.152	0.145	0.189
14	13-Aug-01	0.300	0.188	0.173	0.163	0.139	0.155
15	17-Aug-01	0.288	0.290	0.143	0.122	0.180	0.142
16	20-Aug-01	0.350	0.244	0.122	0.143	0.201	0.100
17	27-Aug-01	0.268	0.205	0.154	0.200	0.162	0.182
18	03-Sep-01	0.244	0.198	0.211	0.182	0.122	0.204
19	10-Sep-01	0.410	0.388	0.124	0.198	0.115	0.166
20	14-Sep-01	0.398	0.340	0.135	0.205	0.134	0.150
21	17-Sep-01	0.326	0.276	0.175	0.184	0.187	0.173
22	24-Sep-01	0.350	0.392	0.194	0.135	0.185	0.189
23	01-Oct-01	0.335	0.356	0.184	0.126	0.166	0.179
24	08-Oct-01	0.321	0.347	0.155	0.115	0.178	0.166
25	12-Oct-01	0.289	0.263	0.185	0.166	0.133	0.162
26	15-Oct-01	0.245	0.350	0.205	0.111	0.109	0.105
27	19-Oct-01	0.288	0.290	0.184	0.156	0.112	0.150
28	22-Oct-01	0.300	0.320	0.188	0.166	0.132	0.122
29	26-Oct-01	0.280	0.410	0.165	0.150	0.100	0.140
30	29-Oct-01	0.380	0.388	0.150	0.160	0.120	0.108
31	02-Nov-01	0.298	0.395	0.142	0.130	0.111	0.119
32	05-Nov-01	0.403	0.407	0.183	0.114	0.116	0.103
33	09-Nov-01	0.423	0.354	0.165	0.123	0.105	0.109
34	12-Nov-01	0.410	0.409	0.154	0.120	0.119	0.10
35	16-Nov-01	0.407	0.388	0.140	0.111	0.110	0.12
36	19-Nov-01	0.399	0.456	0.123	0.115	0.120	0.112
37	23-Nov-01	0.452	0.398	0.152	0.128	0.119	0.108
38	26-Nov-01	0.411	0.412	0.145	0.120	0.111	0.114
39	30-Nov-01	0.400	0.405	0.130	0.113	0.114	0.120
40	03-Dec-01	0.356	0.423	0.146	0.142	0.123	0.119

41	07-Dec-01	0.469	0.455	0.119	0.124	0.120	0.100
42	10-Dec-01	0.444	0.395	0.120	0.122	0.119	0.108
43	14-Dec-01	0.500	0.369	0.111	0.100	0.150	0.110
44	17-Dec-01	0.498	0.412	0.113	0.127	0.132	0.100
45	21-Dec-01	0.501	0.498	0.125	0.130	0.125	0.115
46	24-Dec-01	0.512	0.466	0.144	0.129	0.120	0.111
47	28-Dec-01	0.520	0.450	0.152	0.135	0.115	0.109
48	31-Dec-01	0.489	0.421	0.113	0.124	0.112	0.105
49	04-Jan-01	0.504	0.422	0.106	0.119	0.100	0.112
50	07-Jan-02	0.521	0.458	0.111	0.111	0.109	0.110
52	14-Jan-02	0.490	0.455	0.122	0.120	0.104	0.100
56	28-Jan-02	0.500	0.510	0.120	0.100	0.109	0.111
60	11-Feb-02	0.499	0.499	0.110	0.115	0.110	0.111
64	25-Feb-02	0.509	0.480	0.109	0.111	0.100	0.109
68	11-Mar-02	0.510	0.451	0.112	0.130	0.109	0.120
72	25-Mar-02	0.478	0.502	0.108	0.121	0.115	0.100

Half-cell potential of 20 mm cover test specimens (Gecor 6 measurements)

Cycle number	Date	Potentials (mV)					
		Control 3	Control 4	BC 7	BC 8	AC 11	AC 12
1	18-Jun-01	-402.3	-415.5	-398.2	-382.5	-399.1	-400.5
2	22-Jun-01	-501.2	-477.3	-450.2	-388.4	-520.4	-510.3
3	25-Jun-01	-545.2	-440.3	-468.5	-523.2	-422.2	-566.7
4	29-Jun-01	-592.6	-555.4	-455.2	-502.5	-405.3	-520.3
5	02-Jul-01	-645.0	-581.5	-543.6	-499.3	-539.0	-535.2
6	06-Jul-01	-594.3	-555.5	-401.2	-521.3	-560.1	-410.2
7	09-Jul-01	-622.9	-534.8	-509.5	-586.0	-453.7	-413.8
8	13-Jul-01	-600.2	-599.4	-469.5	-455.5	-520.1	-588.8
9	16-Jul-01	-657.5	-557.5	-547.0	-643.2	-553.2	-576.4
10	23-Jul-01	-393.3	-354.6	-434.8	-362.3	-352.8	-332.2
11	26-Jul-01	-389.0	-361.3	-380.9	-340.1	-312.2	-320.7
12	30-Jul-01	-545.2	-522.2	-498.3	-455.2	-420.1	-466.5
13	06-Aug-01	-255.2	-399.0	-458.1	-371.5	-426.5	-356.3
14	13-Aug-01	-581.3	-558.1	-492.6	-577.1	-469.6	-400.9
15	17-Aug-01	-473.8	-472.5	-457.6	-489.4	-428.6	-361.9
16	20-Aug-01	-602.0	-539.5	-476.5	-600.0	-434.1	-381.8
17	27-Aug-01	-535.6	-445.6	-451.7	-410.4	-384.5	-360.8
18	03-Sep-01	-360.7	-346.3	-426.3	-333.0	-342.2	-322.4
19	10-Sep-01	-359.5	-345.7	-368.4	-328.0	-371.8	-320.9
20	14-Sep-01	-223.4	-200.2	-400.2	-326.8	-331.3	-313.5
21	17-Sep-01	-356.6	-335.2	-414.7	-344.4	-335.0	-316.3
22	24-Sep-01	-354.6	-332.6	-417.1	-373.8	-381.2	-324.2
23	01-Oct-01	-385.6	-365.2	-344.2	-325.6	-358.9	-340.2
24	08-Oct-01	-387.2	-389.5	-350.2	-321.4	-326.2	-322.1
25	12-Oct-01	-346.3	-318.5	-401.1	-300.2	-403	-367.4
26	15-Oct-01	-395.8	-344.6	-438.5	-355.2	-357.0	-322.2
27	19-Oct-01	-488.1	-490.0	-486.2	-449.4	-394.1	-400.2
28	22-Oct-01	-452.3	-425.1	-412.3	-398.6	-385.2	-335.6
29	26-Oct-01	-388.7	-366.8	-332.5	-322.1	-320.0	-333.1
30	29-Oct-01	-400.6	-412.5	-398.6	-387.5	-356.1	-385.2
31	02-Nov-01	-458.6	-423.5	-398.6	-358.2	-397.1	-366.5
32	05-Nov-01	-411.3	-364.7	-455.0	-343.3	-344.6	-312.6
33	09-Nov-01	-423.2	-412.5	-399.8	-365.8	-325.6	-333.3
34	12-Nov-01	-417.5	-412.5	-398.5	-366.5	-325.2	-356.1
35	16-Nov-01	-415.6	-412.0	-399.3	-365.2	-326.5	-333.1
36	19-Nov-01	-410.2	-510.1	-360.2	-352.1	-333.2	-330.0
37	23-Nov-01	-500.1	-455.2	-399.5	-405.1	-325.2	-312.2
38	26-Nov-01	-489.0	-497.5	-375.2	-395.2	-320.0	-355.4
39	30-Nov-01	-480.4	-482.0	-330.8	-375.2	-330.6	-335.0
40	03-Dec-01	-455.8	-512.2	-385.0	-388.5	-350.1	-348.9
41	07-Dec-01	-522.4	-555.2	-356.2	-365.3	-365.1	-321.5
42	10-Dec-01	-510.7	-480.0	-350.0	-398.6	-350.0	-320.0
43	14-Dec-01	-567.9	-452.1	-320.2	-312.6	-345.2	-340.0

44	17-Dec-01	-560.0	-500.3	-333.5	-350.0	-320.0	-302.5
45	21-Dec-01	-588.8	-522.1	-354.1	-366.9	-336.5	-350.0
46	24-Dec-01	-589.2	-550.0	-411.2	-422.3	-411.0	-423.5
47	28-Dec-01	-590.0	-555.6	-421.5	-415.6	-450.2	-435.6
48	31-Dec-01	-512.3	-503.2	-400.6	-432.5	-420.2	-411.2
49	04-Jan-01	-515.0	-510.0	-405.8	-421.3	-402.0	-413.5
50	07-Jan-02	-522.6	-536.5	-425.6	-430.0	-412.3	-425.6
52	14-Jan-02	-510.3	-505.6	-430.0	-444.5	-410.5	-400.9
56	28-Jan-02	-511.0	-521.2	-432.1	-429.0	-419.6	-410.2
60	11-Feb-02	-498.3	-510.3	-420.0	-425.8	-420.0	-425.0
64	25-Feb-02	-514.2	-502.3	-410.9	-415.0	-410.3	-422.6
68	11-Mar-02	-510.2	-500.1	-412.5	-411.3	-421.5	-425.8
72	25-Mar-02	522.0	-505.3	-423.0	-400.4	-420.0	-411.9

Resistance of 20 mm cover test specimens (Gecor 6 measurements).

Cycle number	Date	Resistance (kOhms)					
		Control 3	Control 4	BC 7	BC 8	AC 11	AC 12
1	18-Jun-01	1.12	1.52	1.03	1.00	0.99	1.00
2	22-Jun-01	1.23	1.44	1.13	0.99	1.20	1.03
3	25-Jun-01	1.30	1.15	1.02	1.24	1.00	0.99
4	29-Jun-01	1.13	1.03	1.25	0.99	1.06	1.11
5	02-Jul-01	1.29	1.02	1.14	1.11	1.12	1.21
6	06-Jul-01	1.24	1.45	1.20	1.02	0.98	1.05
7	09-Jul-01	1.47	1.23	1.37	1.44	1.30	1.52
8	13-Jul-01	1.72	1.22	1.05	0.98	1.00	1.00
9	16-Jul-01	1.34	1.50	1.50	1.43	1.60	1.58
10	23-Jul-01	1.47	1.27	1.36	1.39	1.40	1.62
11	26-Jul-01	1.21	0.97	1.09	1.16	1.12	1.12
12	30-Jul-01	2.55	1.56	1.82	1.54	2.00	2.11
13	06-Aug-01	3.24	1.97	2.07	2.56	2.69	2.76
14	13-Aug-01	2.01	1.73	1.99	2.30	2.30	2.43
15	17-Aug-01	1.42	1.27	1.36	1.36	1.44	1.59
16	20-Aug-01	2.41	2.43	2.35	2.59	2.89	3.00
17	27-Aug-01	2.11	1.99	2.06	1.98	2.21	2.30
18	03-Sep-01	1.36	1.16	1.15	1.38	1.27	1.53
19	10-Sep-01	1.59	1.37	1.29	1.66	1.63	1.82
20	14-Sep-01	3.36	3.24	4.63	5.12	5.47	6.57
21	17-Sep-01	1.79	1.72	1.69	1.79	2.15	2.28
22	24-Sep-01	2.02	1.88	1.94	2.85	2.52	2.69
23	01-Oct-01	2.55	2.41	2.12	2.32	2.06	1.99
24	08-Oct-01	2.35	2.03	1.99	2.54	2.20	2.02
25	12-Oct-01	2.46	2.20	2.00	2.10	1.98	1.55
26	15-Oct-01	2.32	2.05	1.97	2.23	2.33	2.45
27	19-Oct-01	2.04	2.11	1.88	2.24	2.16	2.55
28	22-Oct-01	2.32	2.10	1.99	2.02	2.15	2.33
29	26-Oct-01	2.56	2.45	2.03	2.11	2.13	2.01
30	29-Oct-01	2.41	2.12	2.06	1.98	2.08	2.11
31	02-Nov-01	1.11	1.05	1.65	1.98	1.99	1.80
32	05-Nov-01	1.02	0.78	0.89	0.10	1.06	1.10
33	09-Nov-01	0.99	0.89	0.75	0.65	0.60	1.00
34	12-Nov-01	1.10	0.95	0.88	0.85	0.74	0.55
35	16-Nov-01	0.56	0.90	0.87	0.56	0.60	0.70
36	19-Nov-01	0.88	0.75	0.56	0.88	0.97	0.95
37	23-Nov-01	0.63	0.56	0.87	0.55	0.69	0.58
38	26-Nov-01	0.98	1.00	1.01	0.99	0.87	0.96
39	30-Nov-01	1.00	1.20	1.05	0.87	0.98	1.11
40	03-Dec-01	1.20	0.57	0.68	0.65	0.89	0.74
41	07-Dec-01	0.99	0.88	0.80	0.88	0.69	0.98
42	10-Dec-01	0.85	0.65	0.60	0.53	0.87	0.58
43	14-Dec-01	0.96	0.98	0.80	0.90	0.65	0.66

44	17-Dec-01	0.87	1.10	1.00	0.99	0.85	0.77
45	21-Dec-01	0.99	1.03	0.98	0.85	0.98	0.69
46	24-Dec-01	1.00	1.11	0.98	0.87	0.80	0.70
47	28-Dec-01	0.85	0.70	0.75	0.96	0.58	0.56
48	31-Dec-01	0.80	0.90	0.85	0.82	0.75	0.66
49	04-Jan-01	0.75	0.70	0.85	0.9	0.95	0.68
50	07-Jan-02	1.20	1.11	1.06	0.98	0.96	0.99
52	14-Jan-02	0.98	0.56	0.80	0.90	0.99	1.00
56	28-Jan-02	0.80	0.58	0.70	0.60	0.66	0.65
60	11-Feb-02	0.99	0.79	0.70	0.68	0.52	0.56
64	25-Feb-02	0.98	0.66	0.87	0.75	0.87	0.95
68	11-Mar-02	0.99	1.12	1.05	0.88	0.85	0.76
72	25-Mar-02	0.70	0.65	0.88	0.85	0.60	0.81

Corrosion rates of 20 mm cover test specimens (Coulostaic method measurements).

Cycle number	Date	Corrosion rate (uA/cm^2)					
		Control 3	Control 4	BC 7	BC 8	AC 11	AC 12
1	18-Jun-01	0.155	0.149	0.109	0.110	0.122	0.115
2	22-Jun-01	0.135	0.144	0.108	0.112	0.285	0.150
3	25-Jun-01	0.250	0.205	0.132	0.141	0.158	0.210
4	29-Jun-01	0.302	0.288	0.145	0.200	0.142	0.250
5	02-Jul-01	0.400	0.240	0.111	0.268	0.213	0.195

$Cu/CuSO_4$ Half-cell potential of 20 mm cover test specimens.

Cycle number	Date	Potentials (mV)					
		Control 3	Control 4	BC 7	BC 8	AC 11	AC 12
1	18-Jun-01	-398.0	-399.8	-375.0	-365.2	-395.1	-399.0
2	22-Jun-01	-489.6	-466.5	-450.8	-355.4	-512.0	-500.3
3	25-Jun-01	-540.1	-438.5	-460.2	-511.3	-410.0	-555.2
4	29-Jun-01	-567.3	-550.2	-444.9	-500.0	-400.9	-518.5
5	02-Jul-01	-600.8	-558.2	-540.2	-487.5	-526.3	-531.0

Resistivity measurements for 20 mm cover test specimens (using the Wenner probe)

Cycle number	Date	Resistivity (k.ohms.cm)					
		Control 3	Control 4	BC 7	BC 8	AC 11	AC 12
1	18-Jun-01	35	48	30	25	28	31
2	22-Jun-01	40	45	35	28	32	35
3	25-Jun-01	45	35	28	40	35	32
4	29-Jun-01	32	30	35	29	35	38
5	02-Jul-01	40	35	35	43	40	46
6	06-Jul-01	42	48	36	32	28	35
7	09-Jul-01	47	38	42	46	40	48
8	13-Jul-01	40	37	37	32	35	31
9	16-Jul-01	42	45	48	42	52	50
10	23-Jul-01	45	41	43	42	46	51
11	26-Jul-01	35	33	38	36	34	31
12	30-Jul-01	80	44	56	47	65	61
13	06-Aug-01	102	64	66	96	89	101
14	13-Aug-01	60	55	62	71	65	76
15	17-Aug-01	44	50	45	42	40	51
16	20-Aug-01	72	90	80	102	98	109
17	27-Aug-01	65	58	59	62	68	72
18	03-Sep-01	41	39	35	38	43	47
19	10-Sep-01	49	45	37	52	45	55
20	14-Sep-01	105	149	154	166	210	200
21	17-Sep-01	55	59	49	54	65	75
22	24-Sep-01	62	55	62	85	71	86
23	01-Oct-01	80	76	64	72	60	54
24	08-Oct-01	74	59	55	78	67	58
25	12-Oct-01	71	69	55	62	65	50
26	15-Oct-01	80	65	52	70	63	75
27	19-Oct-01	59	65	58	70	57	76
28	22-Oct-01	85	85	69	62	64	70
29	26-Oct-01	65	75	58	65	65	59
30	29-Oct-01	75	64	63	55	61	65
31	02-Nov-01	34	39	58	63	60	75
32	05-Nov-01	30	35	30	54	63	65
33	09-Nov-01	50	33	31	25	20	31
34	12-Nov-01	35	32	25	30	28	20
35	16-Nov-01	21	30	28	25	25	22
36	19-Nov-01	29	20	26	26	28	31
37	23-Nov-01	25	22	23	20	21	25
38	26-Nov-01	66	55	32	35	28	30
39	30-Nov-01	50	38	63	58	38	35
40	03-Dec-01	49	21	28	26	30	25
41	07-Dec-01	32	28	25	23	21	30
42	10-Dec-01	33	30	29	20	26	22
43	14-Dec-01	30	30	39	32	22	25

44	17-Dec-01	27	35	38	30	28	25
45	21-Dec-01	35	29	31	29	32	28
46	24-Dec-01	32	35	28	27	31	24
47	28-Dec-01	28	28	25	30	20	21
48	31-Dec-01	25	31	30	24	25	26
49	04-Jan-01	23	25	26	30	31	25
50	07-Jan-02	30	32	30	28	35	35
52	14-Jan-02	29	25	29	28	30	32
56	28-Jan-02	26	20	25	21	21	39
60	11-Feb-02	30	28	23	21	20	25
64	25-Feb-02	32	22	28	26	26	69
68	11-Mar-02	28	35	32	30	25	23
72	25-Mar-02	25	22	29	30	20	31

APPENDIX F

Corrosion rates for Parapet walls 1, Sports Centre Building, UCT

Date	Number of days	Corrosion rate (uA/cm^2)					
		A			**B**		
		1	2	3	1	2	3
01-Oct-01	1	0.007	0.008	0.008	0.006	0.009	0.010
02-Oct-01	2	0.015	0.020	0.018	0.020	0.019	0.011
06-Oct-01	6	0.025	0.085	0.049	0.020	0.035	0.019
07-Oct-01	7	0.035	0.027	0.027	0.012	0.014	0.019
13-Oct-01	13	0.040	0.030	0.035	0.025	0.020	0.018
14-Oct-01	14	0.035	0.028	0.031	0.019	0.020	0.021
20-Oct-01	20	0.035	0.041	0.038	0.018	0.025	0.022
21-Oct-01	21	0.014	0.019	0.035	0.024	0.040	0.066
27-Oct-01	27	0.015	0.019	0.020	0.030	0.029	0.011
28-Oct-01	28	0.009	0.014	0.012	0.028	0.034	0.045

Half-cell potentials for Parapet walls 1, Sports Centre Building, UCT

Date	Number of days	Potential (mV)					
		A			**B**		
		1	2	3	1	2	3
01-Oct-01	1	-41.4	-50.6	-54.6	-12.8	-52.4	-63.5
02-Oct-01	2	-50.4	-54.3	-52.3	-64.3	-61.4	-55.6
06-Oct-01	6	-65.1	-71.1	-103.0	-267.3	-144.2	-13.2
07-Oct-01	7	-99.2	-62.2	-70.3	-14.3	-34.8	-25.4
13-Oct-01	13	-98.4	-59.3	-65.4	-36.2	-44.3	-30.4
14-Oct-01	14	-105.2	-58.6	-74.3	-20.2	-29.8	-35.2
20-Oct-01	20	-101.2	-84.8	-61.3	-30.1	-41.5	-42.3
21-Oct-01	21	-60.3	-55.2	-71.4	-45.0	-35.3	-56.3
27-Oct-01	27	-45.6	-54.3	-62.1	-77.4	-68.0	-50.2
28-Oct-01	28	-40.5	-50.3	-45.4	-60.3	-65.8	-110.0

Resistance measurements for Parapet walls 1, Sports Centre Building, UCT

Date	Number of days	Resistance (k. ohms)					
		A			**B**		
		1	2	3	1	2	3
01-Oct-01	1	2.44	2.02	1.88	2.99	2.06	1.98
02-Oct-01	2	2.41	1.99	2.00	2.01	1.94	2.98
06-Oct-01	6	9.36	7.80	10.02	9.42	9.56	8.95
07-Oct-01	7	10.24	12.61	9.85	10.74	10.00	9.85
13-Oct-01	13	10.44	13.22	10.10	11.64	9.99	10.23
14-Oct-01	14	10.25	13.10	9.89	11.21	10.40	8.89
20-Oct-01	20	10.26	11.10	9.88	12.44	10.21	9.99
21-Oct-01	21	12.04	9.80	10.33	10.40	8.88	11.54
27-Oct-01	27	10.11	9.90	8.85	12.12	10.10	9.99
28-Oct-01	28	9.80	12.88	13.40	11.20	8.88	10.200

APPENDIX G

Corrosion rates for Parapet walls 2, Sports Centre Building, UCT

Date	Number of days	Corrosion rate (uA/cm^2)					
		C			D		
		1	2	3	1	2	3
01-Oct-01	1	0.008	0.010	0.014	0.011	0.008	0.007
02-Oct-01	2	0.021	0.016	0.019	0.015	0.025	0.031
06-Oct-01	6	0.031	0.021	0.015	0.030	0.024	0.032
07-Oct-01	7	0.015	0.011	0.011	0.033	0.015	0.030
13-Oct-01	13	0.032	0.025	0.019	0.045	0.030	0.034
14-Oct-01	14	0.03	0.028	0.017	0.041	0.034	0.029
20-Oct-01	20	0.019	0.035	0.018	0.033	0.040	0.021
21-Oct-01	21	0.022	0.028	0.016	0.025	0.030	0.020
27-Oct-01	27	0.034	0.019	0.025	0.012	0.018	0.022
28-Oct-01	28	0.044	0.015	0.010	0.017	0.023	0.030

Half-cell potentials for Parapet walls 1, Sports Centre Building, UCT

Date	Number of days	Potential (mV)					
		C			D		
		1	2	3	1	2	3
01-Oct-01	1	-41.1	-50.3	-64.6	-65.2	-54.3	-40.4
02-Oct-01	2	-54.6	-49.2	-45.3	-40.4	-55.3	-64.5
06-Oct-01	6	-86.6	-110.7	-63.7	-117.1	-69.9	-70.8
07-Oct-01	7	-110.9	-106.5	-79.9	-116.4	-84.5	-82.7
13-Oct-01	13	-90.1	-112.4	-60.4	-122.4	-72.1	-69.9
14-Oct-01	14	-100.3	-111.2	-60.9	-122.4	-71.5	-68.8
20-Oct-01	20	-64.2	-112.4	-60.1	-66.5	-100.6	-71.5
21-Oct-01	21	-55.4	-68.2	-48.9	-68.2	-111.5	-70.3
27-Oct-01	27	-115.4	-89.9	-90.4	-71.4	-80.3	-110.2
28-Oct-01	28	-44.3	-56.0	-40.2	-65.3	-70.1	-99.4

Resistance measurements for Parapet walls 1, Sports Centre Building, UCT

Date	Number of days	Resistance (k. ohms)					
		C			D		
		1	2	3	1	2	3
01-Oct-01	1	2.84	2.02	1.99	2.11	2.24	2.98
02-Oct-01	2	2.55	3.10	2.98	3.02	2.40	1.98
06-Oct-01	6	11.19	13.57	20.82	6.00	12.49	10.41
07-Oct-01	7	19.56	23.70	32.63	6.60	12.22	11.02
13-Oct-01	13	11.91	12.45	16.20	5.85	12.62	11.10
14-Oct-01	14	10.84	14.22	15.16	7.22	11.50	9.99
20-Oct-01	20	9.88	10.14	11.20	10.99	12.20	14.10
21-Oct-01	21	13.14	8.99	9.90	8.90	10.00	12.44
27-Oct-01	27	9.89	10.00	10.11	10.84	11.12	10.20
28-Oct-01	28	10.56	11.45	12.88	11.34	8.44	10.20.

APPENDIX H

Corrosion rates for Concrete Slabs, Civil Engineering Department, UCT

Date	Number of days	Corrosion rate (uA/cm^2)					
		E			**F**		
		1	2	3	1	2	3
15-Oct-01	1	0.025	0.052	0.026	0.082	0.099	0.045
16-Oct-01	2	0.090	0.066	0.018	0.084	0.056	0.047
22-Oct-01	7	0.090	0.066	0.018	0.084	0.056	0.047
23-Oct-01	8	0.059	0.070	0.036	0.033	0.065	0.010
28-Oct-01	13	0.040	0.058	0.015	0.056	0.044	0.023
29-Oct-01	14	0.044	0.032	0.030	0.050	0.030	0.028

Half-cell potentials for Concrete Slabs, Civil Engineering Department, UCT

Date	Number of days	Potential (mV)					
		E			**F**		
		1	2	3	1	2	3
15-Oct-01	1	-222.4	-225.1	-133.8	-179.5	-232.2	-210.5
16-Oct-01	2	-235.8	-224.5	-211.8	-251.3	-216.8	-210.5
22-Oct-01	7	-228.3	-210.4	-205.3	-198.4	-180.5	-201.1
23-Oct-01	8	-210.8	-224.4	-209.8	-220.6	-245.0	-210.1
28-Oct-01	13	-240.0	-258.9	-199.8	-250.2	-241.5	-205.6
29-Oct-01	14	-240.7	-230.5	-219.4	-266.0	-240.5	-222.0

Resistance measurements for Concrete Slabs, Civil Engineering Department, UCT

Date	Number of days	Resistance (k. ohms)					
		E			**F**		
		1	2	3	1	2	3
15-Oct-01	1	4.73	18.01	9.38	4.71	16.02	39.56
16-Oct-01	2	9.45	10.10	22.11	10.44	8.50	20.48
22-Oct-01	7	9.89	10.50	8.80	10.44	8.10	25.50
23-Oct-01	8	11.46	28.30	16.50	4.74	8.32	11.01
28-Oct-01	13	10.07	22.00	39.40	48.30	36.20	25.11
29-Oct-01	14	10.12	15.34	16.48	22.58	25.01	36.21

APPENDIX I

Corrosion rates for Roof of Menzies Building, UCT

Date	Number of days	Corrosion rate (uA/cm^2)					
		H			**G**		
		1	2	3	1	2	3
02-Oct-01	1	0.069	0.213	0.069	0.037	0.012	0.100
03-Oct-01	2	0.145	0.032	0.386	0.030	0.014	0.020
08-Oct-01	7	0.109	0.150	0.076	0.127	0.276	0.105
09-Oct-01	8	0.099	0.110	0.152	0.100	0.222	0.109
15-Oct-01	14	0.162	0.112	0.210	0.150	0.099	0.160
16-Oct-01	15	0.170	0.155	0.105	0.166	0.112	0.144
23-Oct-01	22	0.222	0.194	0.110	0.180	0.154	0.184
24-Oct-01	23	0.320	0.222	0.190	0.280	0.111	0.326
29-Oct-01	28	0.122	0.189	0.200	0.255	0.156	0.290
30-Oct-01	29	0.280	0.160	0.295	0.200	0.190	0.216
15-Dec-01	75	0.244	0.190	0.250	0.281	0.200	0.199
16-Dec-01	76	0.222	0.215	0.231	0.250	0.198	0.233
22-Dec-01	82	0.185	0.194	0.166	0.210	0.188	0.169
23-Dec-01	83	0.150	0.239	0.142	0.221	0.208	0.190
12-Jan-02	103	0.114	0.125	0.130	0.256	0.291	0.220
13-Jan-02	104	0.166	0.119	0.120	0.240	0.265	0.222
26-Jan-02	117	0.120	0.109	0.118	0.235	0.211	0.219
27-Jan-02	118	0.121	0.108	0.125	0.215	0.280	0.234
09-Feb-02	131	0.114	0.108	0.100	0.210	0.199	0.222
10-Feb-02	132	0.110	0.119	0.120	0.245	0.223	0.211
23-Feb-02	145	0.096	0.114	0.150	0.243	0.215	0.208
24-Feb-02	146	0.111	0.131	0.142	0.208	0.224	0.168
02-Mar-02	152	0.108	0.115	0.134	0.245	0.261	0.247
03-Mar-02	153	0.119	0.121	0.123	0.260	0.243	0.235
16-Mar-02	166	0.128	0.120	0.157	0.198	0.212	0.193
17-Mar-02	167	0.135	0.142	0.137	0.200	0.231	0.199
06-Apr-02	186	0.139	0.138	0.143	0.210	0.217	0.200
07-Apr-02	187	0.142	0.140	0.153	0.218	0.220	0.207
20-Apr-02	200	0.135	0.119	0.130	0.200	0.167	0.197
21-Apr-02	201	0.130	0.108	0.128	0.242	0.188	0.170

Half-cell potentials for Roof of Menzies Building, UCT

Date	Number of days	Half-cell potential (mV)					
		H			**G**		
		1	2	3	1	2	3
02-Oct-01	1	-140.5	-194.5	-159.0	-220.6	-256.6	-229.4
03-Oct-01	2	-111.0	-219.2	-109.4	-128.4	-168.5	-151.5
08-Oct-01	7	-215.4	-284.5	-175.3	-244.5	-270.3	-227.3
09-Oct-01	8	-154.3	-260.5	-270.2	-224.0	-252.4	-211.2
15-Oct-01	14	-220.4	-210.5	-260.2	-210.4	-199.3	-224.5
16-Oct-01	15	-235.0	-220.5	-201.6	-210.5	-244.7	-253.2
23-Oct-01	22	-230.0	-215.5	-256.8	-250.5	-210.1	-256.0
24-Oct-01	23	-264.5	-245.6	-211.1	-240.5	-213.3	-256.8
29-Oct-01	28	-200.6	-224.0	-236.1	-258.0	-200.0	-264.5
30-Oct-01	29	-284.3	-210.5	-232.5	-284.3	-199.3	-205.6
15-Dec-01	75	-277.3	-259.0	-291.2	-288.1	-260.2	-255.9
16-Dec-01	76	-252.8	-240.0	-241.2	-285.6	-256.2	-275.3
22-Dec-01	82	-266.3	-241.5	-230.6	-271.8	-267.4	-248.3
23-Dec-01	83	-241.8	-198.3	-234.4	-258.9	-265.4	-241.2
12-Jan-02	103	-185.4	-234.8	-250.0	-251.3	-198.4	-188.2
13-Jan-02	104	-175.3	-189.2	-199.9	-241.8	-265.4	-199.8
26-Jan-02	117	-184.3	-154.2	-200.3	-249.2	-268.4	-245.1
27-Jan-02	118	-175.2	-221.5	-248.3	-251.2	-264.8	-255.3
09-Feb-02	131	-211.1	-200.2	-198.4	-170.8	-254.2	-288.9
10-Feb-02	132	-210.4	-215.6	-250.2	-288.9	-264.3	-249.1
23-Feb-02	145	-215.6	-222.3	-245.8	-297.5	-288.0	-287.1
24-Feb-02	146	-199.8	-200.5	-240.1	-285.0	-268.5	-288.8
02-Mar-02	152	-200.6	-240.1	-212.2	-258.3	-254.2	-295.0
03-Mar-02	153	-205.3	-234.7	-222.3	-265.8	-266.3	-278.0
16-Mar-02	166	-199.2	-245.5	-236.9	-256.6	-258.6	-295.6
17-Mar-02	167	-185.2	-230.6	-244.4	-266.3	-250.1	-300.5
06-Apr-02	186	-215.9	-225.8	-250.2	-298.5	-274.3	-285.6
07-Apr-02	187	-210.8	-220.0	-245.1	-284.1	-265.0	-280.0
20-Apr-02	200	-200.0	-233.2	-240.0	-258.6	-287.0	-298.6
21-Apr-02	201	-214.2	-245.6	-235.0	-250.1	-265.8	-290.0

Resistance measurements for Roof of Menzies Building, UCT

Date	Number of days	Resistance (k.ohm)					
		H			**G**		
		1	2	3	1	2	3
02-Oct-01	1	4.36	3.83	4.64	5.36	8.55	5.60
03-Oct-01	2	3.59	0.77	2.00	4.10	4.20	4.18
08-Oct-01	7	6.3	6.12	6.59	5.09	3.28	4.25
09-Oct-01	8	7.54	6.22	5.83	6.30	6.52	6.10
15-Oct-01	14	5.44	6.23	7.10	8.90	7.24	7.99
16-Oct-01	15	10.12	9.44	9.00	10.21	9.90	10.01
23-Oct-01	22	10.11	9.80	9.99	12.34	11.20	8.40
24-Oct-01	23	7.32	8.50	10.14	9.80	7.17	8.88
29-Oct-01	28	10.11	11.50	12.84	10.51	9.89	13.44
30-Oct-01	29	11.22	10.90	9.88	11.20	10.99	9.84
15-Dec-01	75	6.30	8.24	4.90	5.85	6.10	8.22
16-Dec-01	76	10.85	8.22	6.95	5.89	7.33	6.58
22-Dec-01	82	6.06	5.85	8.24	5.08	7.86	5.14
23-Dec-01	83	6.60	4.80	5.99	7.24	10.21	6.81
12-Jan-02	103	5.85	4.21	3.91	6.14	7.55	5.80
13-Jan-02	104	4.82	6.91	7.04	7.55	6.19	5.21
26-Jan-02	117	10.11	9.8	7.02	13.81	14.07	10.20
27-Jan-02	118	6.81	7.24	6.98	8.84	9.90	5.83
09-Feb-02	131	4.10	4.20	3.84	6.12	5.44	4.85
10-Feb-02	132	4.36	3.50	4.00	5.12	4.90	2.10
23-Feb-02	145	5.36	2.85	5.63	5.89	6.23	6.58
24-Feb-02	146	4.88	3.02	4.78	5.09	6.00	5.88
02-Mar-02	152	2.54	3.00	2.95	3.21	4.13	5.22
03-Mar-02	153	2.85	3.52	3.01	3.33	3.98	4.52
16-Mar-02	166	10.21	9.89	8.50	6.65	8.45	8.00
17-Mar-02	167	9.95	8.80	9.77	5.68	8.77	9.45
06-Apr-02	186	5.65	6.60	5.89	7.88	8.00	5.45
07-Apr-02	187	4.50	3.98	3.55	4.56	3.00	2.88
20-Apr-02	200	2.12	3.00	2.98	1.90	4.00	2.23
21-Apr-02	201	3.05	2.88	3.11	2.20	3.21	2.00

APPENDIX J

Corrosion monitoring of Roof of Menzies Site, UCT, during application of wetting system (Control site)

Corrosion rates during application of wetting system for Roof of Menzies Building, UCT

Date	Number of days after wetting started	Corrosion rate ($\mu A/cm^2$)			Average Corrosion rate ($\mu A/cm^2$)
		H			
		1	2	3	
16-May-02	0	0.201	0.322	0.188	0.237
19-May-02	3	0.585	0.620	0.441	0.549
21-May-02	5	2.981	4.115	1.985	3.027
23-May-02	7	2.542	3.566	1.708	2.605
26-May-02	10	2.310	3.112	1.875	2.432
28-May-02	12	2.664	3.386	1.600	2.550
31-May-02	15	2.420	2.988	2.000	2.469
03-Jun-02	18	2.322	3.120	1.980	2.474
06-Jun-02	21	2.655	2.560	2.130	2.448
10-Jun-02	25	2.400	2.733	1.895	2.343
13-Jun-02	28	2.056	2.850	2.112	2.339
17-Jun-02	32	2.225	2.113	2.050	2.129
20-Jun-02	35	2.100	2.100	1.954	2.051
27-Jun-02	42	1.880	1.780	1.852	1.837
25-Jul-02	69	0.258	0.320	0.280	0.286
27-Jul-02	71	0.201	0.002	0.155	0.119
03-Aug-02	78	0.024	0.016	0.029	0.023
09-Aug-02	65	0.033	0.025	0.020	0.026
15-Aug-02	71	0.028	0.022	0.031	0.027

Half-cell potentials during application of wetting system for Roof of Menzies Building, UCT

Date	Number of days after wetting started	Half-cell potential (mV)			Average Half-cell potential (mV)
		H			
		1	2	3	
16-May-02	0	-178.0	-184.2	-123.4	-161.9
19-May-02	3	-185.2	-232.4	-190.0	-202.5
21-May-02	5	-192.2	-244.5	-188.8	-208.5
23-May-02	7	-200.5	-251.2	-210.3	-220.7
26-May-02	10	-215.6	-268.9	-200.0	-228.2
28-May-02	12	-232.0	-250.5	-188.4	-223.6
31-May-02	15	-235.6	-244.2	-195.8	-225.2

03-Jun-02	18	-255.8	-268.9	-200.8	-241.8
06-Jun-02	21	-240.2	-260.5	-188.7	-229.8
10-Jun-02	25	-252.0	-271.8	-195.2	-239.7
13-Jun-02	28	-245.0	-240.5	-205.6	-230.4
17-Jun-02	32	-275.1	-255.0	-222.3	-250.8
20-Jun-02	35	-270.1	-260.9	-215	-248.7
27-Jun-02	42	-245.3	-235.0	-225.9	-235.1
25-Jul-02	69	-220.1	-241.8	-209.0	-223.6
27-Jul-02	71	-215.6	-248.6	-199.5	-221.3
03-Aug-02	78	-236.0	-237.0	-220.4	-231.1
09-Aug-02	65	-255.5	-260.8	-210.5	-242.3
15-Aug-02	71	-250.0	-245.6	-218.0	-237.8

Resistance during application of wetting system for Roof of Menzies Building, UCT

Date	Number of days after wetting started	Resistance (k.ohms)			Average Resistance (k.ohms)
		H			
		1	2	3	
16-May-02	0	2.87	2.05	1.95	2.29
19-May-02	3	2.50	1.88	1.65	2.01
21-May-02	5	0.98	0.80	1.12	0.97
23-May-02	7	0.88	0.90	1.05	0.94
26-May-02	10	0.95	0.75	0.98	0.89
28-May-02	12	0.87	0.80	1.09	0.92
31-May-02	15	0.99	0.96	1.08	1.01
03-Jun-02	18	0.85	0.87	0.95	0.89
06-Jun-02	21	0.99	1.10	0.88	0.99
10-Jun-02	25	1.08	1.06	0.96	1.03
13-Jun-02	28	0.85	0.84	1.08	0.92
17-Jun-02	32	0.98	0.98	1.10	1.02
20-Jun-02	35	1.08	1.08	1.09	1.08
27-Jun-02	42	1.12	1.15	1.12	1.13
25-Jul-02	69	2.10	2.3	2.05	2.15
27-Jul-02	71	2.37	2.18	2.27	2.27
03-Aug-02	78	2.98	2.29	2.48	2.58
09-Aug-02	65	2.55	2.08	2.12	2.25
15-Aug-02	71	2.30	1.95	2.00	2.08

Resistivity during application of wetting system for Roof of Menzies Building, UCT

Date	Number of days after wetting started	Resistivity (k.ohm.cm)			Average Resistivity (k.ohm.cm)
		H			
		1	2	3	
16-May-02	0	96	55	68	73
19-May-02	3	84	57	92	78
21-May-02	5	25	30	42	32
23-May-02	7	26	32	45	34
26-May-02	10	28	35	40	34
28-May-02	12	30	29	36	32
31-May-02	15	25	32	41	33
03-Jun-02	18	28	28	35	30
06-Jun-02	21	35	30	31	32
10-Jun-02	25	39	25	28	31
13-Jun-02	28	26	31	30	29
17-Jun-02	32	32	36	32	33
20-Jun-02	35	45	41	36	41
27-Jun-02	42	40	35	30	35
25-Jul-02	69	61	69	65	65
27-Jul-02	71	75	65	69	70
03-Aug-02	78	88	72	75	78
09-Aug-02	65	80	75	81	79
15-Aug-02	71	75	82	78	78

APPENDIX K

Corrosion monitoring of Roof of Menzies Site, UCT, during application of wetting system (Treated site)

Corrosion rates during application of wetting system for Roof of Menzies Building, UCT

Date	Number of days after wetting started	Corrosion rate ($\mu A/cm^2$)			Average Corrosion rate ($\mu A/cm^2$)
		G			
		1	2	3	
06-Jun-02	0	0.255	0.208	0.382	0.282
10-Jun-02	4	0.591	0.745	0.605	0.647
13-Jun-02	7	0.520	0.612	0.548	0.560
17-Jun-02	11	0.512	0.600	0.445	0.519
20-Jun-02	14	0.525	0.640	0.519	0.561
27-Jun-02	21	0.488	0.580	0.468	0.512
25-Jul-02	48	0.100	0.098	0.109	0.102
27-Jul-02	50	0.099	0.085	0.035	0.073
03-Aug-02	57	0.082	0.024	0.029	0.045
09-Aug-02	65	0.091	0.045	0.035	0.057
15-Aug-02	71	0.088	0.034	0.042	0.055

Half-cell potentials during application of wetting system for Roof of Menzies Building, UCT

Date	Number of days after wetting started	Half-cell potential (mV)			Average Half-cell potential (mV)
		G			
		1	2	3	
06-Jun-02	0	-200.0	-185.6	-165.2	-183.6
10-Jun-02	4	-233.3	-250.6	-231.5	-238.5
13-Jun-02	7	-258.9	-270.0	-260.8	-263.2
17-Jun-02	11	-281.0	-276.3	-272.0	-276.4
20-Jun-02	14	-265.4	-288.0	-260.1	-271.2
27-Jun-02	21	-240.3	-238.7	-255.5	-244.8
25-Jul-02	48	-205.8	-212.0	-200.6	-206.1
27-Jul-02	50	-168.7	-188.2	-195.3	-184.1
03-Aug-02	57	-184.2	-192.8	-180.7	-185.9
09-Aug-02	65	-195.0	-181.2	-175.5	-183.9
15-Aug-02	71	-188.4	-190.7	-170.2	-183.1

Resistance during application of wetting system for Roof of Menzies Building, UCT

Date	Number of days after wetting started	Resistance (k.ohms)			Average Resistance (k.ohms)
		G			
		1	2	3	
06-Jun-02	0	3.20	2.88	3.06	3.05
10-Jun-02	4	2.44	2.51	2.72	2.56
13-Jun-02	7	1.25	1.12	1.09	1.15
17-Jun-02	11	0.85	0.95	0.87	0.89
20-Jun-02	14	1.08	1.12	0.96	1.05
27-Jun-02	21	1.02	0.82	0.88	0.91
25-Jul-02	48	2.84	3.08	2.11	2.68
27-Jul-02	50	4.25	3.95	2.54	3.58
03-Aug-02	57	4.39	3.33	2.96	3.56
09-Aug-02	65	3.30	2.89	2.68	2.96
15-Aug-02	71	3.08	2.68	2.55	2.77

Resistivity during application of wetting system for Roof of Menzies Building, UCT

Date	Number of days after wetting started	Resistivity (k.ohm.cm)			Average Resistivity (k.ohm.cm)
		G			
		1	2	3	
06-Jun-02	0	95	86	112	98
10-Jun-02	4	123	108	98	110
13-Jun-02	7	61	58	65	61
17-Jun-02	11	32	41	35	36
20-Jun-02	14	28	25	30	28
27-Jun-02	21	38	31	28	32
25-Jul-02	48	49	52	59	53
27-Jul-02	50	85	75	64	75
03-Aug-02	57	119	92	78	96
09-Aug-02	65	100	85	75	87
15-Aug-02	71	105	88	80	91

APPENDIX L

Relationship between resistance measured using the Gecor instrument and resistivity measured using the Wenner probe.

Resistance measured using Gecor 6 (k.Ohms)	Resistivity measured using Wenner Probe (k.Ohm.cm)
0.56	28
0.70	31
0.91	51
0.85	25
0.77	57
0.71	42
0.64	31
0.77	37
1.09	51
0.85	22
0.97	53
0.95	51
0.54	31
0.66	34
0.88	49
0.85	22
0.78	51
0.68	48
0.77	31
0.74	37
0.99	53
0.83	26
0.83	56
0.74	56
0.82	47
0.63	39
0.91	41
1.03	69
0.77	36
0.88	75
0.92	54
0.62	35
0.76	39
1.05	63
0.83	29
0.87	55
0.99	50

0.70	35
0.94	35
1.26	69
1.02	27
1.04	65
1.21	52
1.23	71
1.20	49
1.30	59
1.38	59
1.22	64
1.33	69
0.80	40
0.80	40
0.94	69
0.83	31
0.92	70
0.93	42
1.03	66
0.89	44
1.07	52
1.09	55
1.53	84
1.15	56
0.64	35
0.84	33
1.12	38
0.87	30
0.95	33
0.99	28
1.29	40
1.02	35
1.14	35
1.11	43
1.12	40
1.21	46
1.75	55
1.41	46
2.15	66
1.86	55
2.22	90
2.02	65
1.47	48

1.17	40
1.62	48
1.41	49
1.57	57
1.66	58
2.41	72
2.43	90
2.35	80
2.59	102
2.89	98
3.00	109
3.36	105
3.24	149
4.63	154
5.12	166
5.47	210
2.32	86
2.32	80
2.10	85
1.99	69
2.02	62
2.15	64
2.33	70
1.79	55
1.72	66
1.69	66
1.79	75
2.15	63
2.28	65
3.24	102
1.97	64
2.07	66
2.56	95
2.69	89
2.76	101
1.72	66
1.22	47
1.05	38
0.98	66
1.00	55
1.00	50